



Numerical Model Study of Proposed Navigation Improvements at the Colorado River Intersection with the Gulf Intra-Coastal Waterway, TX

Volume 1: Report

Gary L. Brown, M. Soraya Sarruff, Timothy L. Fagerburg and Nolan
Raphelt

January 2003

Preface

As part of the continuing studies of the Mouth of Colorado River Project, TX, the US Army Engineer District, Galveston (SWG), requested the US Army Engineer Research and Development Center (ERDC) to perform a numerical model study of hydrodynamics, including currents, salinity, and sediment changes, associated with the plan to open Parker's Cut and or Southwest Cut. A numerical model study and related field data collection were conducted at the Coastal and Hydraulic Laboratory (CHL) of the ERDC, Vicksburg, MS, during 2001-2002 to evaluate if opening any or all of the cuts would improve navigation currents at the intersection of the Gulf Inter-Coastal Waterway (GIWW) and the Mouth of Colorado River bypass channel.

The Galveston District provided funding for this study. Mr. Gary Brown and Ms. Soraya Sarruff, CHL, served as co-principal investigators of the project, while Mr. Nolan Raphelt assisted the team in performing numerical modeling tasks. The Hydraulic Analysis Group of CHL, led by Mr. Tim Fagerburg, undertook the field data collection efforts. Mr. Ed Reindl and Ms. Laura Lynn Robinson provided pertinent data available at the Galveston District.

The study was conducted under general supervision of Dr. Robert T. McAdory, Chief of the Estuarine Engineering Branch, and Mr. Thomas W. Richardson, Director, CHL.

At the time of this publication, Dr. James R. Houston is Director of ERDC, and COL John W. Morris III, EN, is Commander and Executive Director.

Table of Contents

INTRODUCTION	5
BACKGROUND AND PROBLEM STATEMENT	8
OBJECTIVE AND APPROACH	13
NUMERICAL MODEL DESCRIPTION	14
FIELD DATA COLLECTION AND ANALYSIS	14
HYDRODYNAMIC, SALINITY, AND SEDIMENT MODELS	18
<i>Computational Mesh</i>	18
<i>Boundary Conditions</i>	20
a. Hydrodynamic and Salinity Model Boundary Conditions	20
b. Sediment Boundary Conditions	31
CALIBRATION AND VERIFICATION	33
MODEL CALIBRATION.....	33
MODEL VERIFICATION.....	36
<i>Water Surface Elevation Data</i>	36
<i>ADCP Discharge Data</i>	37
<i>Velocity Data</i>	37
<i>Salinity Data</i>	38
<i>Salinity Sensitivity Tests</i>	40
MODEL SCENARIO RUNS	42
DESCRIPTION OF SCENARIOS	42
CURRENTS	42
<i>Currents at the ICWW-Bypass Channel Intersection</i>	43
<i>Currents at the Old River Channel Mouth</i>	46
<i>Currents at Parker's Cut, Southwest Cut, and the Diversion Dam Cut</i>	48
SALINITY	52
<i>Annual Average Salinity Distribution</i>	52
<i>Influence of Parker's Cut on West Matagorda Bay Salinity: Sample Comparison</i>	54
<i>Evaluation of Scenarios: Average Annual Salinity Difference</i>	56
<i>Impact of Parker's Cut on Average Springtime Salinity in West Matagorda Bay</i>	57
SEDIMENT	57
<i>Average Annual Bed Elevation Change</i>	57
<i>Influence of Parker's Cut and the Diversion Dam Cut on Sedimentation in West Matagorda Bay: Sample Comparison</i>	60
<i>Evaluation of Scenarios: Average Annual Bed Elevation Change Difference</i>	62
CONCLUSIONS AND RECOMMENDATIONS.....	64
REFERENCES	67

List of Tables

TABLE 1. DESCRIPTION OF STUDIED SCENARIOS.....	13
TABLE 2. TIDAL BOUNDARY CONDITION ADJUSTMENT FACTORS	20
TABLE 3. LOCKING PROTOCOL APPLIED TO MODEL RUNS.....	21
TABLE 4: MANNING’S N AND HORIZONTAL TURBULENT MIXING PARAMETERS USED IN THE MODEL.....	34
TABLE 5: STATISTICAL SUMMARY OF CALIBRATION: WATER SURFACE ELEVATION	35
TABLE 6: STATISTICAL SUMMARY OF VERIFICATION: WATER SURFACE ELEVATION	37
TABLE 7: STATISTICAL SUMMARY OF VERIFICATION: VELOCITY VARIANCE ELLIPSE ANALYSIS RESULTS	38
TABLE 8: STATISTICAL SUMMARY OF VERIFICATION: SALINITY DATA	40
TABLE 9: SALINITY SENSITIVITY TEST RESULTS	41
TABLE 10: APPROXIMATE VOLUME OF COLORADO RIVER DIVERSION DELTA GROWTH FOR EXISTING CONDITIONS.....	59
TABLE 11: PERCENT REDUCTION OF THE RATE OF GROWTH OF THE COLORADO RIVER DELTA RELATIVE TO EXISTING CONDITIONS.....	63

List of Figures

FIGURE 1. MATAGORDA BAY LOCATION MAP (ADAPTED FROM KRAUS, MARK, & SARRUFF 1999).....	10
FIGURE 2. DEVELOPMENT OF COLORADO RIVER DELTA FROM 1855 TO 1976 (ADAPTED FROM USGS, TOBIN AND KARGL).....	11
FIGURE 3. STUDY AREA FEATURES.....	12
FIGURE 4. DETAILS OF INTERSECTION BETWEEN THE COLORADO RIVER AND THE GULF INTER-COASTAL WATERWAY.....	12
FIGURE 5. WES DATA COLLECTION STATIONS	16
FIGURE 6. LOCATION OF WES ADCP TRANSECTS.....	17
FIGURE 7. AREA OF WES BATHYMETRIC SURVEY	17
FIGURE 8. COMPUTATIONAL MESH AND BATHYMETRY OF STUDY AREA.....	19
FIGURE 9. LOCATION OF BOUNDARY CONDITION STATIONS.....	22
FIGURE 10. RAWLINGS BAIT CAMP TIDE STATION SIGNAL	23
FIGURE 11. MITCHELL’S CUT TIDE STATION SIGNAL	24
FIGURE 12. PORT O’CONNOR TIDE STATION SIGNAL.....	25
FIGURE 13. EAST MATAGORDA BAY STATION (TCOON) WIND SPEED AND DIRECTION	26
FIGURE 14. PORT O’CONNOR STATION (TCOON) WIND SPEED AND DIRECTION	27
FIGURE 15. WES STATION WIND SPEED AND DIRECTION	28
FIGURE 16. DISCHARGE HYDROGRAPH FOR THE COLORADO, TRES PALACIOS, AND LAVACA RIVERS	29
FIGURE 17. APPLIED PRECIPITATION AND EVAPORATION PARAMETERS.....	29
FIGURE 18. RAW AND ATTENUATED BIG BOGGY CREEK UNGAGED FLOW	30
FIGURE 19. SAMPLE LOW, MEDIUM, AND HIGH FLOW YEARS FOR THE COLORADO RIVER (MEASURED AT BAY CITY, TX)	30
FIGURE 20: APPLIED SEDIMENT LOAD ON THE COLORADO RIVER, BY GRAIN SIZE	32

FIGURE 21: APPLIED COLORADO RIVER SUSPENDED SEDIMENT CONCENTRATION	32
FIGURE 22: PERCENT REDUCTION IN AVERAGE PEAK FLOOD-TIDE CURRENTS AT THE ICWW-BYPASS CHANNEL INTERSECTION.....	43
FIGURE 23: PEAK FLOOD-TIDE CURRENTS AT THE BYPASS CHANNEL-ICWW INTERSECTION FOR SCENARIO A	45
FIGURE 24: PEAK FLOOD-TIDE CURRENTS AT THE BYPASS CHANNEL-ICWW INTERSECTION FOR SCENARIO I.....	45
FIGURE 25: PERCENT INCREASE IN THE AVERAGE PEAK FLOOD-TIDE CURRENTS AT THE OLD RIVER CHANNEL MOUTH	46
FIGURE 26: 1 YEAR AVERAGED (RESIDUAL) FLOW AT THE OLD RIVER CHANNEL MOUTH.....	47
FIGURE 27: DIFFERENCE OF 1 YEAR AVERAGED (RESIDUAL) FLOW AT THE OLD RIVER CHANNEL MOUTH	48
FIGURE 28: PEAK VELOCITY AND AVERAGE (RESIDUAL) FLOW CHARACTERISTICS FOR PARKER’S CUT	50
FIGURE 29: PEAK VELOCITY AND AVERAGE (RESIDUAL) FLOW CHARACTERISTICS FOR SOUTHWEST CUT	50
FIGURE 30: FILTERED DISCHARGE AND WIND COMPONENT PROJECTED ALONG THE BAY AXIS, PARKER’S CUT	51
FIGURE 31: FILTERED DISCHARGE AND WIND COMPONENT PROJECTED ALONG THE BAY AXIS, SOUTHWEST CUT	51
FIGURE 32: PERCENT OF COLORADO RIVER DISCHARGE DIVERTED THROUGH THE OLD RIVER CHANNEL	52
FIGURE 33: AVERAGE SALINITY, EXISTING CONDITIONS (SCENARIO A), LOW FLOW YEAR.....	53
FIGURE 34: AVERAGE SALINITY, EXISTING CONDITIONS (SCENARIO A), MEDIUM FLOW YEAR	53
FIGURE 35: AVERAGE SALINITY, EXISTING CONDITIONS (SCENARIO A), HIGH FLOW YEAR.....	54
FIGURE 36: SNAPSHOT OF SALINITY AND CIRCULATION FOR SCENARIO A (EXISTING CONDITIONS)	55
FIGURE 37: SNAPSHOT OF SALINITY AND CIRCULATION FOR SCENARIO M (PARKER’S CUT, 5’X100’)	55

FIGURE 38: APPROXIMATE WESTWARD EXTENT OF 1 PPT SALINITY DIFFERENCE CONTOUR FOR VARIOUS CONFIGURATIONS OF PARKER'S CUT.....	56
FIGURE 39: BED ELEVATION CHANGE, LOW FLOW YEAR.....	58
FIGURE 40: BED ELEVATION CHANGE, EXISTING CONDITIONS (SCENARIO A), MEDIUM FLOW YEAR	58
FIGURE 41: BED ELEVATION CHANGE, EXISTING CONDITIONS (SCENARIO A), HIGH FLOW YEAR.....	59
FIGURE 42: SNAPSHOT OF SUSPENDED SEDIMENT CONCENTRATION FOR SCENARIO A (EXISTING CONDITIONS).....	61
FIGURE 43: SNAPSHOT OF SUSPENDED SEDIMENT CONCENTRATION FOR SCENARIO L (PK,2-4'X350', DDC,4'X20')	61

Introduction

Background and Problem Statement

The Colorado River in Texas reaches the coastline about halfway between Galveston Bay and Corpus Christi Bay (See Figure 1). Historically, the Colorado River discharged directly into Matagorda Bay. However, since 1935 the formation of a delta near the mouth of the Colorado River has separated Matagorda Bay into East and West Matagorda Bay. This delta was created by sediment released due to the demolition of a logjam on the river in 1929. (USACE 1992). Figure 2 depicts the progression of the delta formation. The river eventually discharged directly into the Gulf of Mexico, effectively bypassing Matagorda Bay.

The Gulf Intra-Coastal Waterway (GIWW) intersects the Colorado River near the town of Matagorda, approximately 6.5 miles upstream of its mouth. The GIWW is typically 125 feet wide and 12 feet deep. The Colorado River exchanges some water flow between East and West Matagorda Bay through the GIWW locks, located in the GIWW main channel to each side of the river. The locks are 1,200 feet long and 75 feet wide each (See Figure 4 for location). Their purpose is to control flow and sedimentation, thereby improving navigation across the intersection between the GIWW and the Colorado River. Also, before 1992, Parker's Cut (formerly Tiger Island Channel, located two miles upstream of the river mouth), was open, and permitted some additional exchange of river flow with West Matagorda Bay.

In the late 1970s, various interests expressed a need for additional freshwater inflow into Matagorda Bay. Increased freshwater discharges, as proposed, would enhance seafood productivity of the bay, reduce flood damage potential along the lower Colorado River, and reduce navigation hazards as well as channel maintenance costs (USACE 1981). Consequently, in 1992, the Colorado River was diverted into West Matagorda Bay through a diversion channel, and Parker's Cut was closed. This diversion was accomplished by placing a dam on the existing river channel at a point south of the river's intersection with the GIWW. To bypass the diversion dam, the navigation channel was relocated east of the eastern GIWW lock, before reaching the GIWW/Colorado River intersection. Figure 3 contains all of these features. Parker's Cut was closed because of concerns about losing freshwater through the cut towards the Gulf of Mexico, thereby canceling the potential benefits expected.

Since the river was diverted, a substantial increase in currents at the intersection of the GIWW with the Colorado River has been observed. These currents have adversely affected navigation in various ways. For instance, the barging industry has had to change some of its practices to enable barges to cross the intersection. Typically, tows comprise two to three barges (sometimes up to four), varying in length from 400 to 900 feet. Push boats are usually 70 feet in length (McCollum

2000). Tripping, or the practice of towing only one barge at a time, has become a necessity when currents reach 3 ft/s. Restrictions under these flow conditions specify that only two empty barges or one loaded barge can cross at a time. Exceptions are only made if a bow thruster or a helper boat is available. Otherwise, there is a substantial risk to property damage because of barges colliding with the lock approaches, not to mention the safety hazard to people working the barges. If current velocities exceed 5 ft/s, lock operations have to be shut down altogether at a considerable cost to industry. Appendix A contains some pictures depicting a typical approach to the locks and examples of the damage encountered in the vicinity of the locks.

In addition, tow pilots have historically used Southwest Corner (Figure 4) at the intersection as a pivot point to maneuver the tows when deflected by strong cross-currents. This area has eroded significantly since the modifications to the system were completed and no longer serves as an aid to navigation. It has become increasingly difficult to navigate across the intersection, especially when traveling in a westerly direction. The bypass channel also presents problems when strong tidal currents are present, making it difficult to travel past its opening.

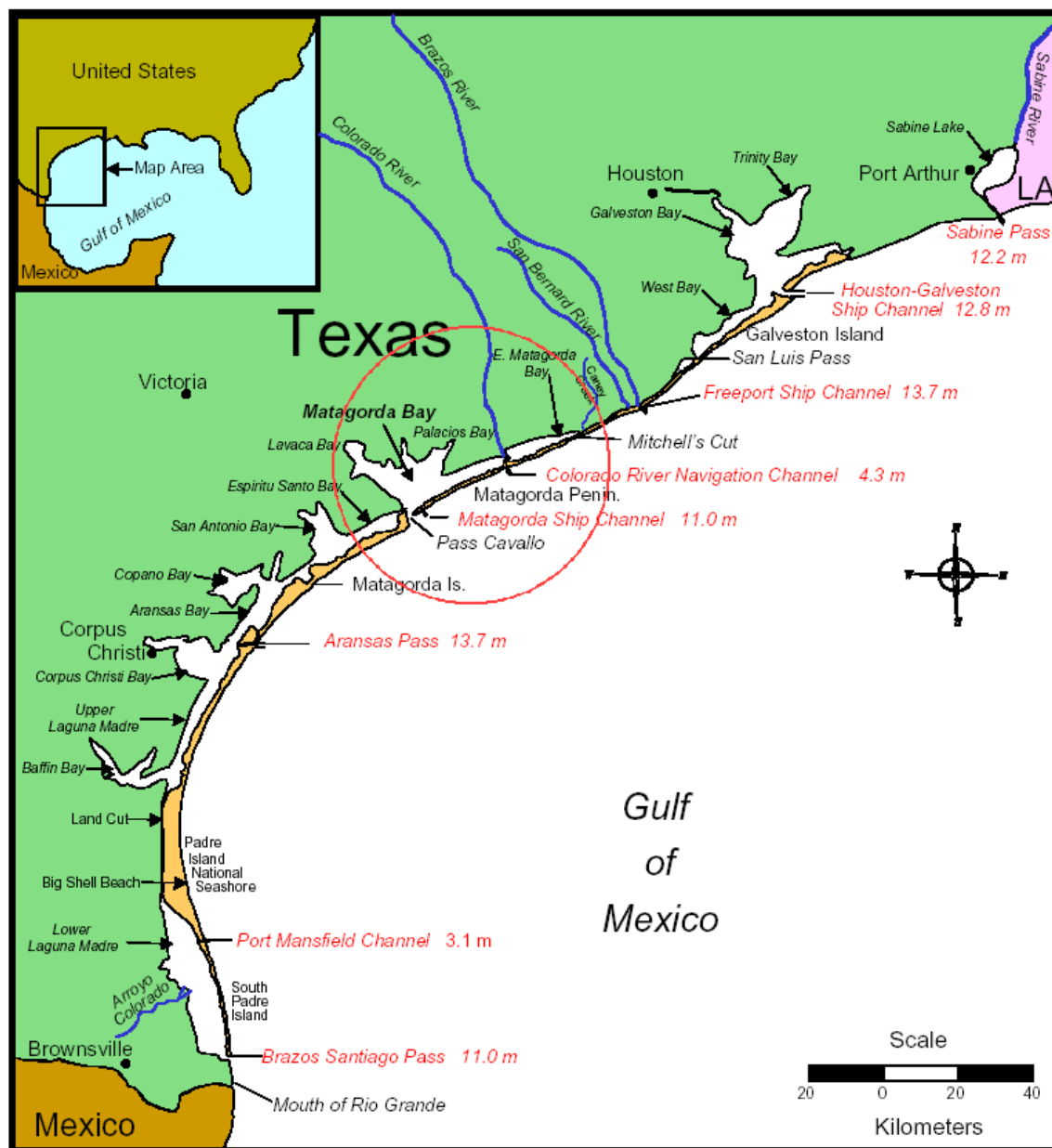


Figure 1. Matagorda Bay Location Map (Adapted from Kraus, Mark, & Sarruff 1999)

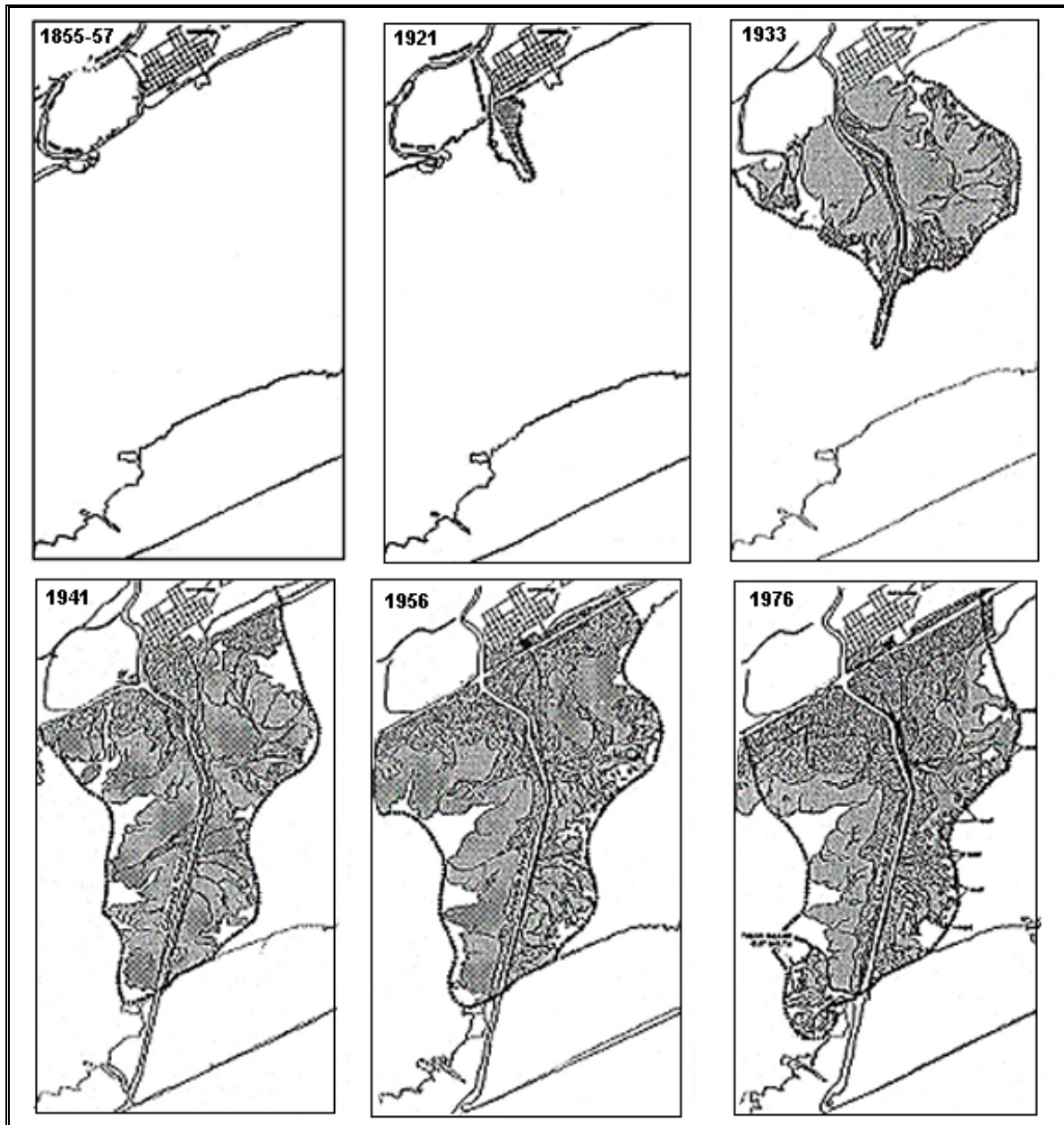


Figure 2. Development of Colorado River Delta from 1855 to 1976 (Adapted from USGS, Tobin and Kargl)

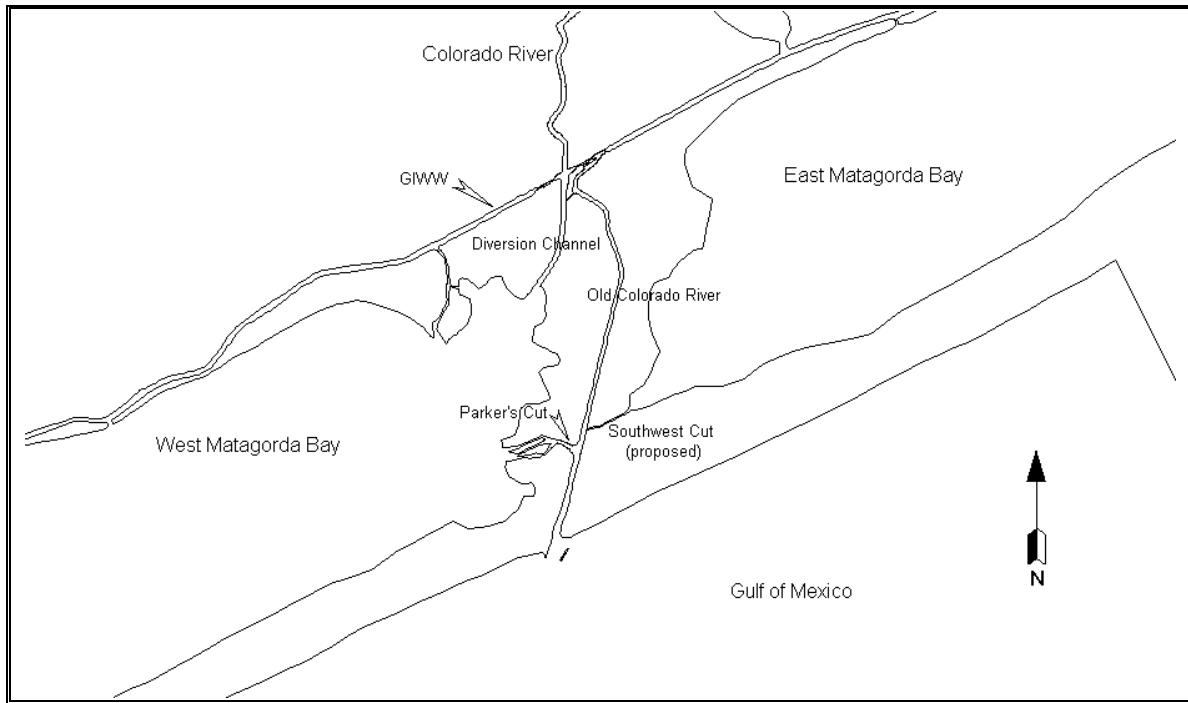


Figure 3. Study area features

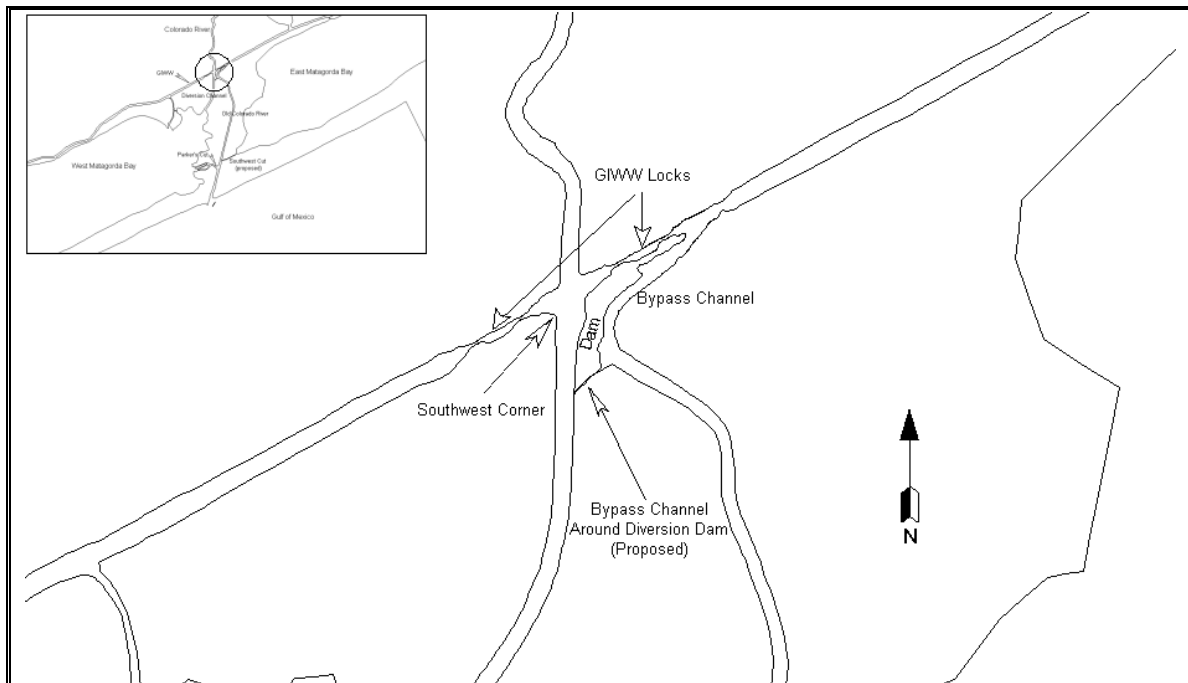


Figure 4. Details of intersection between the Colorado River and the Gulf Inter-Coastal Waterway

Objective and Approach

This report details the development of a numerical model study of hydrodynamics, including currents, salinity, and sediment changes, associated with the different alternatives proposed to alleviate the navigation problems encountered in the intersection of the GIWW and the Colorado River. Specifically, potential impacts on salinity in Matagorda Bay and sedimentation in the area derived from any of the options considered are emphasized, thereby assisting the Galveston District in making sound environmental determinations.

The tasks performed and described by this report are:

- a. Field data collection, data reduction, and laboratory analysis to set up and validate the numerical model,
- b. Development of a two-dimensional numerical model grid and study,
- c. Validation of the model for hydrodynamics, salinity, and sediment, using both historic and field data gathered for this undertaking,
- d. Evaluation of all plan conditions proposed (as detailed in Table 1), and
- e. Comparison and analysis of results.

Table 1. Description of Studied Scenarios

Scenario	Description
Sa	Existing conditions
Sb	Parker's Cut (4ft by 20 ft)
Sc	Parker's Cut (7ft by 50 ft)
Sd	Bypass channel around diversion dam (4ft by 20 ft)
Sg	Southwest Cut (5 ft by 100 ft)
Sh	Southwest Cut (5 ft by 100 ft) with Parker's Cut (4ft by 20 ft)
Si	Southwest Cut (5 ft by 100 ft) with stable sized Parker's Cut (estimated at 2-4 ft x 350 ft)
Sj	Southwest Cut (5 ft by 100 ft) with Bypass channel around diversion dam (4 ft x 20 ft)
Sk	Parker's Cut (4 ft x 20 ft) with Bypass channel around diversion dam (4 ft x 20 ft)
Sl	Stable sized Parker's Cut (estimated at 2-4 ft x 350 ft) with Bypass channel around diversion dam (4 ft x 20 ft)
Sm	Parker's Cut (5 ft by 100 ft)
Sn	Southwest Cut (5 ft by 200 ft)

The number of scenarios and their different combinations attempt to cover the several possibilities available to alleviate navigation currents at the GIWW/Colorado River intersection. As shown in Table 1, Parker's Cut and Southwest Cut were analyzed at various dimensions to evaluate whether the cut's size would effect a reduction in current velocities. Also, analyzing combinations of these options allows for a clear determination of which alternative produces greater benefits.

Numerical Model Description

The TABS-MDS code of ERDC-WES is used for computing hydrodynamics, plus salinity and sediment transport. The model was originally developed as RMA10 by Resource Management Associates (King 1993) and extensively modified by ERDC-WES staff into its present configuration. In agreement with the original author, the ERDC version of the code was given the name TABS-MDS to distinguish it from RMA10. It is a finite element model, which gives it great flexibility in matching complex geometry. Through the solution of equations of conservation of mass and horizontal momentum, as well as the convective-diffusion equation for transport of salinity and heat, the code accounts for forcing due to tides, freshwater inflows, wind, Coriolis effects (where applicable), and density gradients due to salinity and temperature. It also considers evaporation and precipitation to complete an accurate description of the system under study. The sediment transport model was written at ERDC-WES by Teeter (2001). It consists of a multi-grain sized, fine-grain sediment transport algorithm. It incorporates transport, erosion, deposition, and bed consolidation. The model includes the capability to model the wind-wave re-suspension of sediment. It also has a dynamic bathymetry option, for coupling the influence of bed elevation changes to the flow field. For further discussion of TABS-MDS, see Appendix B.

ERDC-WES personnel have used the code extensively over the last decade in a variety of field investigations with excellent results. Its proven effectiveness makes it well suited for this application.

Field Data Collection and Analysis

A numerical hydrodynamic and transport model requires adequate field data to force (run) and validate it. For this study, the Hydraulic Analysis Group of CHL performed an intensive data collection effort to gather information on existing bathymetry, tidal and river currents, water levels, and salinity and sediment concentration changes in the area of interest. Data were collected in three ways:

1. Six-month data collection on water levels and salinity changes at 12 locations throughout the GIWW, old Colorado River, and East and West Matagorda Bay, (See Figure 5 for locations)
2. Intensive 25-hour velocity data and water sampling data collection (Figure 6) through Acoustic Doppler Current Profiling (ADCP), and
3. Bathymetric survey of immediate study area (Figure 7).

The data collection program started in May 2001 with the installation of all the instruments and ended in October of the same year, when instruments were retrieved. During that period, instruments were serviced on a monthly basis. At those times, instruments were cleaned and

recalibrated, and data were retrieved.

The extent of field data collection has been described in detail previously on the Memorandum for Record “Field Data Collection at the Colorado River and Gulf Inter-coastal Waterway, Matagorda, TX” dated January 2002. The memorandum is being reproduced in its entirety and published as Volume 2 of this report.

In addition, the modeling team supplemented this information with freshwater inflow data from United States Geological Survey (USGS) stations and water level data at Texas Coastal Observation Network (TCOON) stations outside the immediate study area (See Figure 9).

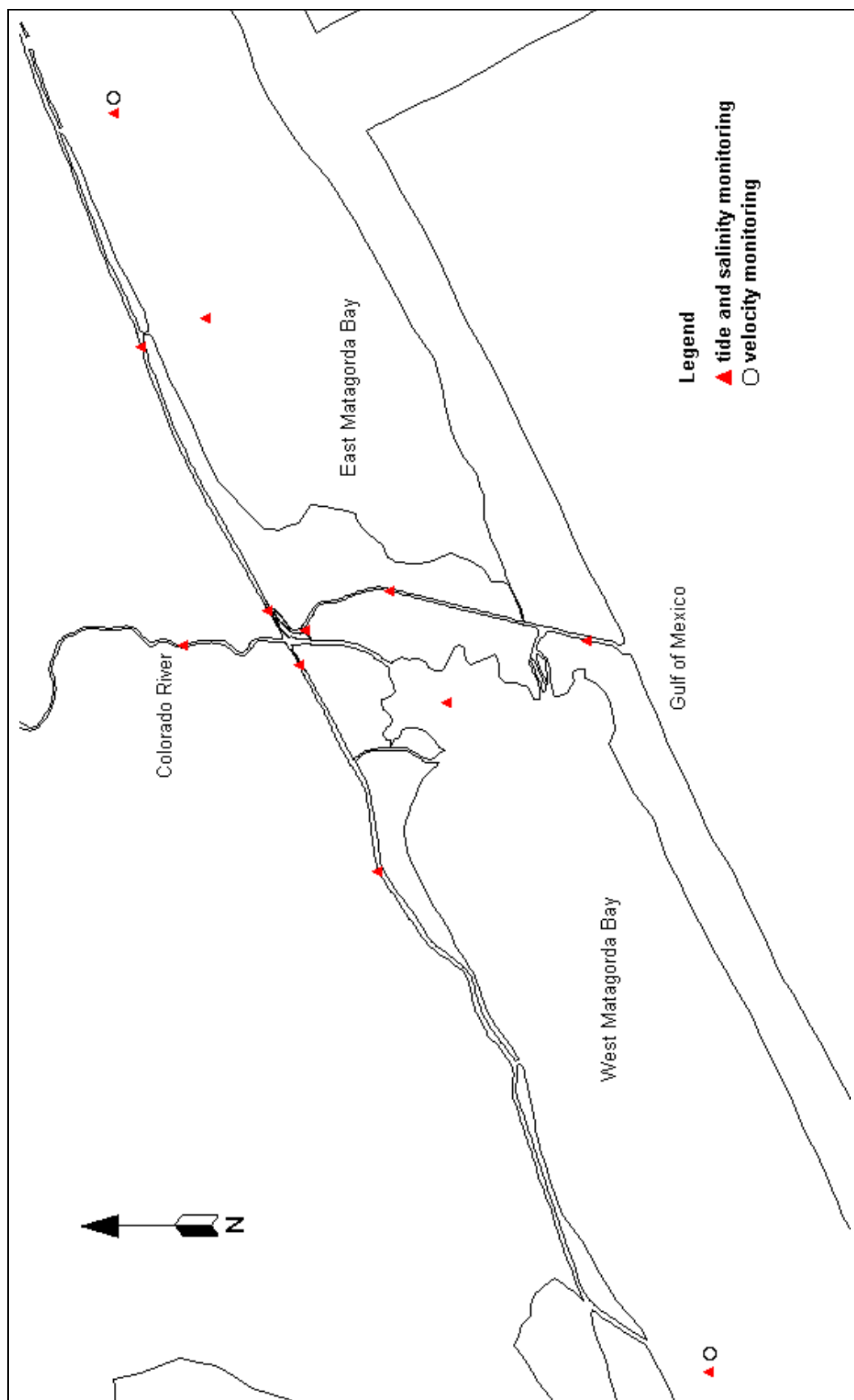


Figure 5. WES data collection stations

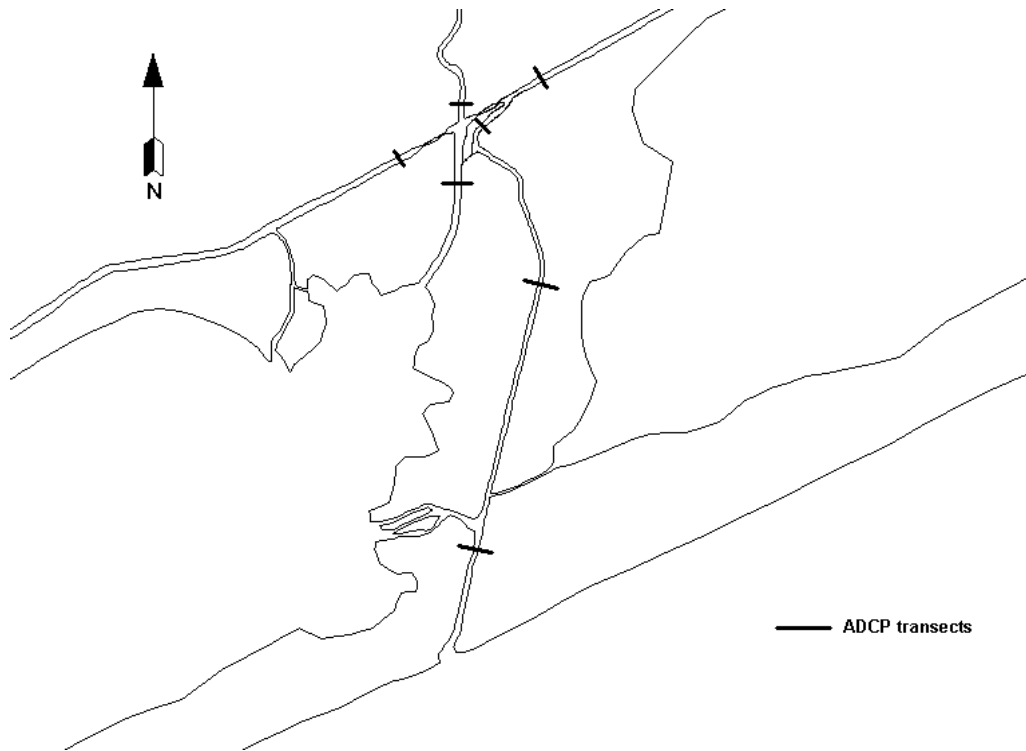


Figure 6. Location of WES ADCP transects

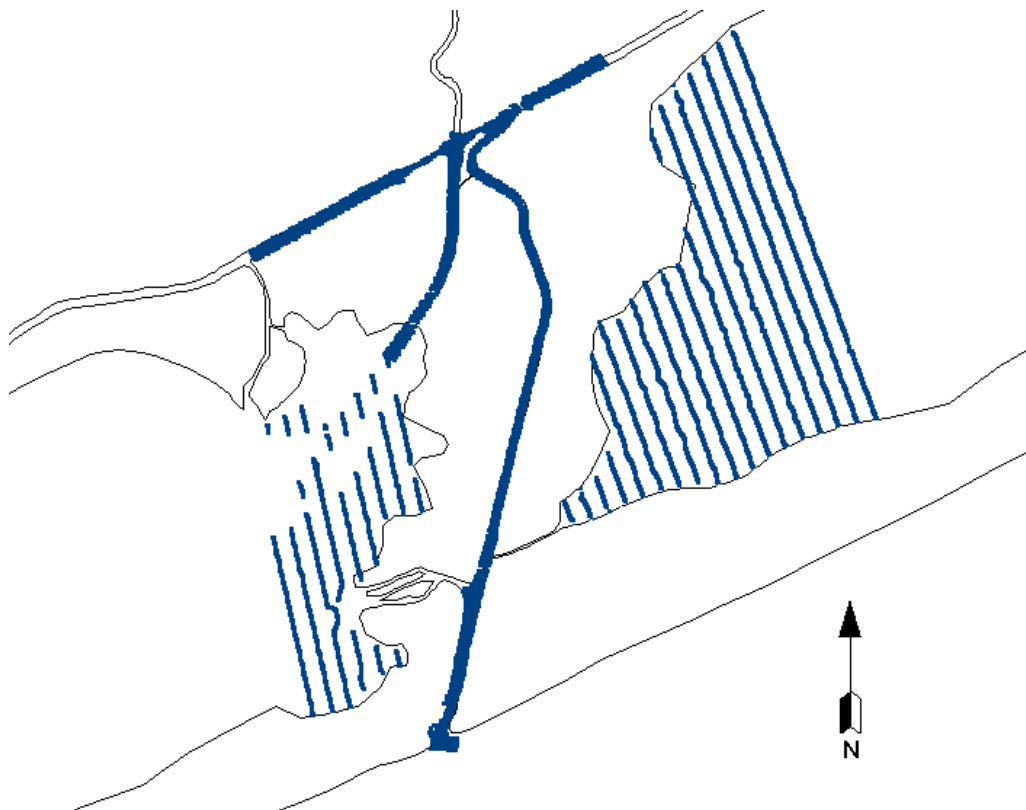


Figure 7. Area of WES bathymetric survey

Hydrodynamic, Salinity, and Sediment Models

Computational Mesh

The TABS-MDS code uses a computational mesh, or grid, as a mathematical representation of the physical environment under study. A mesh typically includes information on the extent and depth of the area involved. The area of interest for the purposes of this study is limited to the mouth of the Colorado River up to the intersection with the GIWW and immediate surroundings, yet the grid actually encompasses all of East and West Matagorda Bay, along with the adjacent GIWW and the Colorado River all the way up to Bay City, Texas (Figure 8). Part of the Gulf of Mexico and cuts feeding water into the system, such as Pass Cavallo, the Colorado River itself, and Mitchell's Cut, are included as well. Extending the mesh to these larger areas ensures that near-field effects imposed by the boundary conditions of the model will not adversely affect the area of interest. The same mesh was used for hydrodynamics, salinity, and sediment calculations.

For the sake of computational efficiency, the grid is more highly resolved in the areas of interest to this study than it is elsewhere. This practice reduces the need for extensive computational time, while still maintaining an accurate description of the entire region. By practical standards, the mesh is average in size, with 10,351 elements and 32,955 nodes.

The necessary bathymetry was taken from a variety of sources. Initially, the mesh was outlined using National Oceanic and Atmospheric Administration (NOAA) charts of the region. To supplement the charts, USGS QUAD maps provided bathymetry for the Colorado River up to Bay City. Aerial pictures aided in determining the proper configuration for Mitchell's Cut, which historically has changed faster than maps of the area have been updated. The survey described in the field data section of this report provided detailed water surface elevations in the area of interest. Elsewhere, depths were taken from an Advanced Circulation (ADCIRC) model grid developed by Kraus (2002).

East and West Matagorda Bay are fairly shallow, with depths of 2 to 3 feet adjacent to the study area. The Gulf Intra-Coastal Waterway and the Old Colorado River channel are, of course, much deeper (about 12 and 15 feet respectively), while the intersection of the GIWW and the Colorado River shows the largest depths in the area, reaching around 20 feet at certain locations.

To adequately characterize bottom features, the numerical grid is also divided into sections, or material types, so that different parameters can be applied to various areas of the model, according to their specific properties.

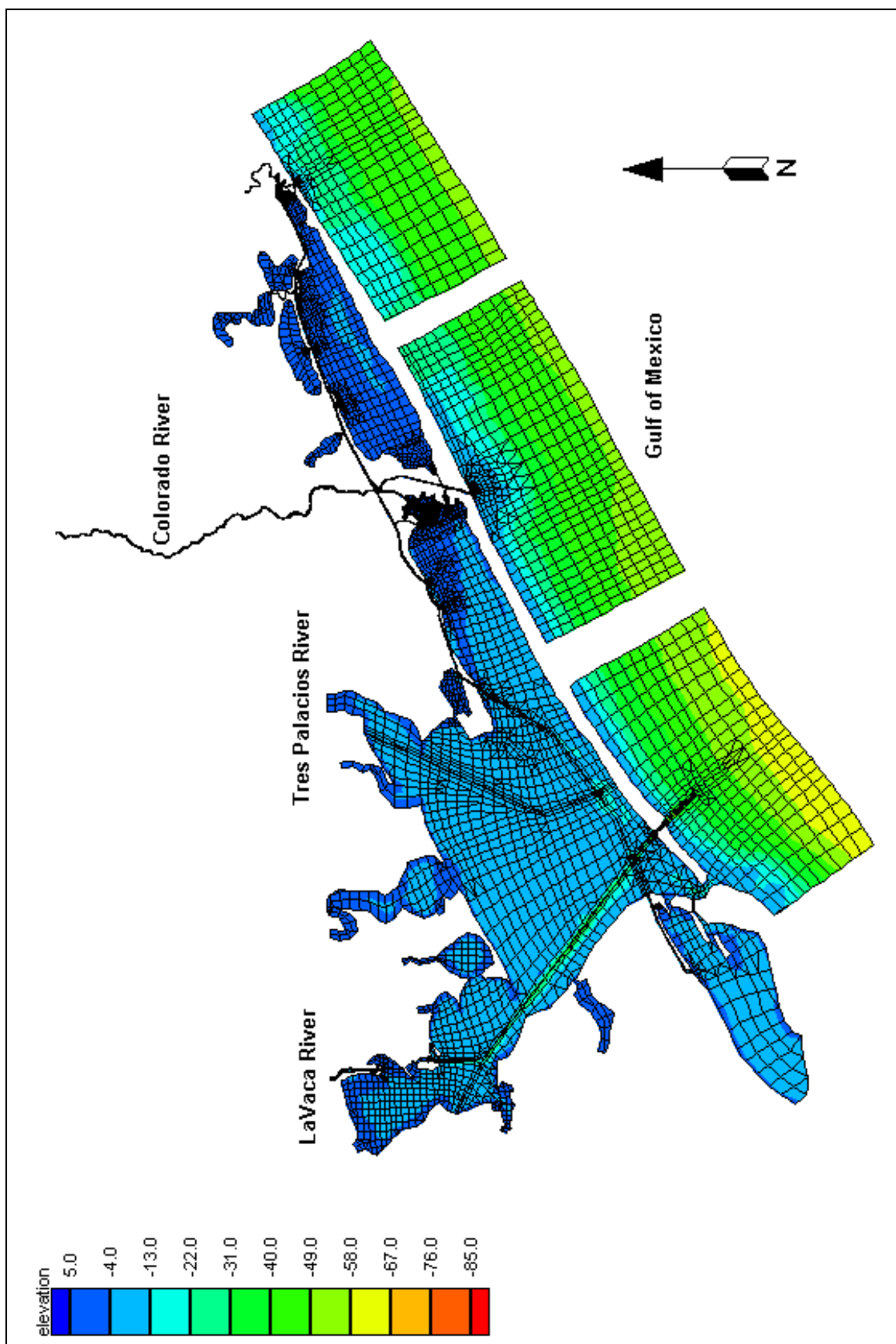


Figure 8. Computational mesh and bathymetry of study area

Boundary Conditions

a. Hydrodynamic and Salinity Model Boundary Conditions

Texas A&M University (TAMU), USGS, and TCOON stations furnished the data used to force the model. As described in Figure 9, there are four major types of data applied: tides, wind, flows, and evaporation and precipitation. Data was downloaded for the period May through October of 2001, complementing the field data collected by WES, and used during calibration and verification of the model. For scenario runs, a whole year (2001) was simulated, once the model was verified against field data, to evaluate the different options presented.

The Rawlings Bait Camp TCOON station, adjusted to reflect the distance between the boundary and the actual station, provided the ocean boundary tides. Table 2 describes the adjustment factors applied to the three tide stations. Port O'Connor (TCOON), Mitchell's Cut (USGS), and Rawlings Bait Camp tide stations were then used to check the accuracy of the adjusted signal (See Figures 10, 11, and 12).

Table 2. Tidal boundary condition adjustment factors

Location	Vertical datum shift (ft)	Phase shift (hrs)	Tidal amplitude multiplication factor
Port O' Connor	-.031	-.25	1.125
Rawlings Bait camp	-.01	-.25	1.25
Mitchell's Cut	-.085	-.25	1.5

Given the importance of wind effects on a shallow system such as Matagorda Bay, the East Matagorda Bay and Port O'Connor wind stations, as well as WES wind data, were used to complete the wind field affecting the region. Specifically, the East Matagorda Bay wind gage (TCOON) provided wind data for East Matagorda Bay and the eastern part of West Matagorda Bay. The WES wind gage covered the vicinity of the Colorado River locks, while the Port O'Connor wind gage (TCOON) covered the western part of West Matagorda Bay. See Figures 13, 14, and 15 for the magnitude and prevalent wind direction applied during calibration and verification. Evidently, wind predominates from the east and southeast, with some incidence of winds from the northeast.

In terms of flow, the most relevant freshwater inflow to the system was that of the Colorado River itself because of its proximity to the study area. To avoid near-field effects from this freshwater inflow, the bathymetry was extended north to Bay City, where a USGS flow station is located. During its trajectory towards Matagorda Bay, the river encounters an intake from the South Texas Nuclear Project, which has been subtracted from the total flow. This intake is small in relation to total river flow, yet not insignificant, since it can be as much as 600 cubic feet/second (cfs) when the river is at high flow. USGS LaVaca River and Tres Palacios River flows were also applied into West Matagorda Bay. Figure 16 shows the hydrograph for all three rivers.

Rainfall and evaporation data were collected from NOAA's gage at Matagorda and TAMU's Jackson TX stations, respectively. Figure 17 shows the net cumulative rainfall experienced over the study area.

To account for ungaged flows into the system, Texas Water Development Board (TWDB) estimates for the Big Boggy Creek watershed (north of East Matagorda Bay) were applied at Lake Austin, where it connects to the GIWW. Raw data from TWDB were attenuated with a generic synthetic hydrograph to simulate the reduction of the peak flow as it passes through the basin. The total ungaged inflow volume, however, was conserved in the flow attenuation process. Both the original and attenuated hydrographs are depicted in Figure 18.

The salinity at the ocean boundaries was taken from the 30-year, monthly averaged salinity, measured offshore at Galveston, TX (Cochrane and Kelly, 1986).

Once the model was calibrated and verified, the scope of this study called for modeling three different flow regimes for all scenarios to test the sensitivity of the system to various conditions. These scenarios were to be run for a full year. Low, medium, and high flow years for the Colorado River were chosen to simulate extreme events, as well as prevalent circumstances. These years were 1996, 1997, and 1998, respectively. Figure 19 shows the hydrograph for these years at the Bay City USGS station on the Colorado River. Even though 1997 presented a higher volume of water for the year, 1998 contained an extreme high flow event, which allowed for the assessment of the system's sensitivity to such an episode. The corresponding flows for the Tres Palacios and LaVaca Rivers were also applied in the model.

Throughout all of the modeling tasks, the locking operations at the Colorado River locks were considered. A locking schedule was implemented such that the frequency of lock operations increased as the Colorado River velocity increased. The specific locking protocols are described in Table 3 below.

Table 3. Locking protocol applied to model runs

River velocity (ft/sec)	Locking Protocol
0 – 1.5	Locks are OPEN.
1.5 – 4.5	Locks are OPERATING, but not LOCKING. That is, the when the gates are open, flow can pass freely through the locks. An exception is made on weekends. From 8:00 AM to 6:00 PM on Saturdays and Sundays, the locks are OPEN.
4.5 - 6	Locks are LOCKING. That is, when one gate in a lock is open, the other gate remains closed, so water does not flow freely through the locks.
>6	Locks are CLOSED.

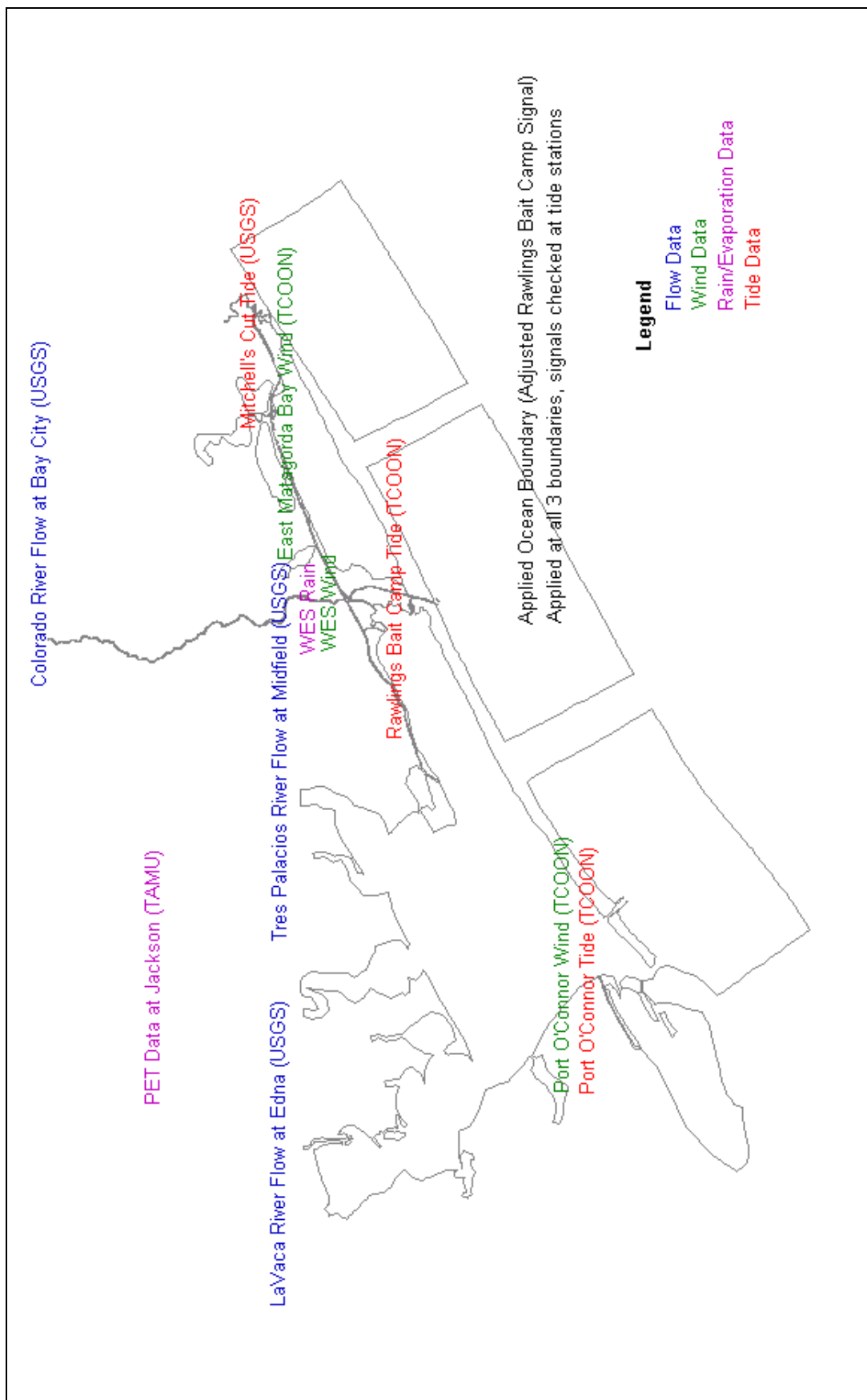


Figure 9. Location of boundary condition stations

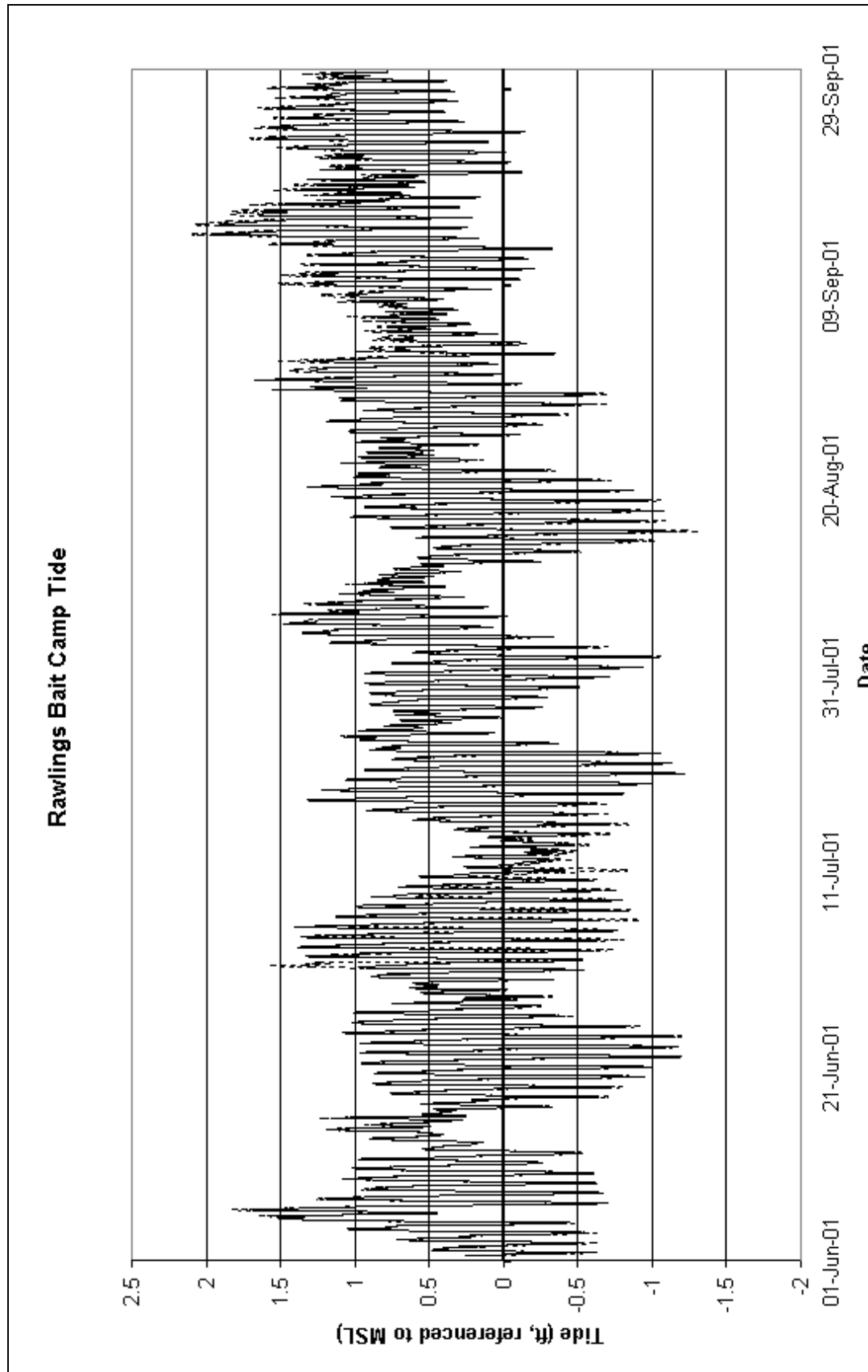


Figure 10. Rawlings Bait Camp tide station signal

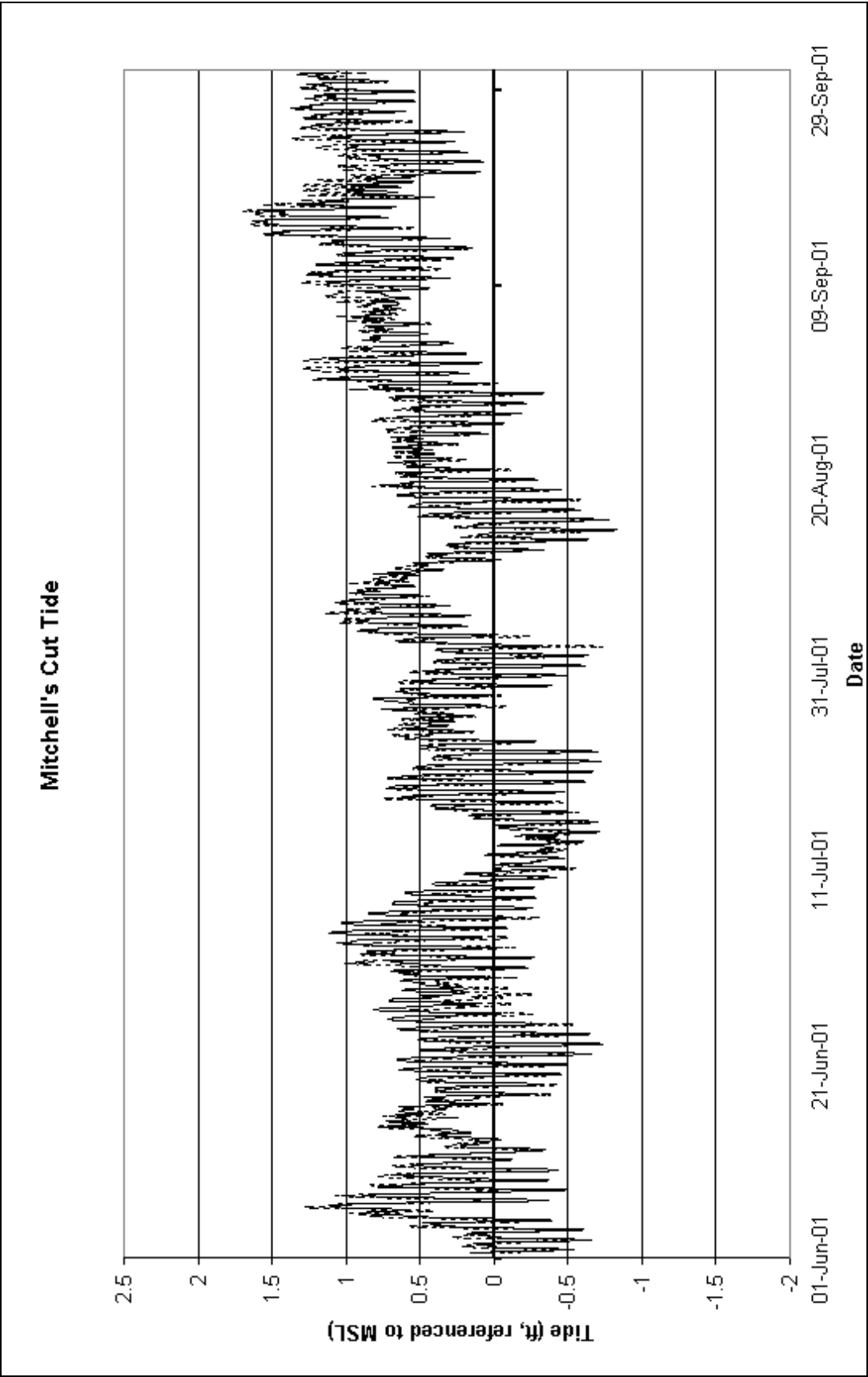


Figure 11. Mitchell's Cut tide station signal

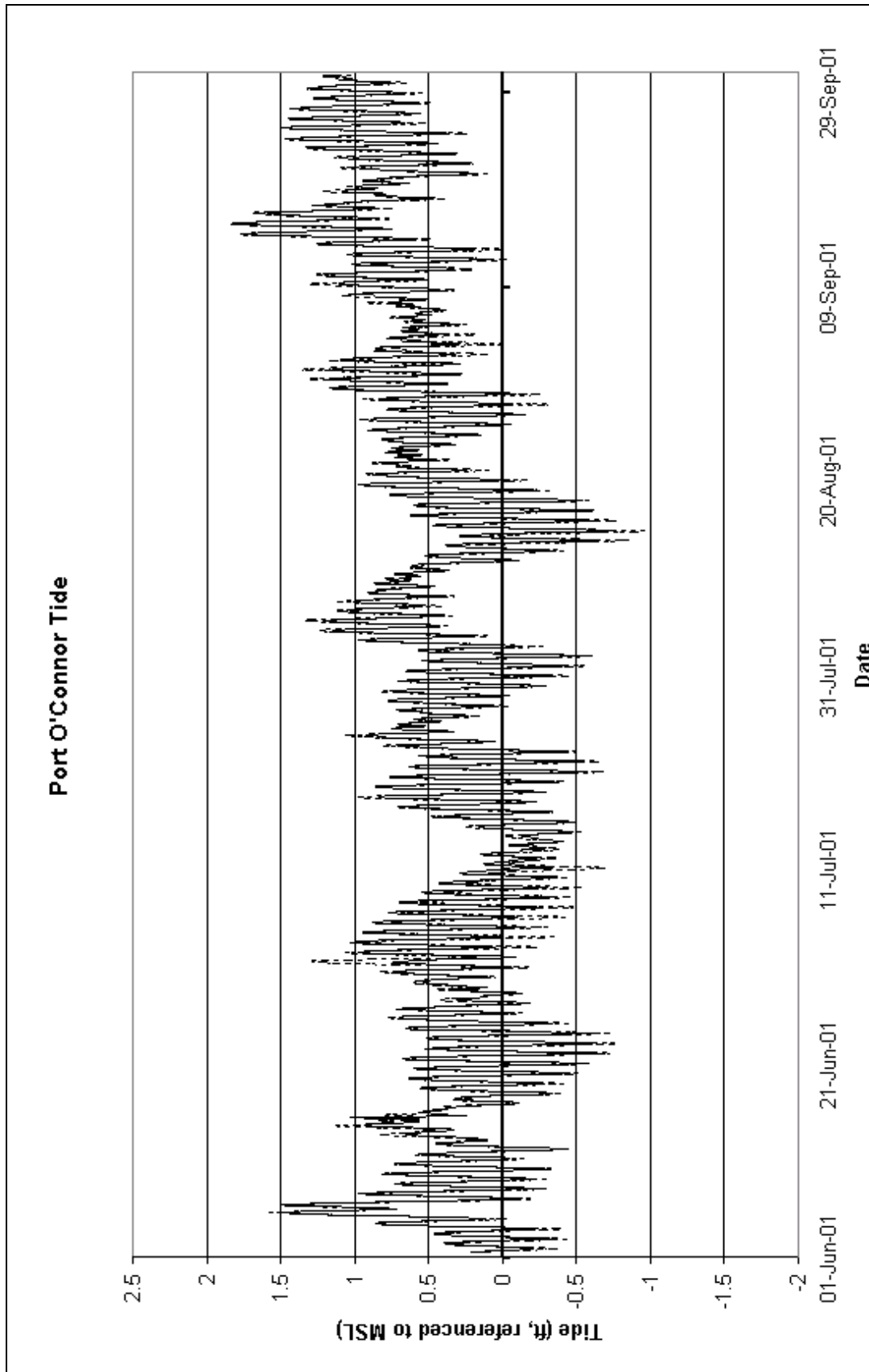


Figure 12. Port O'Connor tide station signal

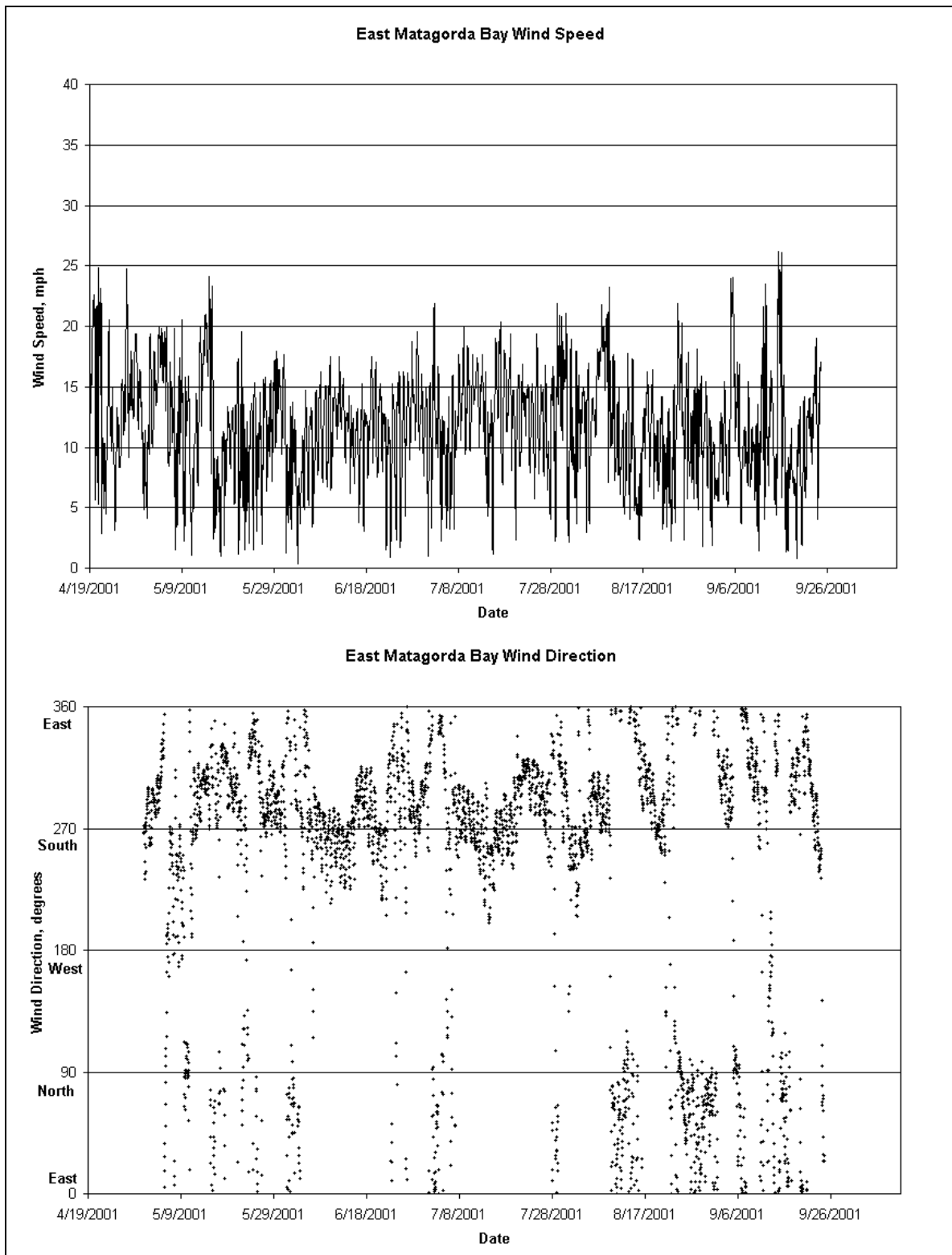


Figure 13. East Matagorda Bay station (TCOON) wind speed and direction

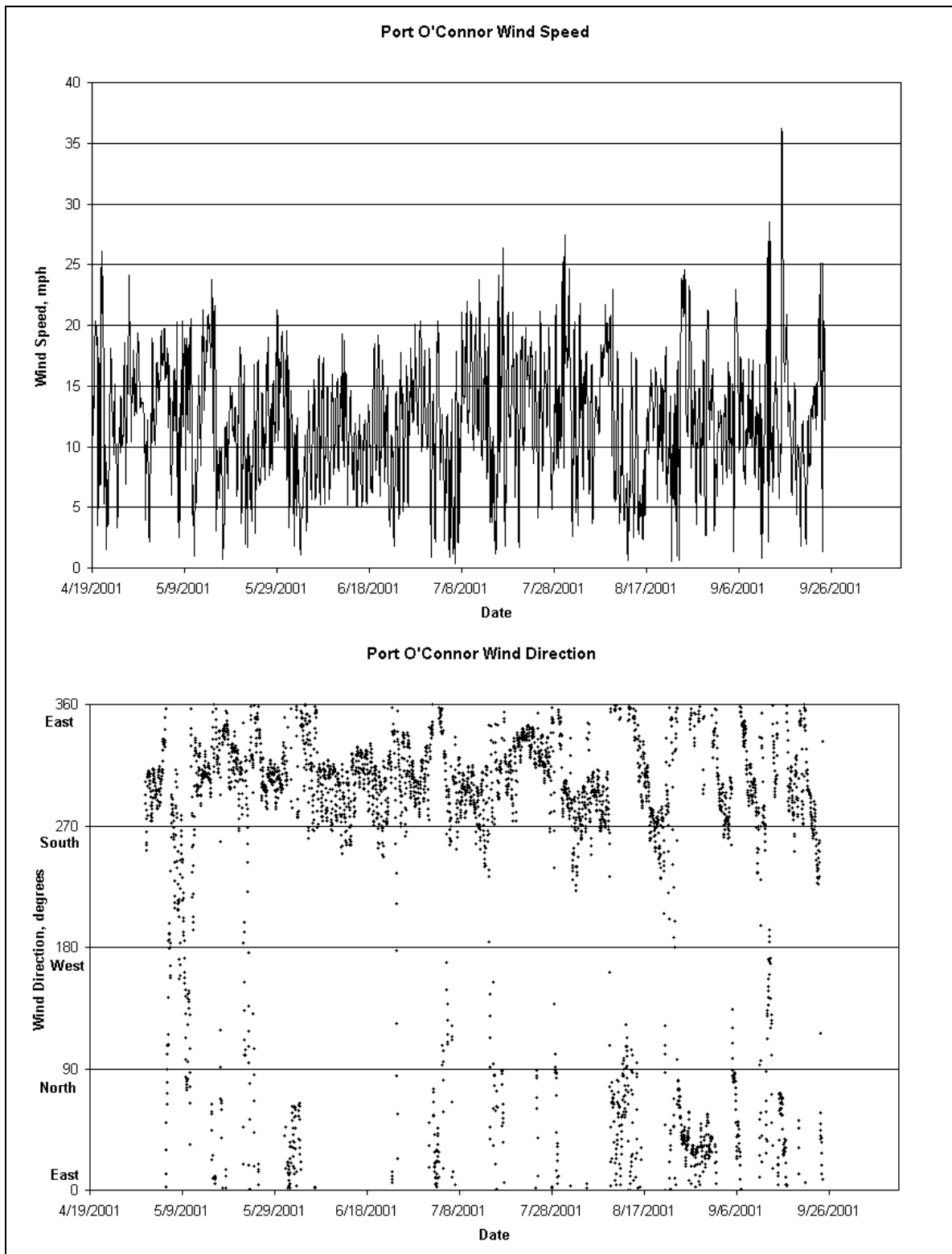


Figure 14. Port O'Connor station (TCOON) wind speed and direction

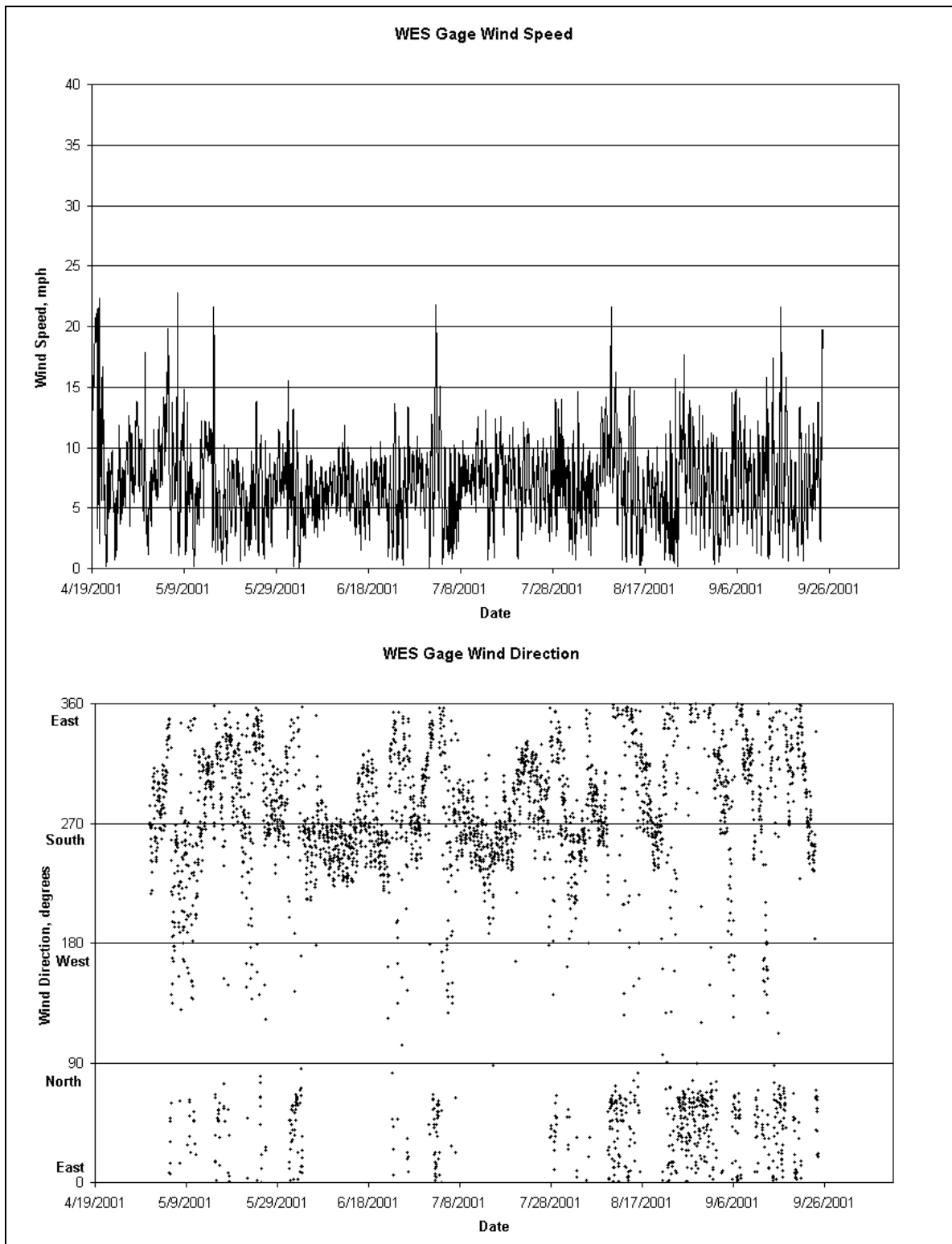


Figure 15. WES station wind speed and direction

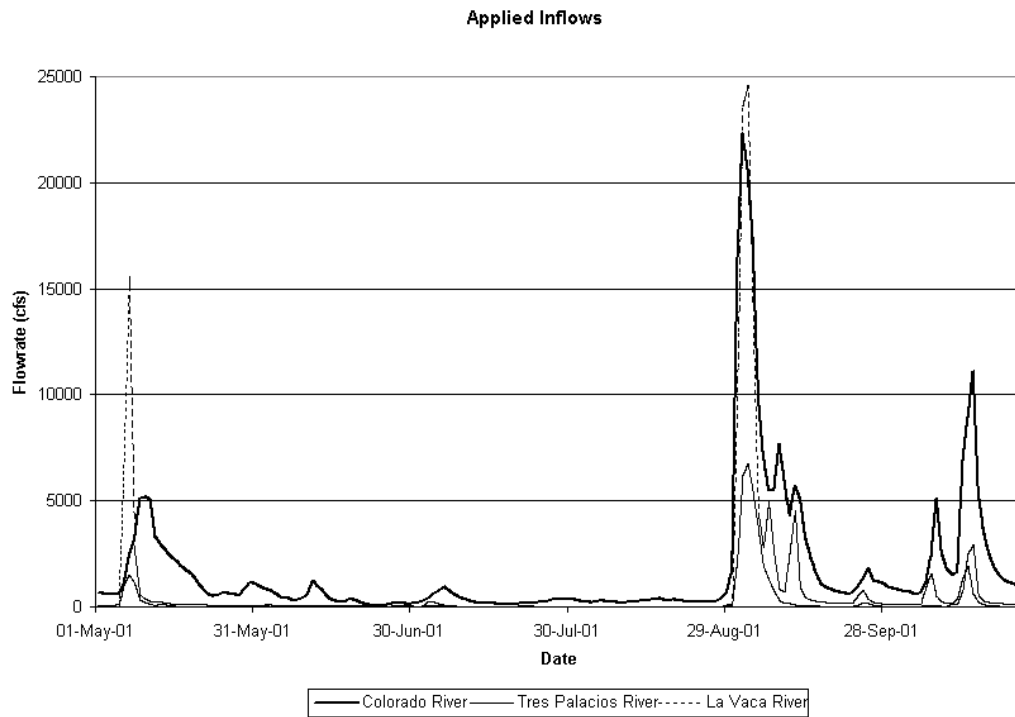


Figure 16. Discharge hydrograph for the Colorado, Tres Palacios, and LaVaca Rivers

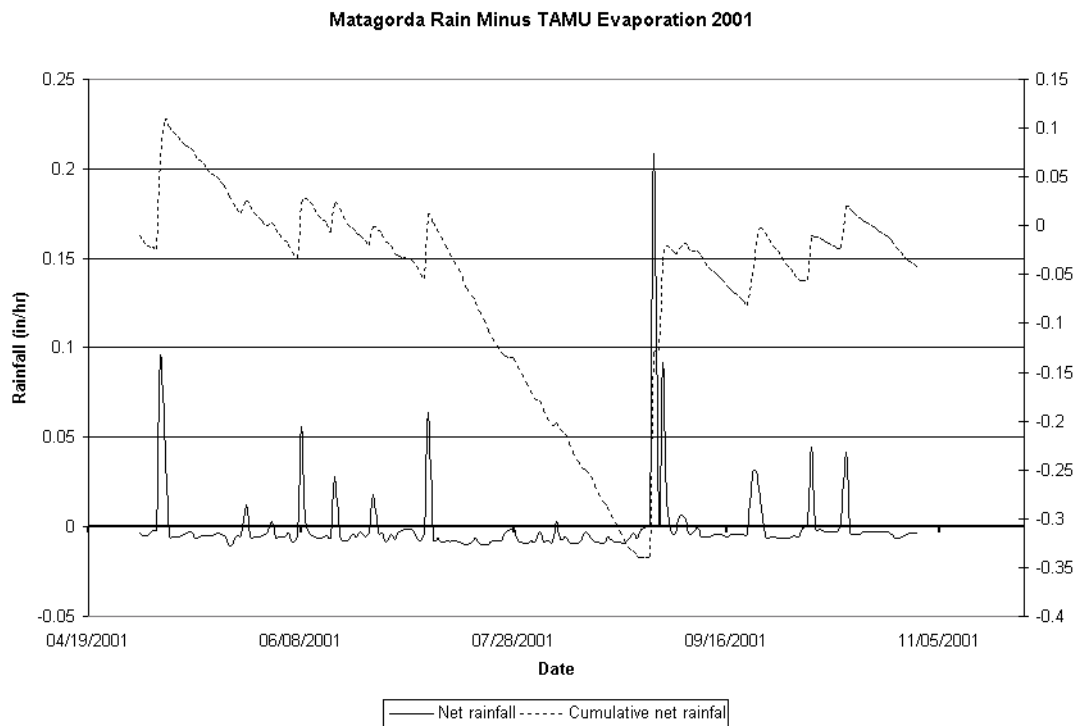


Figure 17. Applied precipitation and evaporation parameters

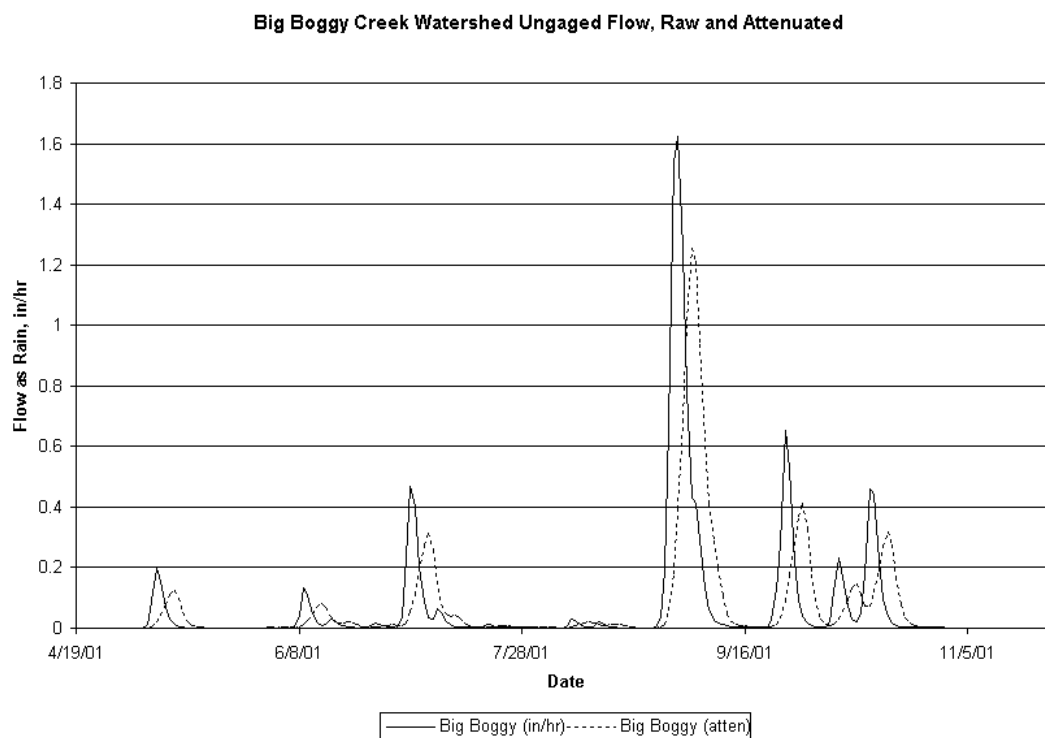


Figure 18. Raw and attenuated Big Boggy Creek ungaged flow

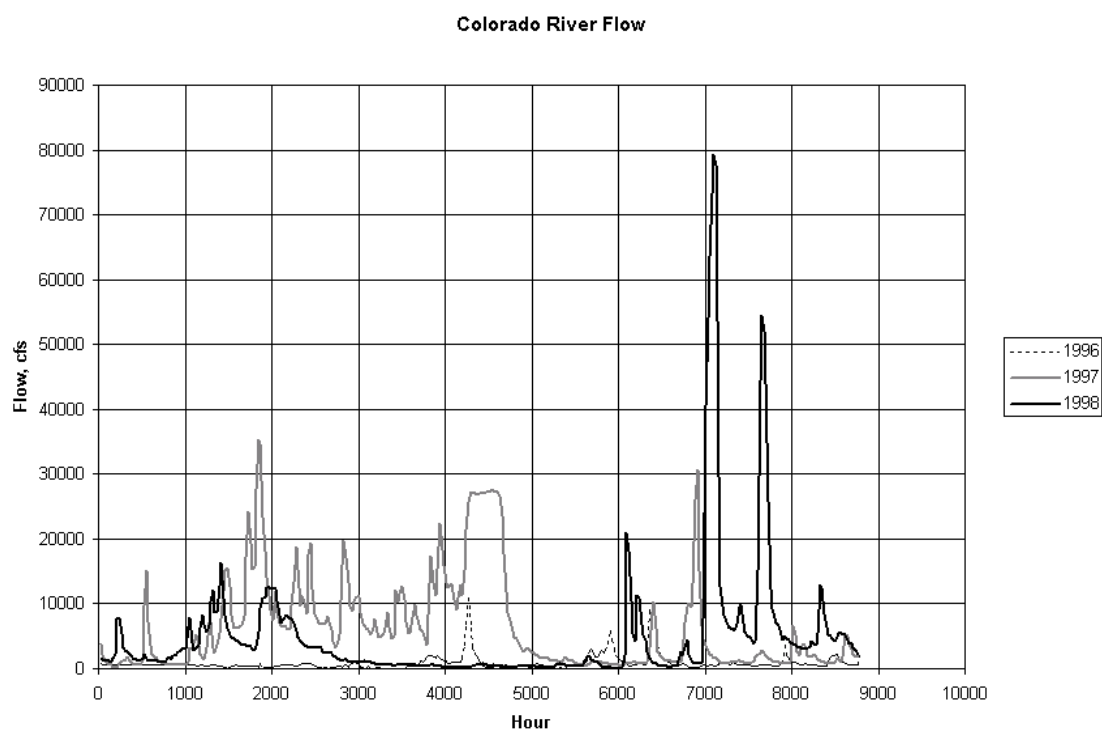


Figure 19. Sample low, medium, and high flow years for the Colorado River (measured at Bay City, TX)

b. Sediment Boundary Conditions

The sediment model was run with 4 different grain classes: 1 clay, 2 silts, and one fine sand. The settling, erosion, deposition, and consolidation properties of each grain class are interdependent in the model. The specific coefficients used to describe each class were taken from values used in a sediment model study of Laguna Madre, Texas (Teeter, et al, 2002). The initial conditions used to describe the physical characteristics of the Bay bottom were taken from the Mouth of Colorado River Texas General Design Memorandum and Environmental Impact Statement (Corps of Engineers, 1981).

In order to model the fate of Colorado River sediment, it was necessary to develop a sediment-rating curve for the Colorado River. Two rating curves were developed: one for total sediment load (clay, silts, and sand), and one for silt and clay only. The sand transport was then found by subtracting the silt and clay transport from the total transport. Finally, the remaining partition of the fines into their respective classes was approximated by a simple lognormal distribution.

The rating curves were derived from data found in (Corps of Engineers, 1981), and also from sediment rating curves developed by the USGS at Wharton, Texas. The equations for the rating curves are as follows:

$$\text{Total Load} = e^{1.99658 * \ln(\text{Colorado River Flow}) - 8.80086} \dots\dots\dots (1)$$

$$\text{Silts and Clay Load} = e^{1.93701 * \ln(\text{Colorado River Flow}) - 8.62843} \dots\dots\dots (2)$$

Where the sediment load is expressed in Tons per Day, and the flow is expressed in cfs. The 4 resulting rating curves are given in Figure 20. Figure 21 shows the inflowing sediment concentration for each of the flow conditions applied to the Colorado River at Bay City.

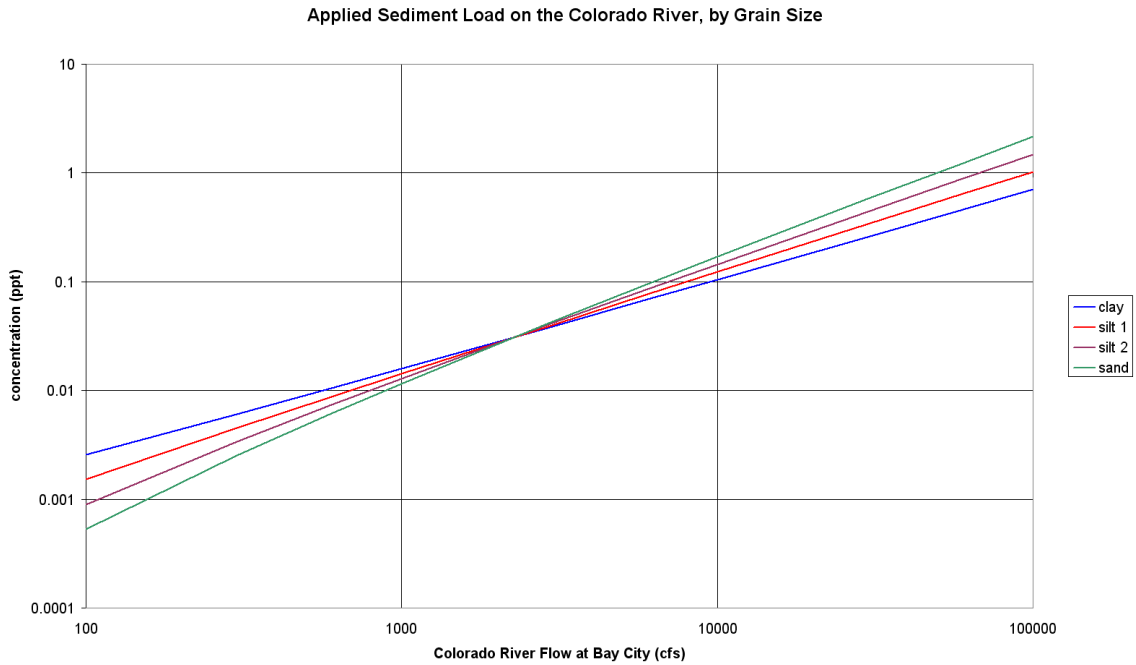


Figure 20: Applied Sediment Load on the Colorado River, by Grain Size

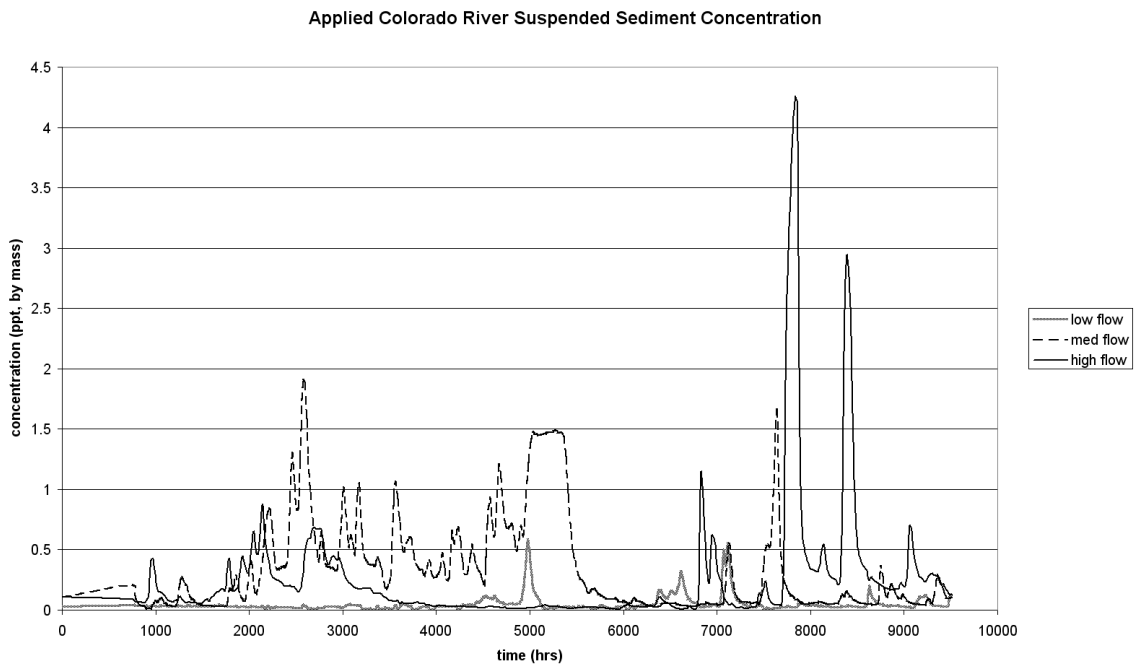


Figure 21: Applied Colorado River Suspended Sediment Concentration

Calibration and Verification

The numerical model was calibrated and verified against the field data collected from May – October of 2001. The results of this effort are covered in this chapter. The specific data and procedures used for both calibration and verification are detailed, and the impact of uncertainties in the applied boundary conditions are analyzed with respect to their influence on the model verification.

Note that the model was calibrated and verified for hydrodynamics and salinity only. The sediment transport model was not calibrated or verified against field data. Hence, the sediment model results should be regarded as qualitative only, useful for predicting the occurrence of changes in erosion and/or deposition in the system, but not useful for predicting the actual amount of those changes.

Model Calibration

The model was calibrated against the 12 water surface elevation stations. The calibration period was chosen from May 15th through July 15th 2001. The model was calibrated by making adjustments to the friction coefficient (Manning's n). Since the model relies on the Smagorinsky (1963) approximation for both horizontal turbulence closure and for horizontal salt diffusivity, these values were not adjusted as a calibration parameter. The Smagorinsky parameter was adjusted at specific locations within the domain, but this was done to provide numerical stability rather than to calibrate the model.

The discharge measurements and salinity measurements were not used for calibration per se. However, they were periodically inspected during the calibration process, in order to determine whether or not errors in the physical description of the system were present in the model. For example, early in the calibration process, it was noticed that the discharges measured in the model were much lower than those measured in the field. This discrepancy was not remedied by adjusting a calibration parameter. Rather, the model geometry was compared against satellite imagery of the system, and it was determined that several of the channels in the model needed to be widened in order to match the physical system. Since no calibration parameters were adjusted to force the model data to match the field data, this procedure is not classified as calibration, but rather as merely a correction of the system description, based on observations of the prototype.

Table 4 contains the final values of Manning's n used to calibrate the system. It also gives the time-averaged eddy viscosities and turbulent diffusion coefficients used to describe the system, as given by the Smagorinsky method. These values are classified according the region of the domain over which they are applied. The Manning's n values used here are appropriate for a relatively smooth bay bottom with little or no vegetation (see Chow 1959). The system is generally homogeneous with respect to bottom roughness, except for the values assigned to the reefs. Some

of the eddy viscosity and turbulent diffusion values in regions of the domain which are far away from the study area were made large, to ensure stability.

Table 4: Manning's n and Horizontal Turbulent Mixing Parameters Used in the Model

<i>Location</i>	<i>Manning's n</i>	<i>Eddy Viscosity (slugs/ft-sec)</i>	<i>Diffusion Coefficient (ft²/sec)</i>
Ocean Boundaries	.02	401	404
Inlets	.02	202	105
Tres Palacios and La Vaca River Inflows	.02	426	217
West-West Matagorda Bay	.02	70	94
East-West Matagorda Bay	.02	50	38
East Matagorda Bay	.02	45	35
Intra-Coastal Waterway (ICWW)	.016	12	11
Colorado River Diversion Channel	.016	11	8
Old River Channel	.016	12	8
Colorado River	.015	8	7
ICWW-Old River Channel Intersection	.016	44	28
Reefs	.025	135	14
Colorado River Locks	.015	93	158
Lake Austin and Wetlands North of East Matagorda Bay	.027	224	114
Colorado River Diversion delta	.020	38	16
Colorado River Diversion delta (emergent areas)	.025	137	53
Additional Wetlands North of East Matagorda Bay	.045	244	123

The water surface elevation observations for both the model and the field for the calibration period are given in plates 1-12 (calibration plates are on the top of each page). Since the field data are not referenced to a vertical datum, the mean water surface elevation has been subtracted from the field data, and the mean water surface elevation observed in the model has been added back in. This makes it easier to visually inspect the amplitude and phase comparisons between the model and the

field.

Any of the field data that was obviously corrupted by bio-fouling of the sensor was omitted from this comparison and analysis. Also, the field data has been filtered to remove noise in the signal. Signals with a period of 6 hours or less were omitted from the data set.

A statistical summary of these results is given in Table 5. A mathematical description of each of these statistics is given in Appendix C. Note that the Index of Agreement, or “d”, is a very useful statistic for evaluating the success of model-to-field comparisons in estuarine systems (Willmott, 1982). It is a measure of the ability of the model to duplicate the variability of the physical system. For this statistic, the degree of agreement between the model and the field is evaluated on a scale from 0 to 1, with 1 representing perfect agreement.

Note that the mean difference between the model and the field is omitted from this statistical summary, since the lack of a vertical datum for the field data renders this statistic meaningless.

Table 5: Statistical Summary of Calibration: Water Surface Elevation

<i>Gage Number</i>	<i>mean absolute error (MAE)(ft)</i>	<i>root mean square error (RMS)(ft)</i>	<i>index of agreement (d)</i>
1	0.14	0.184	0.941
2	0.094	0.122	0.974
3	0.07	0.089	0.989
4	0.175	0.233	0.963
5	0.142	0.184	0.951
6	0.131	0.171	0.958
7	0.11	0.133	0.963
8	0.064	0.083	0.974
9	0.145	0.186	0.943
10	0.11	0.141	0.973
11	0.06	0.073	0.983
12	0.068	0.087	0.973

Model Verification

The model hydrodynamics were verified against 3 separate types of data: Water surface elevation data (from July 15th – October 28th, 2001), ADCP 25-hour discharge data (from July 20th-21st, 2001), and velocity data (from May 15th- October 28th, 2001). The model salinities were verified against salinity data (from May 15th- October 28th, 2001). The following section contains a summary and discussion of these results.

Water Surface Elevation Data

The water surface elevation observations for both the model and the field for the verification period are given in plates 1-12 (verification plates are on the bottom of each page). Since the field data are not referenced to a vertical datum, the mean water surface elevation has been subtracted from the field data and the mean water surface elevation observed in the model has been added back in, just as they were for the calibration period (see **Model Calibration**, above). This makes it easier to visually inspect the amplitude and phase comparisons between the model and the field.

Any of the field data that was obviously corrupted by bio-fouling of the sensor was omitted from this comparison and analysis. Also, the field data has been filtered to remove noise in the signal. Signals with a period of 6 hours or less were omitted from the data set.

A statistical summary of these results is given in Table 6. These statistics are the same as those used to summarize the calibration data. Note that no data was available for verification for gages 3, 4, 7, and 10.

Table 6: Statistical Summary of Verification: Water Surface Elevation

<i>Gage Number</i>	<i>Mean absolute error (MAE)(ft)</i>	<i>Root mean square error (RMS)(ft)</i>	<i>Index of agreement (d)</i>
1	0.148	0.19	0.975
2	0.109	0.139	0.981
3	----	----	----
4	----	----	----
5	0.136	0.173	0.973
6	0.125	0.162	0.978
7	----	----	----
8	0.09	0.111	0.985
9	0.198	0.239	0.945
10	----	----	----
11	0.064	0.084	0.954
12	0.108	0.132	0.983

ADCP Discharge Data

The discharge observations at all 7 transects given in the field data are plotted against model results in plates 13-16. Note that the magnitude of the observed velocities for ranges 1-3 was very low. Hence, it is difficult to determine the cross-sectionally averaged direction of flow at these ranges, for a given time. Therefore, the apparent discrepancy between the direction of flow in the model and in the field for these ranges may be merely a result of this difficulty in processing the field data.

Velocity Data

The velocity observations (from gage 10, in West Matagorda Bay, and gage 12, in East Matagorda Bay) for both the model and the field are given in plates 17-18. The velocities are plotted over 2 separate time intervals: June 15th – July 15th, 2001, and August 15th – August 20th, 2001. This was done in lieu of plotting the entire time series for each gage on a single plot, so that the model to field comparison could be more easily determined by visual inspection. The field data has been filtered to remove noise in the signal. Signals with a period of 10 hours or less were omitted from the data set.

In order to plot the velocities, it was necessary to choose a direction along which to project the velocity components. This direction was determined by performing a variance ellipse analysis on the model and field data. This analysis determines the direction and magnitude of the maximum

and minimum variance of time-series data. Hence, it is useful for determining the dominant direction of flow for tidally influenced velocities. The results of the variance ellipse analysis are given in Table 7. The Table contains the direction of maximum variance, as well as the maximum velocity standard deviation (in the direction of maximum variance) and the minimum velocity standard deviation (in a direction perpendicular to the direction of maximum variance).

Table 7: Statistical Summary of Verification: Velocity Variance Ellipse Analysis Results

<i>Gage Number</i>	<i>Direction of maximum variance (degrees, CCW from positive X-Axis)</i>	<i>Maximum velocity standard deviation (ft/sec)</i>	<i>Minimum velocity standard deviation (ft/sec)</i>
Gage 10 (model)	27.36	0.215	0.037
Gage 10 (field)	42.49	0.153	0.074
Gage 12 (model)	46.2	0.045	0.023
Gage 12 (field)	128.05	0.089	0.038

Note that, although the dominant direction for the model and field velocities at gage 10 are similar, the dominant direction for the model and field velocities for gage 12 are approximately 90° out of phase. The reason for this is uncertain. It could be a real discrepancy between the model and field results. It is also possibly the consequence of a local bathymetric feature in the field, such as a small shoal, in the vicinity of the gage. For a shallow bay like East Matagorda Bay, such local features can have a significant influence on the principle direction of the velocity.

However, at the time of publication of this report, the discrepancy is unresolved. Therefore, the velocity components have been projected along the lines determined by the variance ellipses analysis for both the model and the field, with acknowledgement to the fact that the model results are actually 90° out of phase with the field results at station 12.

The agreement between the model and field velocities at gages 10 and 12 is not as good as the agreement observed in the water surface elevation comparisons. However, it should be noted that the model is being run in depth-averaged mode. The field data, however, consists of several measurements throughout the water column, which are then arithmetically averaged to arrive at a single depth-averaged value. Hence, the field data will show a greater response to such things as wind forcing, which tend to primarily influence only the upper part of the water column. Also, the process of depth averaging the data imposes some additional error on the final depth-averaged field result. Finally, local eccentricities in the currents and the bathymetry may be present in the field, but not accounted for in the model. These will have little effect on the water surface elevations, but they can influence the velocities measured at a point. This is especially true for these velocity gages since they are located in the middle of the bays, with no nearby land boundaries to rectify the direction of flow along a predictable angle.

Salinity Data

The salinity observations for both the model and the field for the verification period are given in plates (19-24). Any of the field data that was obviously corrupted by bio-fouling of the sensor was

omitted from this comparison and analysis. Also, the field data has been filtered to remove noise in the signal. Signals with a period of 6 hours or less were omitted from the data set.

Note that the model salinity at gage 1 is consistently lower than the values observed in the field at gage 1. This is most likely due to the fact that the model is a depth-averaged model. Hence, the model is unable to stratify, and is therefore unable to simulate the baroclinic effects which typically serve to pump salt water upstream along the riverbed in estuarine systems. Salinity stratification is observed in the lower Colorado River at low flows (see Appendix D). This observation indicates that the model would require 3D resolution in the Colorado River channel in order to accurately simulate the salinity in the river north of the locks. However, for the purposes of this study, this limitation should not adversely impact the modeling results. This is evidenced by the comparison between the model and field salinity elsewhere in the study area.

A statistical summary of the salinity results is given in Table 8. These statistics are the same as those used to summarize the calibration data, except that the mean difference has been added as an additional statistic.

Table 8: Statistical Summary of Verification: Salinity Data

<i>Gage Number</i>	<i>Mean error (ME)(ppt)</i>	<i>mean absolute error (MAE)(ppt)</i>	<i>Root mean square error (RMS)(ppt)</i>	<i>index of agreement (d)</i>
1	4.926	5.097	6.965	0.665
2	-0.756	3.165	4.01	0.772
3	0.221	3.529	4.624	0.786
4	0.042	3.751	4.82	0.77
5	0.263	3.887	4.951	0.866
6	1.154	3.019	4.044	0.902
7	-0.553	3.404	4.521	0.82
8	-1.804	2.984	4.056	0.794
9	0.657	3.662	4.638	0.903
10	0.456	2.234	3.079	0.914
11	0.777	1.235	1.707	0.954
12	0.203	1.944	2.445	0.939

Salinity Sensitivity Tests

In order to determine the influence of uncertainties in the boundary conditions and in the Colorado River lock operations on the verification of the salinity modeling results, a series of sensitivity tests were conducted. In these tests, various boundary conditions were perturbed by an amount estimated to be representative of the error in the boundary condition value. The model was run over the verification period with these perturbed boundary conditions, and the results were compared to the original model results. There were 4 sensitivity runs conducted. They are as follows:

Sensitivity run #1 - The ocean salinity was increased by 2 ppt.

Sensitivity run #2 - The freshwater inflows were decreased by 10%.

Sensitivity run #3 - The ungaged inflow was eliminated.

Sensitivity run #4 - The lock operations were altered such that the locks are continuously operational throughout the simulation period.

The results of these runs are given in Table 9. In this table, the Mean Absolute Error (MAE) is given for each sensitivity run at each of the 12 salinity gage locations. This value represents the mean absolute value of the difference between a given sensitivity run and the verification run. The table also gives the MAE for the model validation results (as given in Table 8). This is compared

to the vector sum of the MAE values for the 4 sensitivity runs. If the vector sum of the MAE values for the 4 sensitivity runs is greater than the MAE of the model validation results, then we can infer that the model is verified to within the tolerance of the error inherent in the field data.

The analysis shows that the model results fall within the tolerance of the uncertainty of the field data for all but 4 of the 12 salinity gages. The gages that exceed the tolerance are gages 1, 4, 6, and 10. The result for gage 1 is due to consistently low model salinity at this location. This is discussed in the **Salinity Data** section of this report. The discrepancy at gage 4 appears to be due primarily to the difference in tidal amplitude in the model and field salinity signals. This could be a consequence of the depth-averaged assumption in the model. An inspection of the salinity plots for gages 6 and 10 (see plates 21 and 23) shows that they simulate the pattern of salinity change in the field to a high degree of fidelity. This conclusion is borne out by the high Index of Agreement value given for these gages in Table 8.

Table 9: Salinity Sensitivity Test Results

<i>Gage</i>	<i>Sensitivity Run #1: MAE</i>	<i>Sensitivity Run #2: MAE</i>	<i>Sensitivity Run #3: MAE</i>	<i>Sensitivity Run #4: MAE</i>	<i>Vector Sum of MAE's</i>	<i>MAE of salt verification (from Table 8)</i>	<i>MAE Difference</i>
1	0.1	0.27	0.02	1.68	1.71	5.097	-3.387
2	1	0.31	0.6	3.84	4.02	3.165	0.855
3	1.1	0.29	0.59	3.36	3.59	3.529	0.061
4	1.35	0.23	0.42	2.07	2.53	3.751	-1.221
5	0.46	0.57	0.55	8.51	8.56	3.887	4.673
6	0.38	0.68	0.53	1.52	1.79	3.019	-1.229
7	0.88	0.33	0.46	4.57	4.69	3.404	1.286
8	0.79	0.17	1.52	2.68	3.18	2.984	0.196
9	0.39	0.64	0.33	9.54	9.58	3.662	5.918
10	0.45	0.59	0.26	1.09	1.35	2.234	-0.884
11	0.52	0.12	1.11	1.94	2.3	1.235	1.065
12	0.51	0.08	2.92	1.82	3.48	1.944	1.536

Model Scenario Runs

This chapter contains an analysis and discussion of the scenario runs. The influence of the various scenarios on the currents at the Bypass Channel - ICWW intersection is analyzed in detail, together with the general impact on currents and circulation within the system. The impact of the various scenarios on the salinity and the sediment transport patterns in the system is also analyzed and discussed.

Description of Scenarios

As was mentioned in the **Introduction**, 12 separate scenarios were analyzed for this study: the existing system configuration, and 11 proposed configuration designs (see Table 1). Each of these scenarios was run for 3 separate flow years, which were selected as representative low, medium, high flow years for the Colorado River.

There are three separate proposed cuts being analyzed in these 11 proposed configurations: Parker's Cut (PK), Southwest Cut (SWC) and the Diversion Dam Cut in the existing diversion dam (DDC). In order to implement these cuts in the hydrodynamic model, it was necessary to select an appropriate value of the hydraulic roughness (Manning's n) for each cut. The value of Manning's n assigned to Southwest Cut and to the Diversion Dam Cut was 0.02, based on the assumption that both of these cuts would be comprised primarily of concrete. The value assigned to all but one of the configurations of Parker's Cut was 0.027, based on the assumption that the cut would be a riprap-protected channel. The exception to this is the large configuration of Parker's Cut (used in scenarios I and L). Since this configuration is intended to approximate the dimensions of a stable cut, it is assumed that the bed will consist of sand, with riprap-protected banks. Therefore, the value of Manning's n chosen is indicative of that used for a sand bed: 0.018.

Currents

The influence of the scenario configurations on currents and circulation in the system is discussed with respect to several different specific issues. These are as follows:

- The currents at the ICWW, Bypass Channel Intersection. The flood-tide currents at this intersection represent the principle navigation hazard that these scenarios are designed to alleviate.
- The Currents at the Old River Channel Mouth. Changes to the currents at the Old River Channel Mouth can potentially impact both navigation and sedimentation at this location.
- Currents in Parker's Cut, Southwest Cut, and the Diversion Dam Cut. The currents and

circulation in these cuts can impact salinity and sedimentation in East and West Matagorda Bays, and in the Old River Channel. For Parker's Cut, an understanding of the currents is important to assess the navigation conditions in the cut for small craft boat traffic.

Currents at the ICWW-Bypass Channel Intersection

Figure 22 shows the percent reduction in the peak flood-tide currents in the Bypass Channel-ICWW Intersection. The currents were measured across the Bypass Channel, just south of the intersection with the ICWW. The percent reduction represents the reduction in the peak current magnitude relative to the peak current magnitude for the existing system configuration (i.e., Scenario A). Only flood-tide currents greater than 2 fps were factored into the analysis, so that the influence of the various scenarios on the peak currents could be determined. These flood-tide currents are present in the intersection approximately 4-6% of the year.

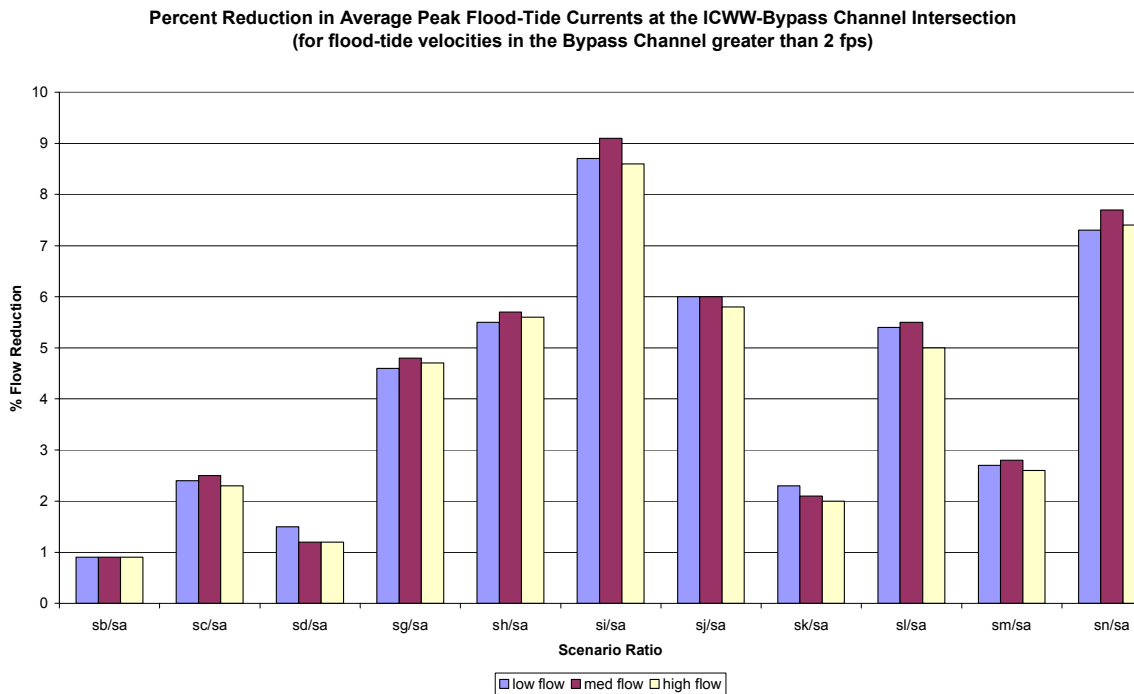


Figure 22: Percent Reduction in Average Peak Flood-Tide Currents at the ICWW-Bypass Channel Intersection

The largest reduction in peak currents is between 8-9%, for Scenario I (PK, 2-4X350, and SWC, 5X100). A comparison of Scenario M (PK, 5X100) and Scenario N (SWC, 5X100) indicates that, for a given cross-sectional area, Southwest Cut is more efficient than Parker's Cut at mitigating the peak flood-tide currents at the intersection. The results given for scenario D (DDC, 4X20) indicate that it has minimal impact on the flood-tide currents in the intersection. This is likely due to the small size of the proposed Diversion Dam Cut.

Figures 23 and 24 are vector plots of the peak flood-tide currents in the Bypass Channel-ICWW Intersection. Figure 23 represents the currents for the existing configuration (Scenario A) and

Figure 24 represents the currents for Scenario I, which is the scenario that yields the maximum impact on the peak currents (as discussed above). These figures are useful for evaluating the impact of the design scenarios on the spatial distribution of the velocities in the Bypass Channel-ICWW Intersection, at peak flood-tide. An inspection of both plots reveals that the spatial distribution of the velocities is virtually unchanged from Scenario A to Scenario I. Therefore, it is reasonable to conclude that the scenarios have little influence on the distribution of the velocities, and therefore the impact of each scenario can be comprehensively assessed by examining its influence on the flood-tide current magnitude (i.e. Figure 22).

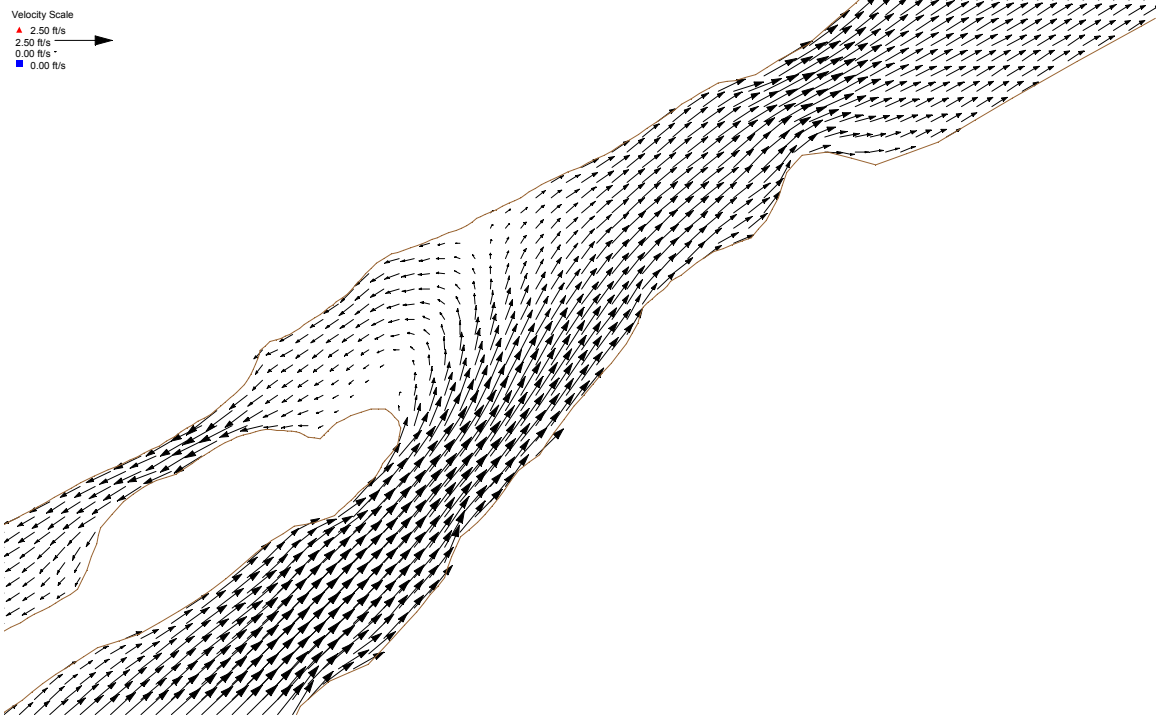


Figure 23: Peak Flood-Tide Currents at the Bypass Channel-ICWW Intersection for Scenario A

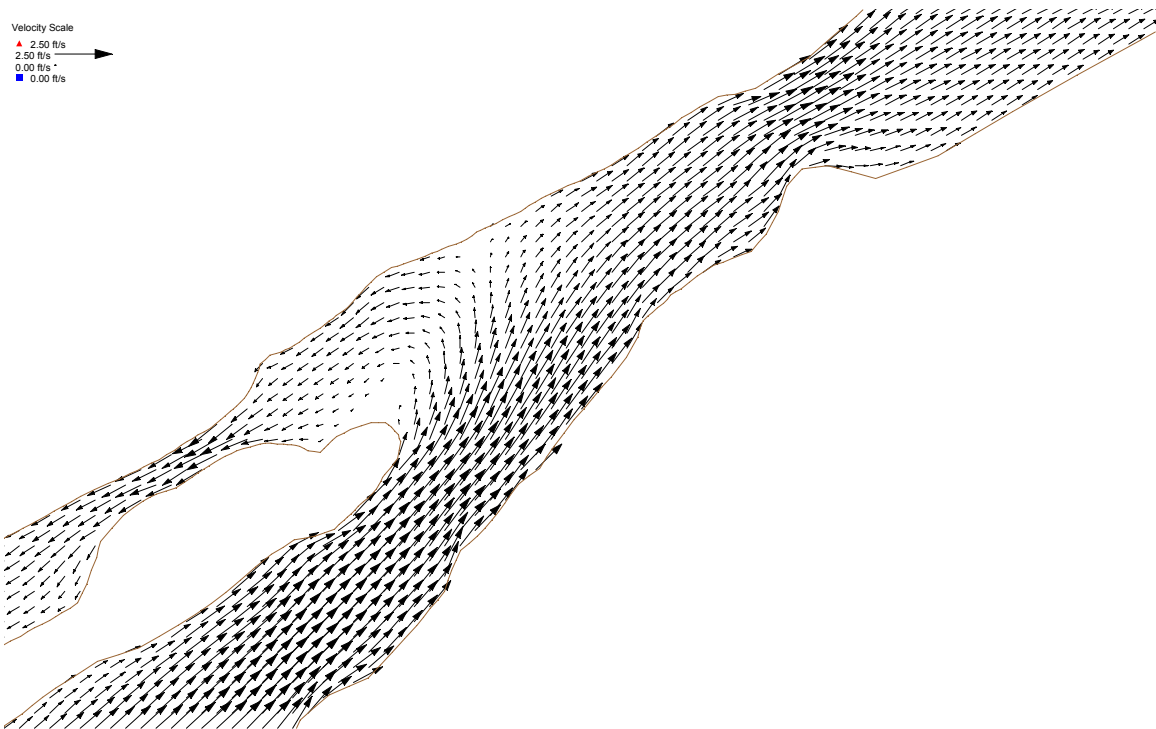


Figure 24: Peak Flood-Tide Currents at the Bypass Channel-ICWW Intersection for Scenario I

Currents at the Old River Channel Mouth

Figure 25 shows the percent increase in the peak flood-tide currents at the Old River Channel Mouth. As with the analysis done in the previous section, only currents greater than 2 fps were examined.

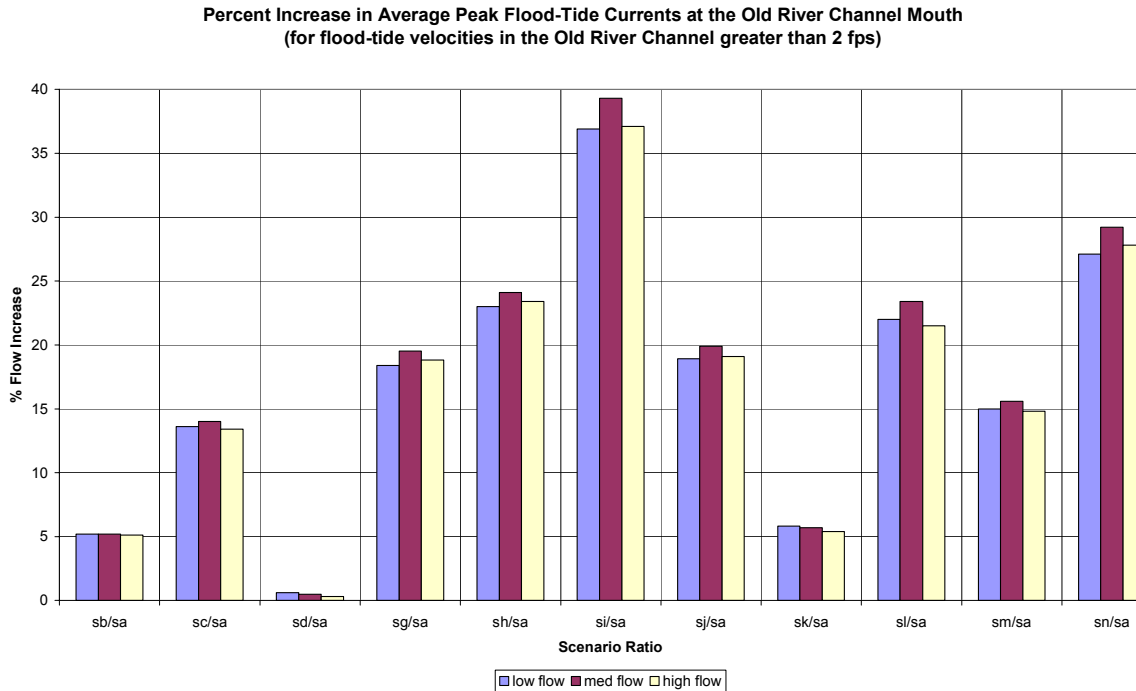


Figure 25: Percent Increase in the Average Peak Flood-Tide Currents at the Old River Channel Mouth

The percent increase in peak flood-tide currents at the Old River Channel Mouth is considerably greater than the percent reduction in peak flood-tide currents at the ICWW Intersection. For example, there is a 35-40% increase in the peak flood-tide current at Scenario I, whereas there is a 8-9% *reduction* in the peak flood-tide currents at the ICWW Intersection. In order to understand this, we can examine an arbitrary scenario (e.g., Scenario M, PK5X100) by using the following simple conservation of mass equation:

$$\text{Flow In} - \text{Flow Out} = \text{Change in Storage With Respect to Time} \dots\dots\dots (3)$$

If we assume there is little or no storage in the Old River Channel itself (that is, if we assume that most of the flood-tide flow passing through the Old River Channel Mouth reaches the ICWW Intersection) then we can set the change in storage = 0, and simplify equation (3) as follows:

$$\text{Flow In} = \text{Flow Out} \dots\dots\dots (4)$$

We can then write the equation for our existing system configuration (Scenario A):

$$\text{Flow into the Old River Channel Mouth} = \text{Flow Out to the ICWW} \dots\dots\dots (5)$$

And we can write the equation for our sample scenario (Scenario M):

$$\text{Flow into the Old River Channel Mouth} = \text{Flow Out to the ICWW} + \text{Flow Out Through PK (6)}$$

Equation 6 indicates that Scenario M has an extra outlet for flow to leave the channel before it reaches the ICWW. Therefore, although more flow is drawn into the system, some of the flow exits the Old River Channel through Parker's Cut, and hence the *net* flow that reaches the ICWW is less than it is for the existing configuration.

The increase in peak flood-tide flow at the Old River Channel mouth indicates a general increase in the tidal currents at this location. This increase in currents will serve to increase the bed shear stress, and hence inhibit shoaling. However, the increase in currents can also serve to create shoaling problems further upstream, by pumping larger volumes of sediment into the system.

In order to determine the likelihood of this, the average current over 1 year was calculated for the Old River Channel Mouth. This average (or residual) current represents the net movement of water. By comparing the average currents for each of the scenarios to the average current for the existing condition, the relative increase in the flood-tide residual can be determined. This can be used as an indicator of the risk of further shoaling upstream, since an increase in the flood-tide residual represents an increase in the capacity for sediment to be transported into the system.

Figure 26 depicts the residual currents at the Old River Channel Mouth. Note that all of the scenarios are flood-tide dominant for the low flow condition, and ebb-tide dominant for the medium and high flow conditions. The medium and high flow cases are ebb dominant because some of the Colorado River flow passes through the East Lock and into the Old River Channel through the Bypass Channel.

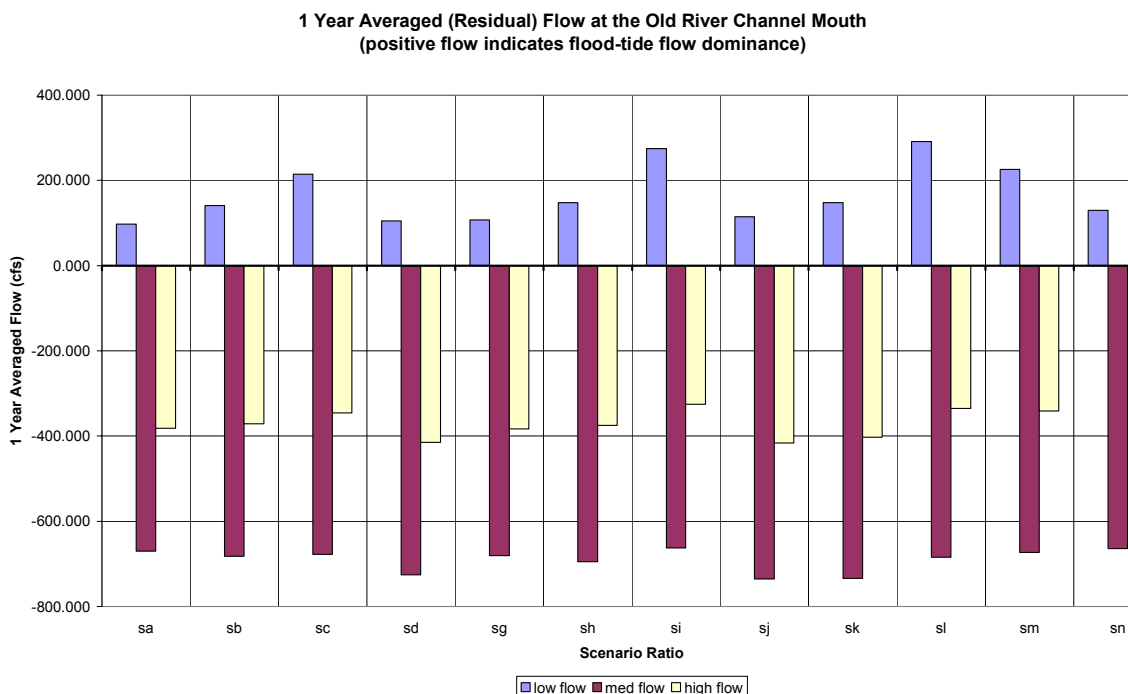


Figure 26: 1 Year Averaged (Residual) Flow at the Old River Channel Mouth

Figure 27 shows the differences between the residual currents at the Old River Channel Mouth for each design scenario, and the residual currents for the existing condition (Scenario A). This plot is useful for evaluation the relative risk of an increased flood-tide residual, and hence an increase in

sediment transport potential into the Old River Channel. Note that the scenarios which incorporate Parker's Cut (Scenarios B, C, H, I, K, L, and M) tend to show a larger increase in the flood-tide residual than do the other scenarios, for the low flow condition. The scenarios involving the Diversion Dam Cut (Scenarios D, J, and K) all exhibit an increase in ebb-tide flow for the medium and high flow conditions. This is due to the fact that the Diversion Dam Cut serves to capture some of the Colorado River Flow and redirect it through the Old River Channel. This could serve to help pump sediment out of the Old River Channel, during high river flow events.

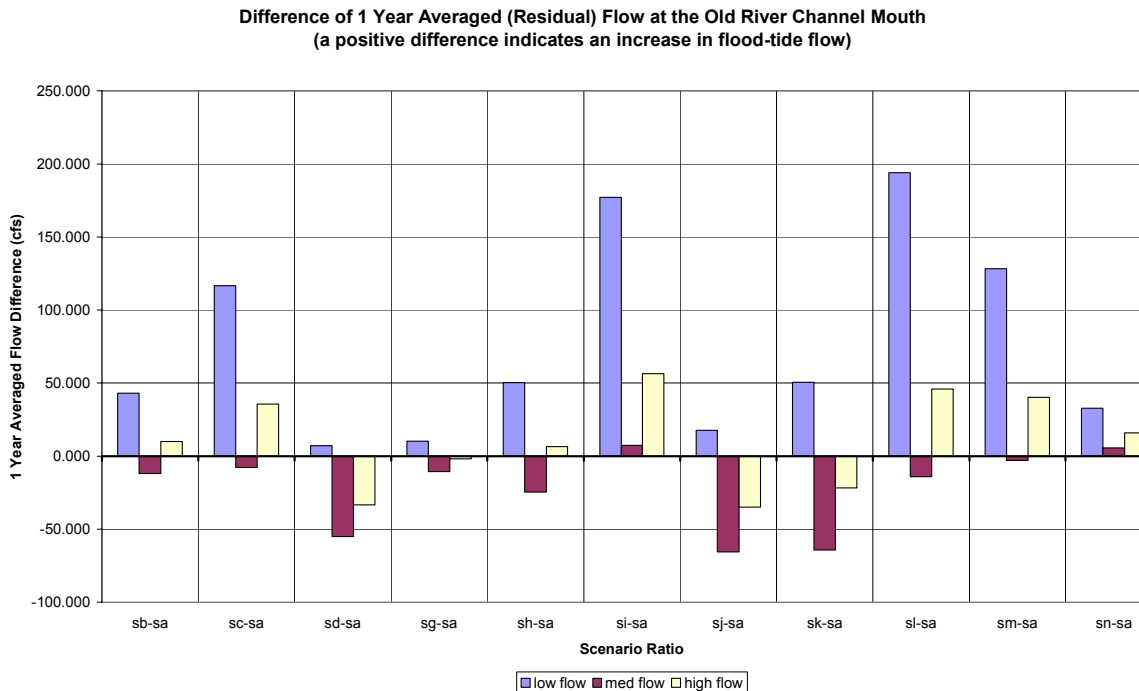


Figure 27: Difference of 1 Year Averaged (Residual) Flow at the Old River Channel Mouth

Currents at Parker's Cut, Southwest Cut, and the Diversion Dam Cut

Figures 28 and 29 show the peak tidal current velocities and residual velocities for the various configurations of Parker's Cut and Southwest Cut, respectively. These values were taken for the Low Flow Year, so that the effects of river flows on the tidal currents could be minimized.

Note that the peak velocities in Parker's Cut for the smallest configuration (4'X20') reach 3 fps. This velocity in a 20 foot wide channel could create navigation problems for small craft attempting to use the cut. The peak velocities are more reasonable for the larger configurations. Also, the minimum flood-tide residual discharge occurs for the 5'X100' configuration.

It should be noted that the information for the 2-4'X350' Parker's Cut configuration was taken from Scenario I, which also contains a 5'X100' Southwest Cut configuration. However, analysis of the results indicates that, with respect to currents, Southwest Cut and Parker's Cut serve to act independently. That is, they have little interdependence with respect to their influence on the currents, and the impact of each can effectively be treated separately.

As with Parker's Cut, the residual discharges in Southwest Cut are flood-tide dominant. However, this is not necessarily indicative of the average condition. To illustrate this, consider Figures 30 and 31. These figures are intended to depict the influence of the wind on the residual flows in

Parker's Cut and Southwest Cut, respectively. For each figure, the wind has been projected along an angle that is roughly parallel to the length of the Bay (26 degrees North of East). This is plotted together with the velocity in each cut, defined as flood-tide positive. Two separate configurations of each cut have been plotted, to show the influence of the configurations on the magnitude of the residual response. Both the wind and the velocity signals have been filtered to remove high frequency signals (i.e. signals with a frequency greater than 1/week). The resulting plots show the response of the residual discharge to the wind. Note that, although Parker's Cut only shows a response to wind components from the east (mostly Northeast), Southwest Cut responds to both east and west wind components. The response for Southwest cut is somewhat ambiguous at times, especially in the first part of the year. However, examination of the wind data indicates that, in general, Southwest Cut is flood-tide dominant for North and Northeasterly winds, and ebb-tide dominant for south and southwesterly winds.

There is a marked correlation between currents in the cuts and seasonal winds. During the simulation year, Parker's Cut is weakly flood-tide dominant in the summer and winter, and more strongly flood tide dominant in the spring and fall. Southwest Cut is flood-tide dominant in the summer, ebb-tide dominant in the fall and early winter, and alternately flood-tide and ebb-tide dominant in the late winter and early spring. This seasonal characteristic is significant with respect to the transport of coastal sediments. Coastal sediment is supplied to the Old River Channel mouth via longshore sediment transport. Longshore sediment transport rates along at the Old River Channel Mouth vary seasonally. The longshore sediment transport rate is highest in the late fall and winter, and lowest in the summer and early fall (King, and Prickett, 1998). Hence, at the times when more sediment is available for transport, Parker's Cut is strongly flood-tide dominant, and Southwest Cut is either ebb-tide dominant or is exhibiting alternate flood-tide and ebb -tide dominance. This indicates that, in general, Parker's Cut will have a tendency to entrain more sediment into the Old River Channel mouth when coastal sediment transport rates are highest, whereas Southwest Cut will have a tendency to push the sediment back towards the Gulf at these times.

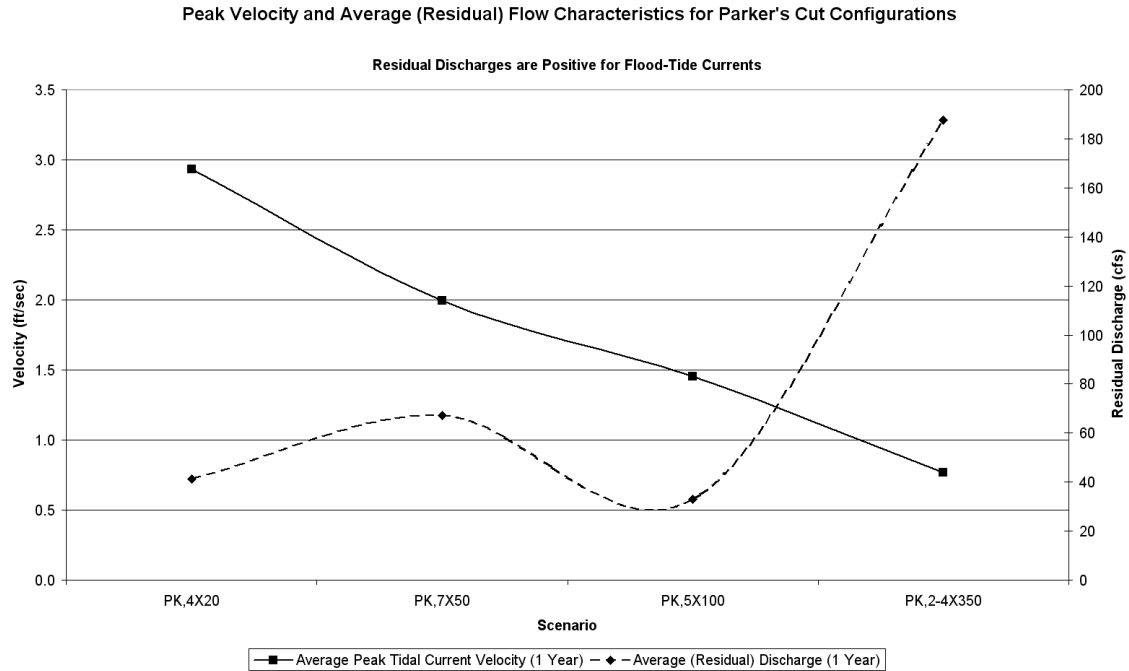


Figure 28: Peak Velocity and Average (Residual) Flow Characteristics for Parker's Cut

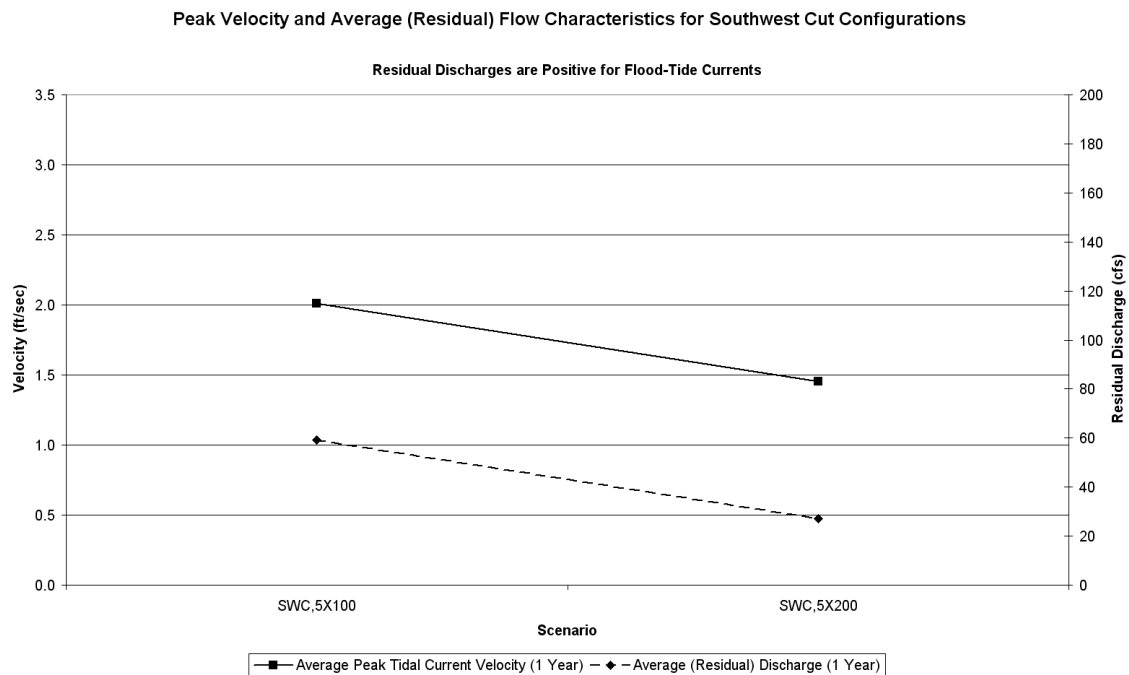


Figure 29: Peak Velocity and Average (Residual) Flow Characteristics for Southwest Cut

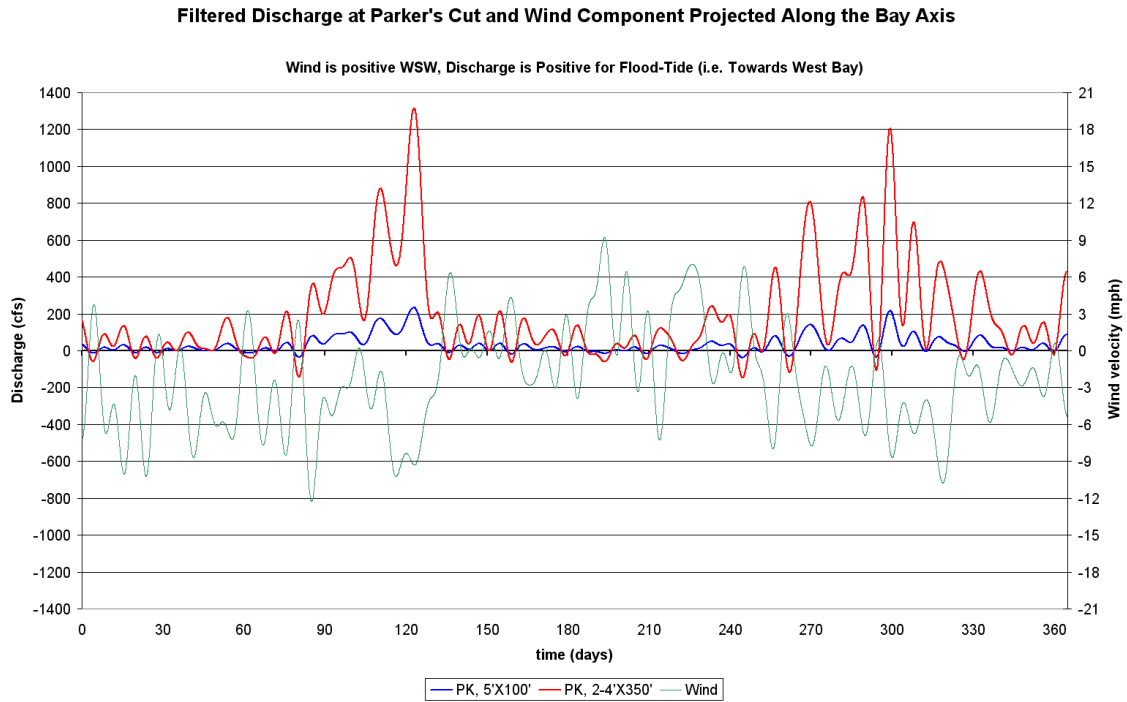


Figure 30: Filtered Discharge and Wind Component Projected Along the Bay Axis, Parker's Cut

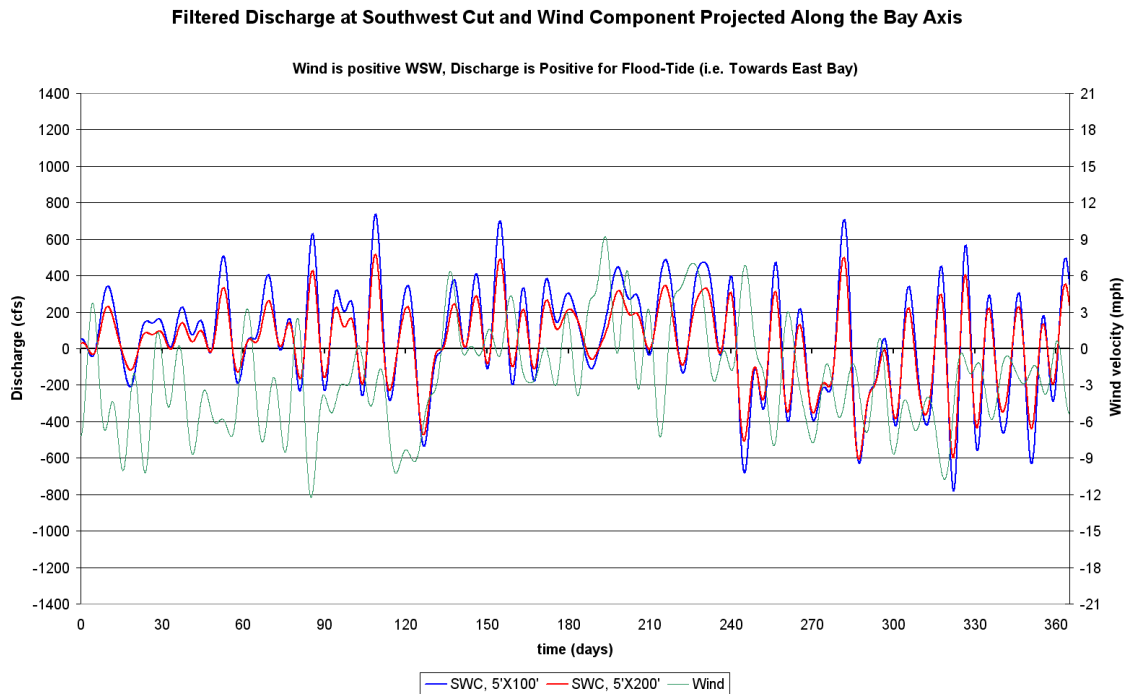


Figure 31: Filtered Discharge and Wind Component Projected Along the Bay Axis, Southwest Cut

Figure 32 depicts the percent of the Colorado River Discharge to West Matagorda Bay that is diverted through the Old River Channel for each scenario. The analysis is done for the high flow year. The figure illustrates that none of the proposed design scenarios will redirect greater than 3% of the Colorado River discharge from West Matagorda Bay to the Old River Channel.

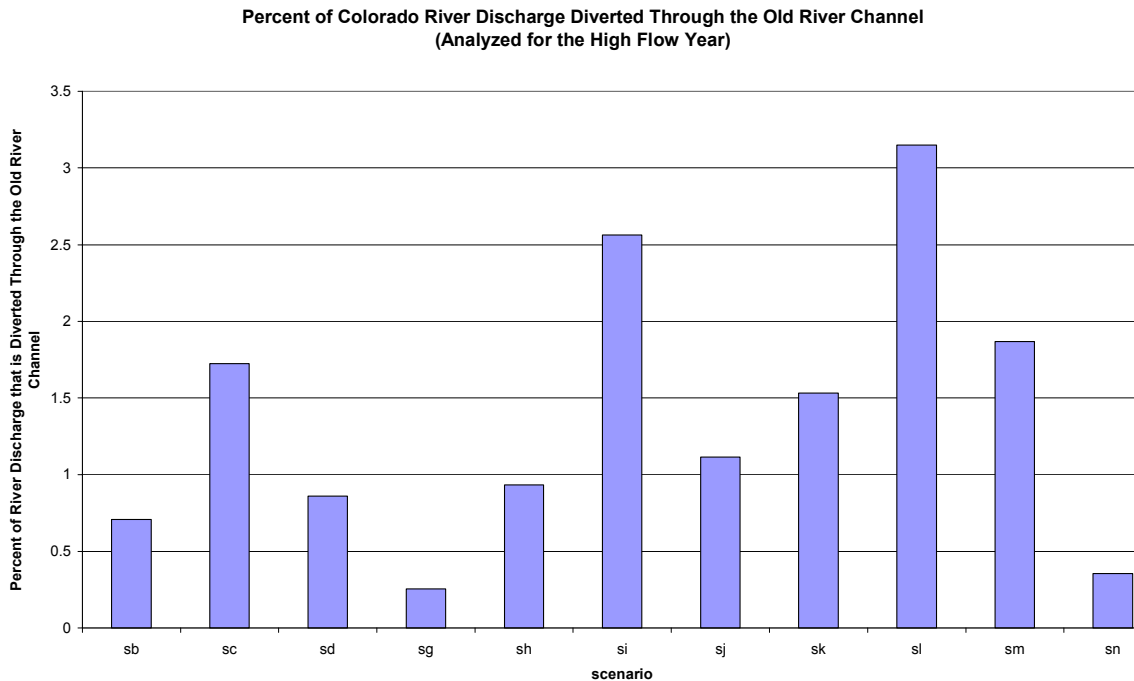


Figure 32: Percent of Colorado River Discharge Diverted Through the Old River Channel

Salinity

Annual Average Salinity Distribution

Figures 33 - 35 depict the average salinity concentrations in East and West Matagorda Bays for each for the 3 design flow years. The plots depict the salinities for the existing condition scenario (Scenario A). These figures show that there is considerable variability in the average salinity of the Bays between lower flow and higher flow years. Also, the spatial distribution of salinity in the eastern arm of West Matagorda Bay confirms the results of the model study found in Corps of Engineers (1981), in which they concluded that the average circulation in the eastern arm is counterclockwise.

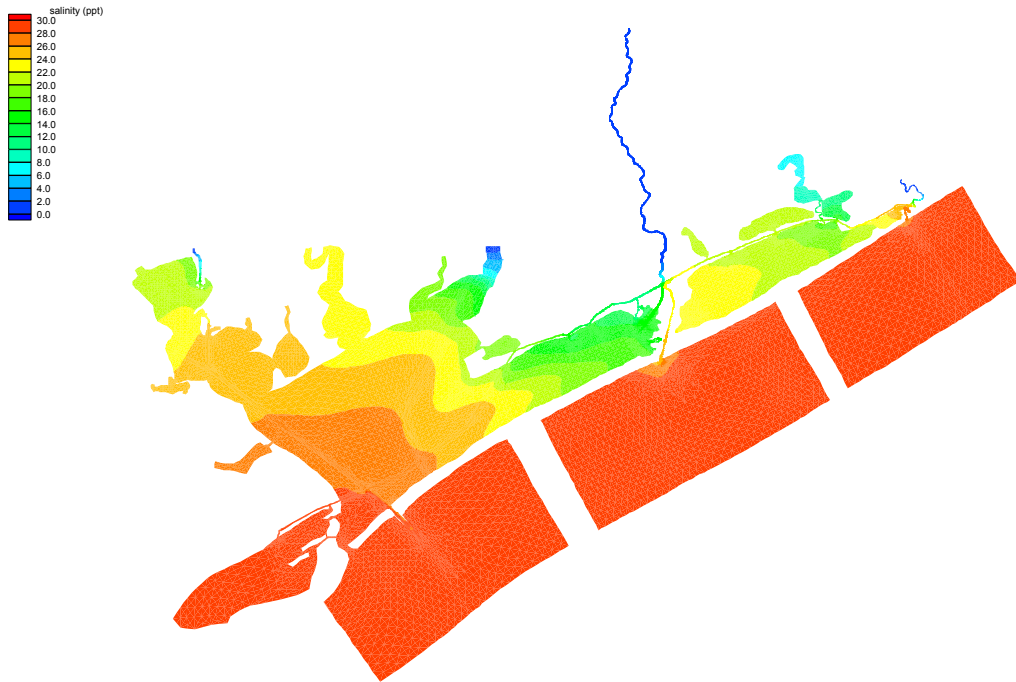


Figure 33: Average Salinity, Existing Conditions (Scenario A), Low Flow Year

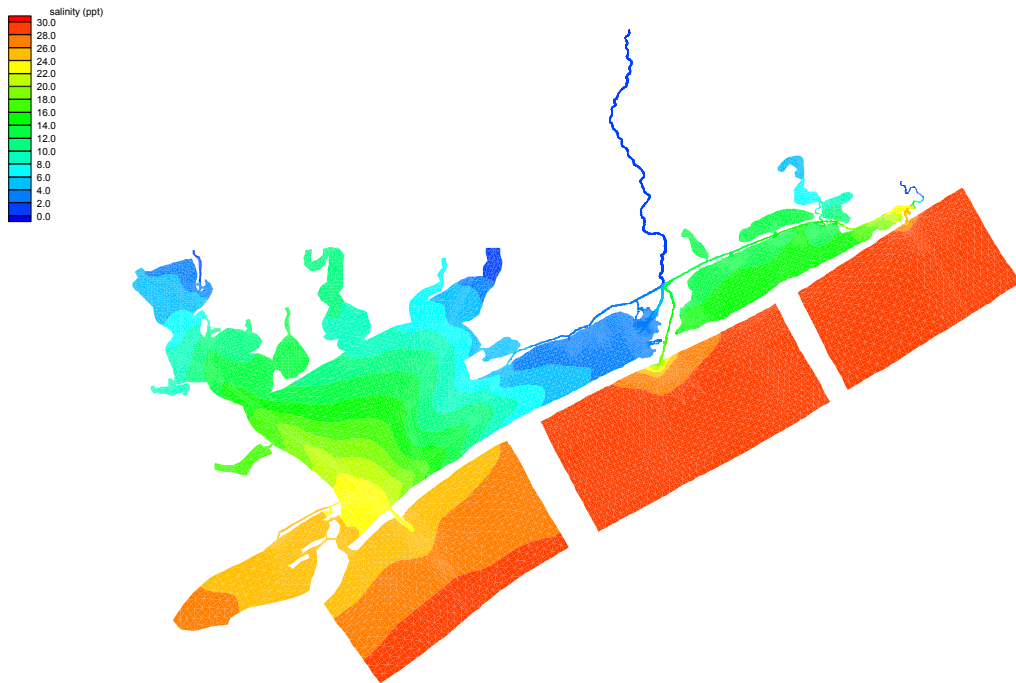


Figure 34: Average Salinity, Existing Conditions (Scenario A), Medium Flow Year

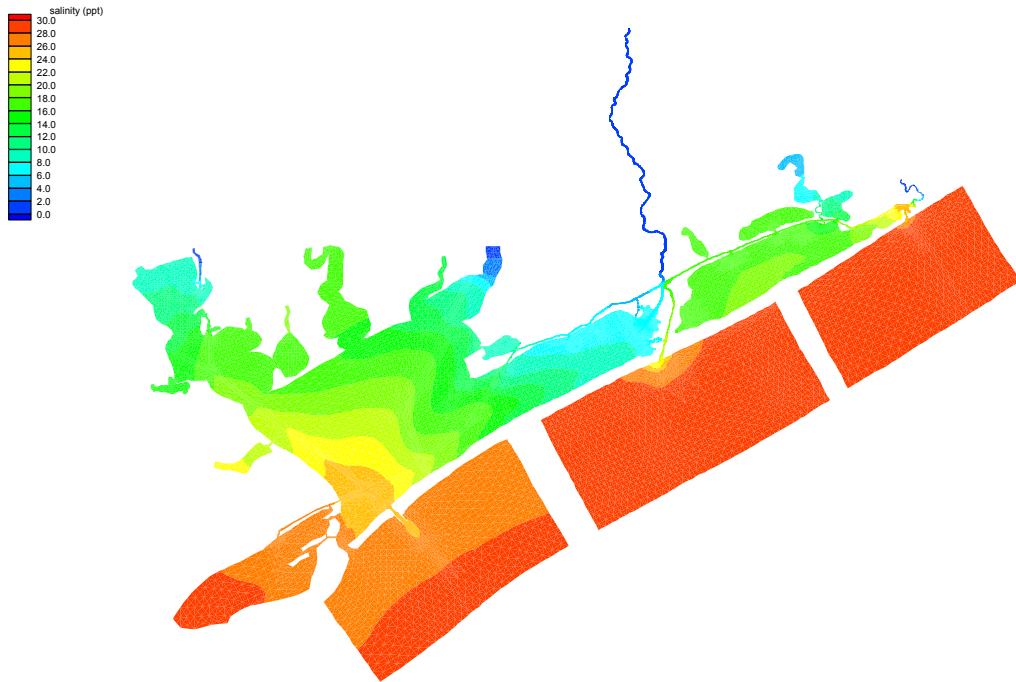


Figure 35: Average Salinity, Existing Conditions (Scenario A), High Flow Year

Influence of Parker's Cut on West Matagorda Bay Salinity: Sample Comparison

Figures 36 and 37 depict the salinity and circulation resulting from a relatively small Colorado River flow event (with a peak discharge of 10,000 cfs). Unlike the average conditions depicted in Figures 33-35 these figures show a snapshot in time. Specifically, the figures show the system during slack water after flood-tide (i.e. peak tidal elevation). Figure 36 depicts the existing conditions (Scenario A), whereas Figure 37 shows Scenario M (PK, 5'X100') at the same moment in time. An examination of the figures indicates that the Parker's Cut tends to exert influence on the Bay circulation and salinity in a semicircular region with a radius of approximately 3,300 feet, extending into the Bay from the bayside mouth of Parker's Cut.

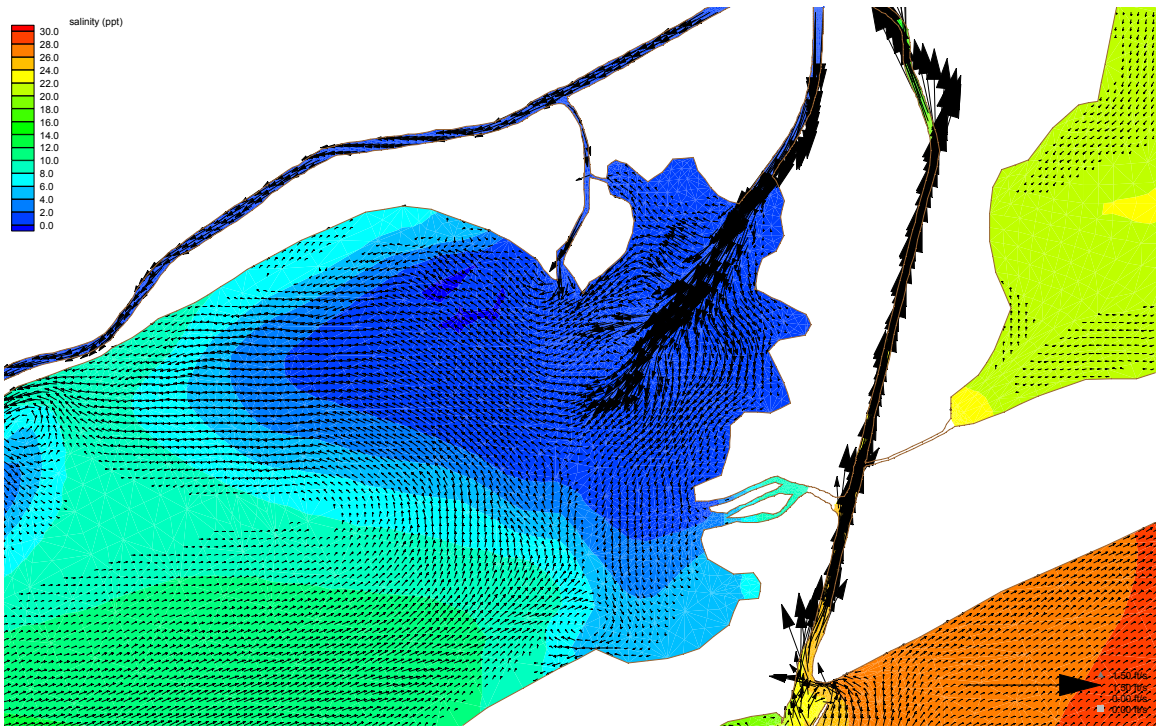


Figure 36: Snapshot of Salinity and Circulation for Scenario A (Existing Conditions)

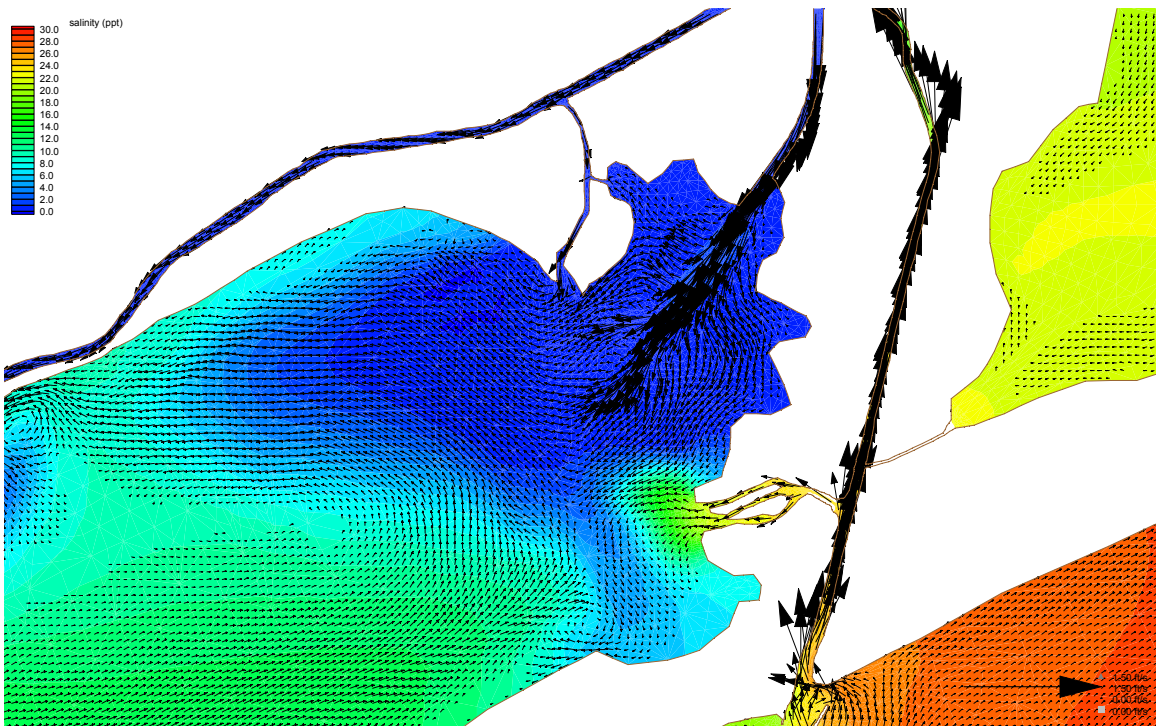


Figure 37: Snapshot of Salinity and Circulation for Scenario M (Parker's Cut, 5'X100')

Evaluation of Scenarios: Average Annual Salinity Difference

Plates 25- 57 depict the average annual salinity difference between each design scenario and Scenario A (existing conditions), for each of the 3 flow year conditions. By examining these plates, several observations can be made.

- By comparing the results from scenarios with multiple cuts (such as Scenarios H and I) against scenarios with single cuts (such as Scenarios B, C, and G) it is apparent that Southwest Cut and Parker's Cut are basically independent of one another with respect to their impact on salinity. That is, each of the cuts exhibits the same basic salinity difference pattern whether it is used in isolation or together with the other cut.
- The Diversion Dam Cut has no measurable impact on the salinity of the system.
- Parker's Cut demonstrates a more spatially confined impact on Bay salinity than does Southwest Cut. However, the magnitude of the impact is greater than for Southwest Cut, reaching as much as 8 ppt in the immediate vicinity of the connection between Parker's Cut and the Bay.
- The spatial extent of the impact of Parker's Cut on Bay salinity increases with increasing cross-sectional area of Parker's Cut. Figure 38 depicts approximate values of the westward extent of the 1ppt salinity difference contour for each configuration of Parker's Cut.

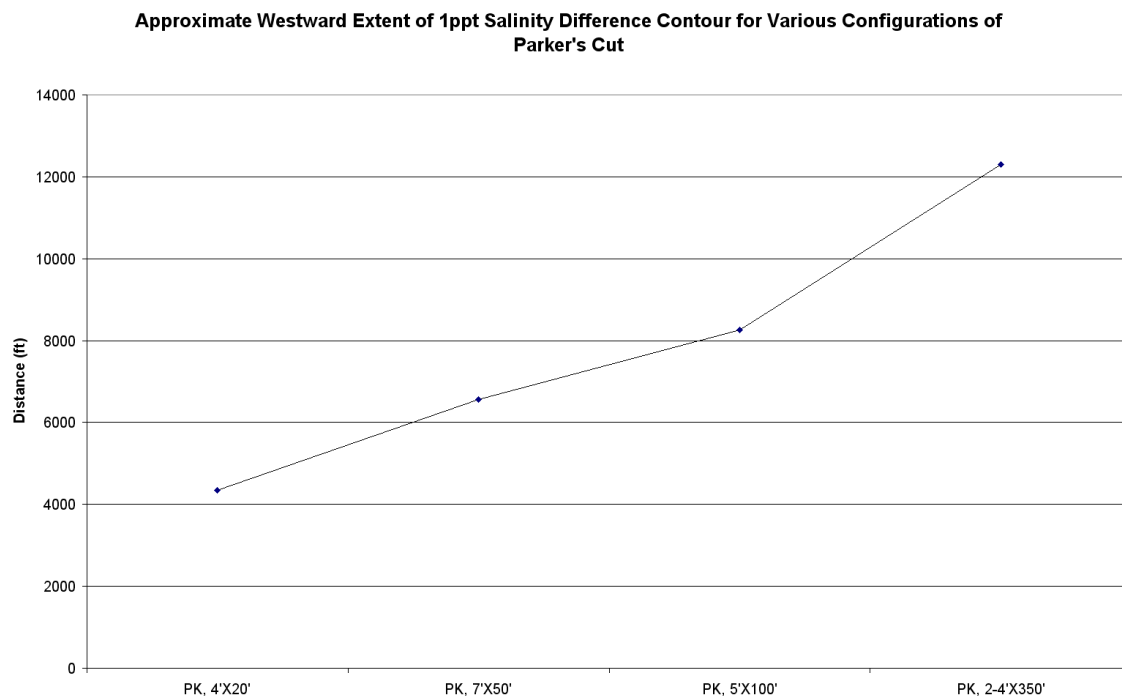


Figure 38: Approximate Westward Extent of 1 ppt Salinity Difference Contour for Various Configurations of Parker's Cut

Impact of Parker's Cut on Average Springtime Salinity in West Matagorda Bay

The average springtime salinity in West Matagorda Bay is of importance to the survivability of oyster larvae in the bay (Bass, 2002). Plates 58 - 66 show the average springtime salinity in the Bay for the existing condition, and for 3 of the Scenarios (B, L, and M) for which Parker's Cut is opened. The contour interval is chosen from 10-20 ppt, so that the location of the mesohaline zone in the Bay can be more clearly delineated. The plates show that no configuration of Parker's Cut should have significant influence on the location of the springtime mesohaline zone in the Bay.

Sediment

The following section presents the results of sediment modeling done for each of the design scenarios and each of the flow conditions. Since these are not calibrated results, they should be useful for predicting trends of erosion and deposition, but not for predicting the actual quantities of those trends. Also, it is important to note that the principle goal of the sediment modeling is to determine the influence of the design scenarios on the fate of Colorado River sediment. Hence, the model used is a fine-grained sediment model, and assumed that the sediment behaves as cohesive sediment. The other primary potential source of sediment for the system is sediment supplied from the longshore transport of coastal sediment through the Old River Channel Mouth. This coastal sediment is sandy, and hence behaves in a much different fashion than the cohesive sediment of the Colorado River. Therefore, these results cannot be considered reliable for predicting the fate of these coastal sediments.

Average Annual Bed Elevation Change

Figures 39-41 depict the average bed elevation changes in East and West Matagorda Bays for each for the 3 design flow years. The plots depict the bed elevation changes for the existing condition scenario (Scenario A). These figures show that the Medium and High Flow years result in much greater delta growth than does the low flow year. Also, note that the delta growth in the high flow year is further west than for the medium flow year. This is a result of the higher current speed during the massive flood event in the high flow year, which forces the sediment further into the Bay. Finally, note that some deposition of Colorado River sediment is observed in the Old River Channel, especially during the Medium Flow year. This sediment is passing through the locks during moderate river flows (when the locks are frequently open) and on into the Old River Channel. This behavior is consistent with observations in the field, where a significant fraction of the Old River Channel sediment has been found to be Colorado River sediment (King and Prickett, 1998).

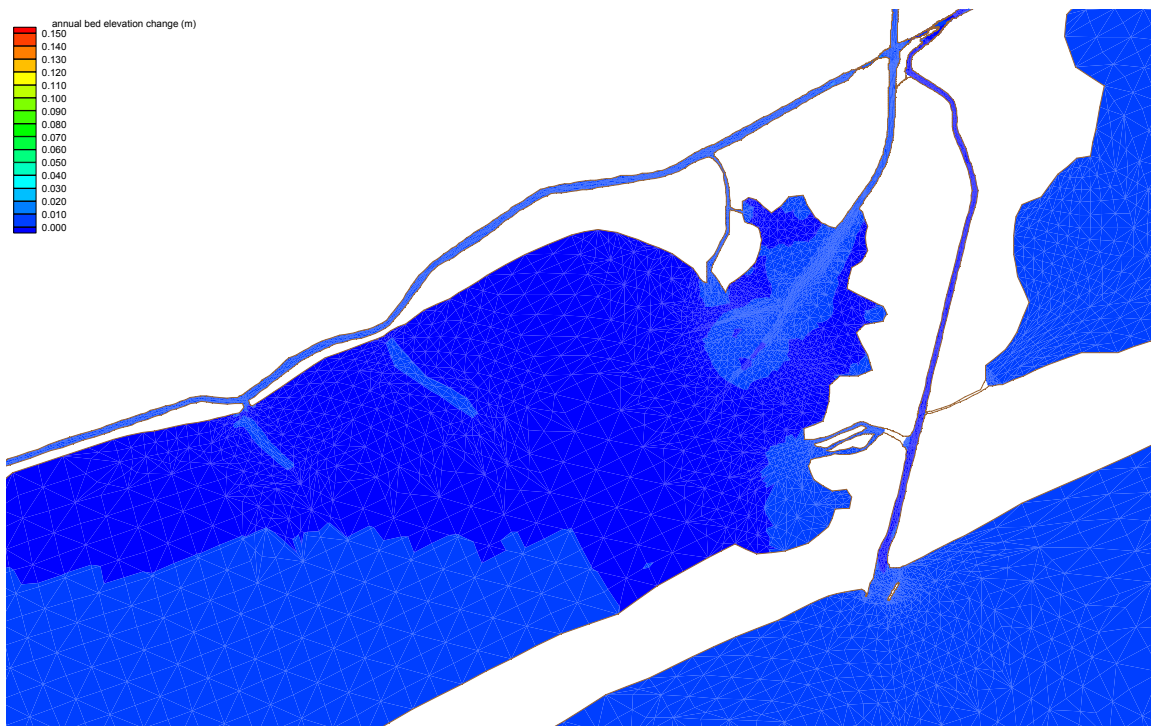


Figure 39: Bed Elevation Change, Low Flow Year

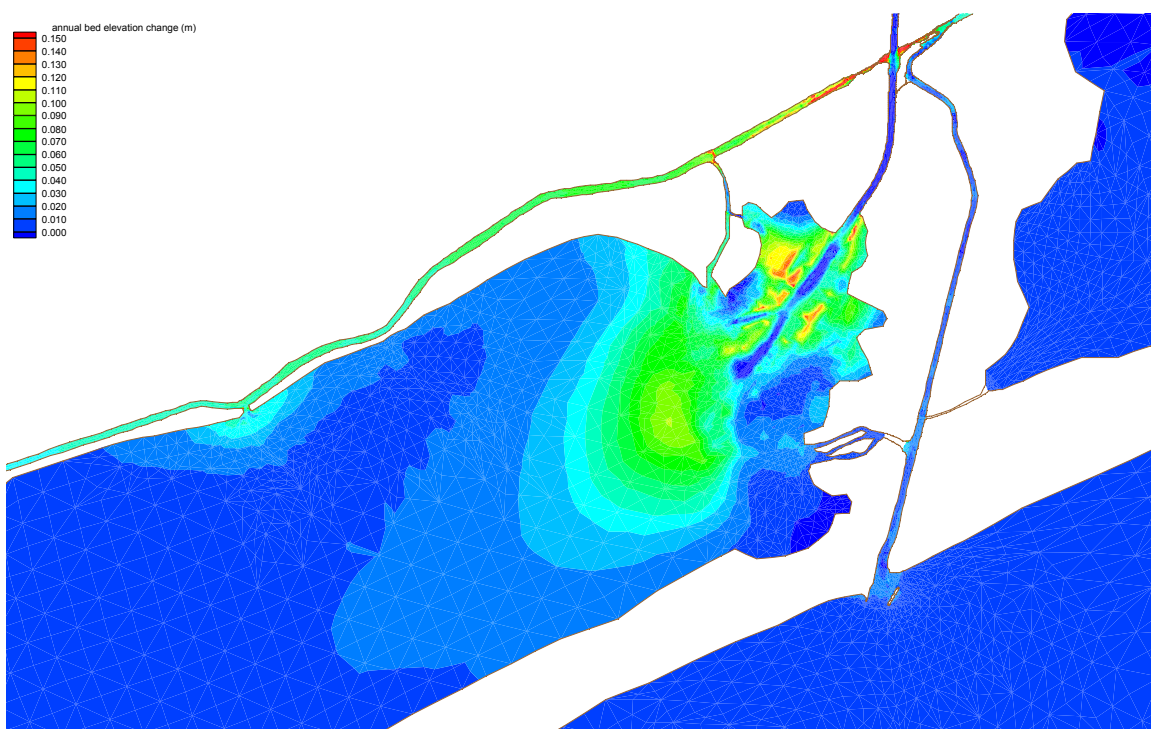


Figure 40: Bed Elevation Change, Existing Conditions (Scenario A), Medium Flow Year

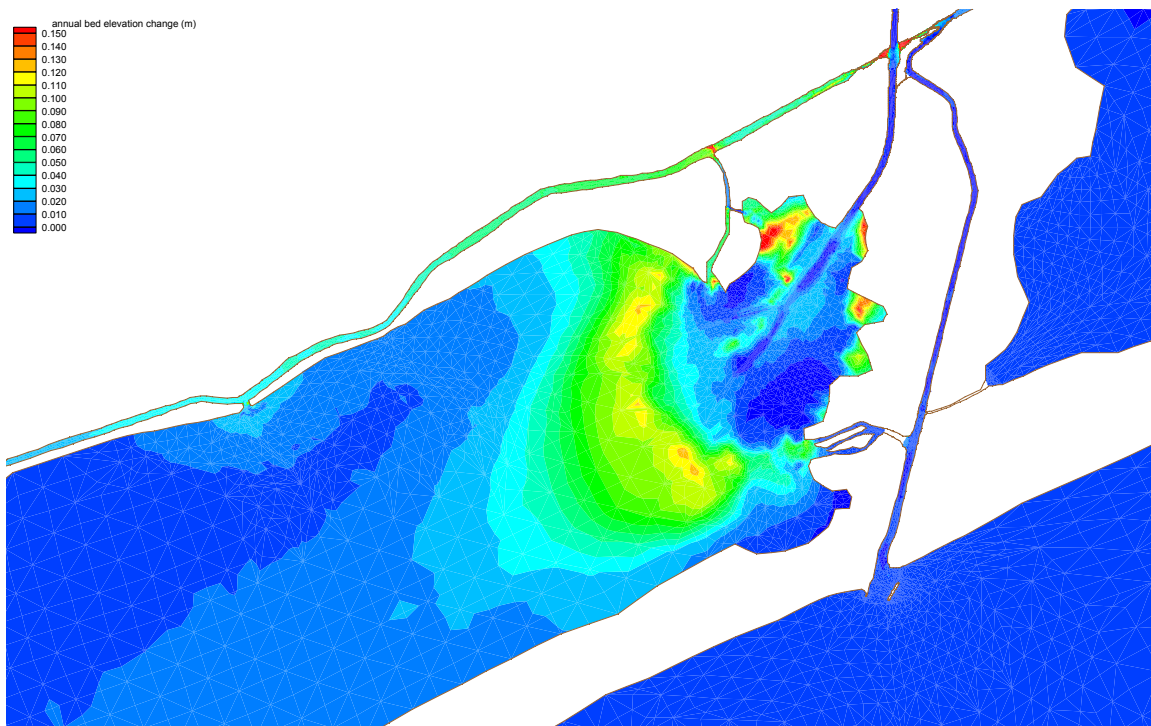


Figure 41: Bed Elevation Change, Existing Conditions (Scenario A), High Flow Year

Table 10 gives the approximate volume of Colorado River Diversion Delta growth for Scenario A (existing conditions) for each of the 3 flow years. Note that the low flow year shows a net erosion of the delta. This is due to the redistribution of the delta sediment via wind-wave re-suspension and bay currents.

Table 10: Approximate Volume of Colorado River Diversion Delta Growth for Existing Conditions

	<i>Volume of Delta Growth (m³)</i>	<i>Volume of Delta Growth (acre-feet)</i>
Low River Flow	-106,144	-86
Medium River Flow	1,744,759	1,414
High River Flow	2,345,551	1,902

Influence of Parker' Cut and the Diversion Dam Cut on Sedimentation in West Matagorda Bay: Sample Comparison

Figures 42 and 43 depict the suspended sediment concentration resulting from a relatively small Colorado River flow event (with a peak discharge of 10,000 cfs). Unlike the average conditions depicted in Figures 39-41 these figures show a snapshot in time. Specifically, the figures show the system during flood-tide (i.e. peak flood-tide current velocity). Figure 42 depicts the existing conditions (Scenario A), whereas Figure 43 shows Scenario L (PK, 2-4'X350' and DDC, 4'X20') at the same moment in time. Note the elevated suspended sediment concentration just west and northwest of the entrance to Parker's Cut. The source of this sediment is actually the Colorado River. Some of the river flow is diverted through the locks and through the Diversion Dam Cut into the Old River Channel, and this sediment is then pumped back into West Matagorda Bay via Parker's Cut.

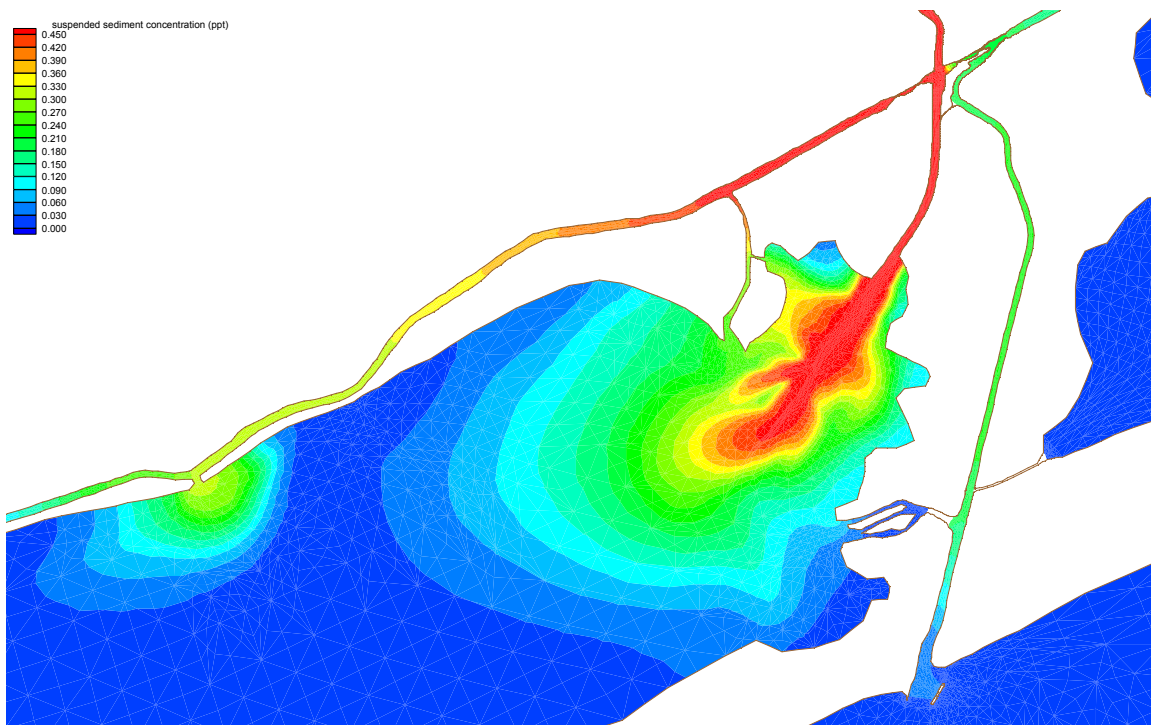


Figure 42: Snapshot of Suspended Sediment Concentration for Scenario A (Existing Conditions)

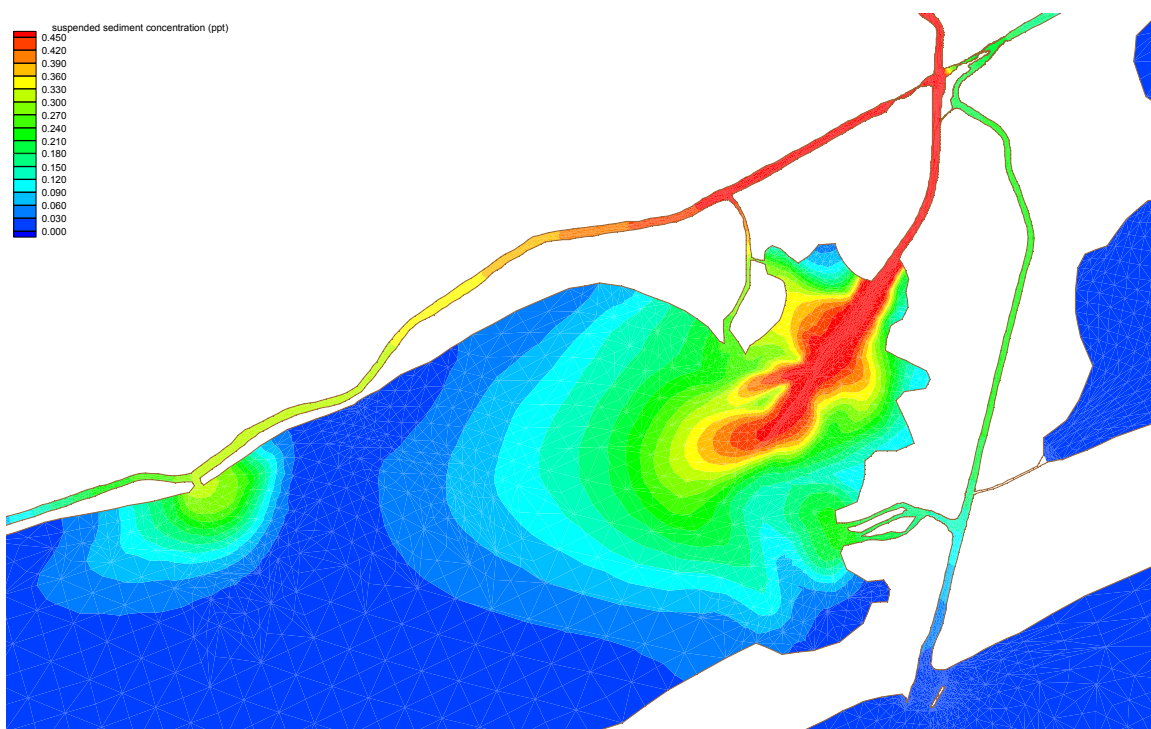


Figure 43: Snapshot of Suspended Sediment Concentration for Scenario L (PK, 2-4'X350', DDC, 4'X20')

Evaluation of Scenarios: Average Annual Bed Elevation Change Difference

Plates 67- 99 depict the average annual bed elevation difference between each design scenario and Scenario A (existing conditions), for each of the 3 flow year conditions. By examining these plates, several observations can be made.

- The Diversion Dam Cut appears to increase shoaling in both the Old River Channel, and in the ICWW east of the locks. This is apparently due to the diversion of Colorado River water during high flow events. This increase in shoaling could be mitigated by installing a gate structure on the west side of the cut (at the confluence with the diversion channel). The gate could be closed during high river flows, thus preventing sediment laden water from passing through the cut into the Old River Channel.
- There is a shoal that develops just west of Parker's Cut. This shoal consists primarily of Colorado River sediment that is pumped through the locks and/or the Diversion Dam Cut into the Old River Channel, and then back through Parker's Cut. It also results from changes in the circulation patterns in the bay as a consequence of the currents in Parker's Cut. Note that the historical shoal that existed at this location consisted primarily of coastal sediment. The coastal sediment source could be mitigated by designing Parker's Cut with a bedload sediment trap at the entrance (the dominant model of transport for the coastal sediment is bedload transport). This would involve designing a riprap-protected channel, with a riprap-protected sill at the eastern end of the cut. This design would inhibit most of the coastal sediment from reaching the Bay, and allow any Colorado River sediment in the Old river Channel to pass through the cut.
- Southwest Cut serves to increase erosion in the lower part of the Old River Channel. This is principally a result of the increased tidal current velocity in the Old River Channel south of the cut. Some increase in deposition is observed in the upper part of the Old River Channel, due to the slight decrease in the tidal currents induced north of the cut. This decrease in the current allows more of the Colorado River sediment to settle in the channel.

Table 11 gives the percent reduction of the rate of growth of the Colorado River Delta (relative to existing conditions) for 3 separate design configurations. Note that the changes for the Medium and High Flow scenarios are all small, and although the changes in the Low Flow year are larger, this year actually shows a small net erosion of the delta in the existing condition.

Table 11: Percent Reduction of the Rate of Growth of the Colorado River Delta Relative to Existing Conditions

	<i>Scenario D</i> <i>DDC, 4'X20'</i>	<i>Scenario M</i> <i>PK, 5'X100'</i>	<i>Scenario L</i> <i>PK, 2-4'X350':DDC, 4'X20'</i>
Low River Flow	0.29	4.93	4.36
Medium River Flow	1.48	0.10	1.42
High River Flow	0.79	0.09	0.70

Conclusions and Recommendations

- The largest reduction in peak currents at the ICWW-Bypass Channel Intersection is between 8-9%, for Scenario I (Parker's Cut, 2-4'X350', and Southwest Cut, 5'X100'). Only flood-tide currents greater than 2 fps were factored into the analysis, so that the influence of the various scenarios on the peak currents could be determined. These flood-tide currents are present in the intersection approximately 4-6% of the year.
- For a given cross-sectional area, Southwest Cut is more efficient than Parker's Cut at mitigating the peak flood-tide currents at the ICWW-Bypass Channel intersection.
- The results given for scenario D (Diversion Dam Cut, 4'X20') indicate that it has minimal impact on the flood-tide currents in the ICWW-Bypass Channel Intersection.
- The scenarios have little influence on the distribution of the velocities in the ICWW-Bypass Channel Intersection, and therefore the impact of each scenario can be comprehensively assessed by examining its influence on the flood-tide current magnitude.
- The percent increase in peak flood-tide currents at the Old River Channel Mouth is considerably greater than the percent reduction in peak flood-tide currents at the Bypass Channel-ICWW Intersection.
- The increase in peak flood-tide flow at the Old River Channel mouth indicates a general increase in the tidal currents at this location. This increase in currents will serve to increase the bed shear stress, and hence inhibit shoaling near the mouth.
- For a given scenario, an increase in the flood-tide dominance of residual currents at the Old Colorado River Mouth are a good indicator of the potential for increased coastal sediment transport into the Old River Channel, and hence additional shoaling in the channel. The scenarios that incorporate Parker's Cut tend to show a larger increase in the flood-tide current residual than do the other scenarios, for the low flow condition. The scenarios involving the Diversion Dam Cut all exhibit an increase in ebb-tide flow for the medium and high flow conditions.
- The peak velocities in Parker's Cut for the smallest configuration (4'X20') reach 3 fps. This velocity in a 20 foot wide channel could create navigation problems for small craft attempting to use the cut. The peak velocities are lower for the larger configurations.
- The minimum flood-tide residual discharge through Parker's Cut occurs for the 5'X100' configuration.
- Southwest Cut and Parker's Cut have little interdependence with respect to their influence on currents, salinity, or sediment transport. Therefore, the impact of each can effectively be modeled separately, and the impact of implementing both cuts can be estimated by superposition of the results.

- Apart from the influence of high flows on the Colorado River, the residual currents in Parker's Cut are always either neutral or flood-tide dominant. It demonstrates a pronounced flood-tide residual flow response to wind components from the east and Northeast. Southwest Cut responds to both east and west wind components. It is flood-tide dominant for North and Northeasterly winds, and ebb-tide dominant for south and southwesterly winds. There is a marked correlation between residual currents in Southwest Cut and seasonal winds.
- In general, Parker's Cut will have a tendency to entrain more coastal sediment into the Old River Channel mouth when coastal sediment transport rates are highest, whereas Southwest Cut will have a tendency to push the sediment back towards the Gulf at these times.
- None of the proposed design scenarios will redirect greater than 3% of the Colorado River discharge from West Matagorda Bay to the Old River Channel.
- The Diversion Dam Cut has no measurable impact on the salinity of the system.
- Parker's Cut demonstrates a more spatially confined impact on changes in bay salinity than does Southwest Cut. The westward extent of the 1ppt salinity difference contour for Parker's Cut ranges between 0.8 and 2.3 miles from the connection between Parker's Cut and West Matagorda Bay. The magnitude of the impact is greater for Parker's Cut than for Southwest Cut, reaching as much as 8 ppt in the immediate vicinity of the connection between Parker's Cut and West Matagorda Bay.
- None of the scenario configurations of Parker's Cut have significant influence on the location of the average springtime mesohaline zone in the Bay.
- The Diversion Dam Cut appears to increase shoaling in both the Old River Channel, and in the ICWW east of the locks. This is apparently due to the diversion of Colorado River water during high flow events.
- The sediment transport model indicates that a shoal develops just west of Parker's Cut. This shoal consists primarily of Colorado River sediment that is pumped through the locks and/or the Diversion Dam Cut into the Old River Channel, and then back through Parker's Cut. It also results from changes in the circulation patterns in the bay as a consequence of the currents in Parker's Cut.
- Southwest Cut serves to increase erosion in the lower part of the Old River Channel. This is principally a result of the increased tidal current velocity in the Old River Channel south of the cut. Some increase in deposition is observed in the upper part of the Old River Channel, due to the slight decrease in the tidal currents induced north of the cut. This decrease in the current allows more of the Colorado River sediment to settle in the channel.
- The percent reduction in the rate of growth of the Colorado River Diversion delta for the Medium and High Flow years is less than 2% in all cases. The changes in the Low Flow year are larger (up to 5%), but the Low Flow year actually shows a small net erosion of the delta in the existing condition.
- If Parker's Cut is implemented, it should be designed to inhibit bedload sediment transport from the Old River Channel into West Matagorda Bay. This would involve designing a riprap-protected channel, with a riprap protected sill at the eastern end of the cut. A small existing embayment at the eastern end of Parker's Cut would then serve as a sediment trap, and may require maintenance dredging. This design would inhibit most of the

coastal sediment from reaching the Bay, and allow any Colorado River sediment in the Old River Channel to pass through the cut.

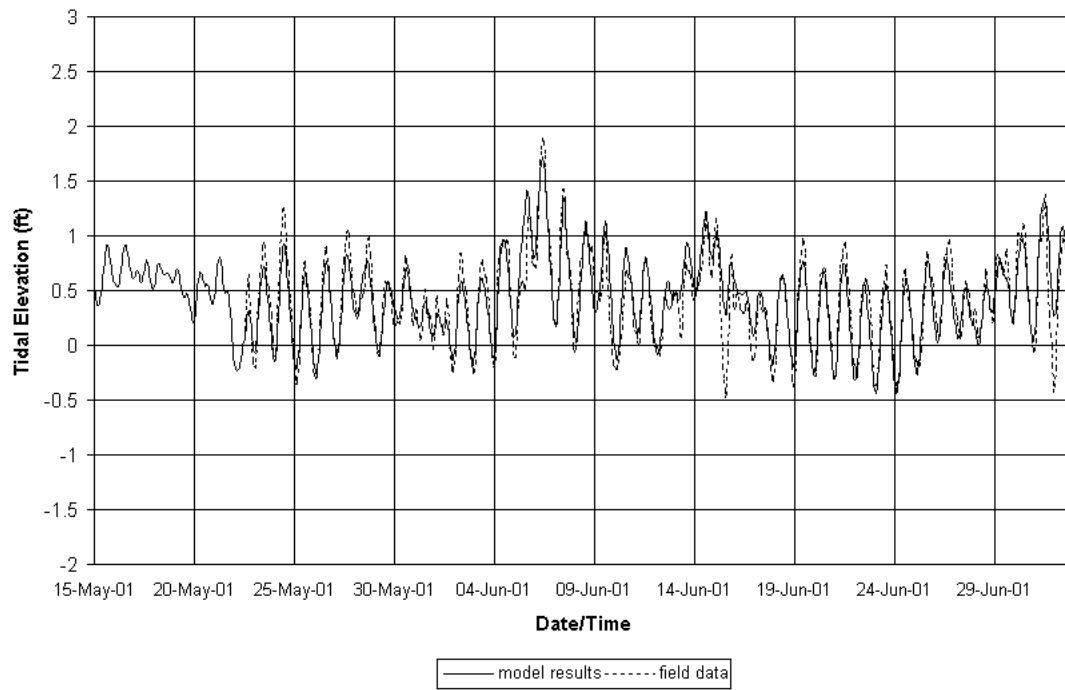
- For the Diversion Dam Cut, the increase in shoaling observed in the Old River Channel could be mitigated by installing a gate structure on the west side of the cut (at the confluence with the diversion channel). The gate could be closed during high river flows, thus preventing sediment laden water from passing through the cut into the Old River Channel.
- Any design selected here should be evaluated with coastal sediment transport model, equipped with the ability to model bedload transport, in order to determine the effect of the design on shoaling and erosion in the Old Colorado River channel and at the Colorado River jetties.

References

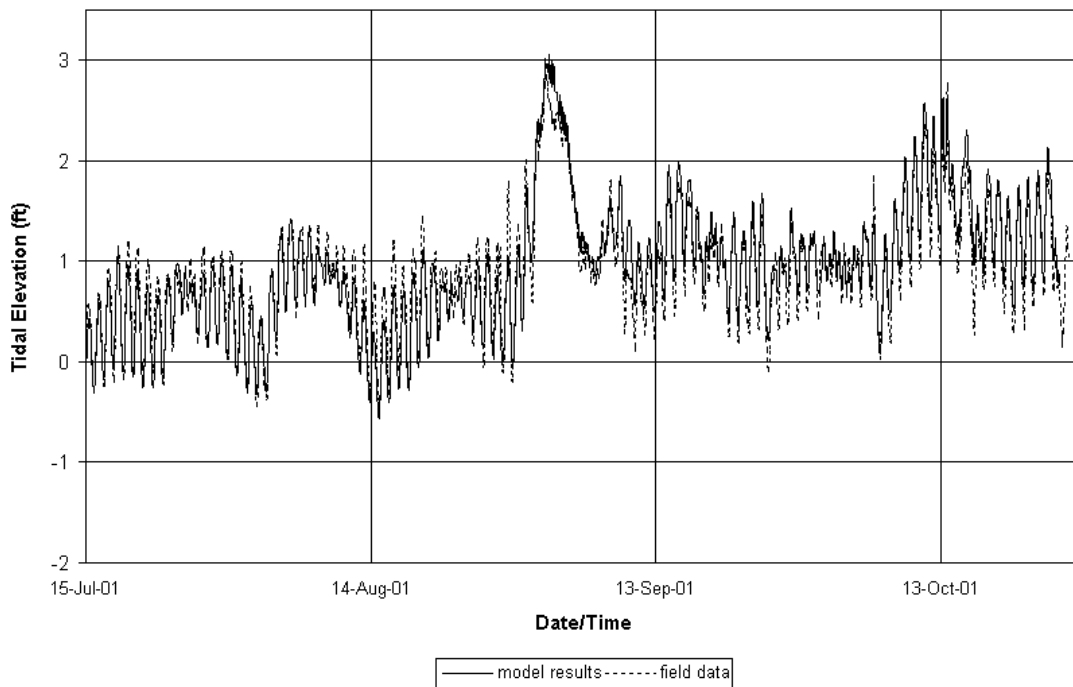
- Bass, Bob (2002) Personal Communication
- Chow, V. T. (1959) "Open Channel Hydraulics". McGraw-Hill, New York.
- King, I.P. (1988) "A Finite Element Model for Three-Dimensional Hydrodynamic System", report prepared by Resource Management Associates, Lafayette California, for U.S. Army Corps of Engineers, Waterways Experiment Station, Vicksburg, MS.
- King, I.P. (1993). "RMA-10, a finite element model for three-dimensional density stratified flow," Department of Civil and Environmental Engineering, University of California, Davis.
- King, D. B., and Prickett, T. L. (1998) "Mouth of the Colorado River Texas, Monitoring Program" Technical report CHL-98-2, prepared for the U.S. Army Corps of Engineers.
- Kraus, N. C., Mark, D. J., and Sarruff, M. S. (2000). "DMS: Diagnostic Modeling System, Report 1, Reduction of sediment shoaling by relocation of the Gulf Intracoastal Waterway, Matagorda Bay, Texas." Technical Report CHL-99-19, U.S. Army Corps of Engineer Waterways Experiment Station, Vicksburg, MS.
- Kraus, N. C., and Militello, A. (1996). "Hydraulic feasibility of proposed Southwest Corner Cut, East Matagorda Bay, Texas." Technical Report TAMU-CC-CBI-96-03, Conrad Blucher Institute for Surveying and Science, Texas A&M University-Corpus Christi, Corpus Christi, Texas.
- Lin, L., Kraus, N. C., and Barcak, R.G. (2002). "Predicting hydrodynamics of a proposed multiple-inlet system, Colorado River, Texas." Proceedings of 7th Coastal and Estuarine Modeling Conference '02, American Society of Civil Engineers, 837-851.
- McCollum, Randy (2000). "Navigation study, Colorado Locks, Colorado River, Matagorda, Texas." Technical Report ERDC/CHL TR-00-26, Engineer Research and Development Center, Waterways Experiment Station, Vicksburg, MS.
- Smagorinsky, J. (1963). "General Circulation Experiments with the Primitive Equations." "Monthly Weather Review", Vol. 93, pp 99 – 165.
- Teeter, A.M., Brown, G. L., Alexander, M. P., Callegan, C. J., Sarruff, M. S., McVan, D. C. (2002) 'Wind-Wave Resuspension and Circulation of Sediment and Dredged Material in Laguna Madre, Texas" U. S. Army Corps of Engineers, Engineer Research and Development Center, Draft Report.

- Teeter, A. M., Johnson, B. H., Berger, C., Stelling, G., Scheffner, N. W., Garcia, M. H., Parchure, T. M.,(2001) “Hydrodynamic and Sediment Transport Modeling With Emphasis on Shallow-water, Vegetated Areas (Lakes, Reservoirs, Estuaries, and Lagoons)”. *Hydrobiologia* 444: 1-23.
- U. S. Army Engineer District, Galveston (1981) “Mouth of Colorado River, Texas, Phase I: General Design Memorandum and Environmental Impact statement (Diversion Features)”
- Willmott, C. J. (1982) “Some Comments on the Evaluation of Model Performance”
Bulletin of the American Meteorological Society, Volume 63, Number 11, pp 1309-1310.

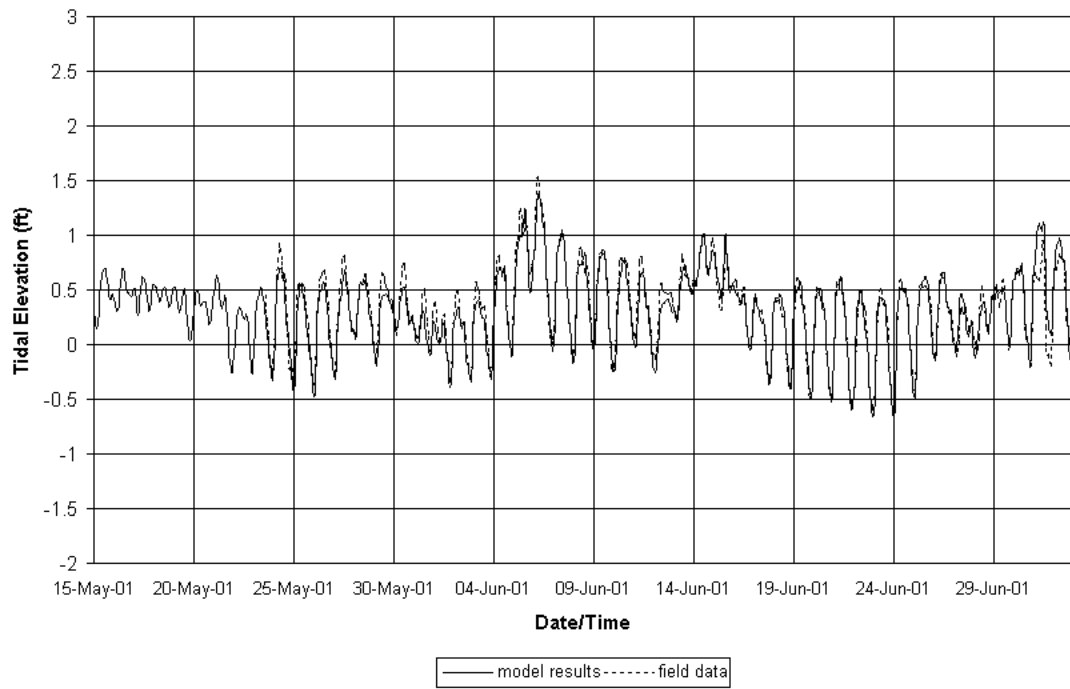
Station 1



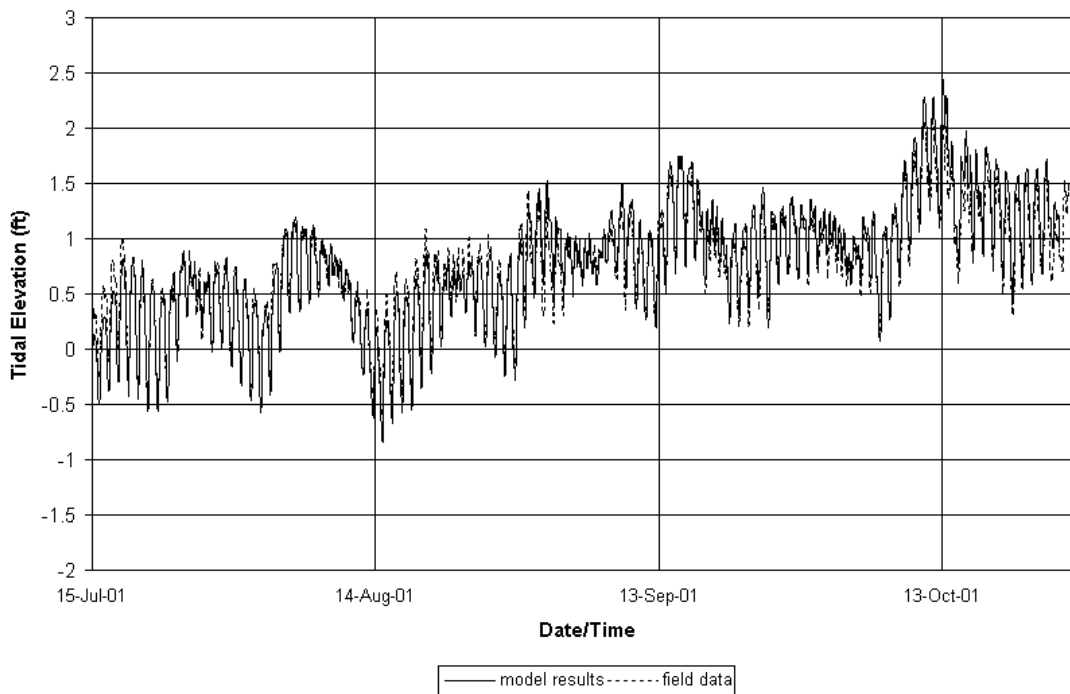
Station 1



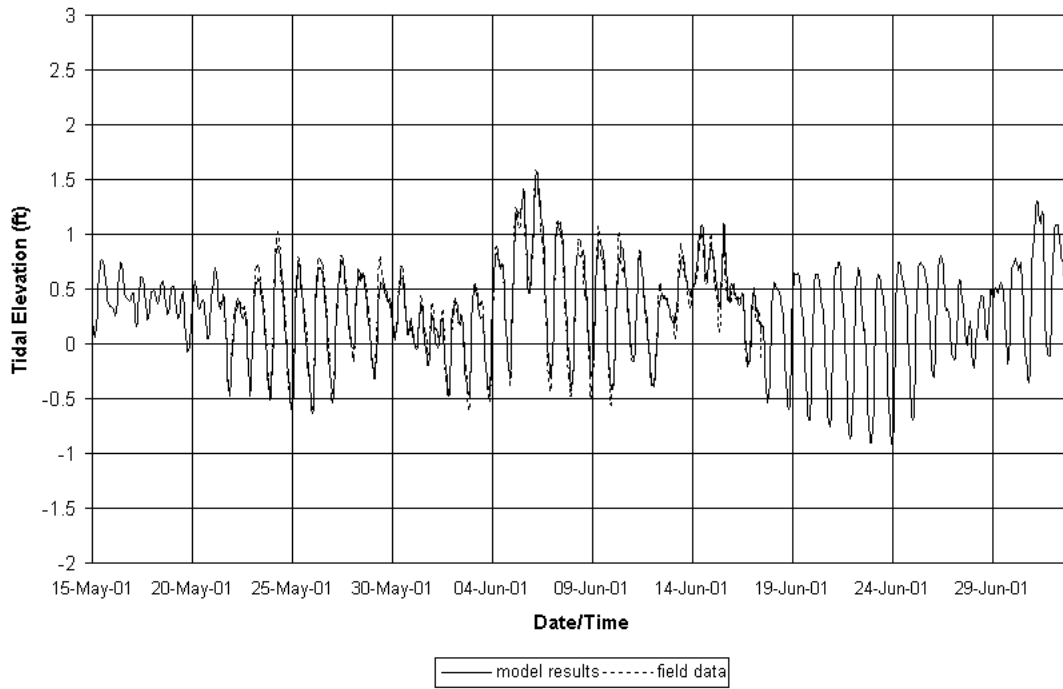
Station 2



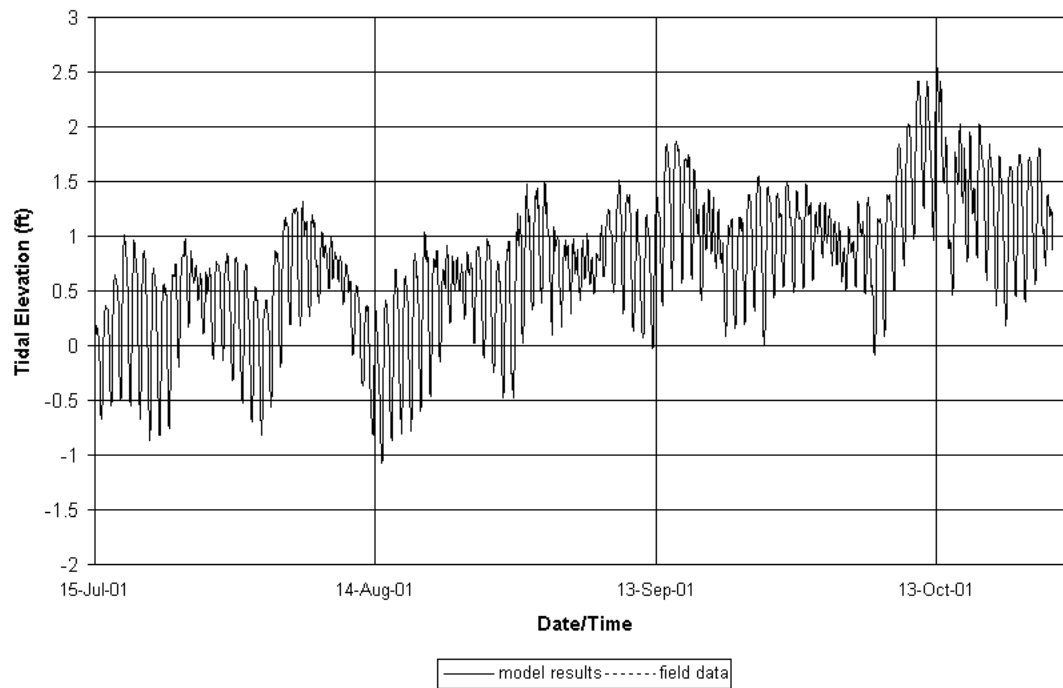
Station 2



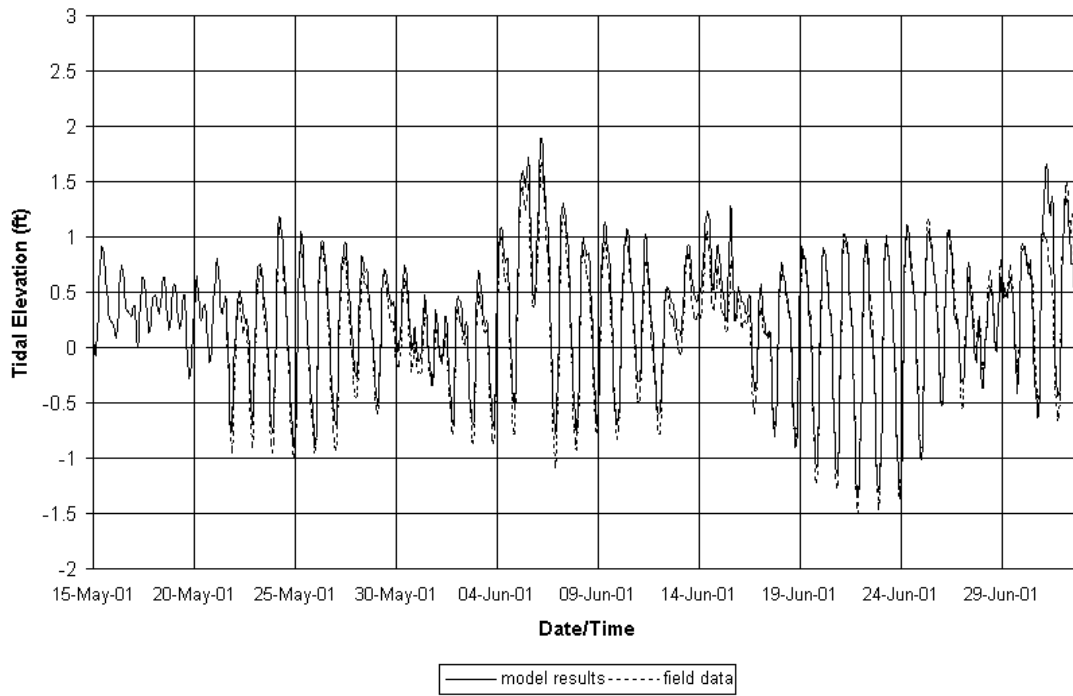
Station 3



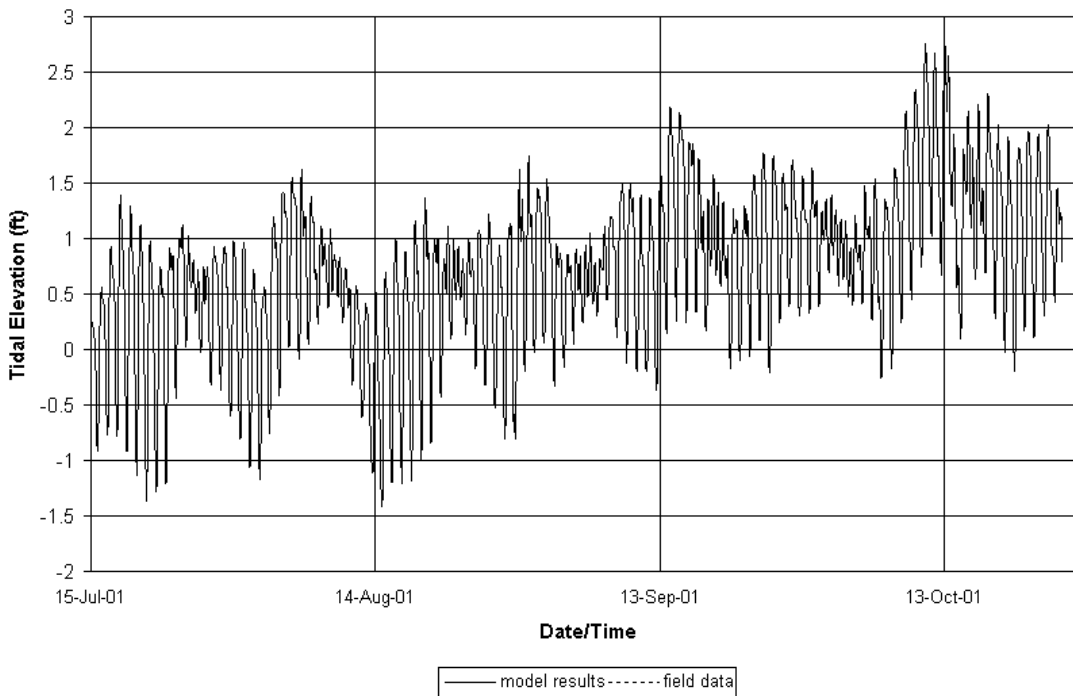
Station 3



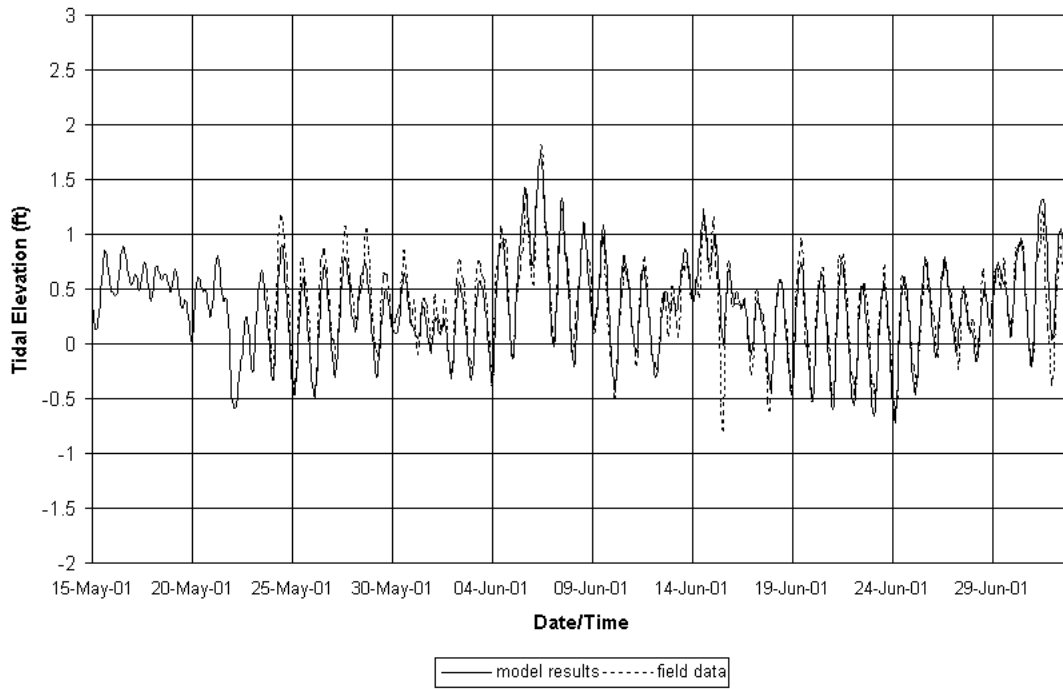
Station 4



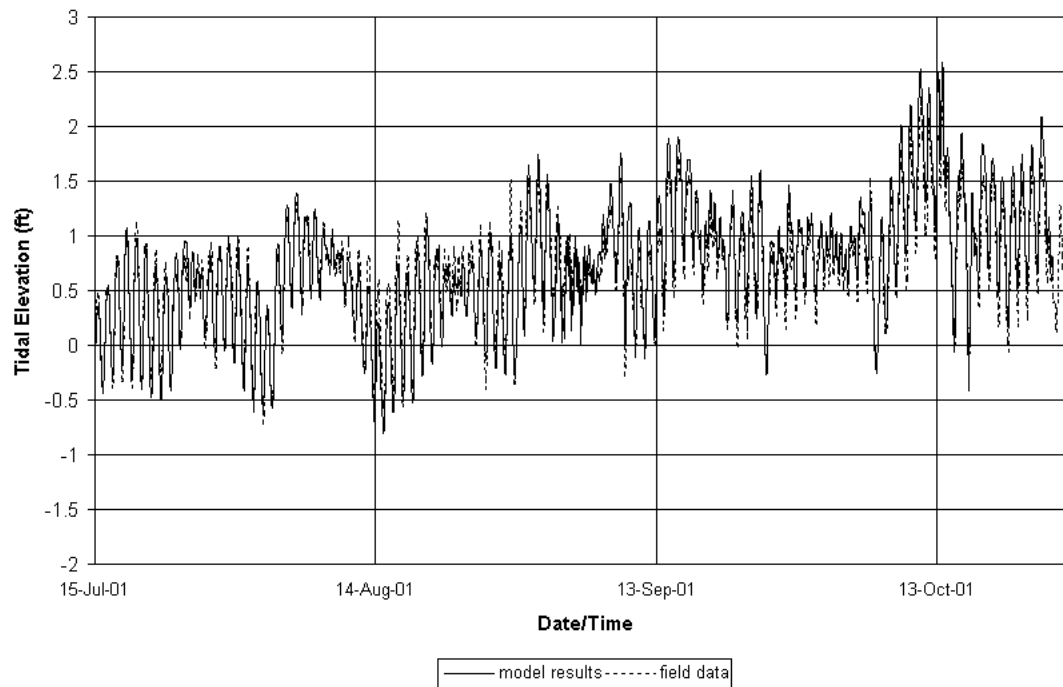
Station 4



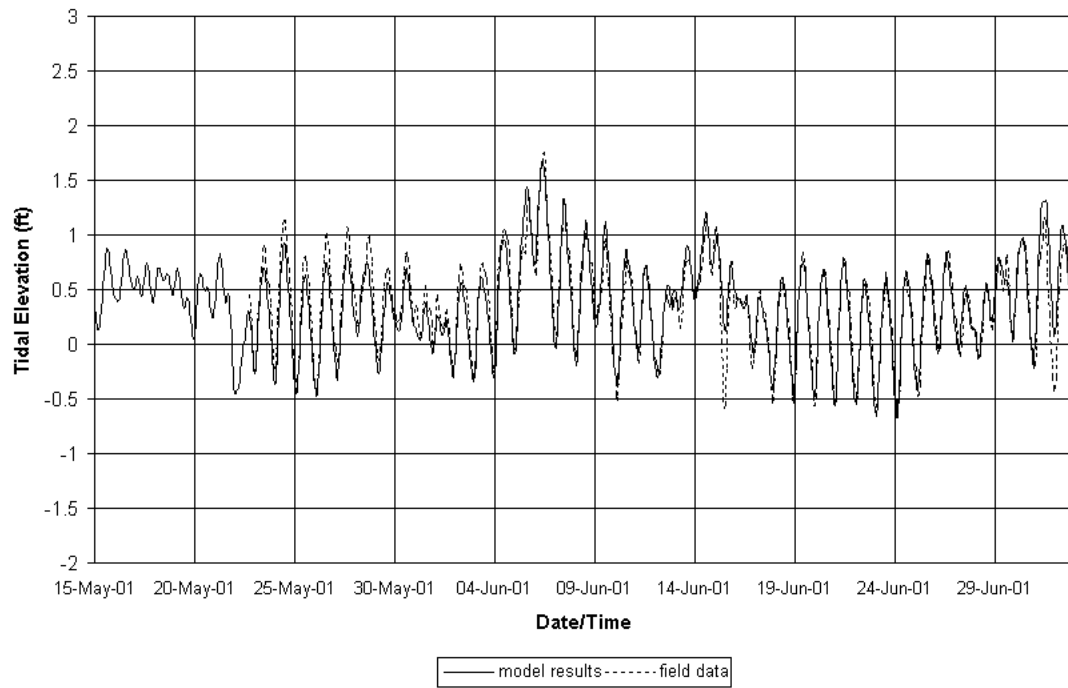
Station 5



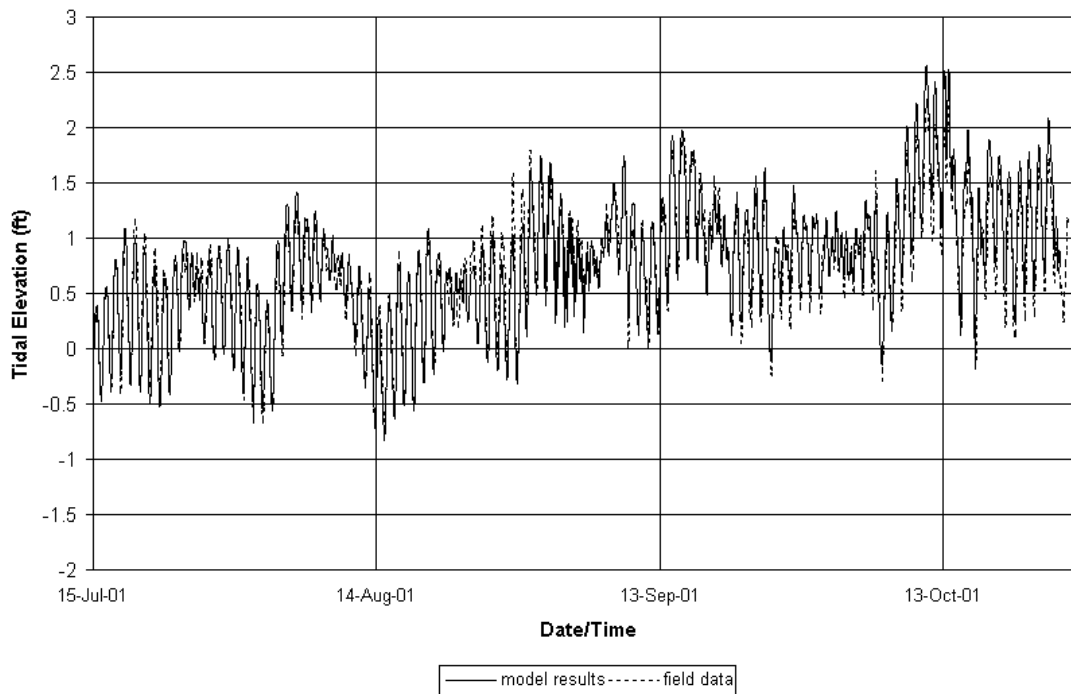
Station 5



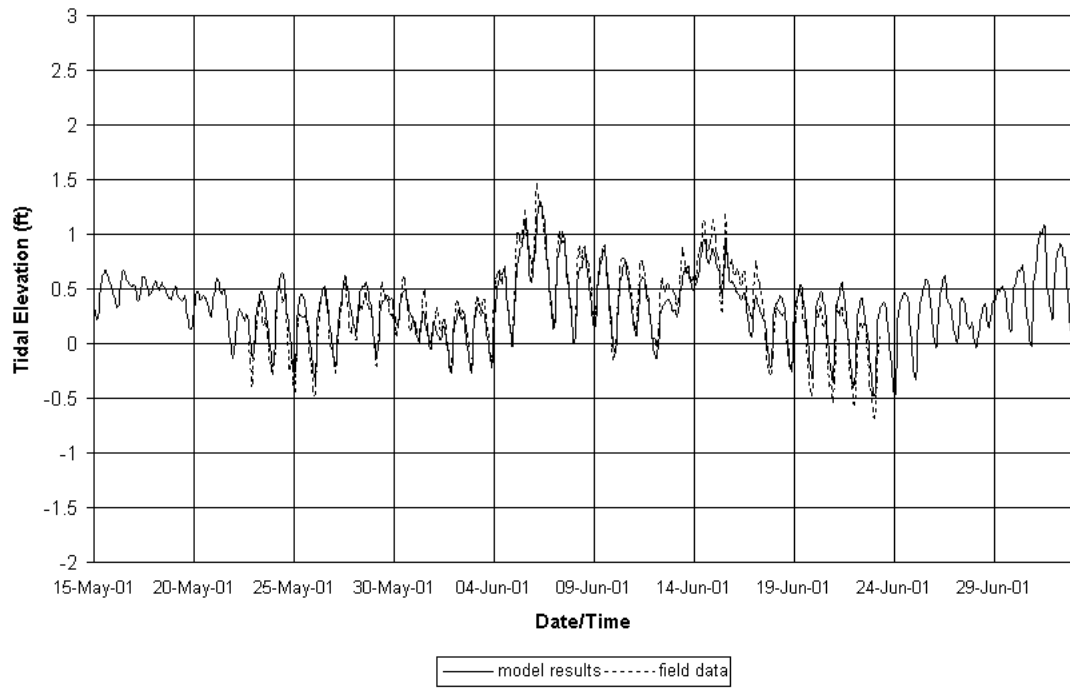
Station 6



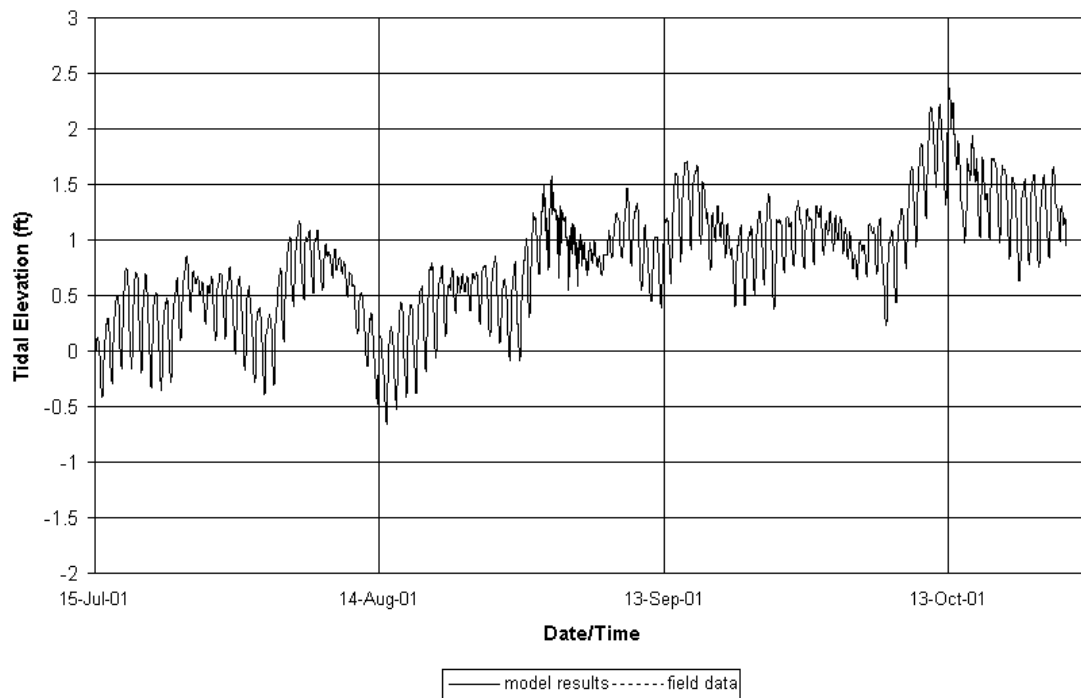
Station 6



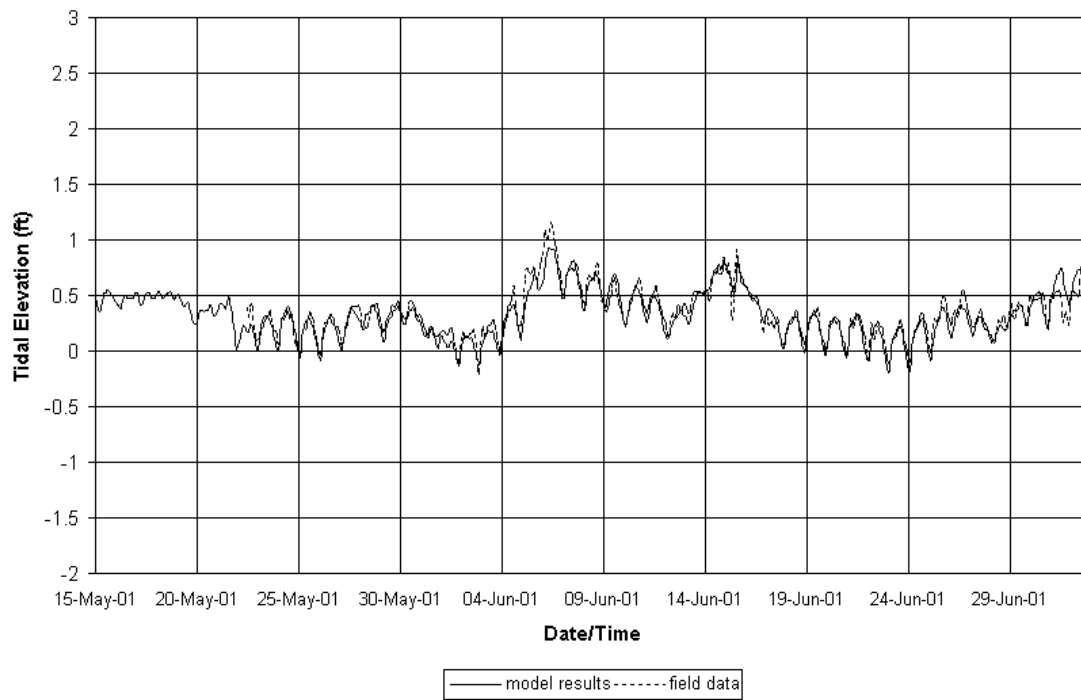
Station 7



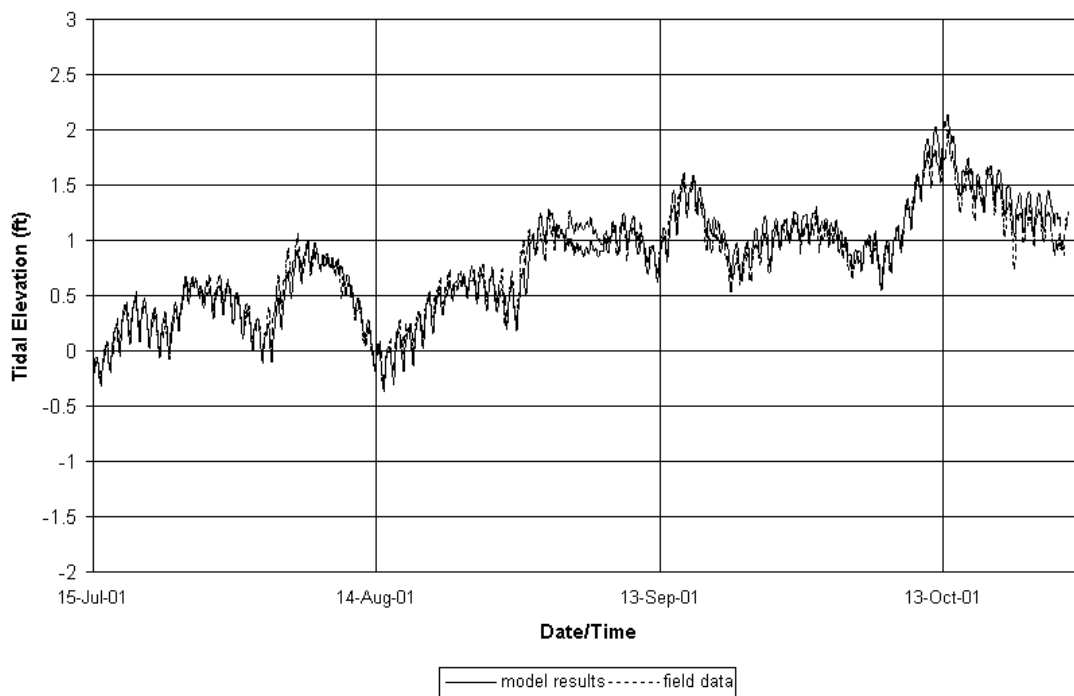
Station 7



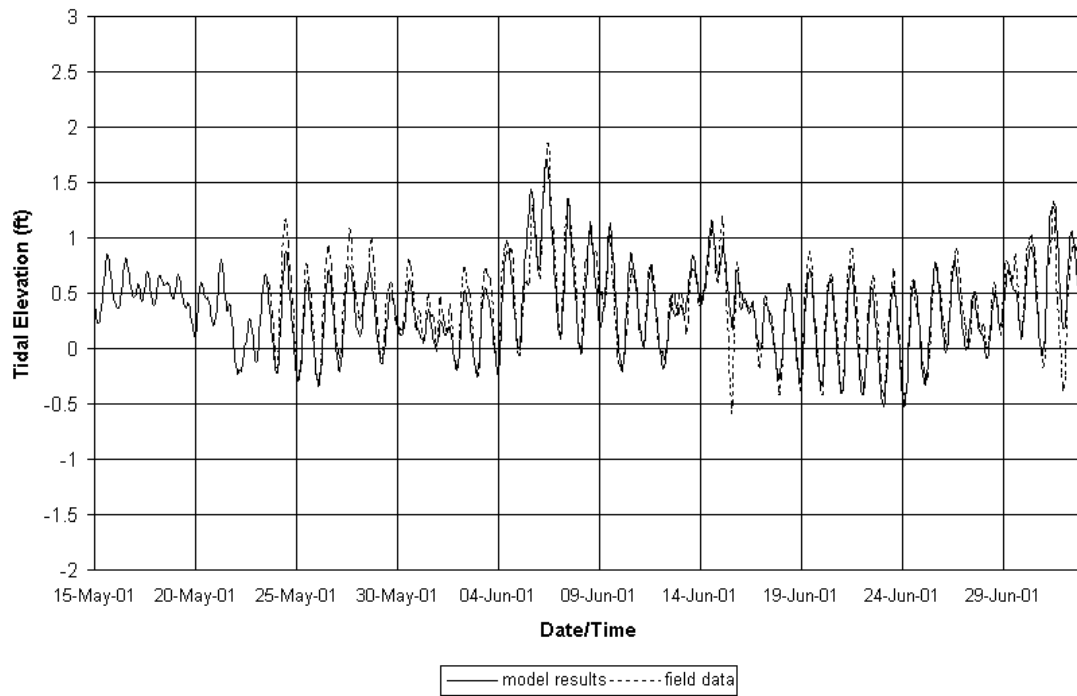
Station 8



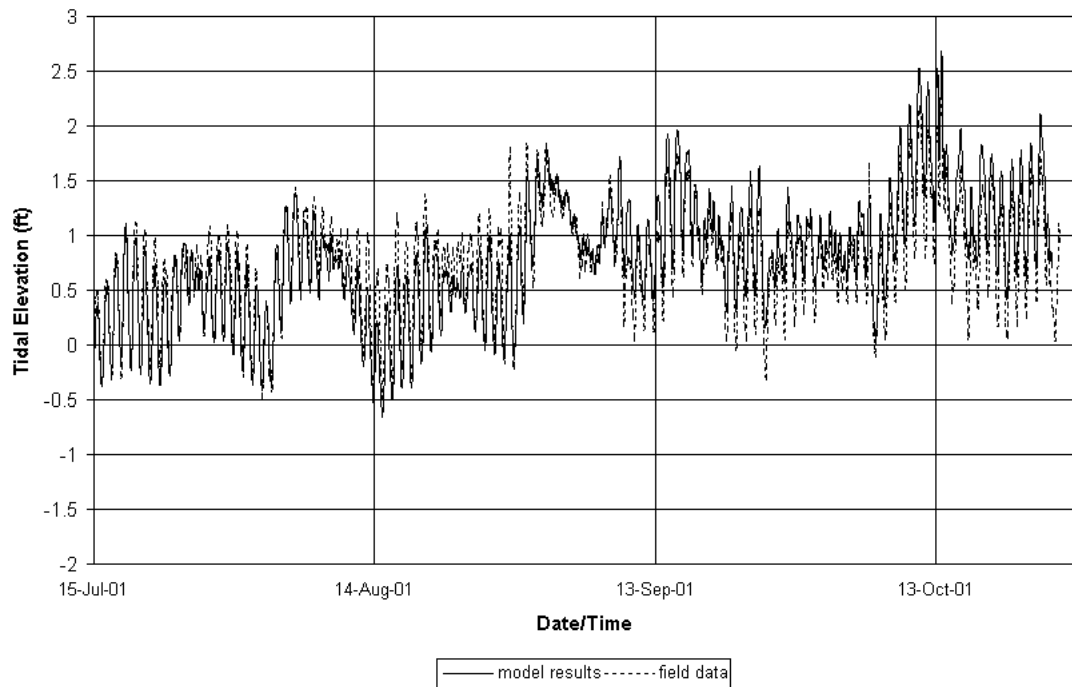
Station 8



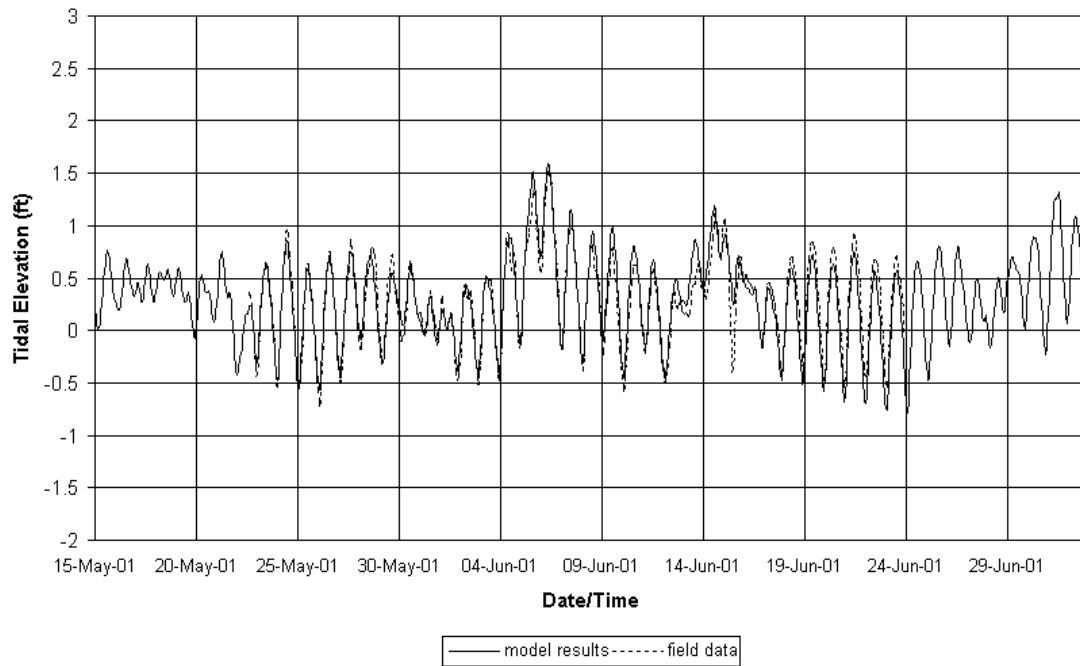
Station 9



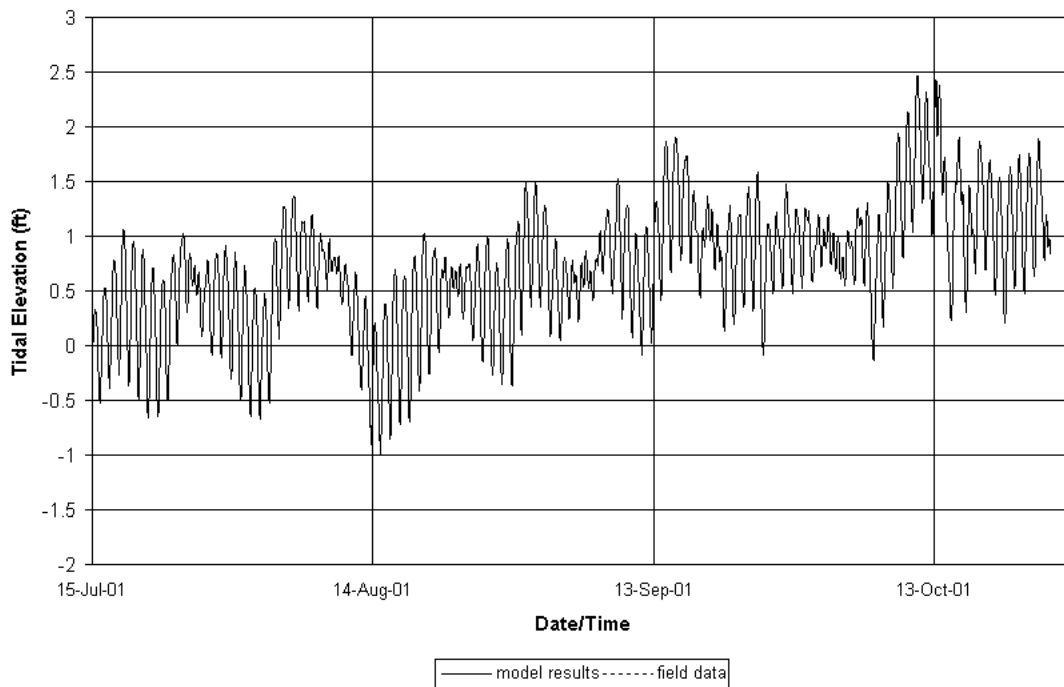
Station 9



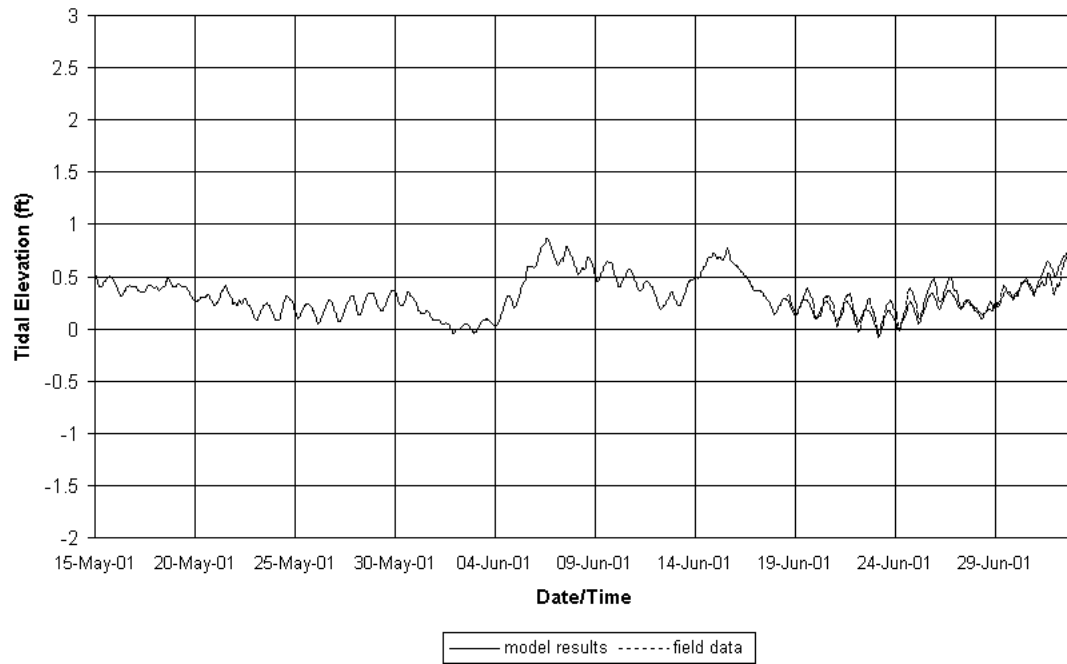
Station 10



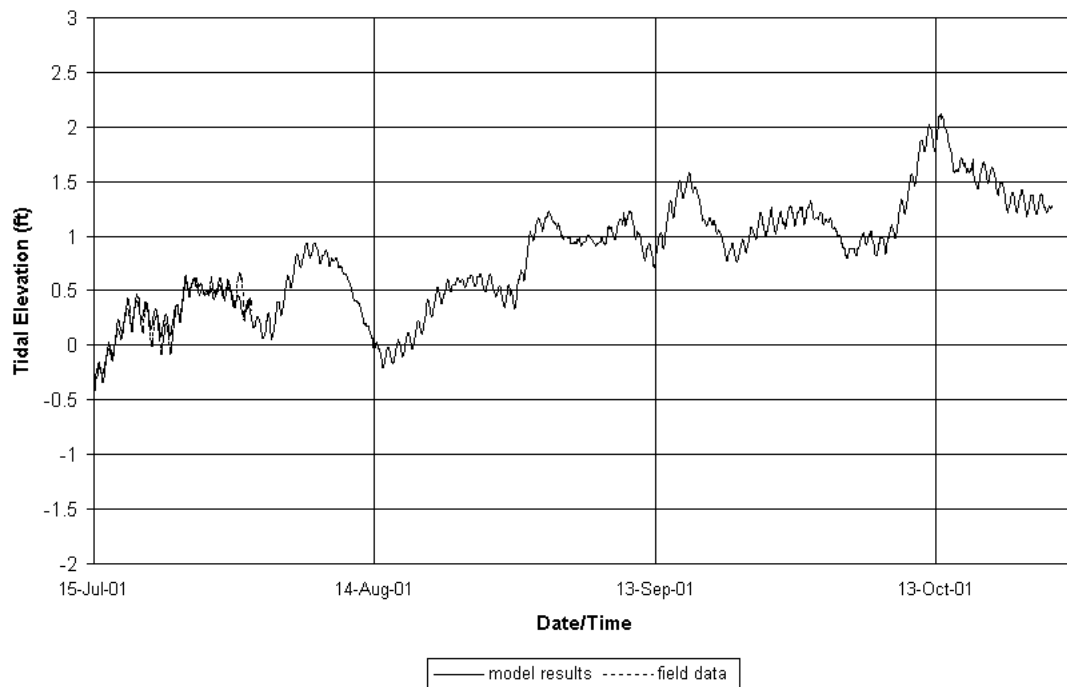
Station 10



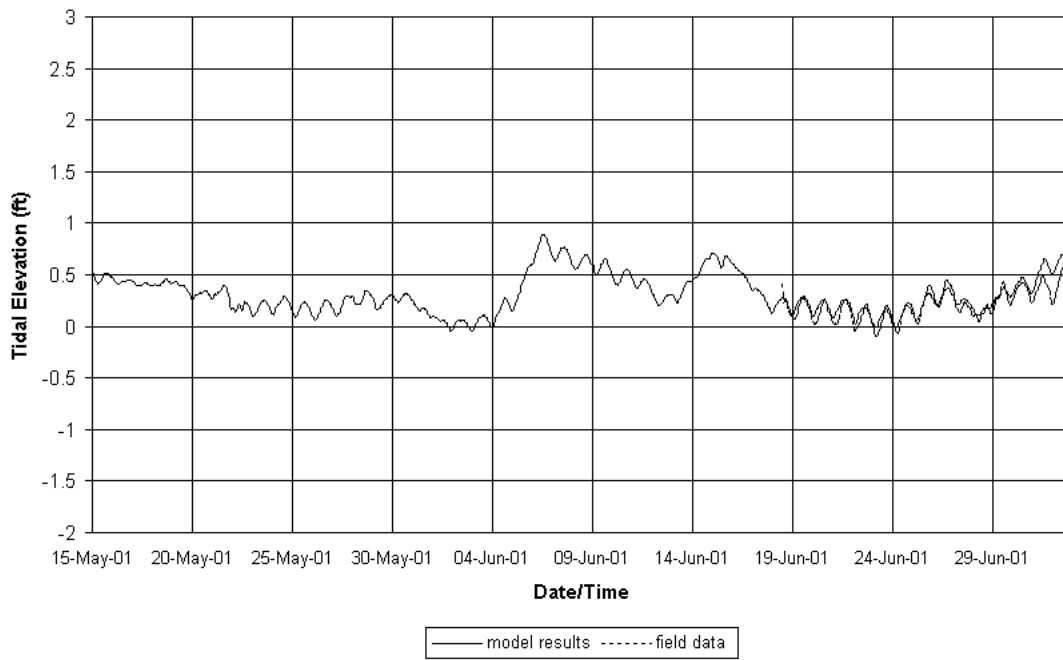
Station 11



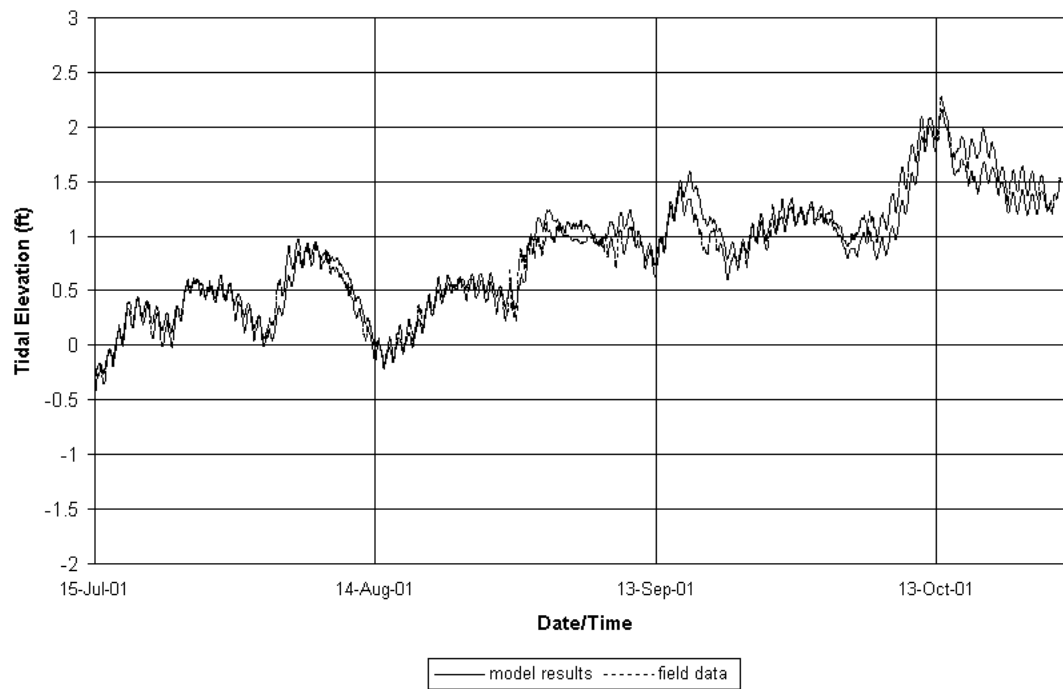
Station 11



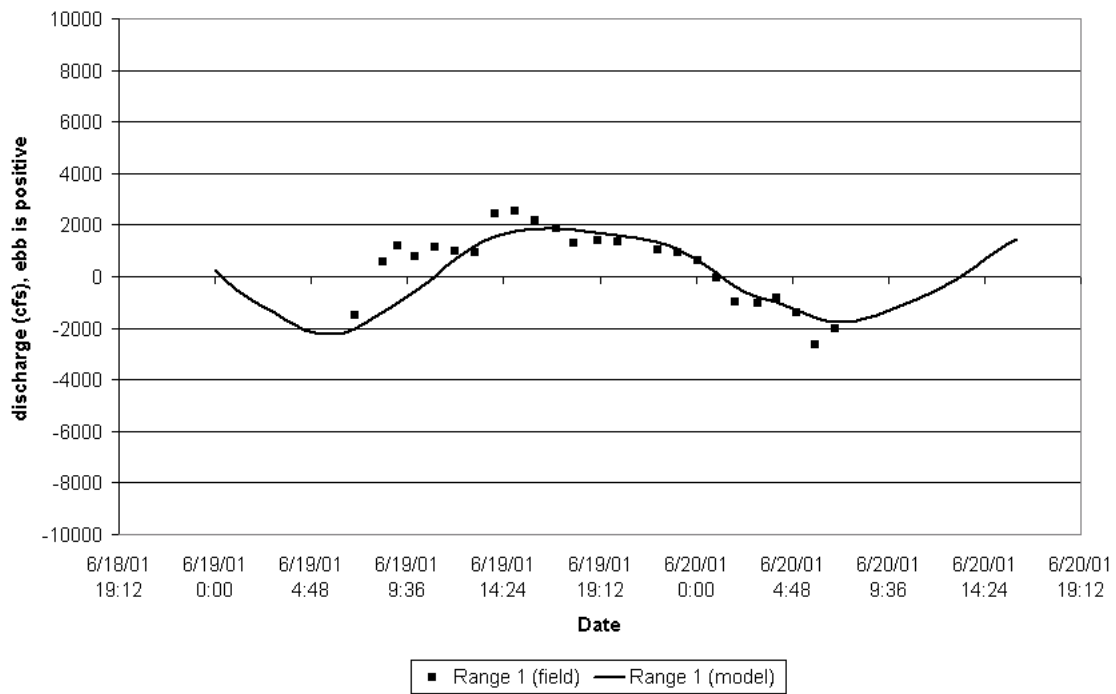
Station 12



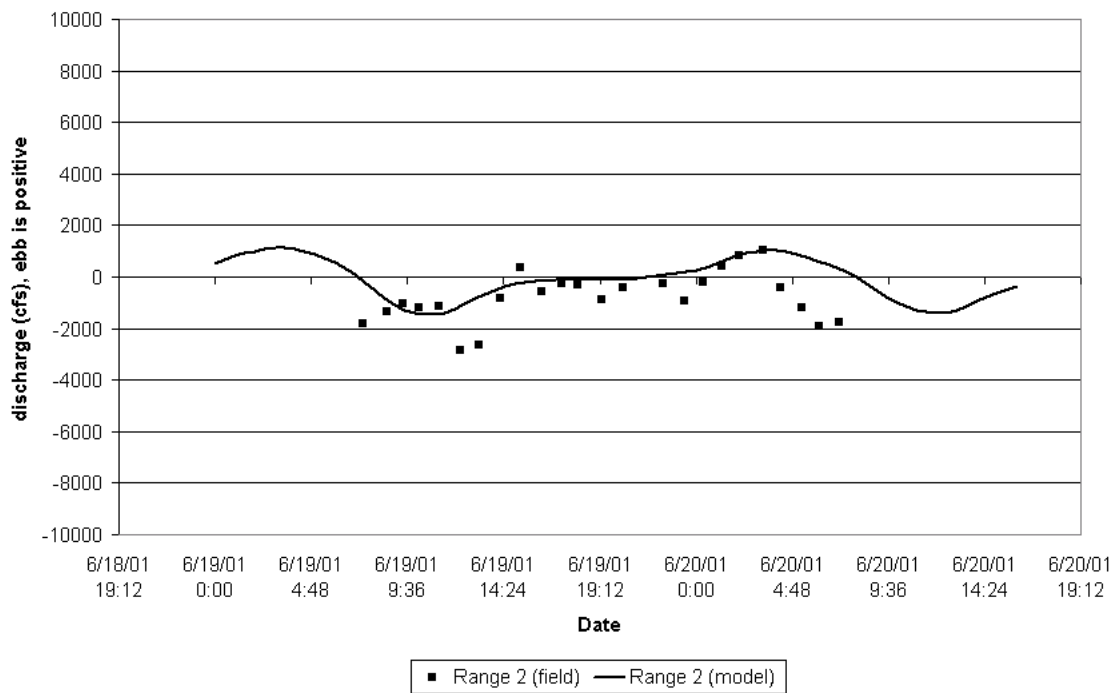
Station 12



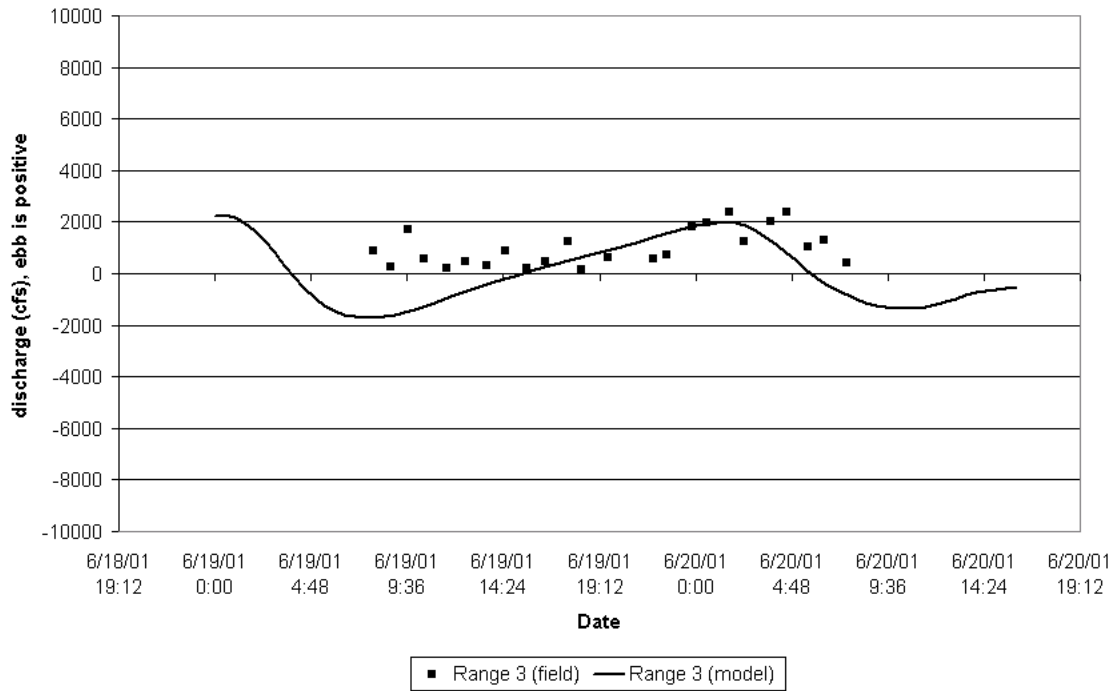
Discharge Comparison at Range 1



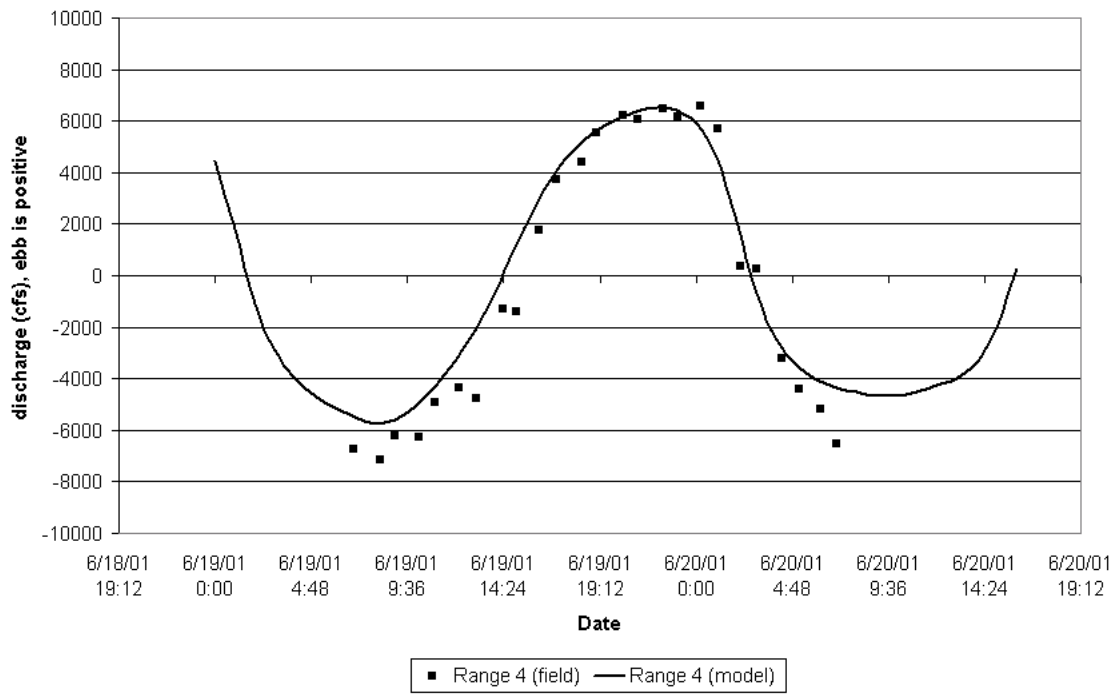
Discharge Comparison at Range 2



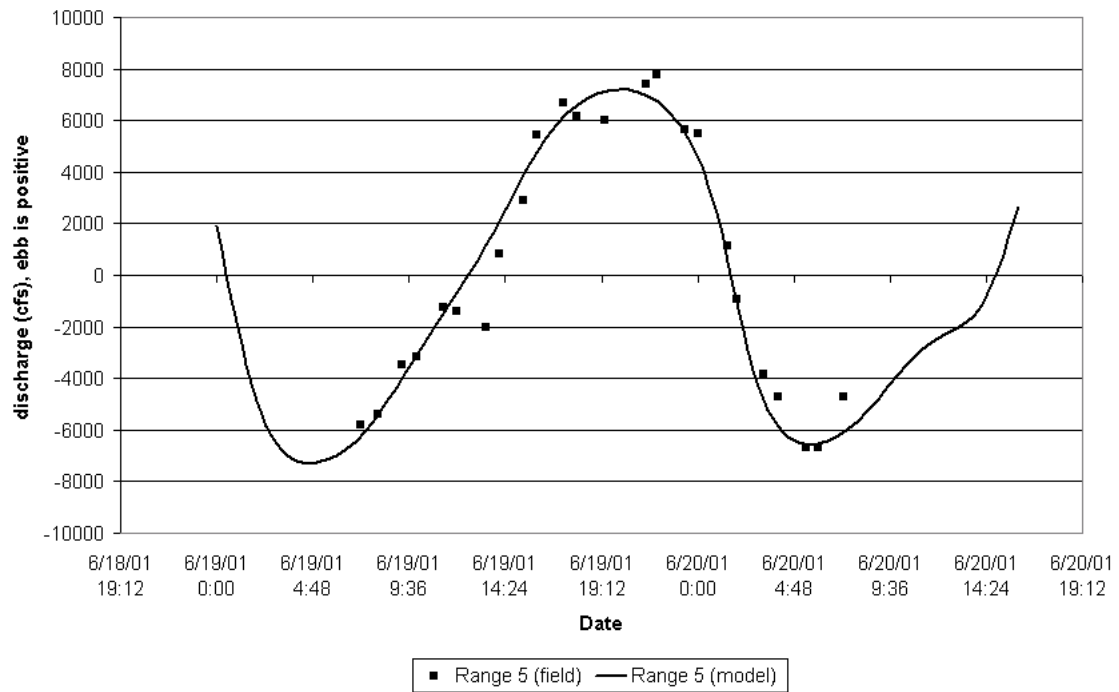
Discharge Comparison at Range 3



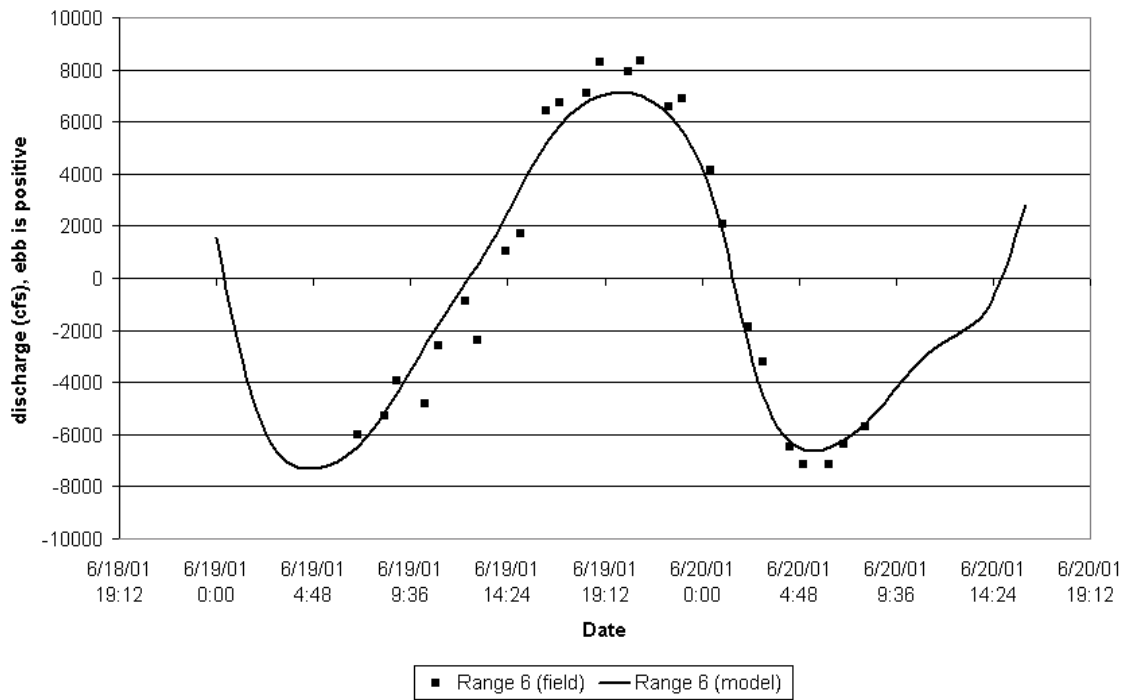
Discharge Comparison at Range 4



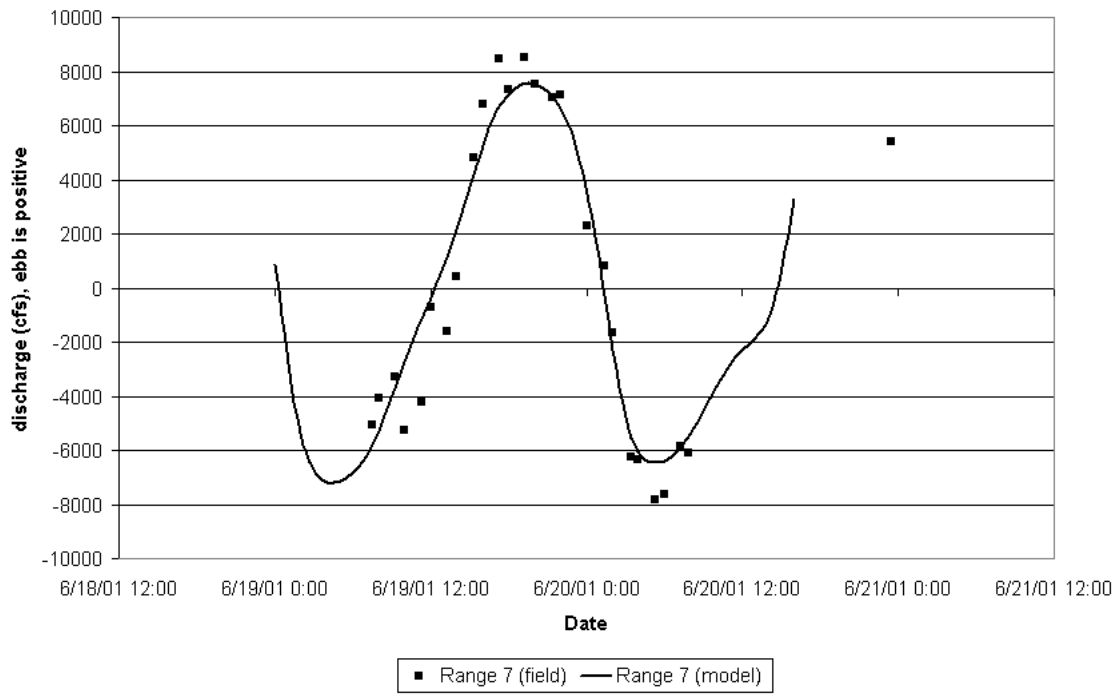
Discharge Comparison at Range 5



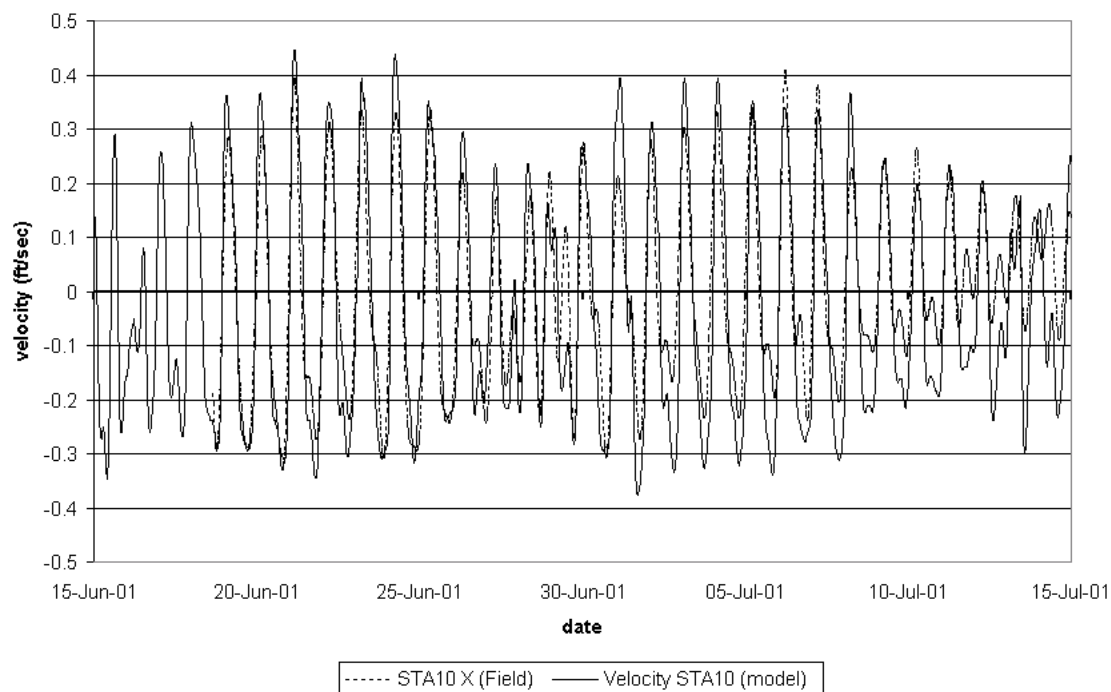
Discharge Comparison at Range 6



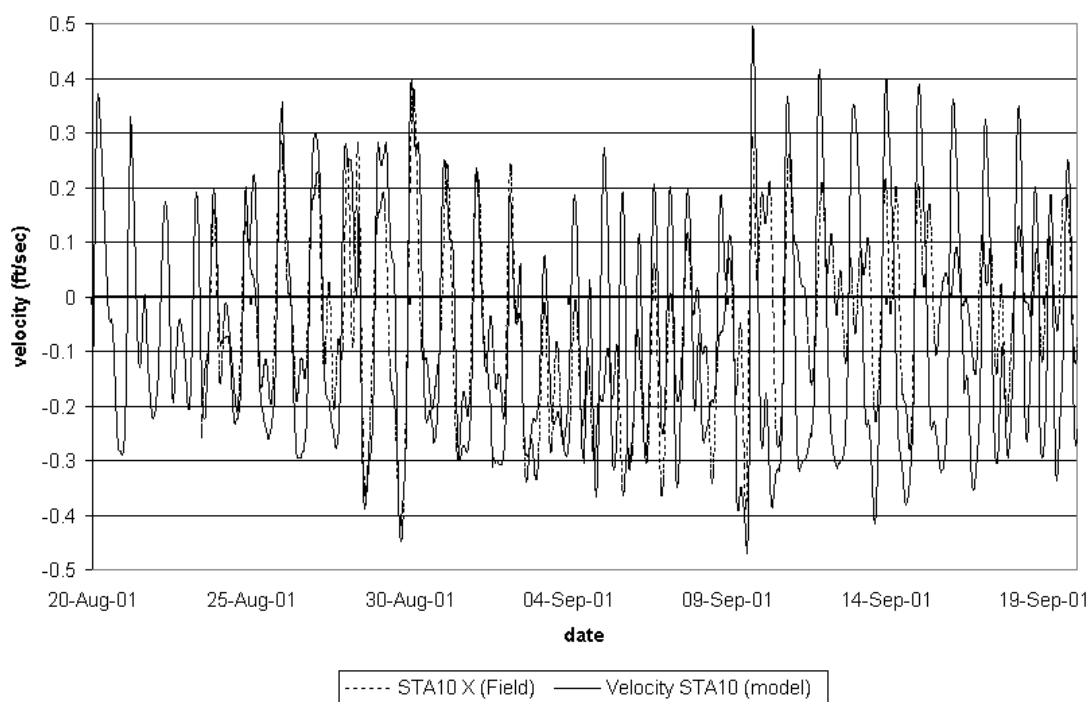
Discharge Comparison at Range 7



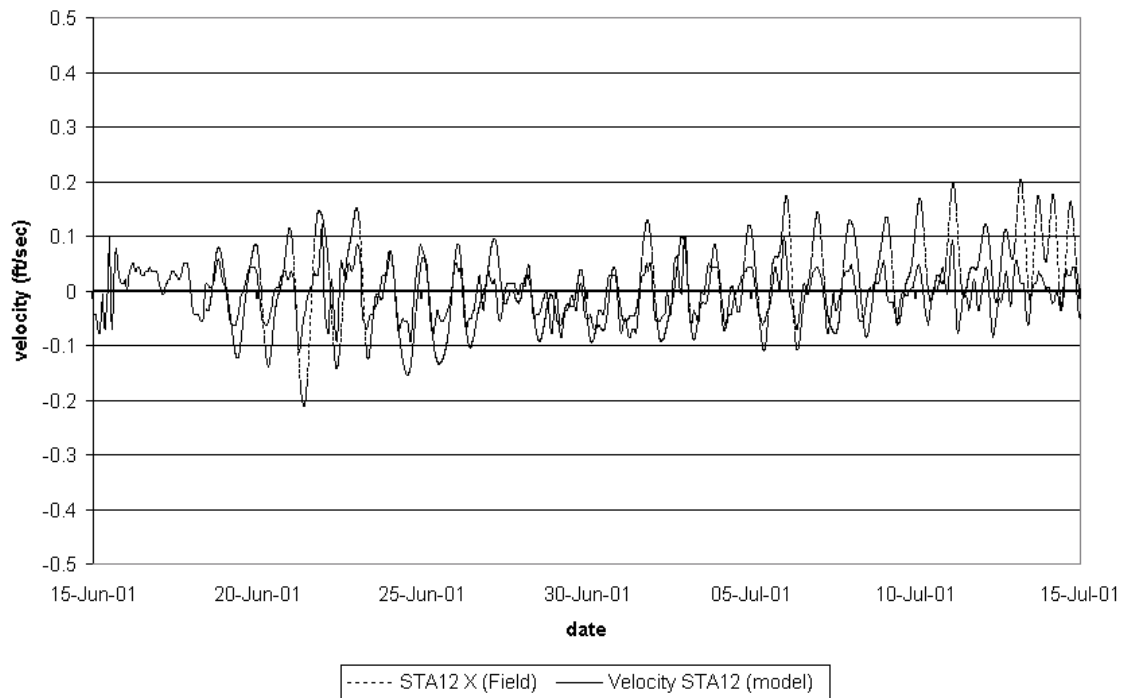
Velocity Comparison at STA 10 (West West Matagorda Bay)



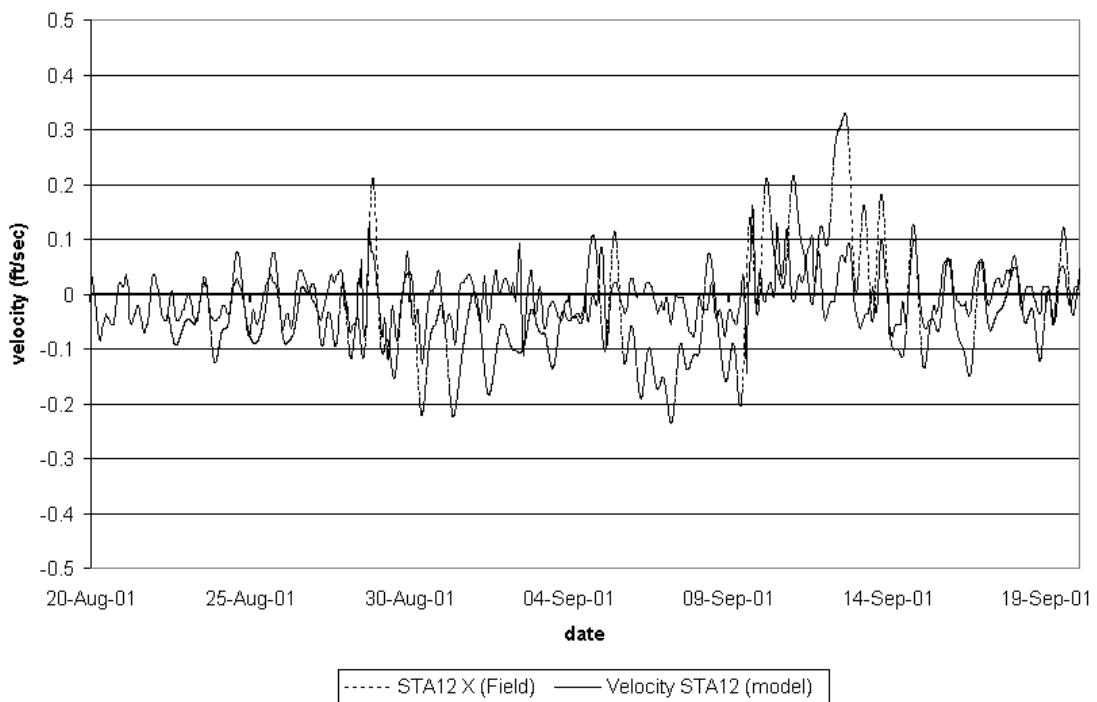
Velocity Comparison at STA 10 (West West Matagorda Bay)



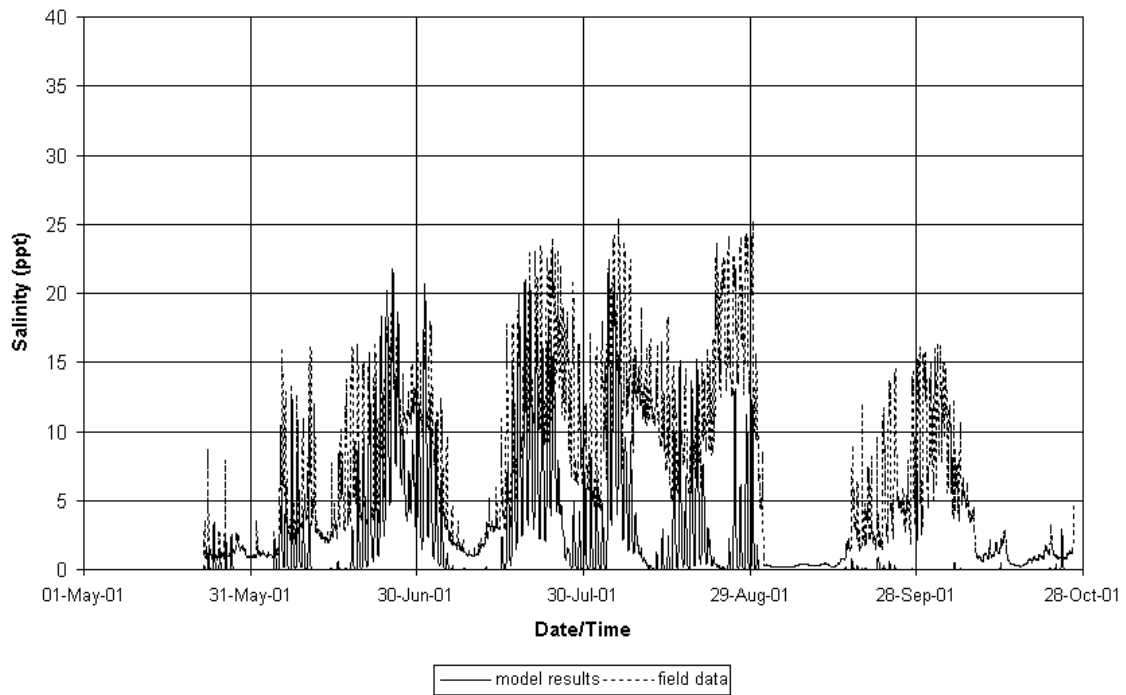
Velocity Comparison at STA 12 (East East Matagorda Bay)



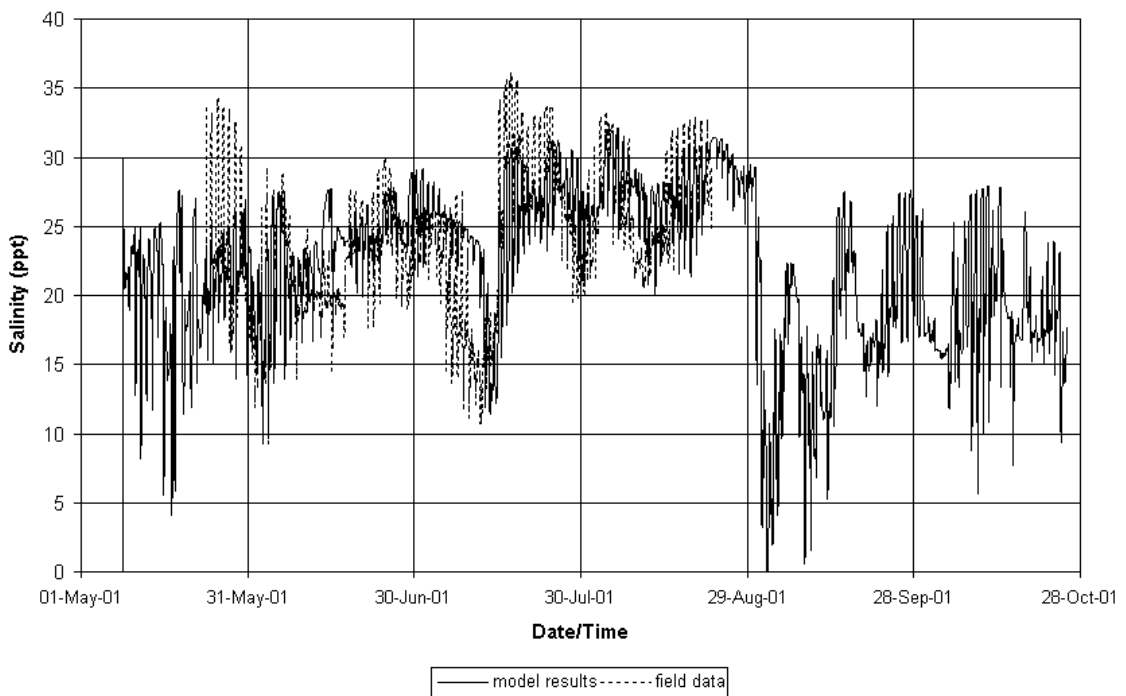
Velocity Comparison at STA 12 (East East Matagorda Bay)



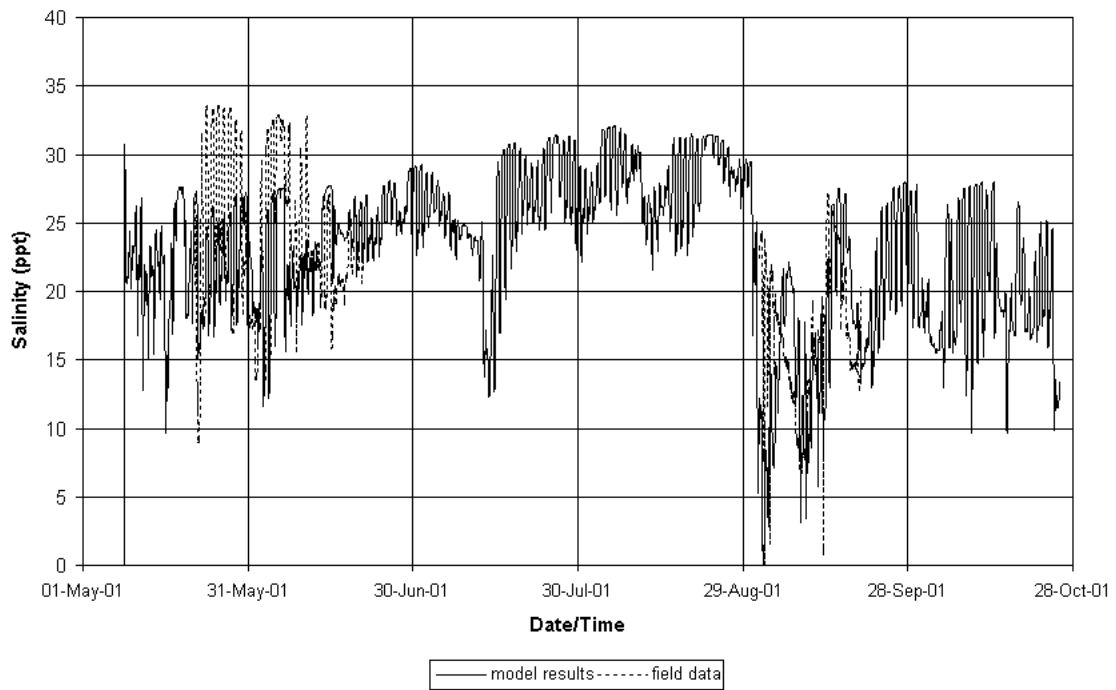
Station 1



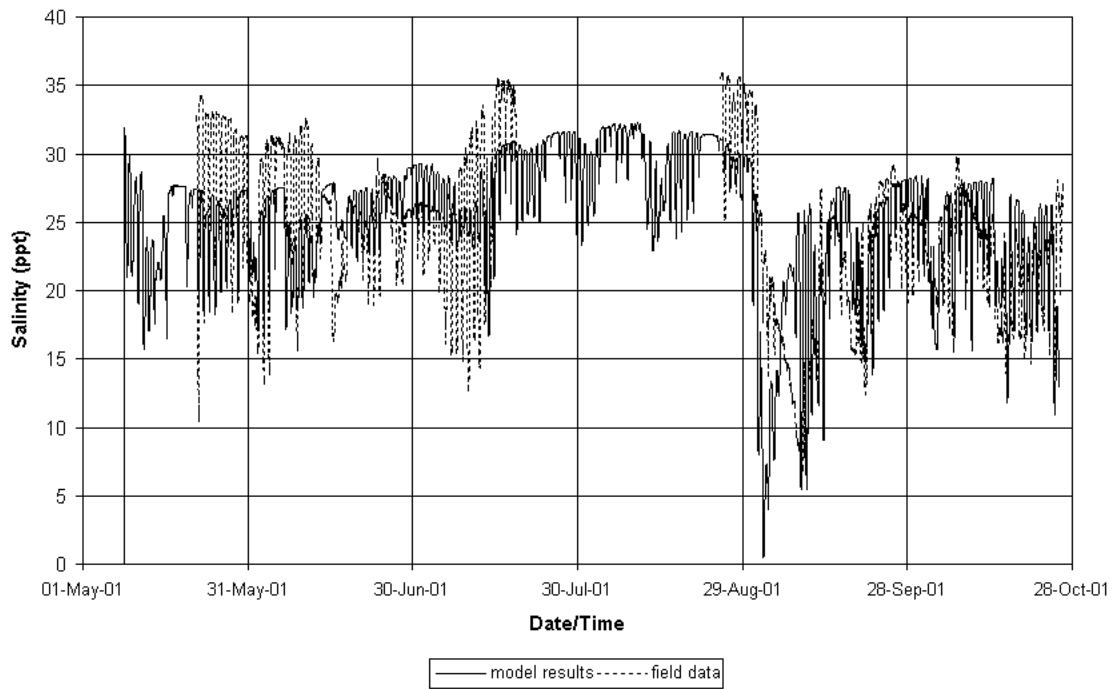
Station 2



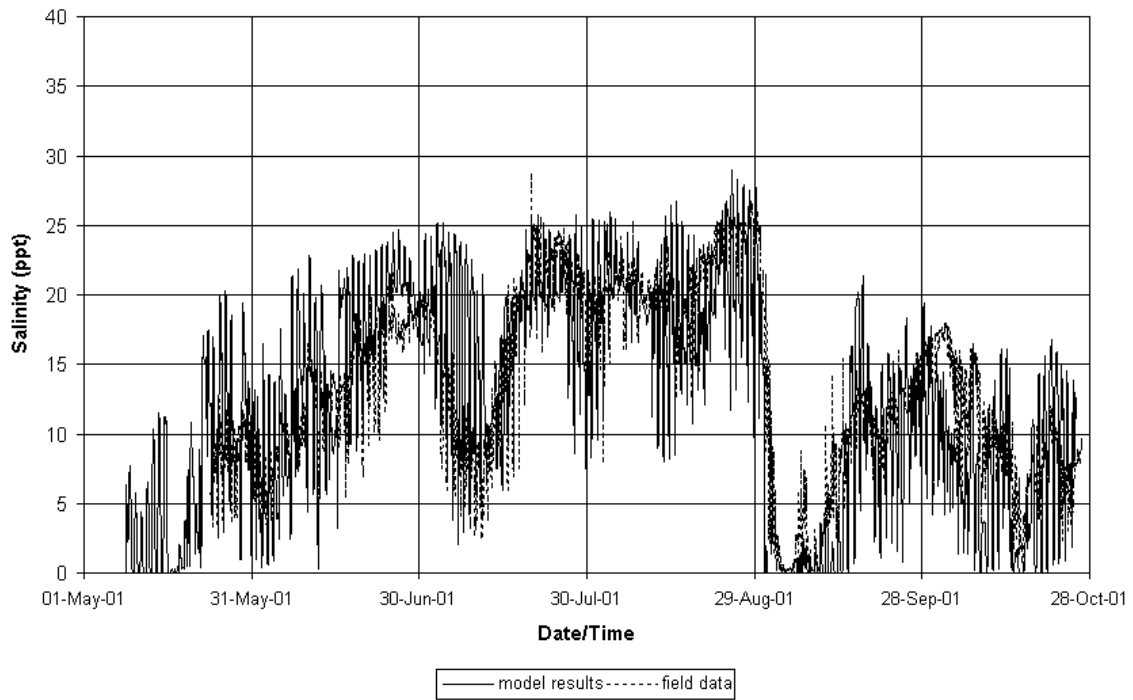
Station 3



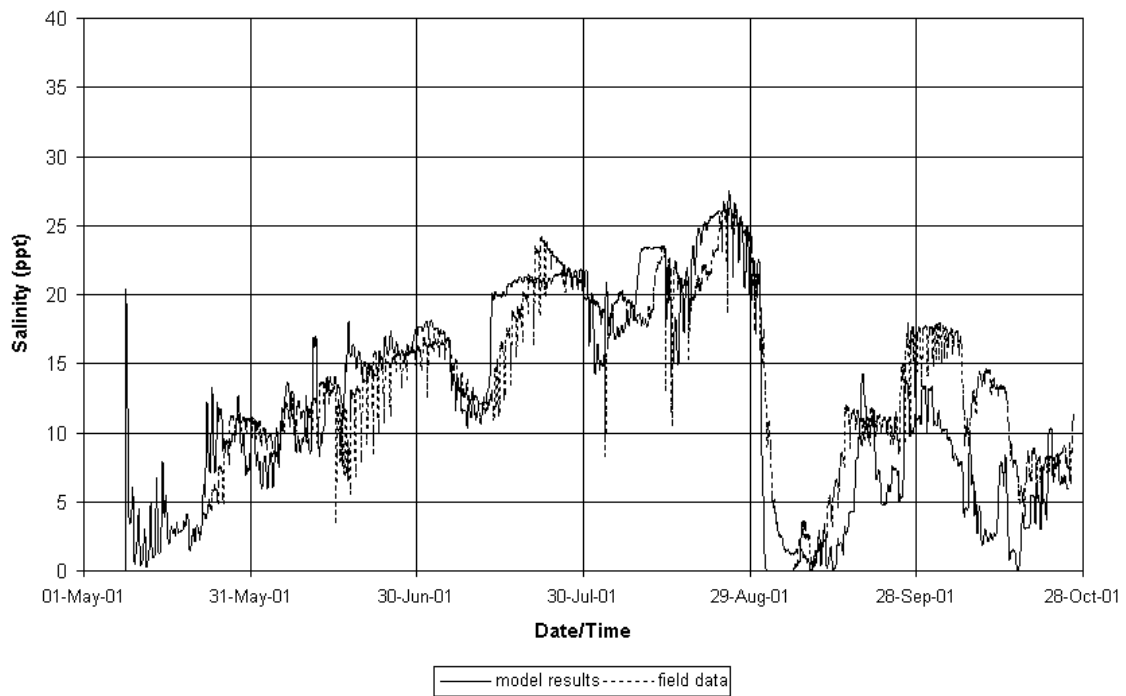
Station 4



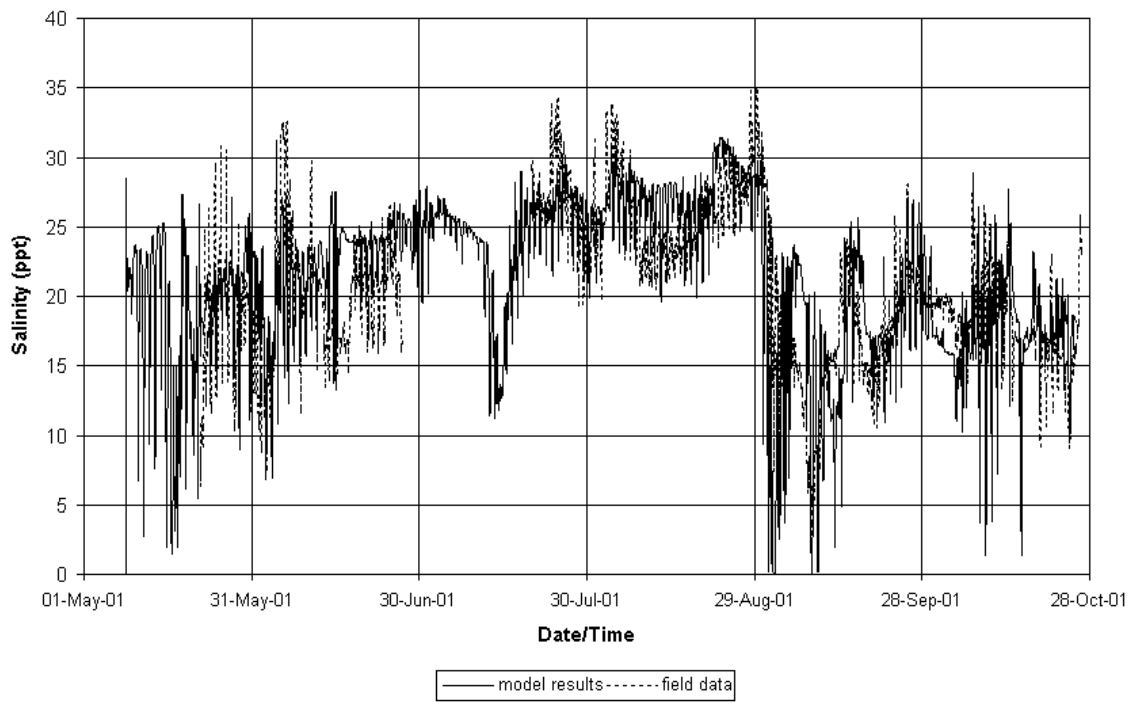
Station 5



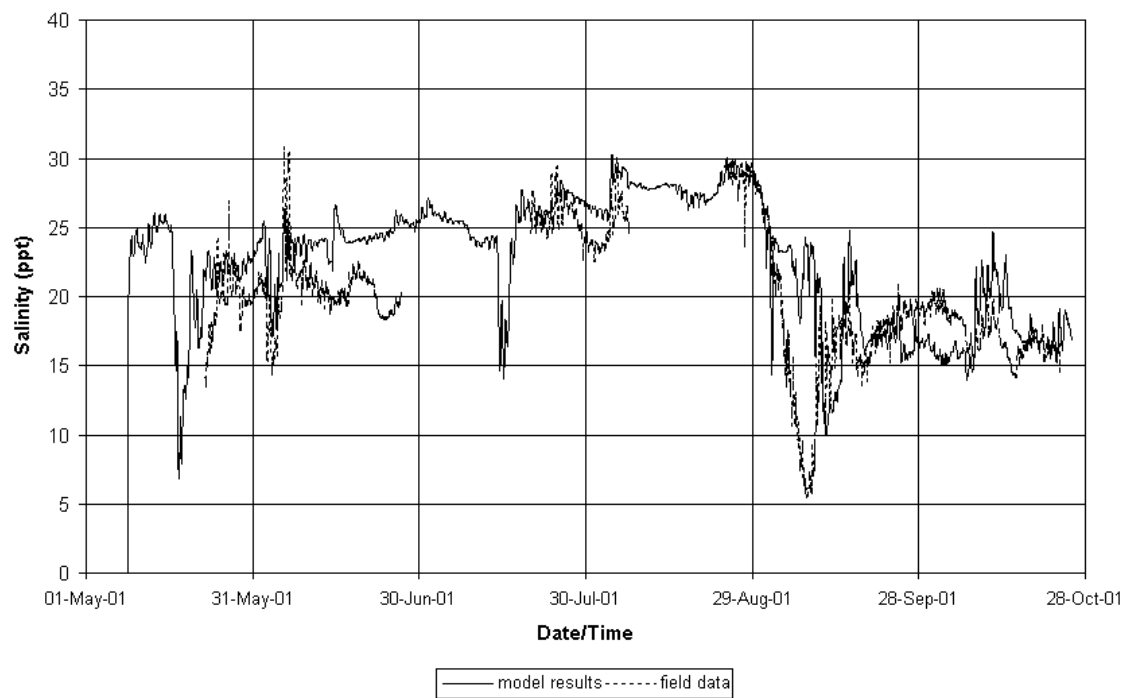
Station 6



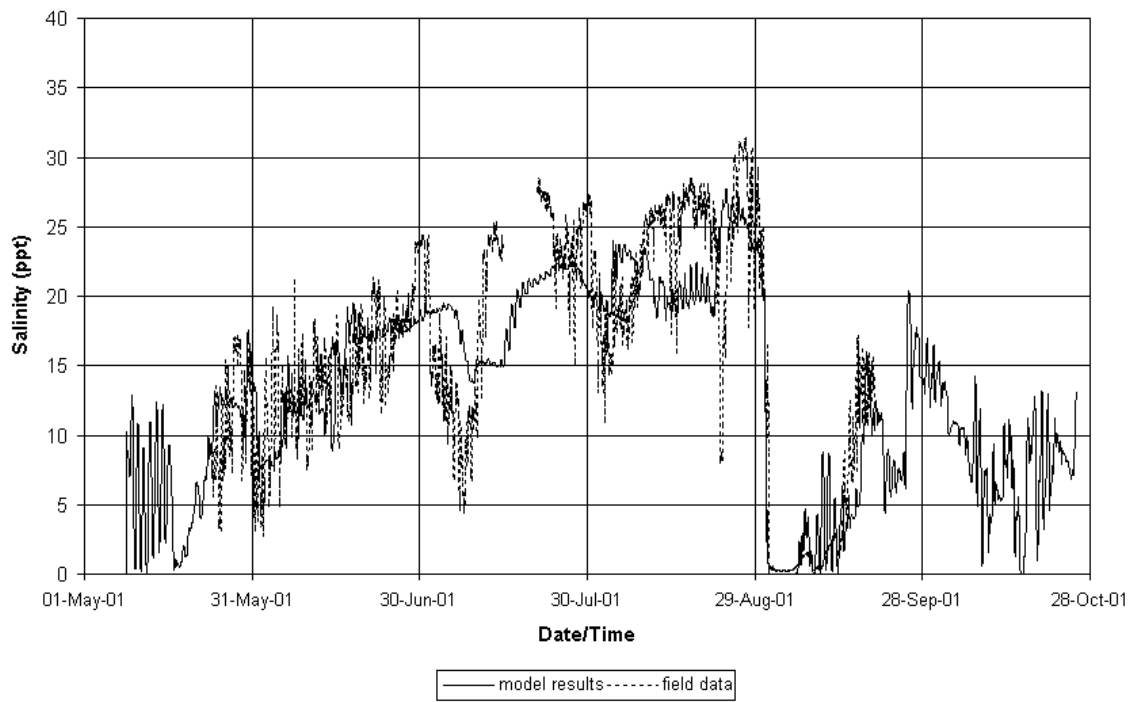
Station 7



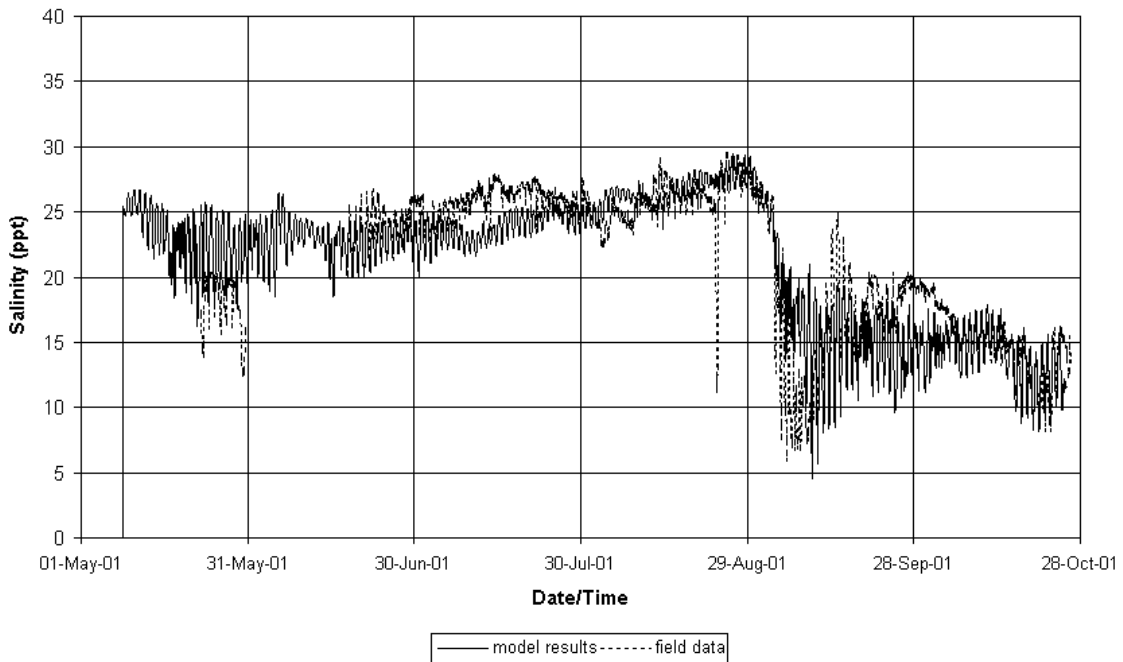
Station 8



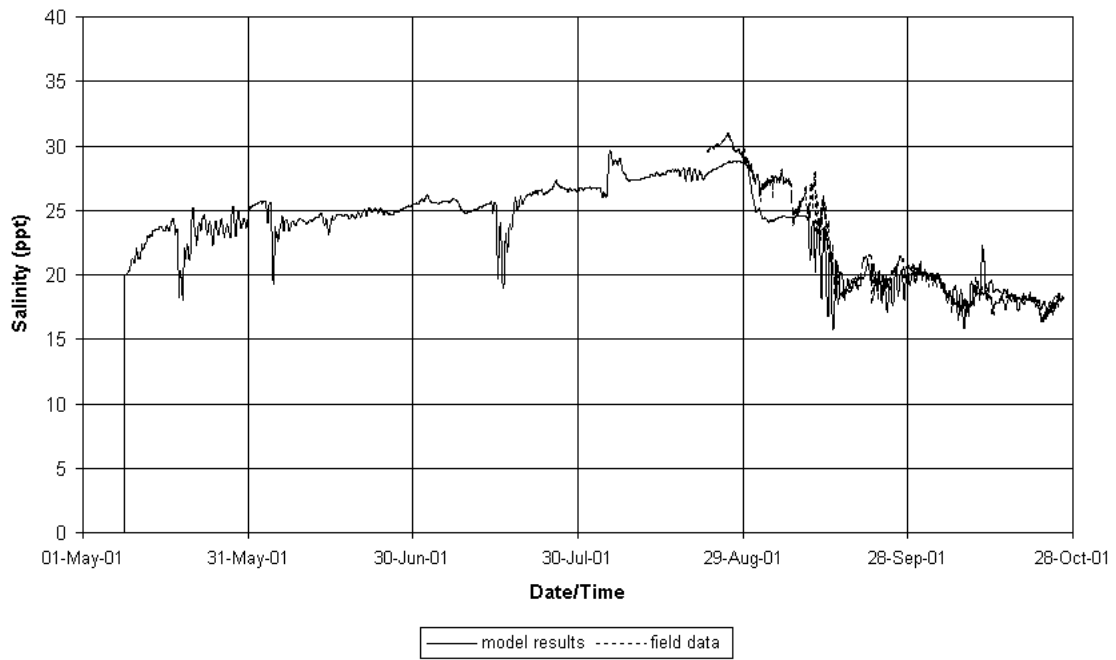
Station 9



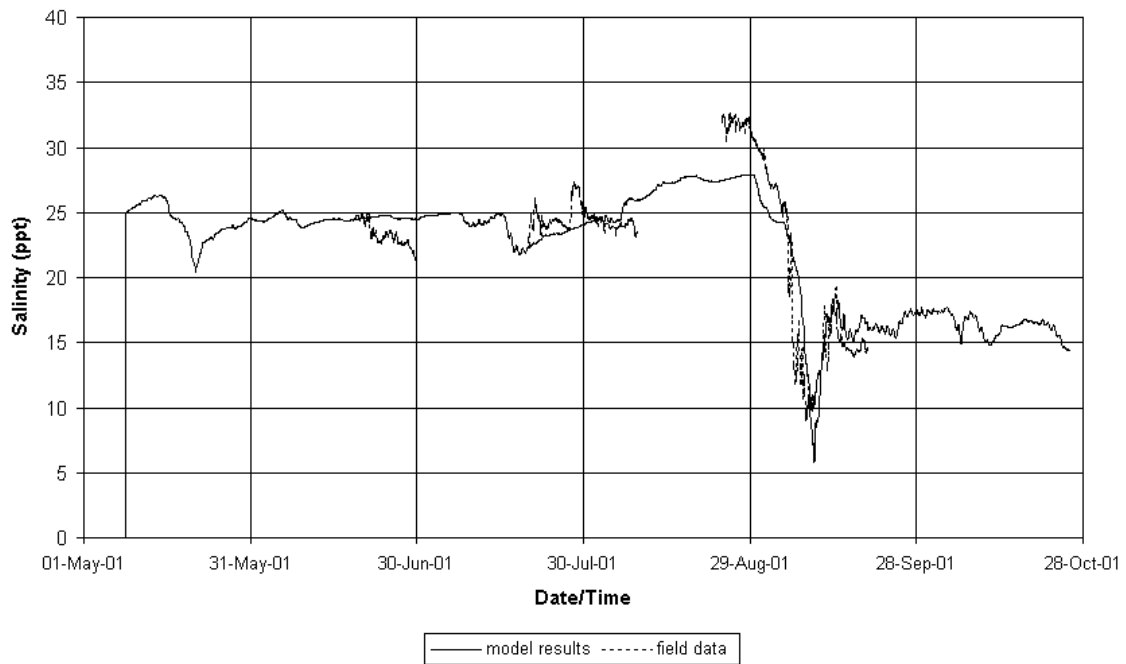
Station 10

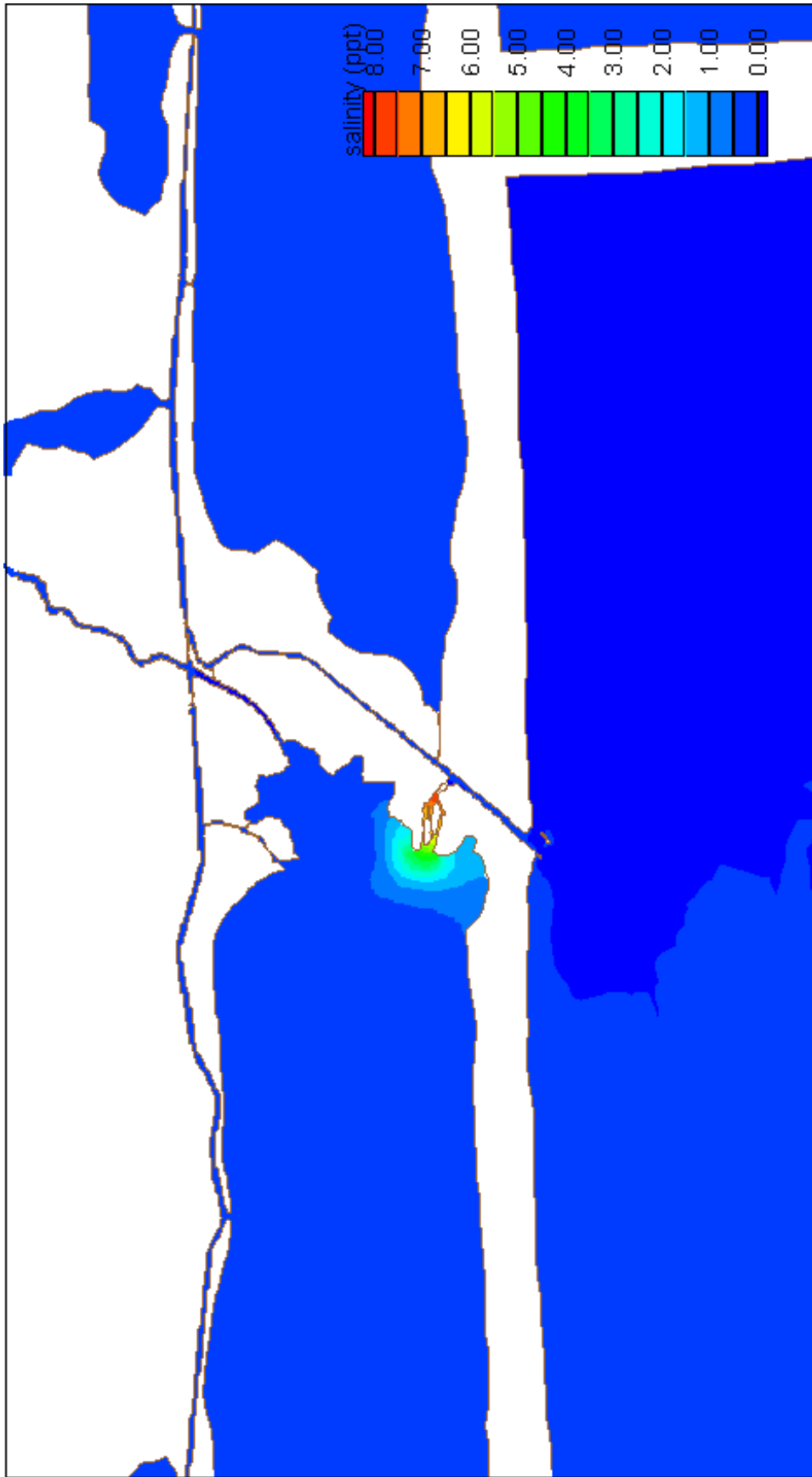


Station 11

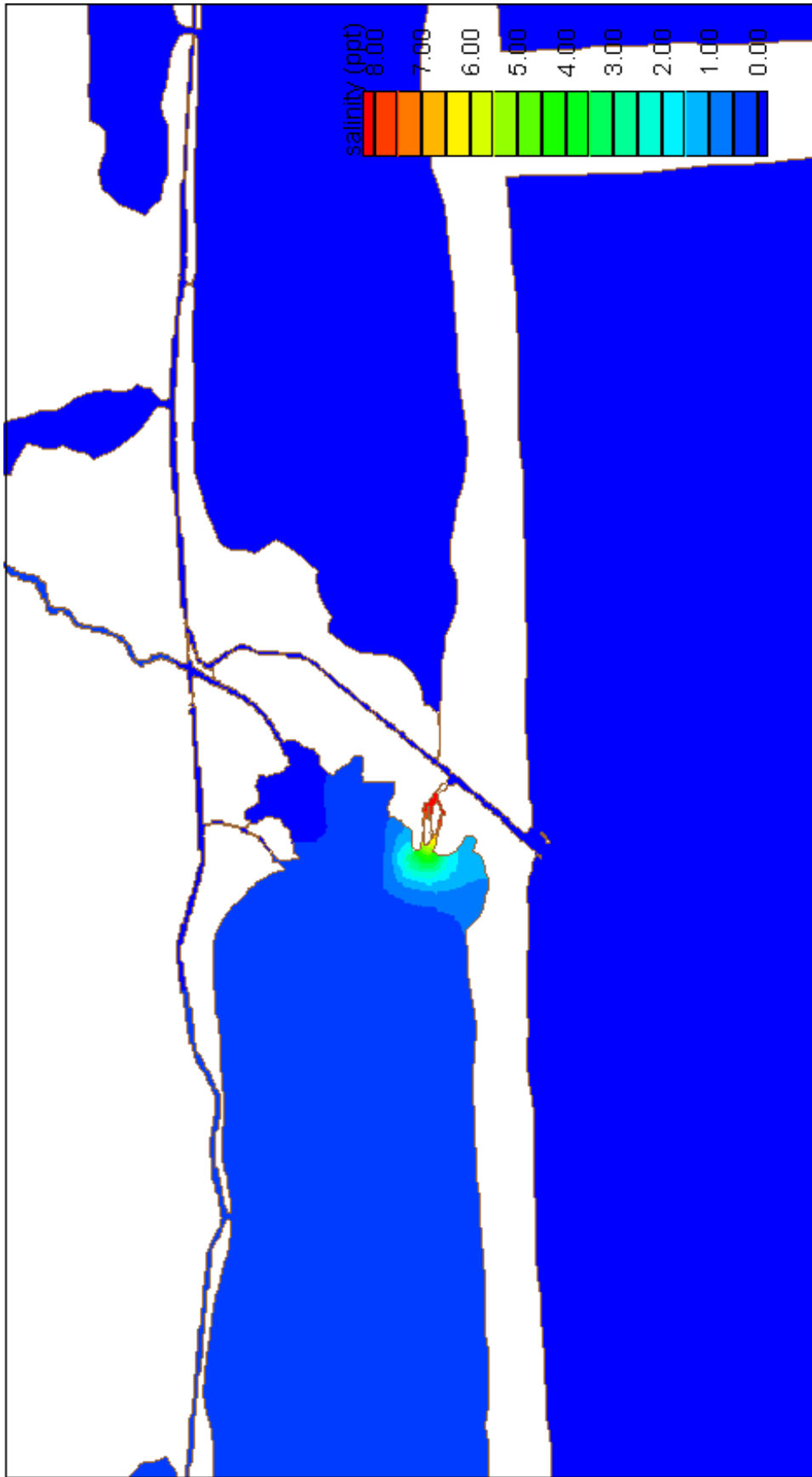


Station 12

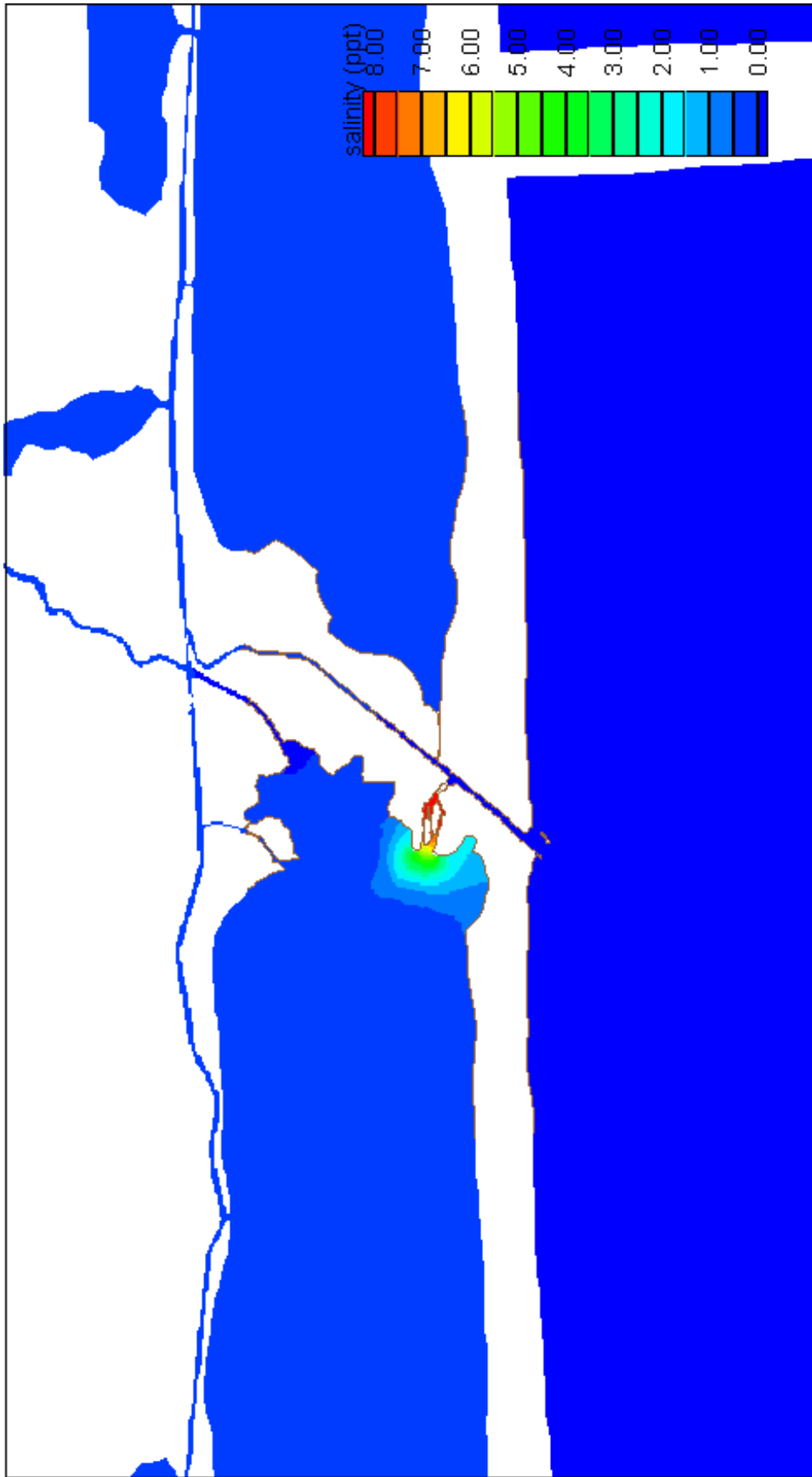




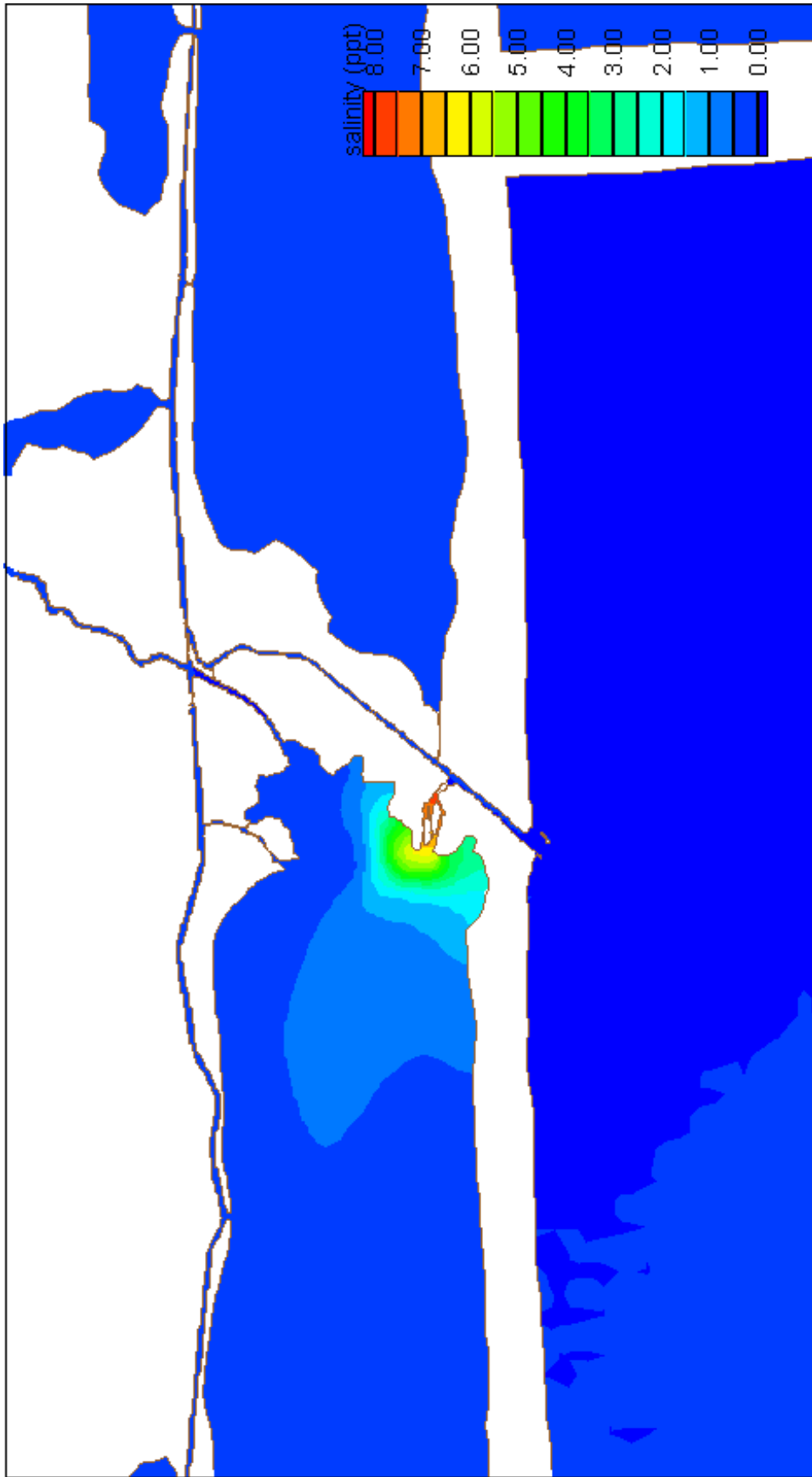
Salinity Difference, Scenario B, Low River Discharge
Scenario B: Parker's Cut (4' X 20')



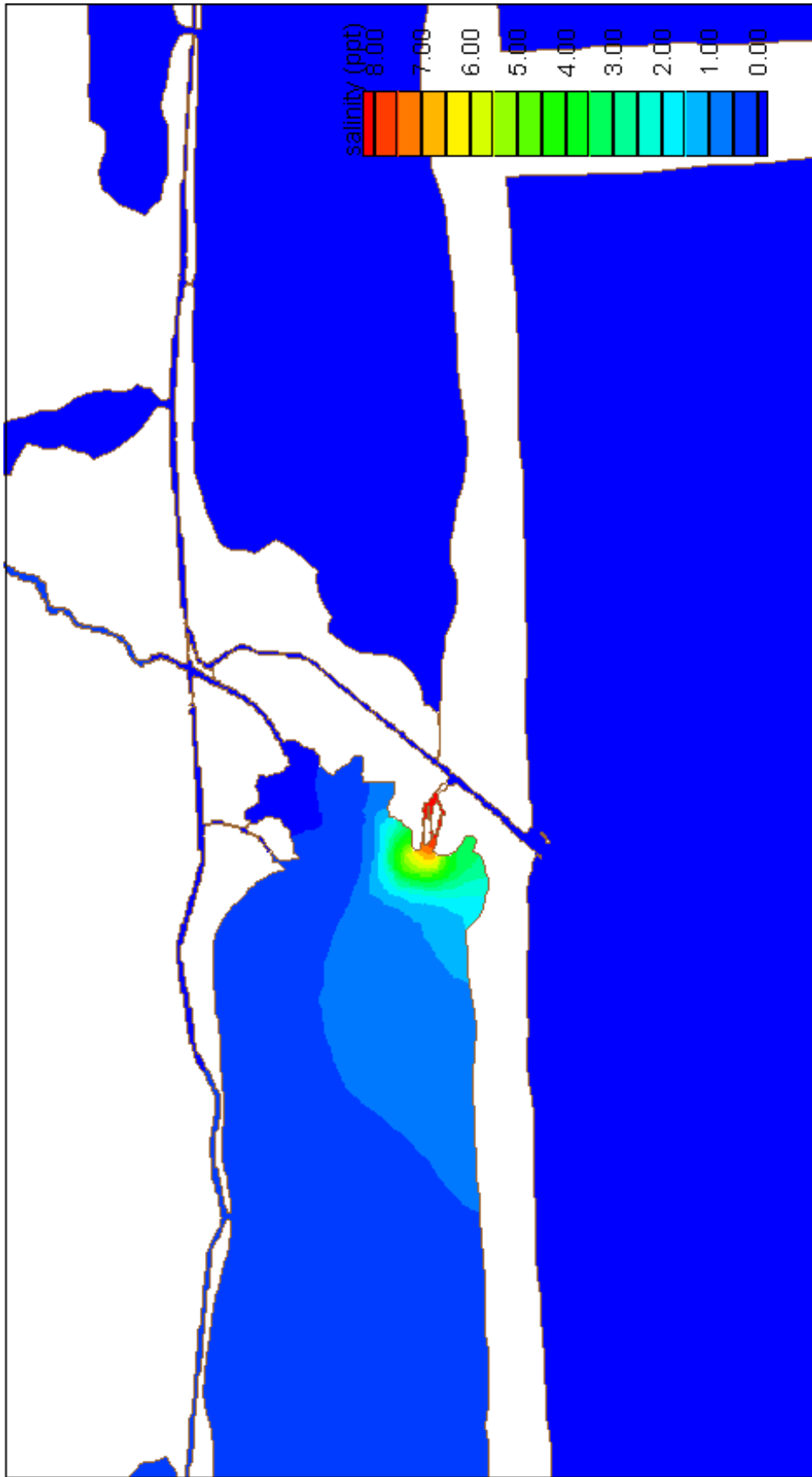
Salinity Difference, Scenario B, Medium River Discharge
Scenario B: Parker's Cut (4' X 20')



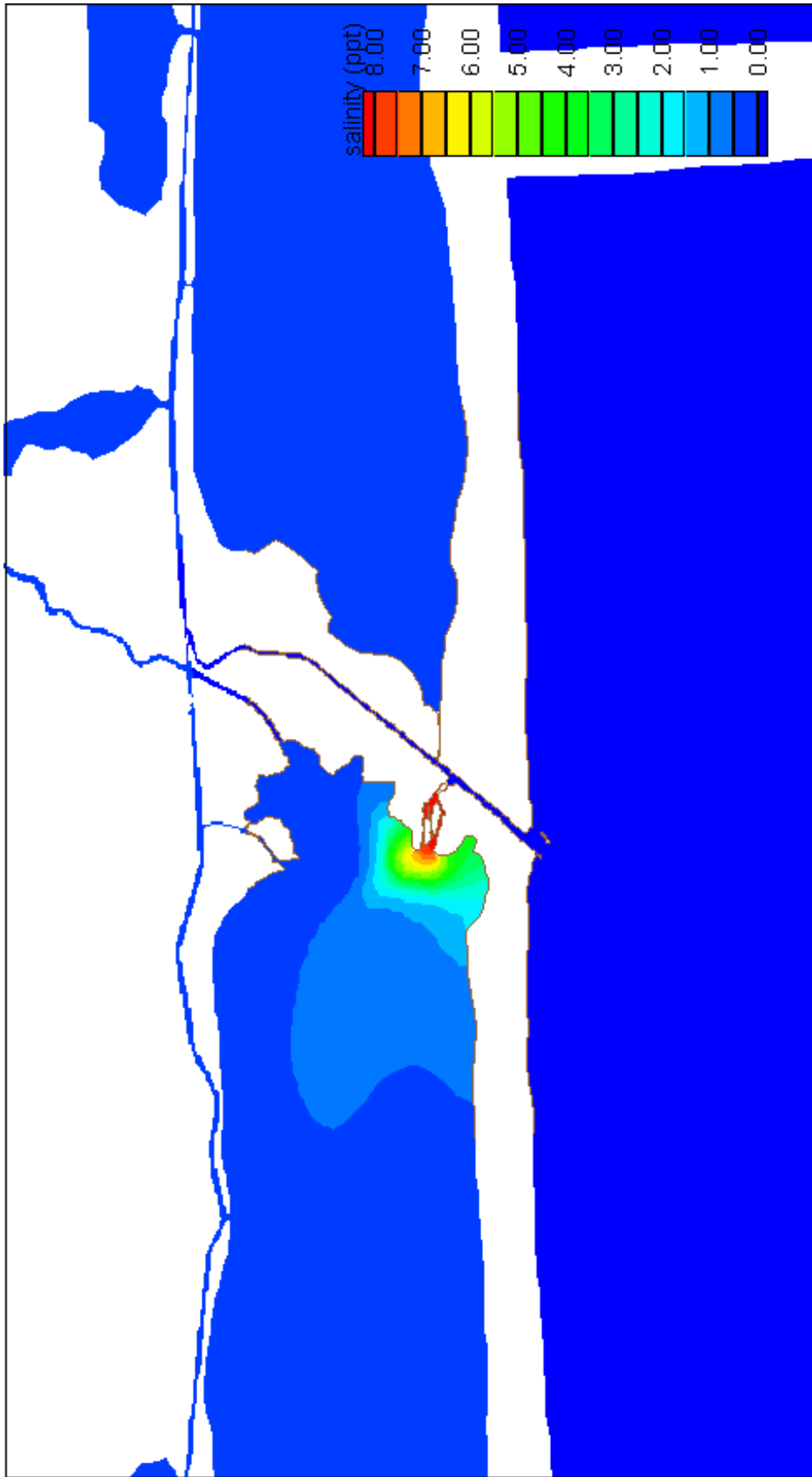
Salinity Difference, Scenario B, High River Discharge
Scenario B: Parker's Cut (4' X 20')



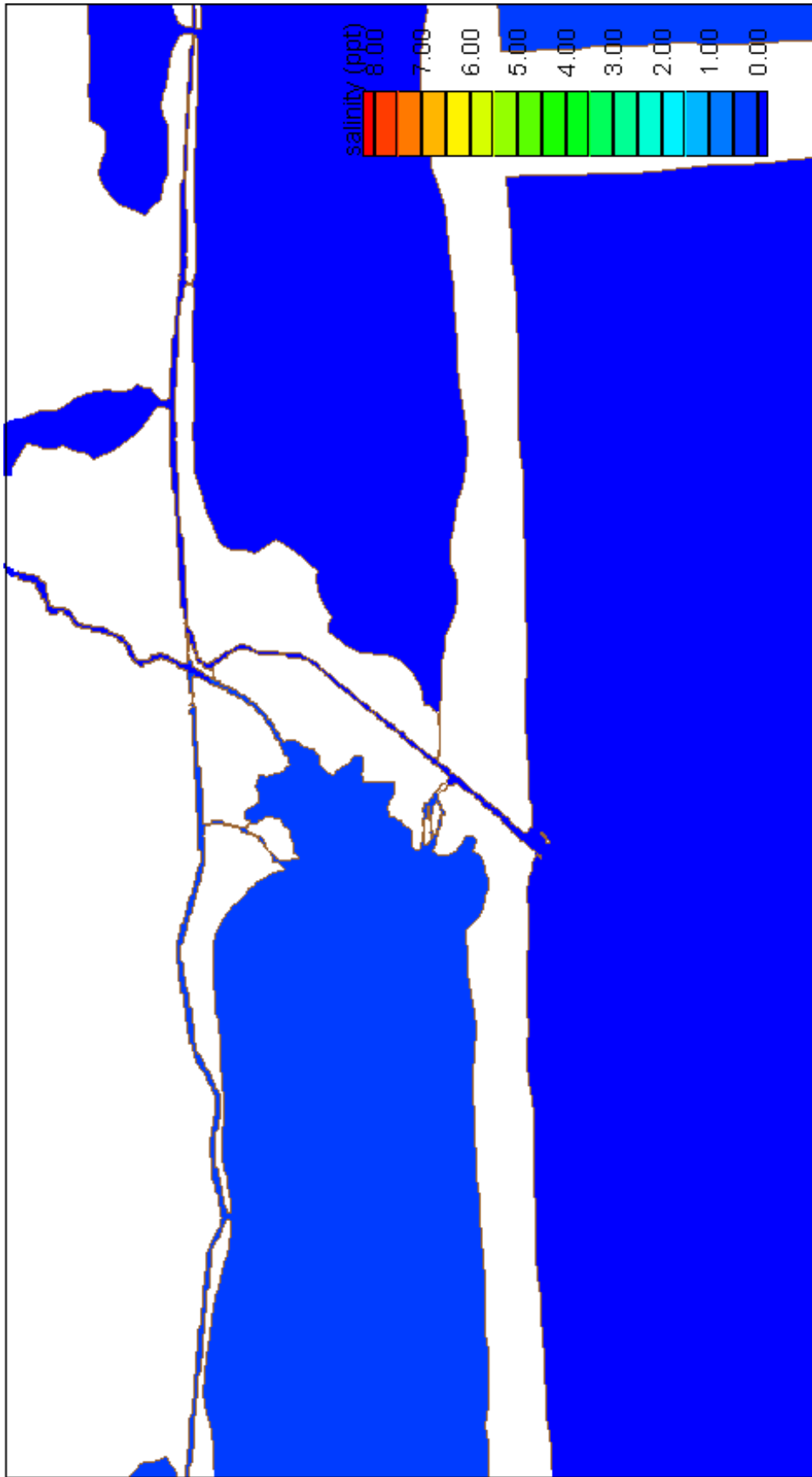
Salinity Difference, Scenario C, Low River Discharge
Scenario C: Parker's Cut (7' X 50')



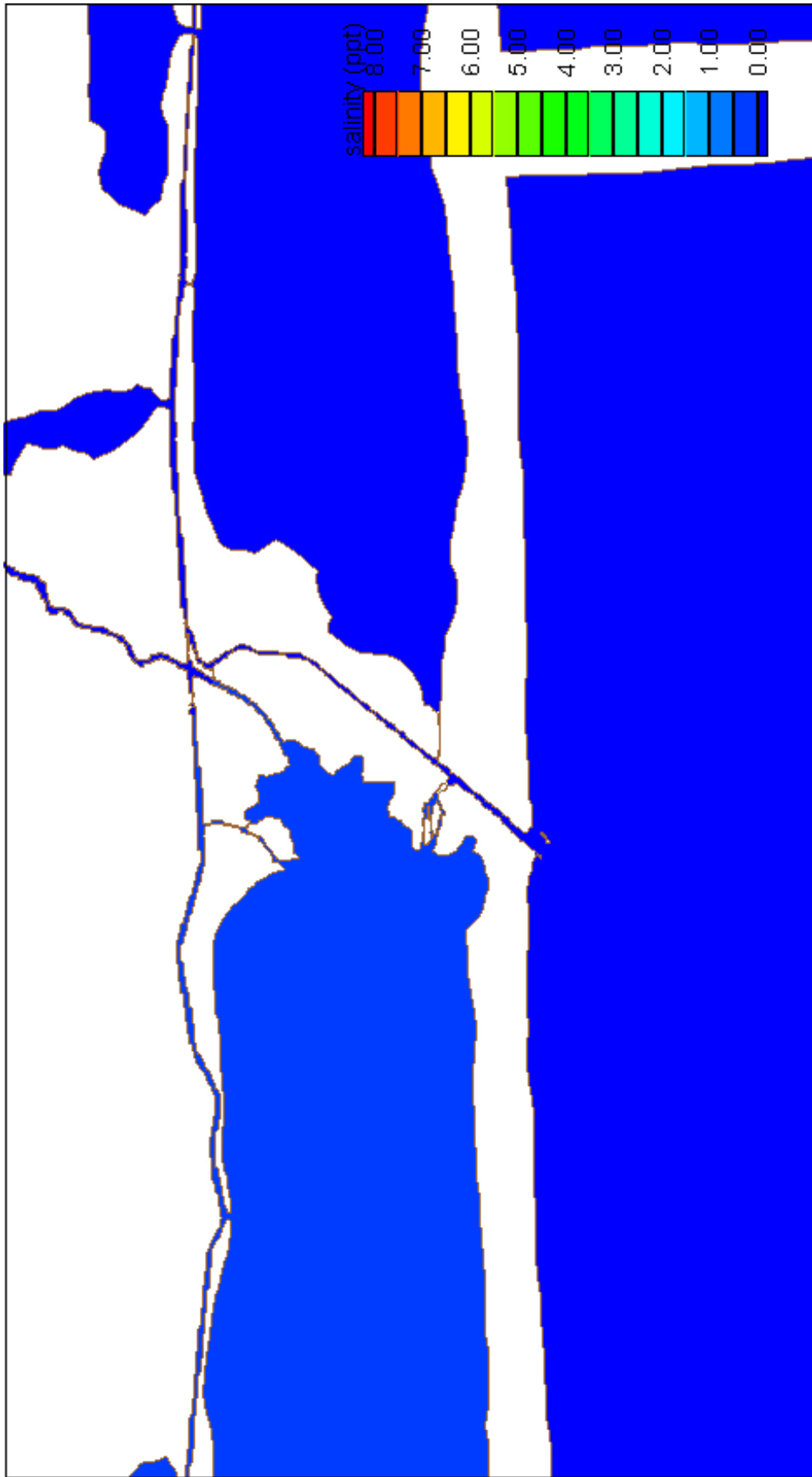
Salinity Difference, Scenario C, Medium River Discharge
Scenario C: Parker's Cut (7' X 50')



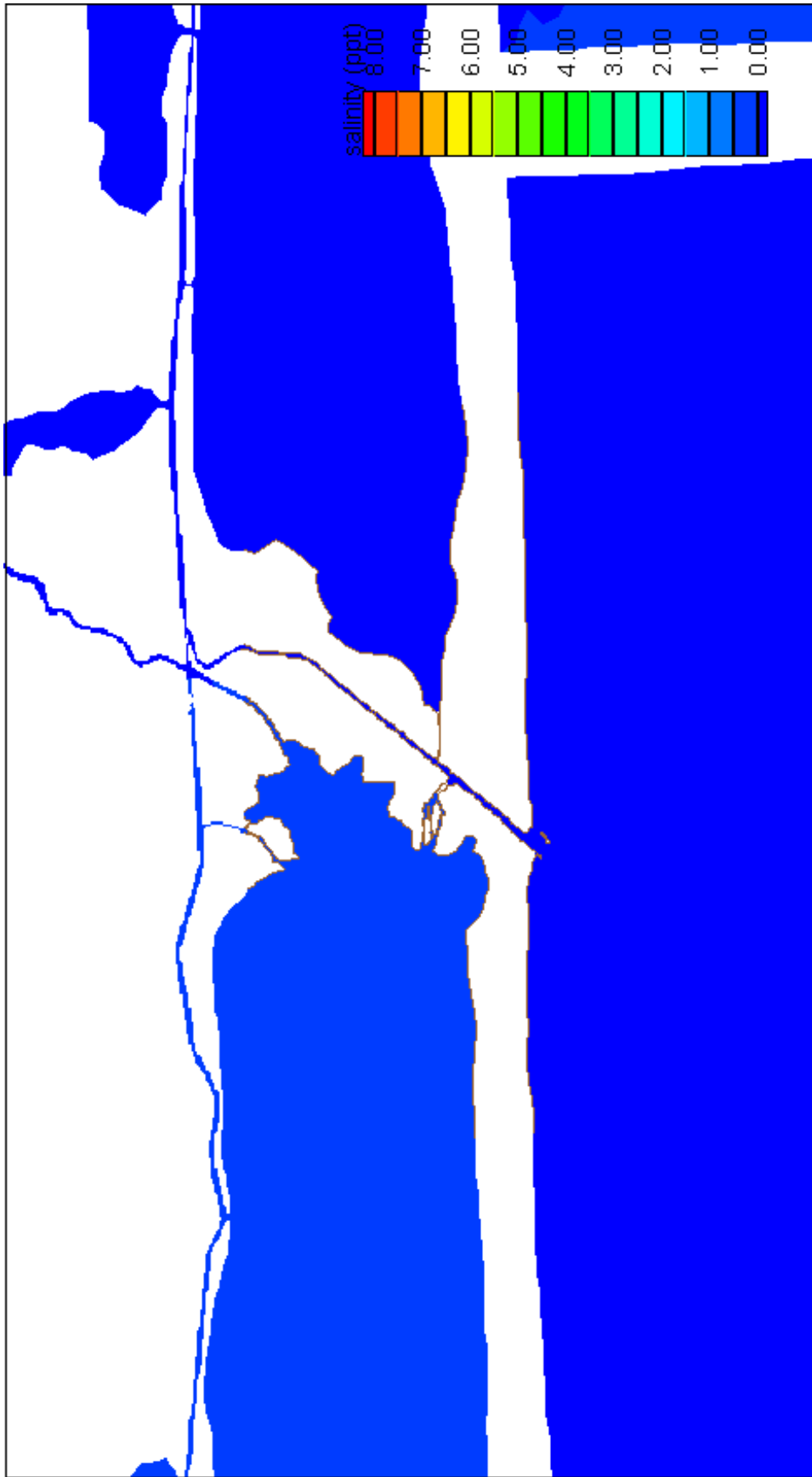
Salinity Difference, Scenario C, High River Discharge
Scenario C: Parker's Cut (7' X 50')



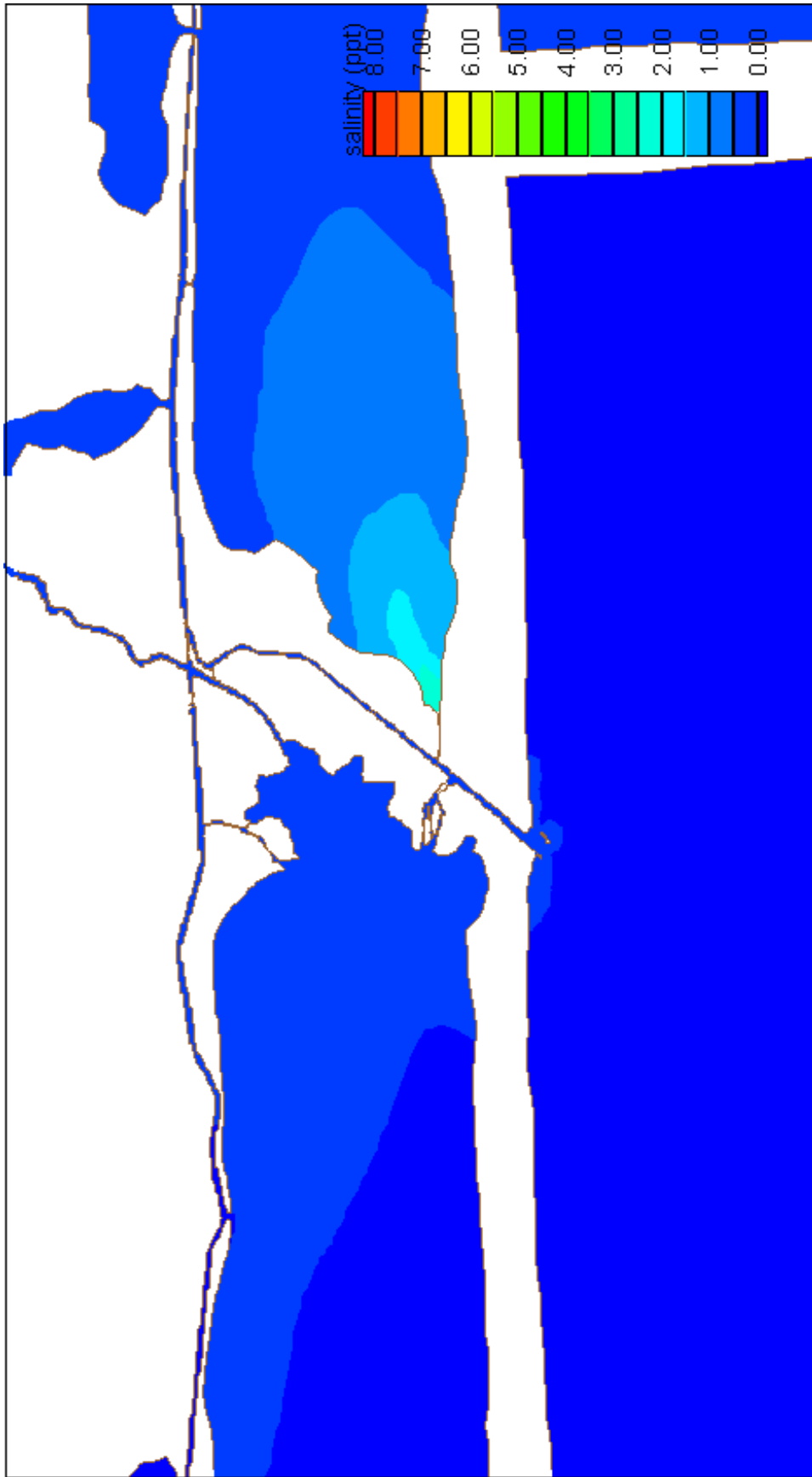
Salinity Difference, Scenario D, Low River Discharge
Scenario D: bypass channel around diversion dam (4' X 20')



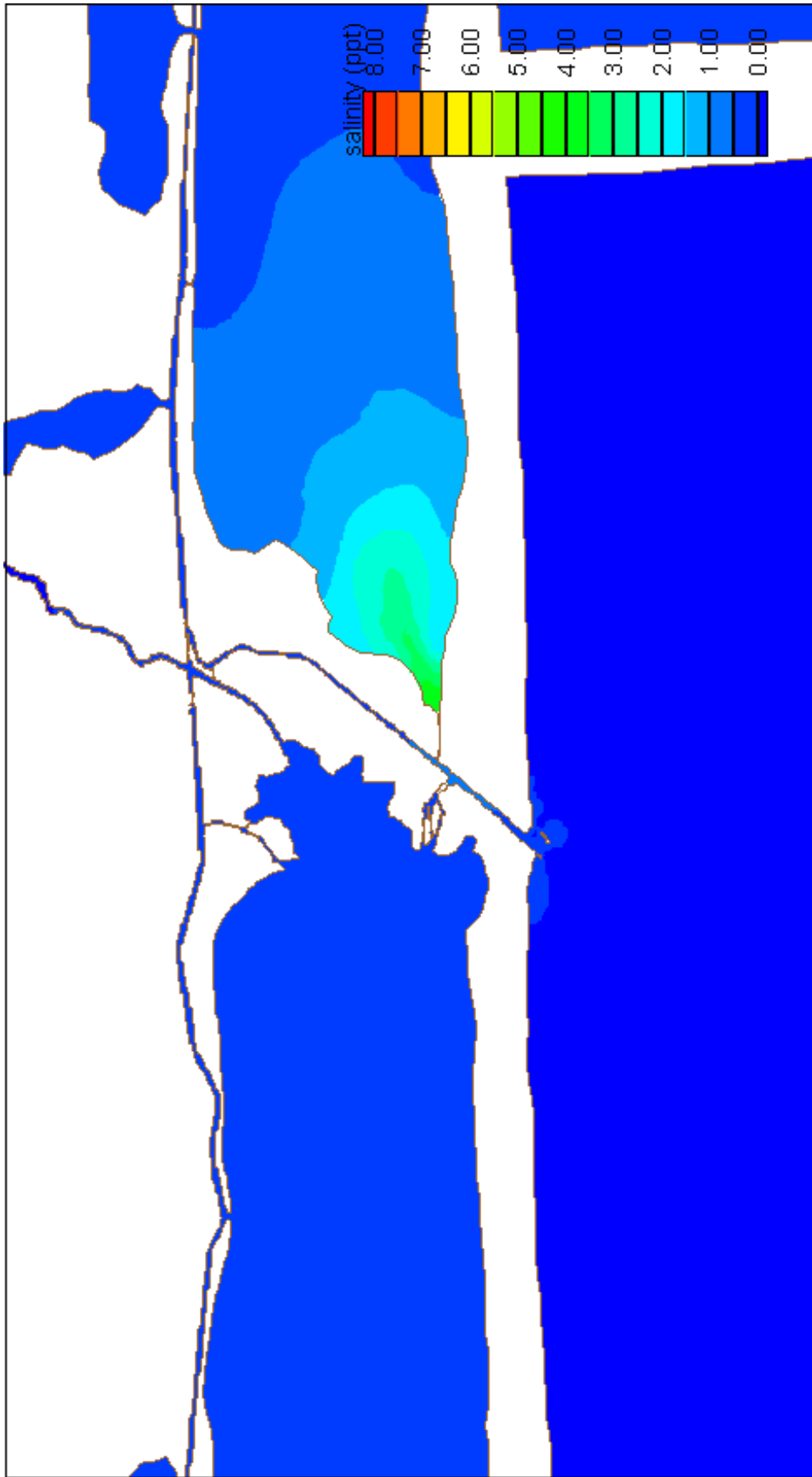
Salinity Difference, Scenario D, Medium River Discharge
Scenario D: bypass channel around diversion dam (4' X 20')



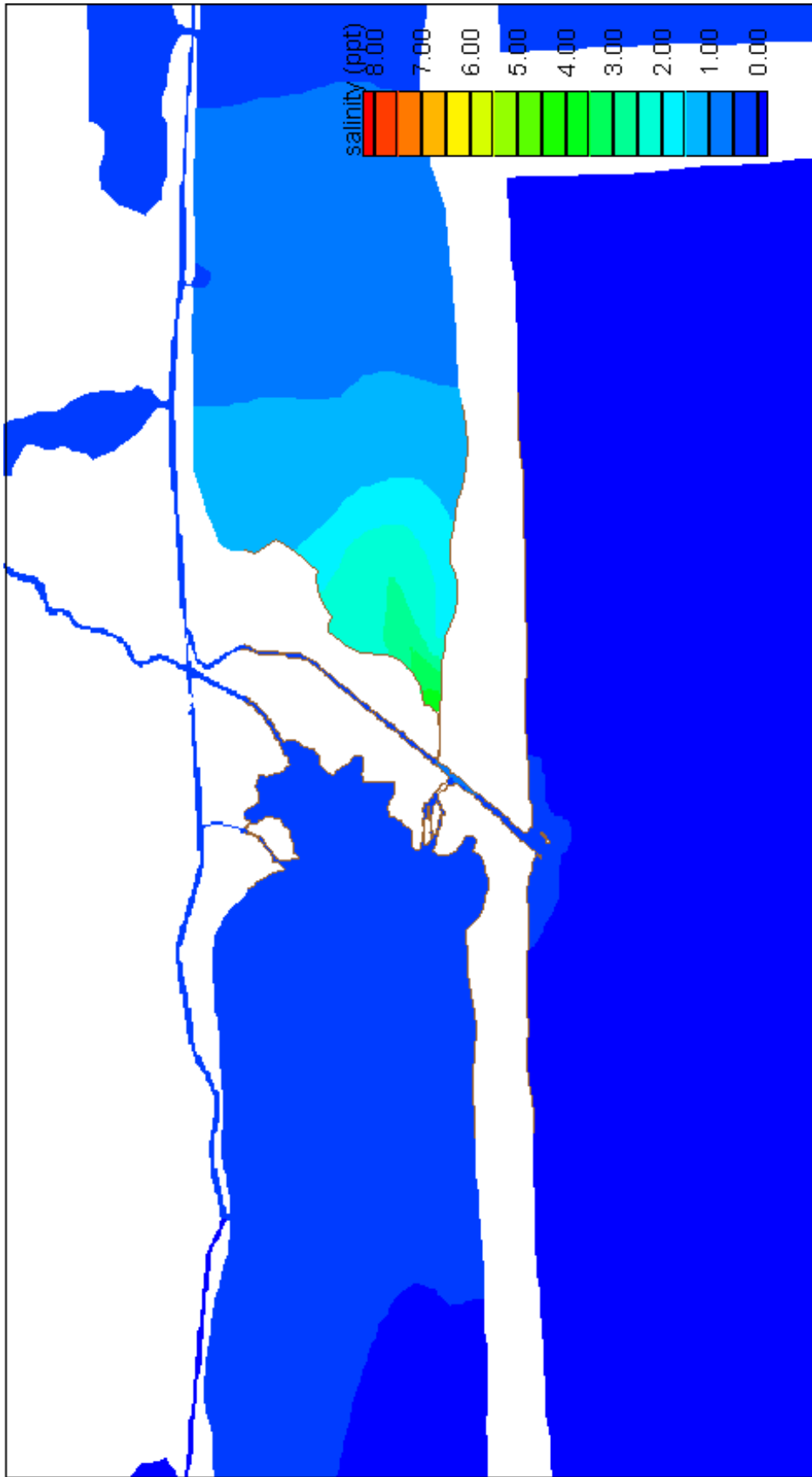
Salinity Difference, Scenario D, High River Discharge
 Scenario D: bypass channel around diversion dam (4' X 20')



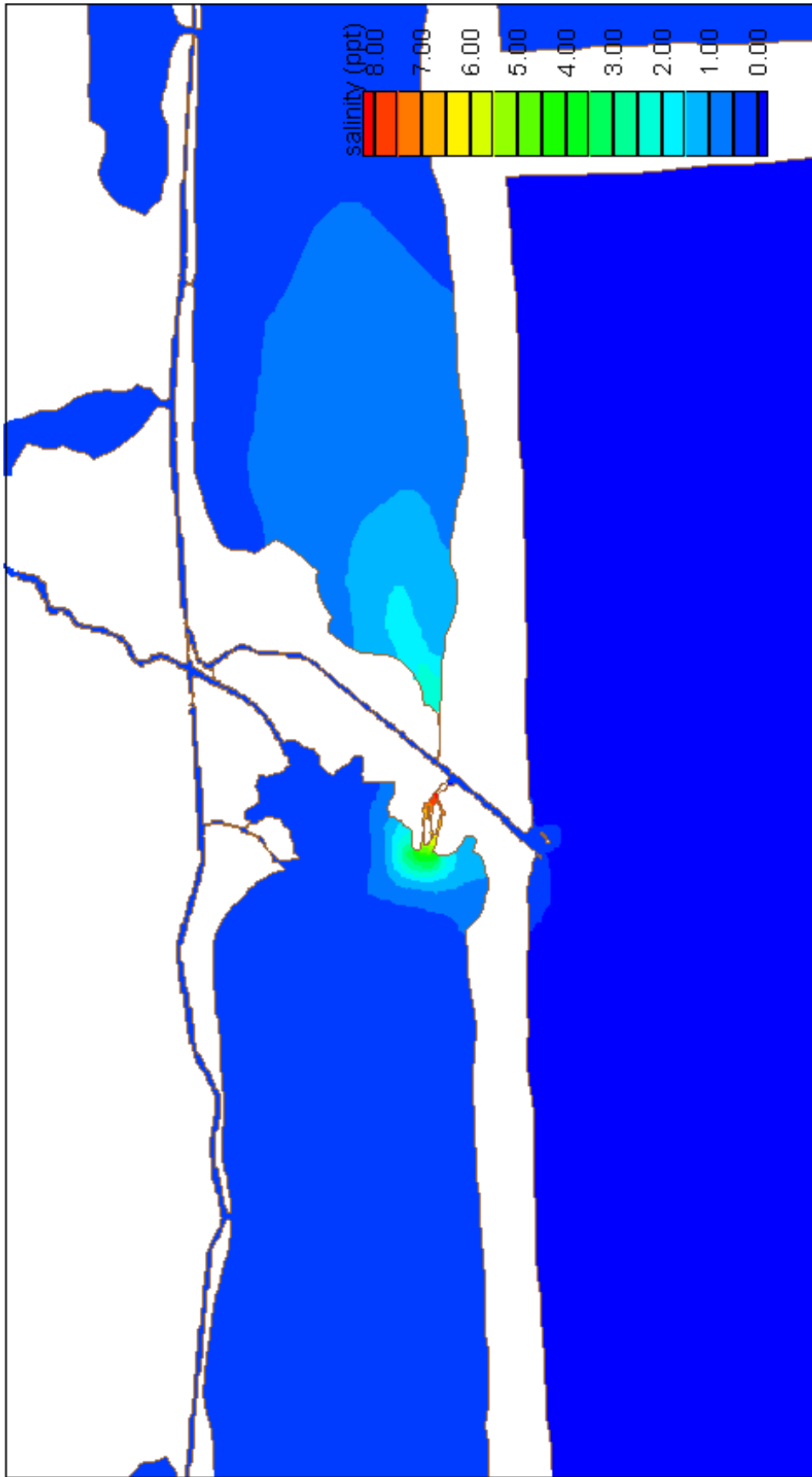
Salinity Difference, Scenario G, Low River Discharge
Scenario G: Southwest Cut (5' X 100')



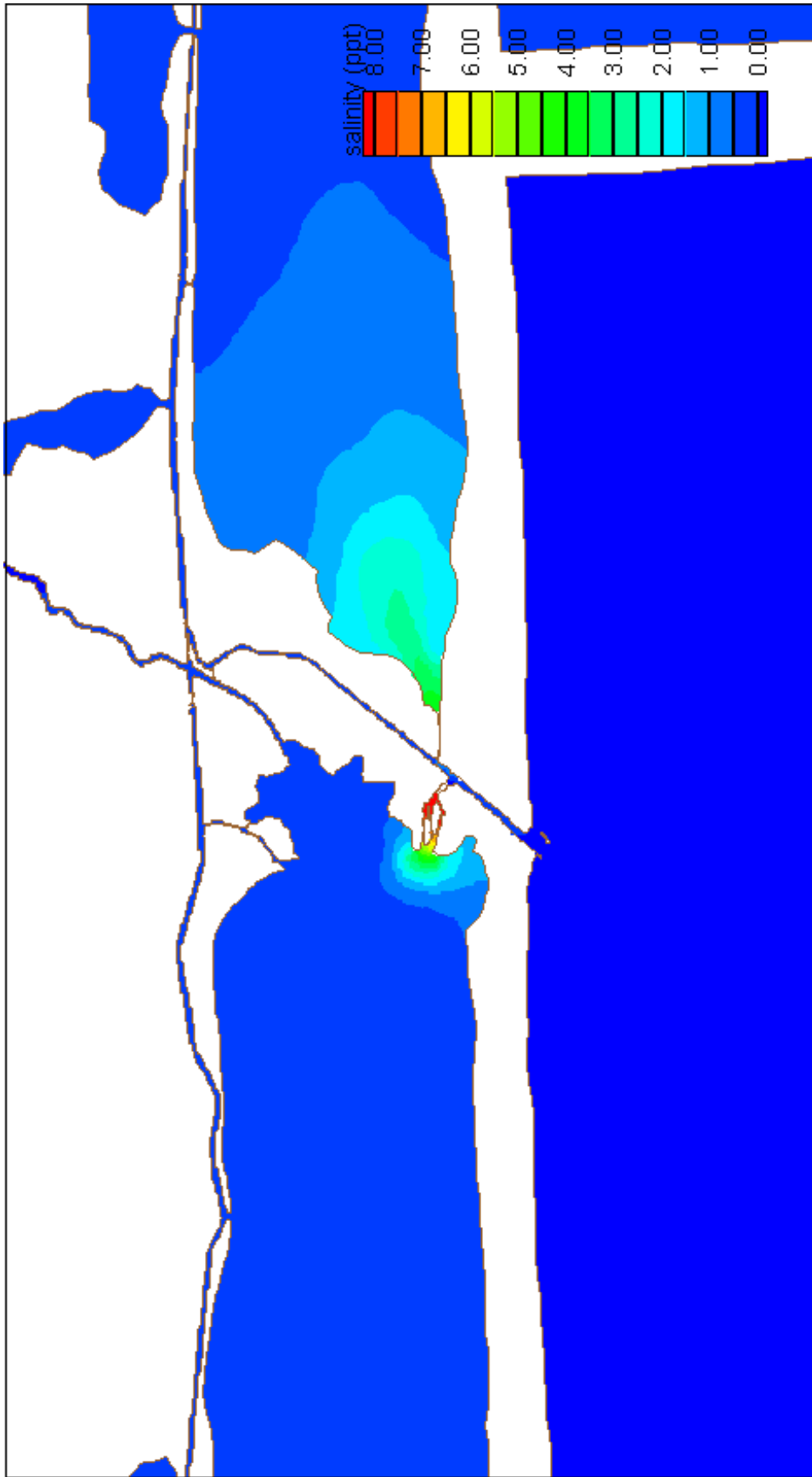
Salinity Difference, Scenario G, Medium River Discharge
Scenario G: Southwest Cut (5' X 100')



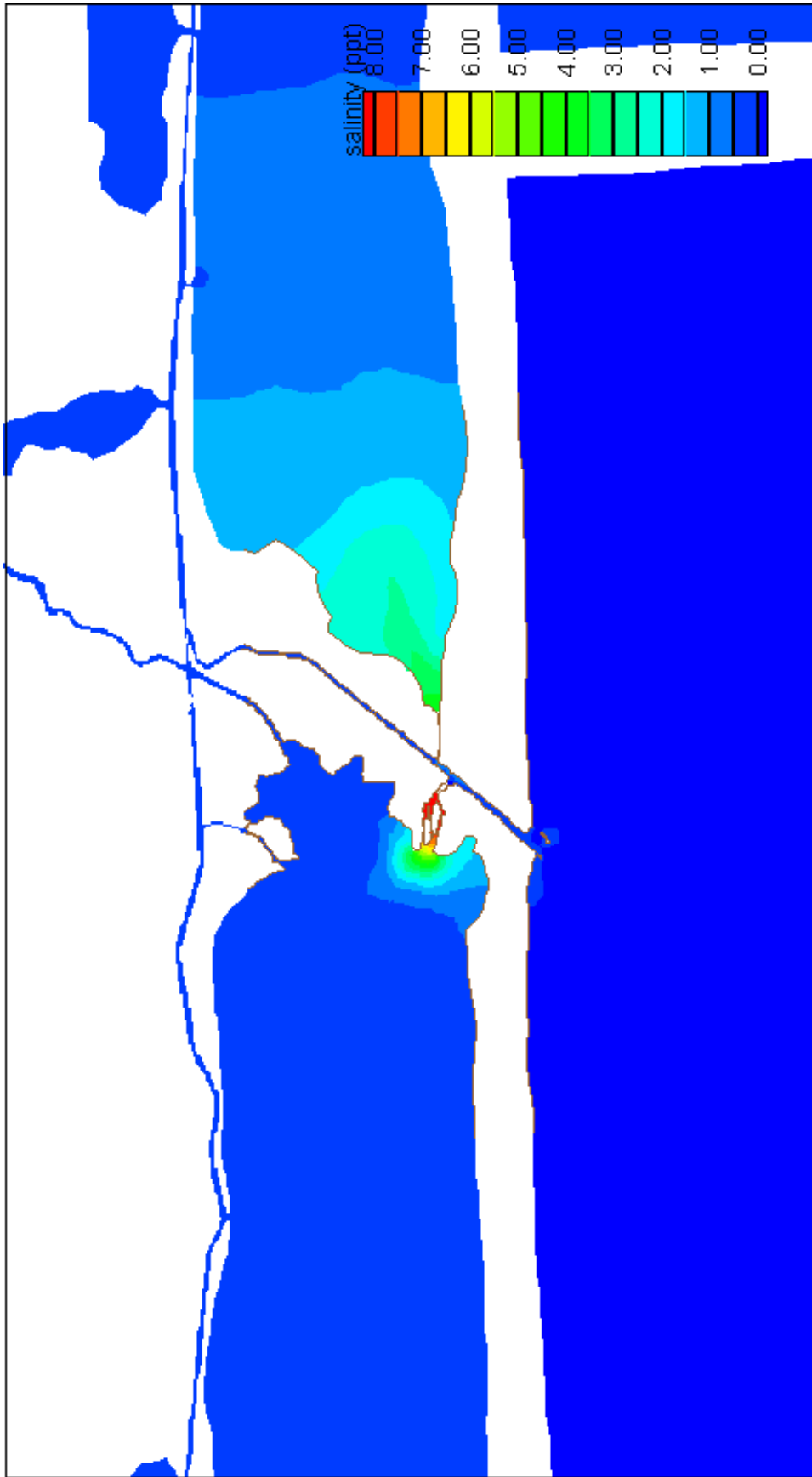
Salinity Difference, Scenario G, High River Discharge
Scenario G: Southwest Cut (5' X 100')



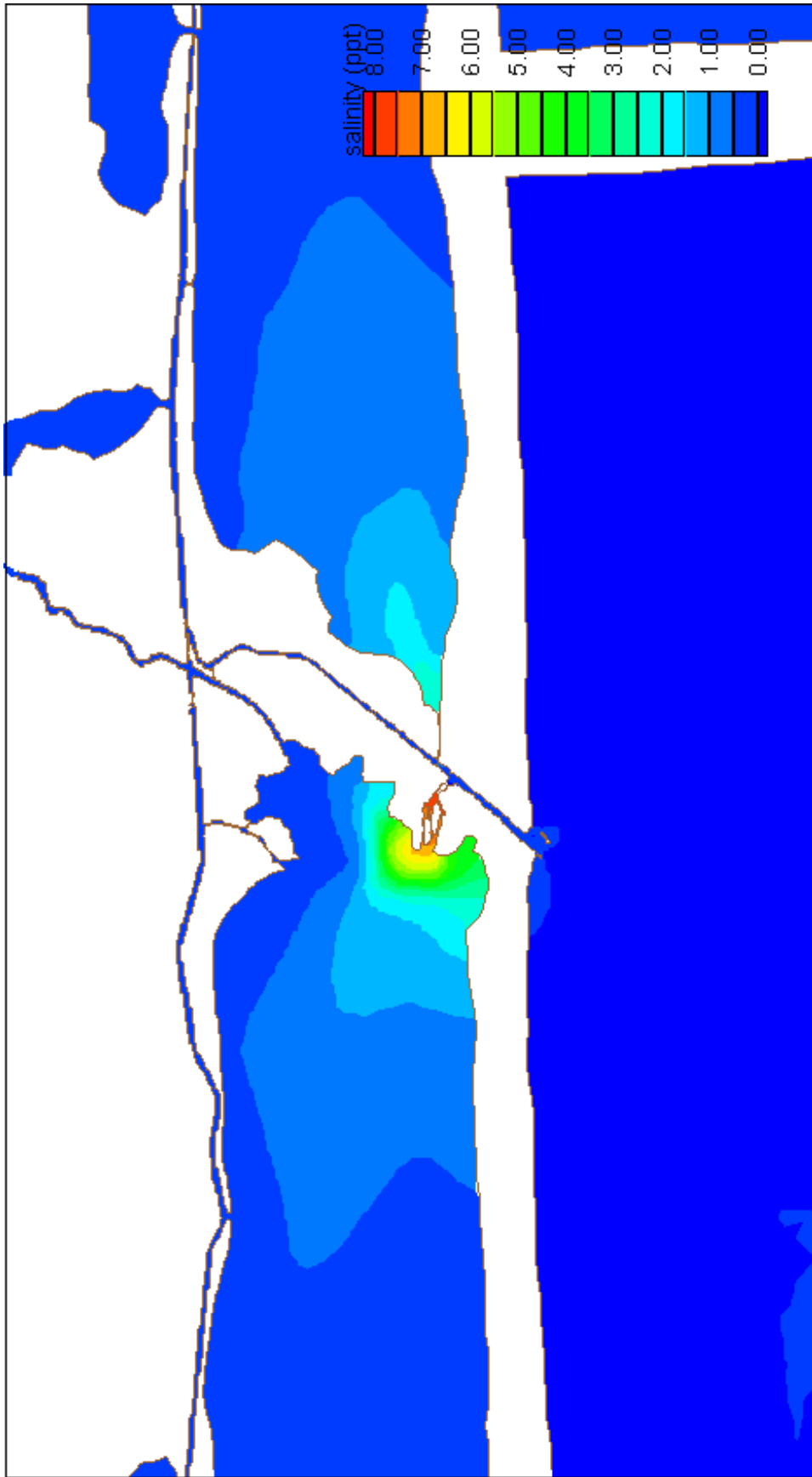
Salinity Difference, Scenario H, Low River Discharge
 Scenario H: Southwest Cut (5' X 100'), with Parker's Cut (4' X 20')



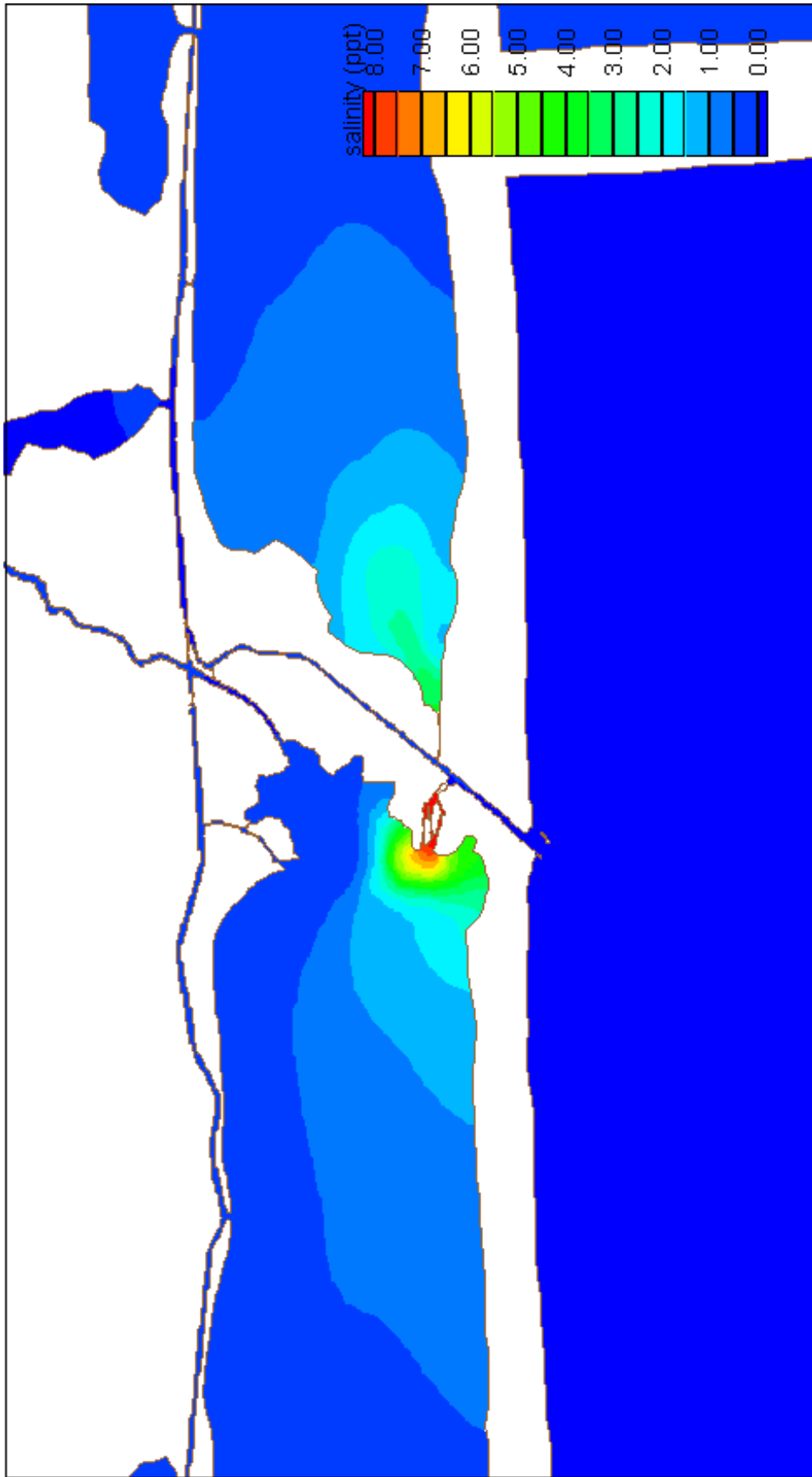
Salinity Difference, Scenario H, Medium River Discharge
Scenario H: Southwest Cut (5' X 100'), with Parker's Cut (4' X 20')



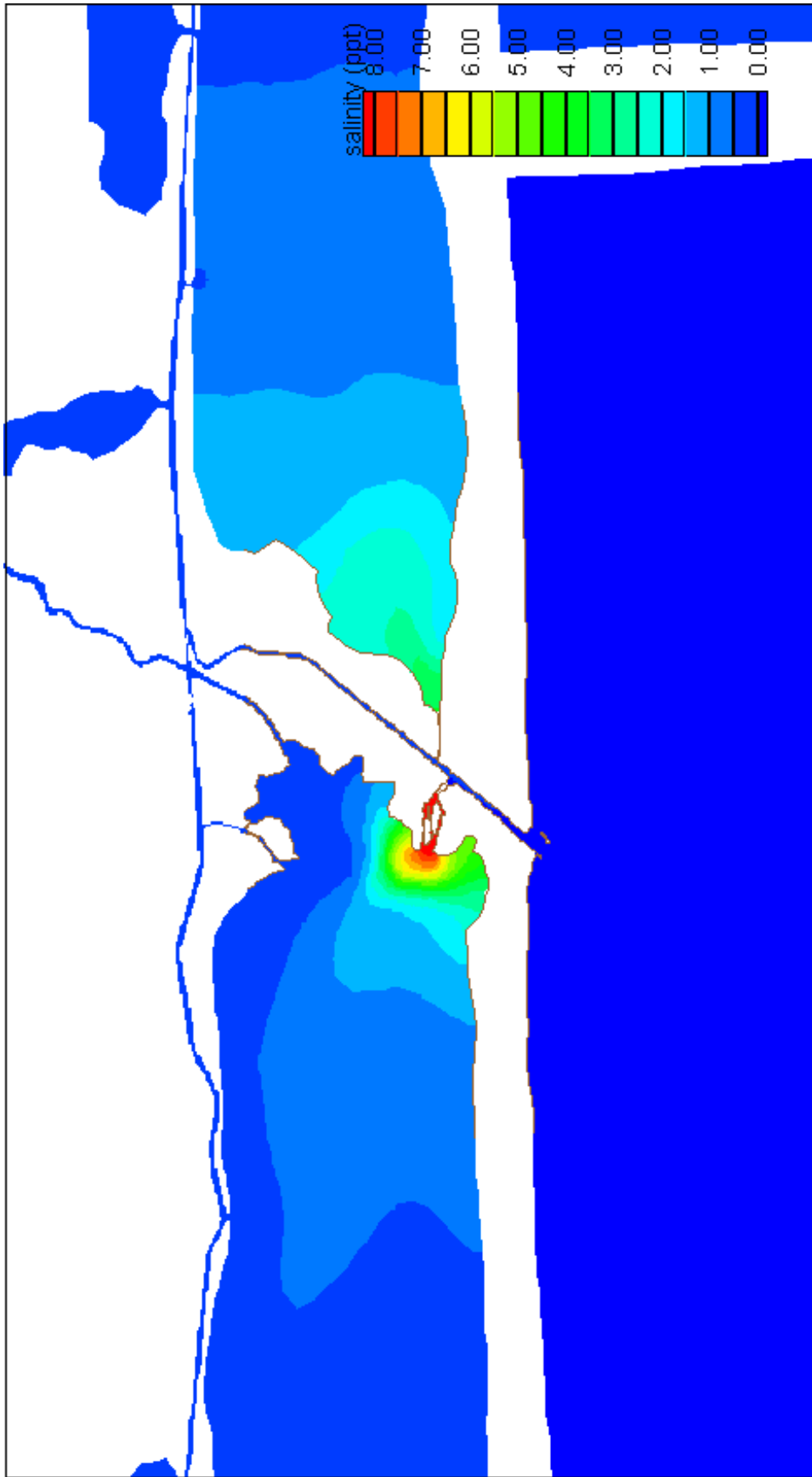
Salinity Difference, Scenario H, High River Discharge
Scenario H: Southwest Cut (5' X 100''), with Parker's Cut (4' X 20')



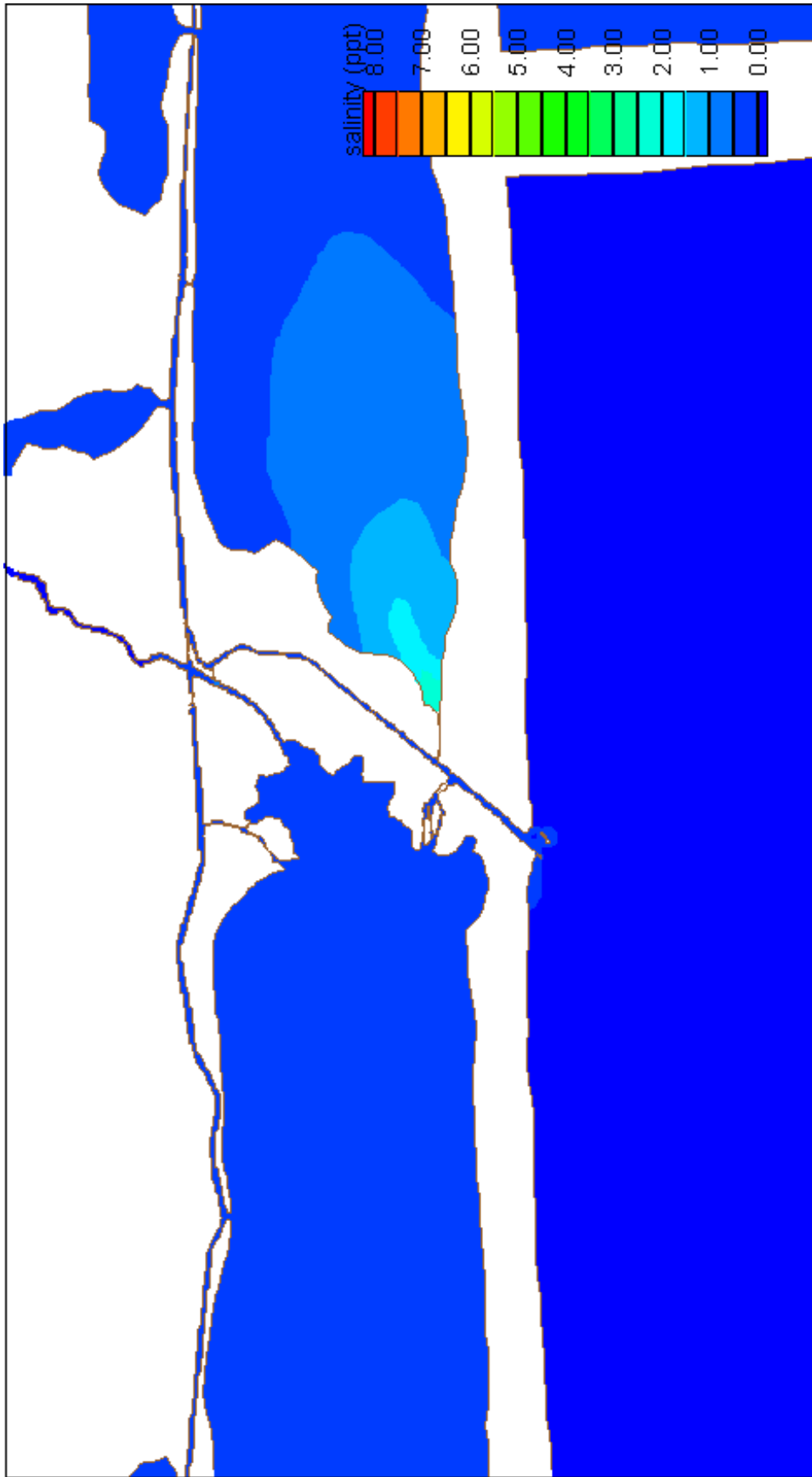
Salinity Difference, Scenario I, Low River Discharge
Scenario I: Southwest Cut (5' X 100'), with Parker's Cut sized to be stable (estimated at 2-4' X 350')



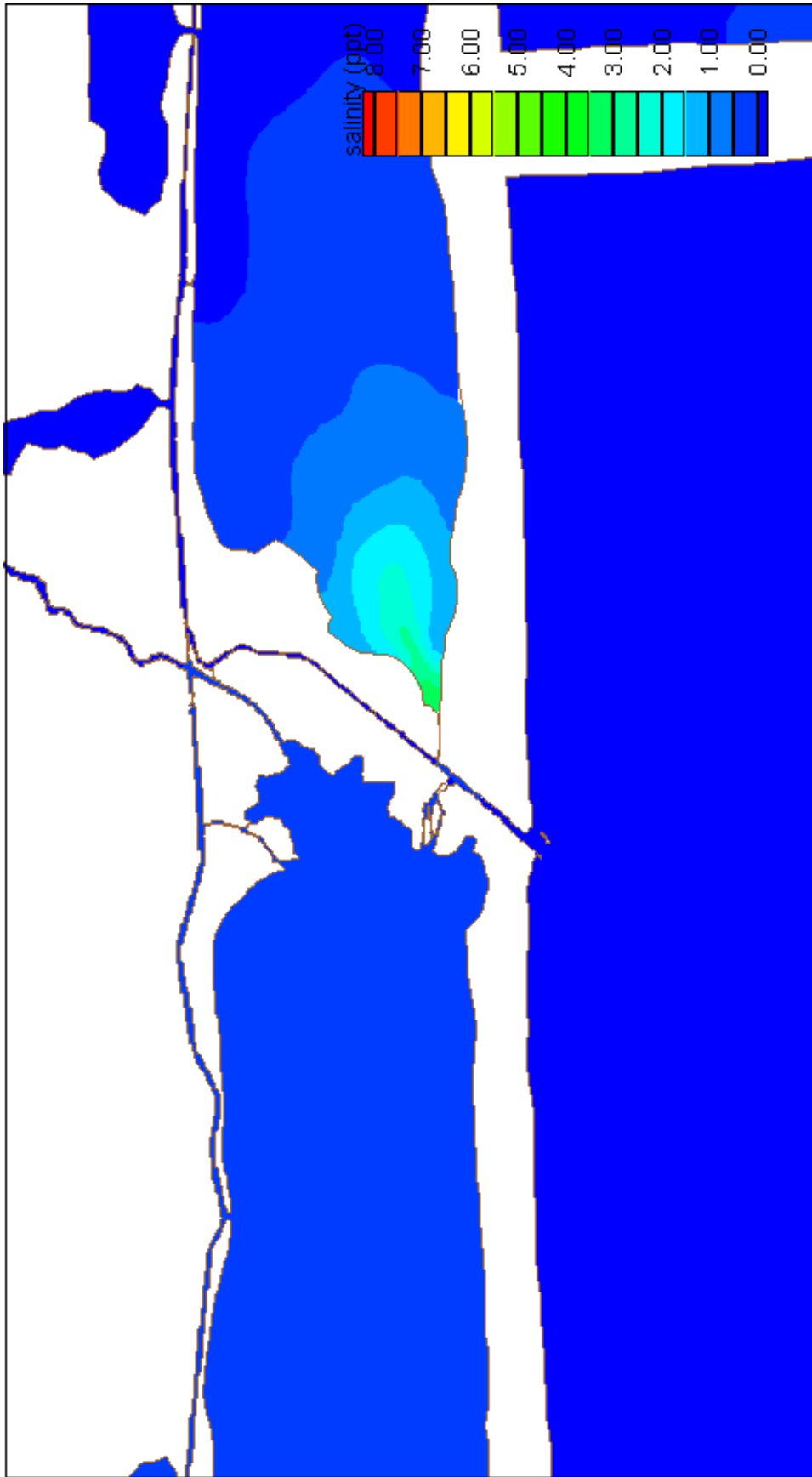
Salinity Difference, Scenario I, Medium River Discharge
 Scenario I: Southwest Cut (5' X 100'), with Parker's Cut sized to be stable (estimated at 2-4' X 350')



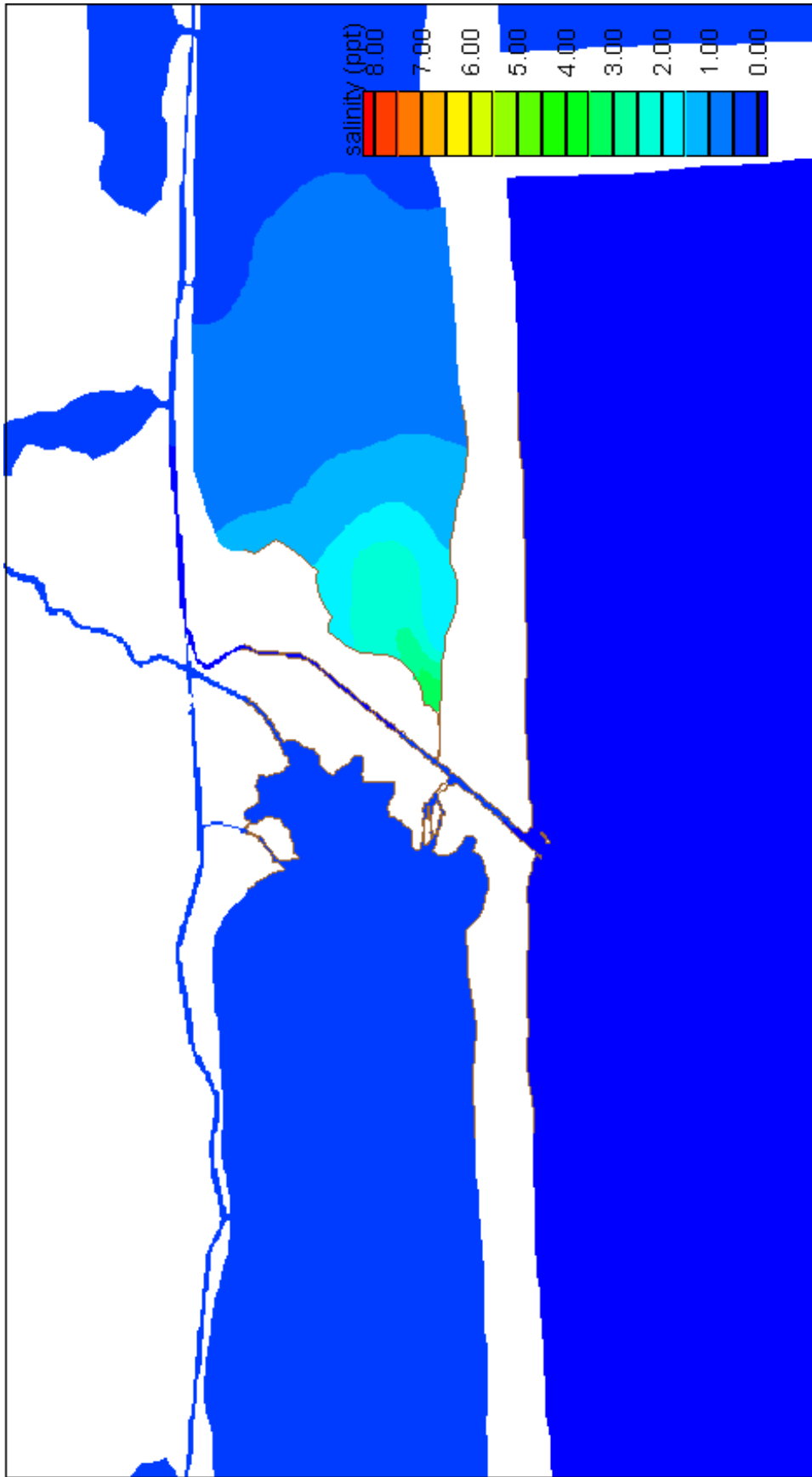
Salinity Difference, Scenario I, High River Discharge
 Scenario I: Southwest Cut (5' X 100'), with Parker's Cut sized to be stable (estimated at 2-4' X 350')



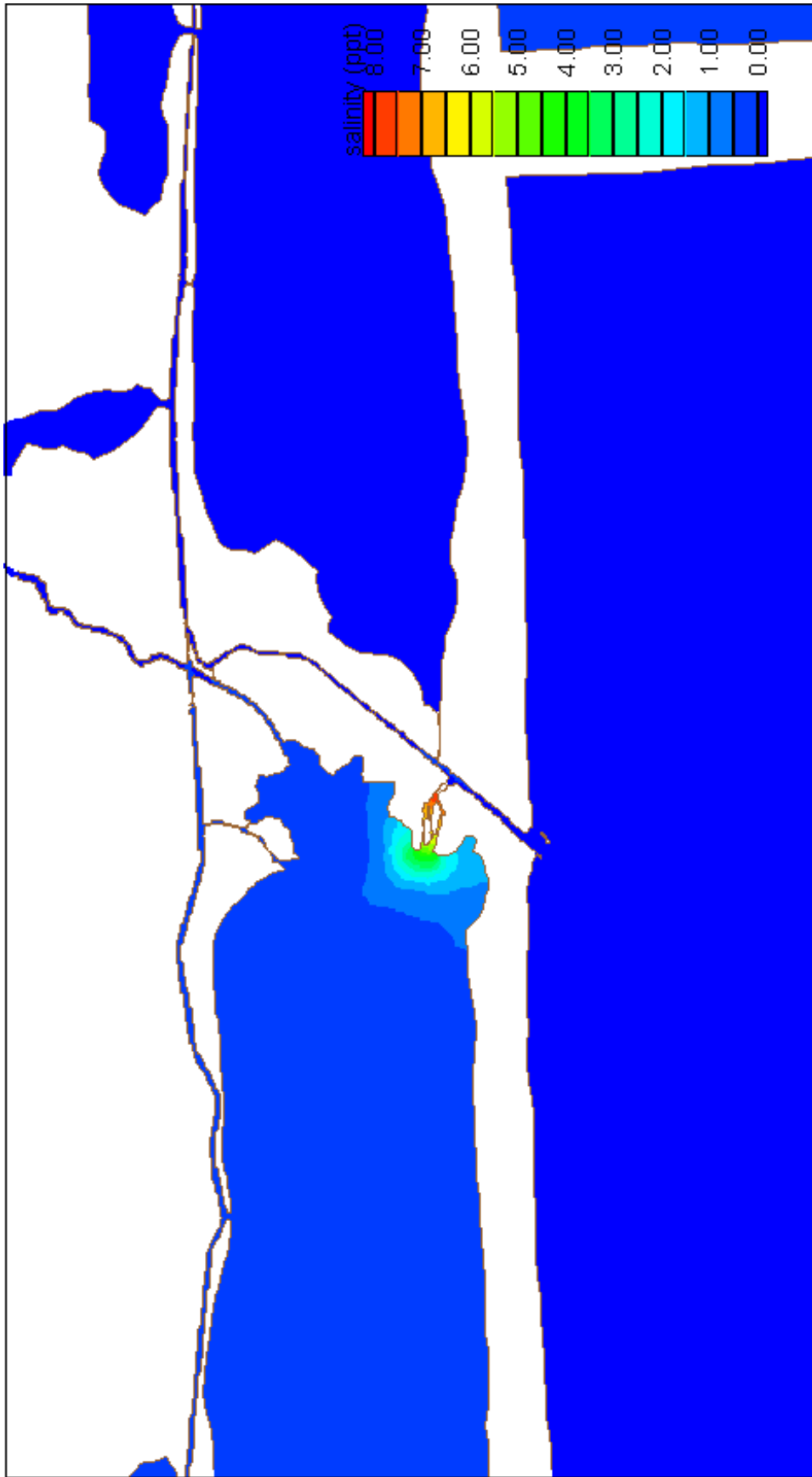
Salinity Difference, Scenario J, Low River Discharge
 Scenario J: Southwest Cut (5' X 100') with bypass channel around diversion dam (4' X 20')



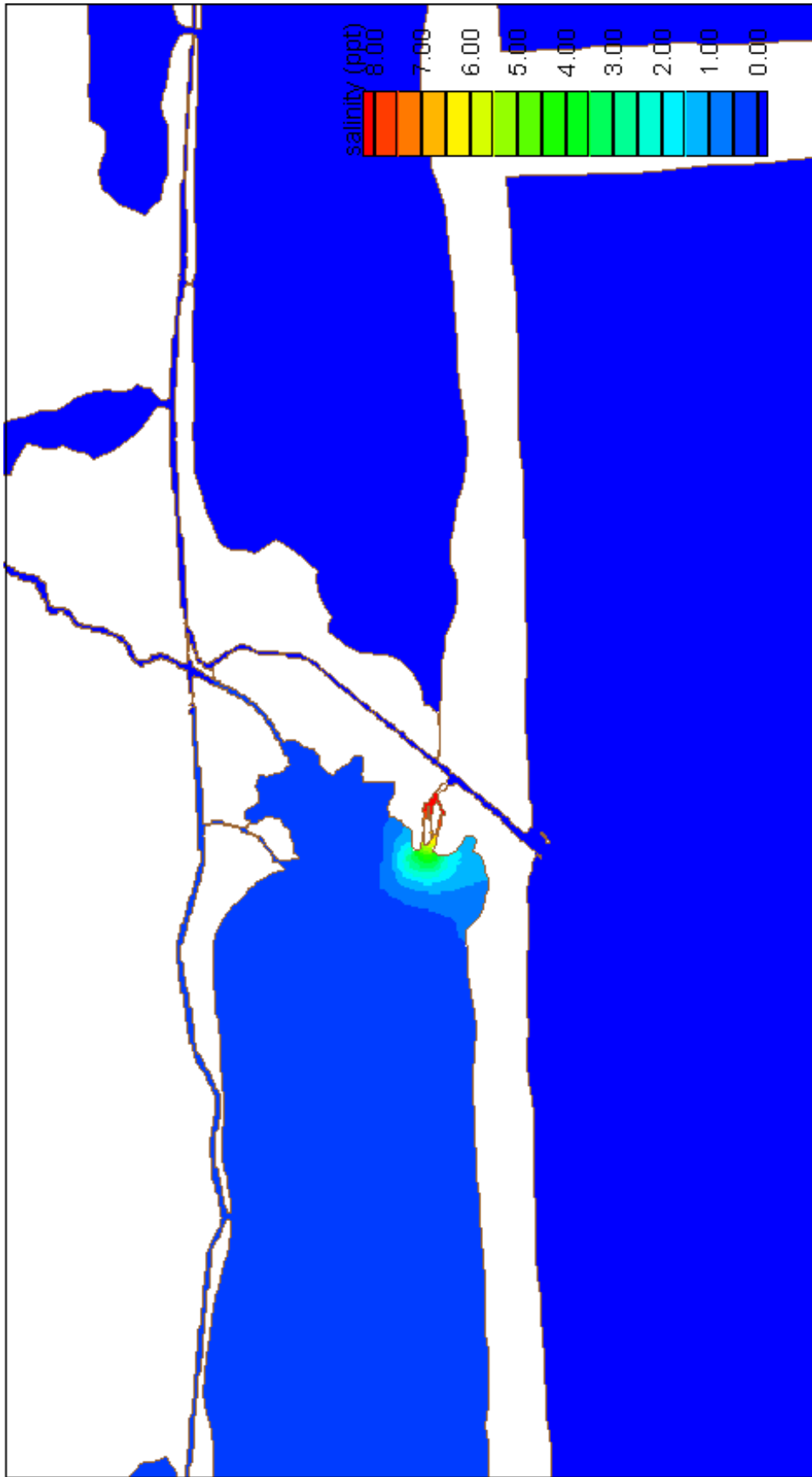
Salinity Difference, Scenario J, Medium River Discharge
 Scenario J: Southwest Cut (5' X 100') with bypass channel around diversion dam (4' X 20')



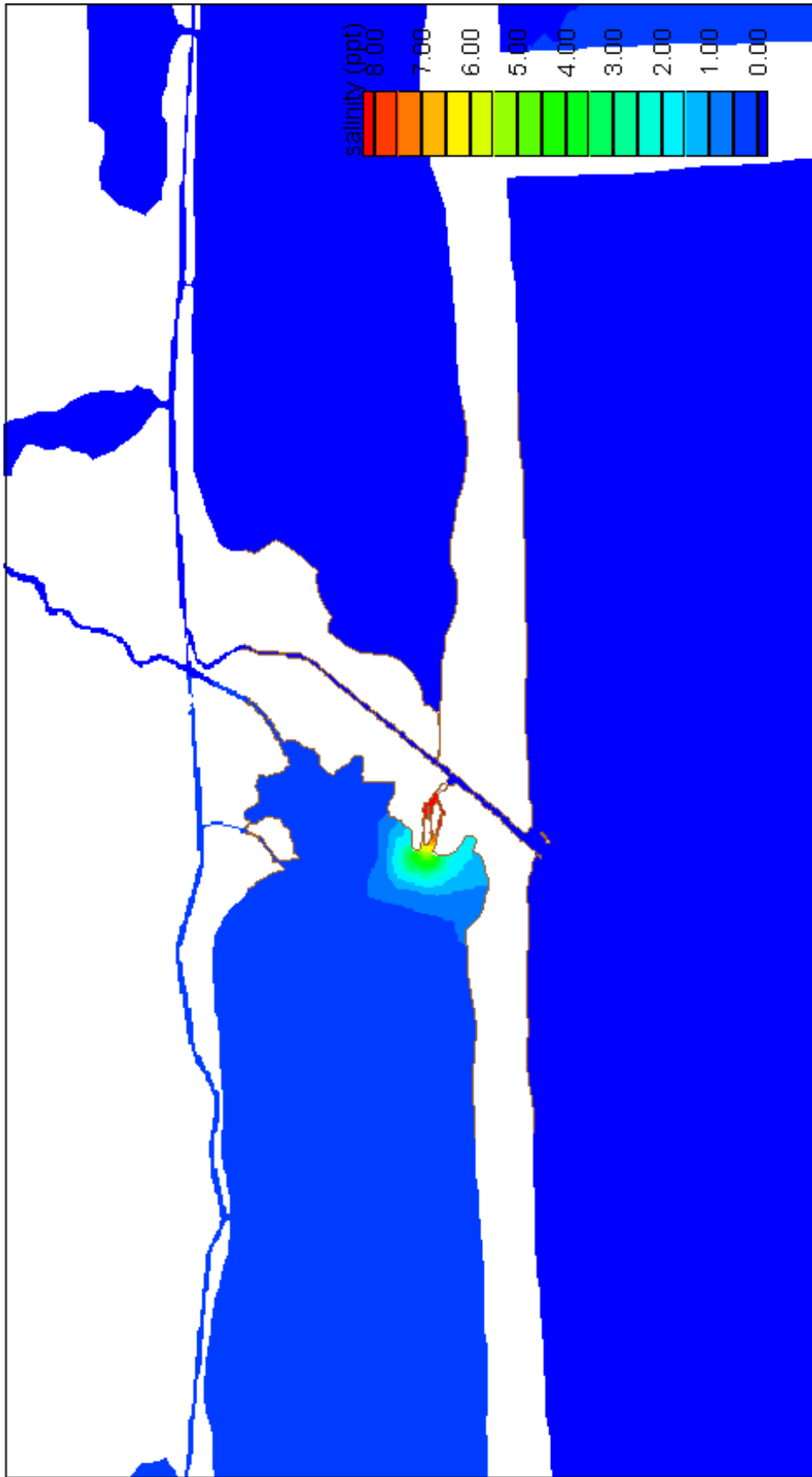
Salinity Difference, Scenario J, High River Discharge
Scenario J: Southwest Cut (5' X 100') with bypass channel around diversion dam (4' X 20')



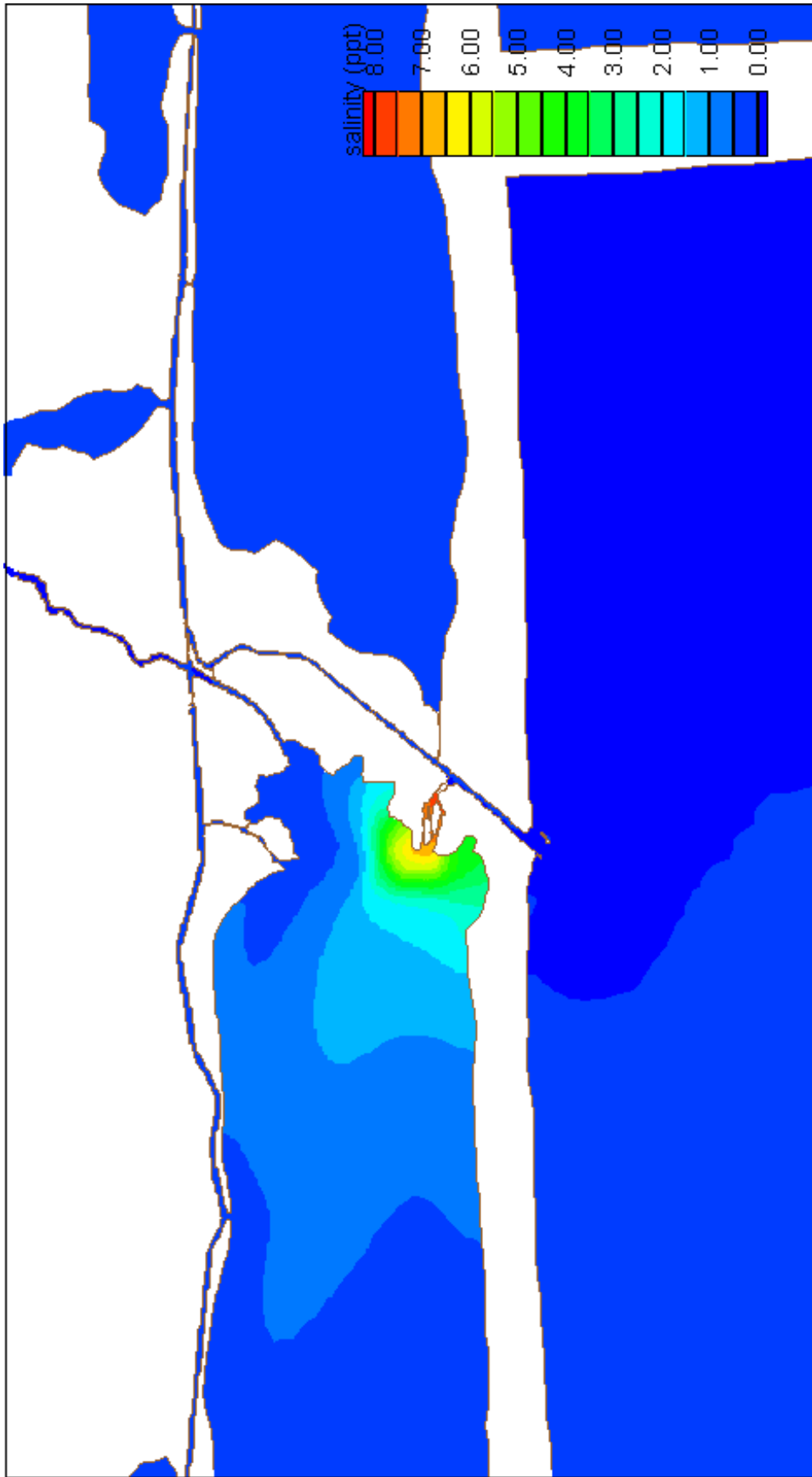
Salinity Difference, Scenario K, Low River Discharge
 Scenario K: Parker's Cut (4' X 20') with bypass channel around diversion dam (4' X 20')



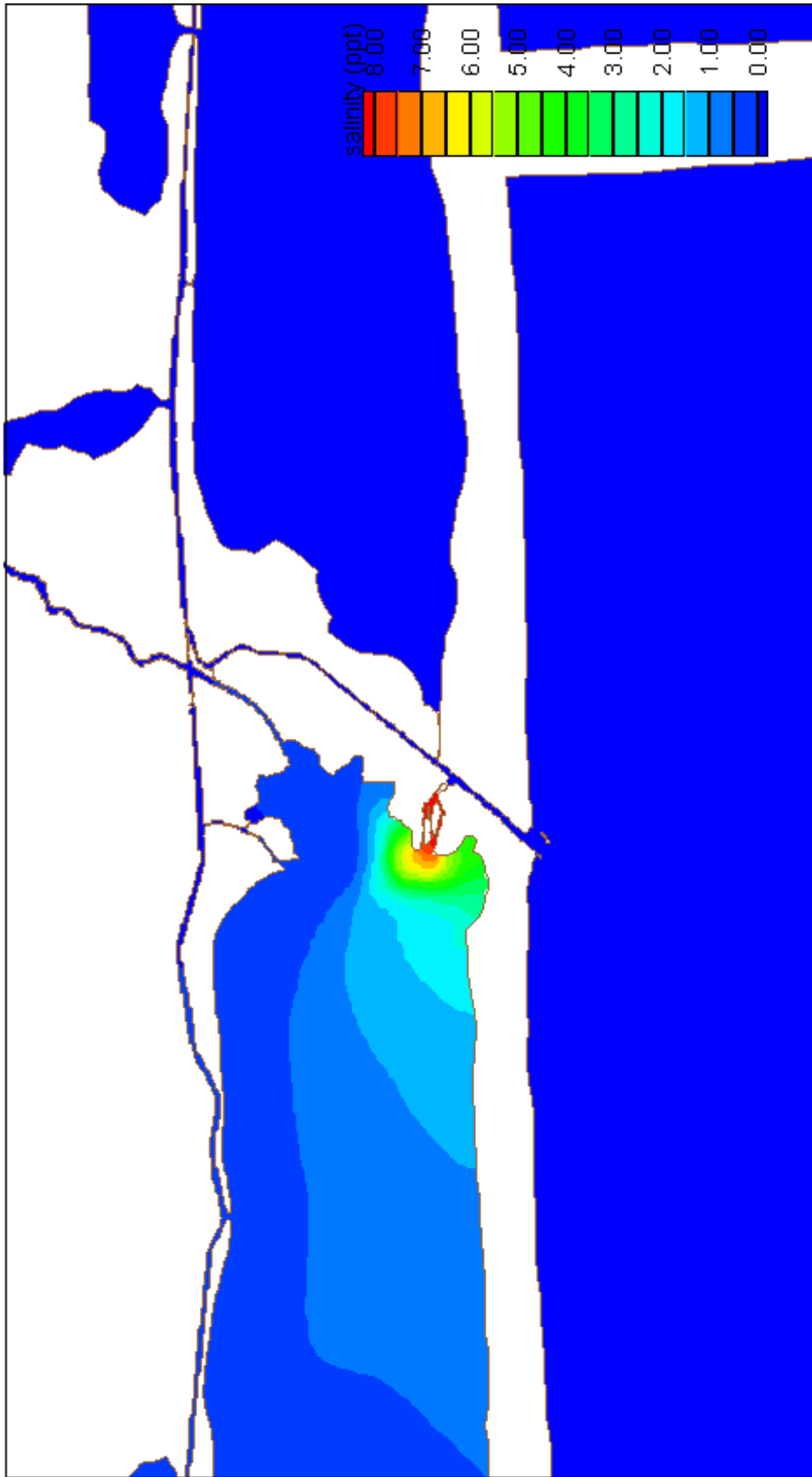
Salinity Difference, Scenario K, Medium River Discharge
 Scenario K: Parker's Cut (4' X 20') with bypass channel around diversion dam (4' X 20')



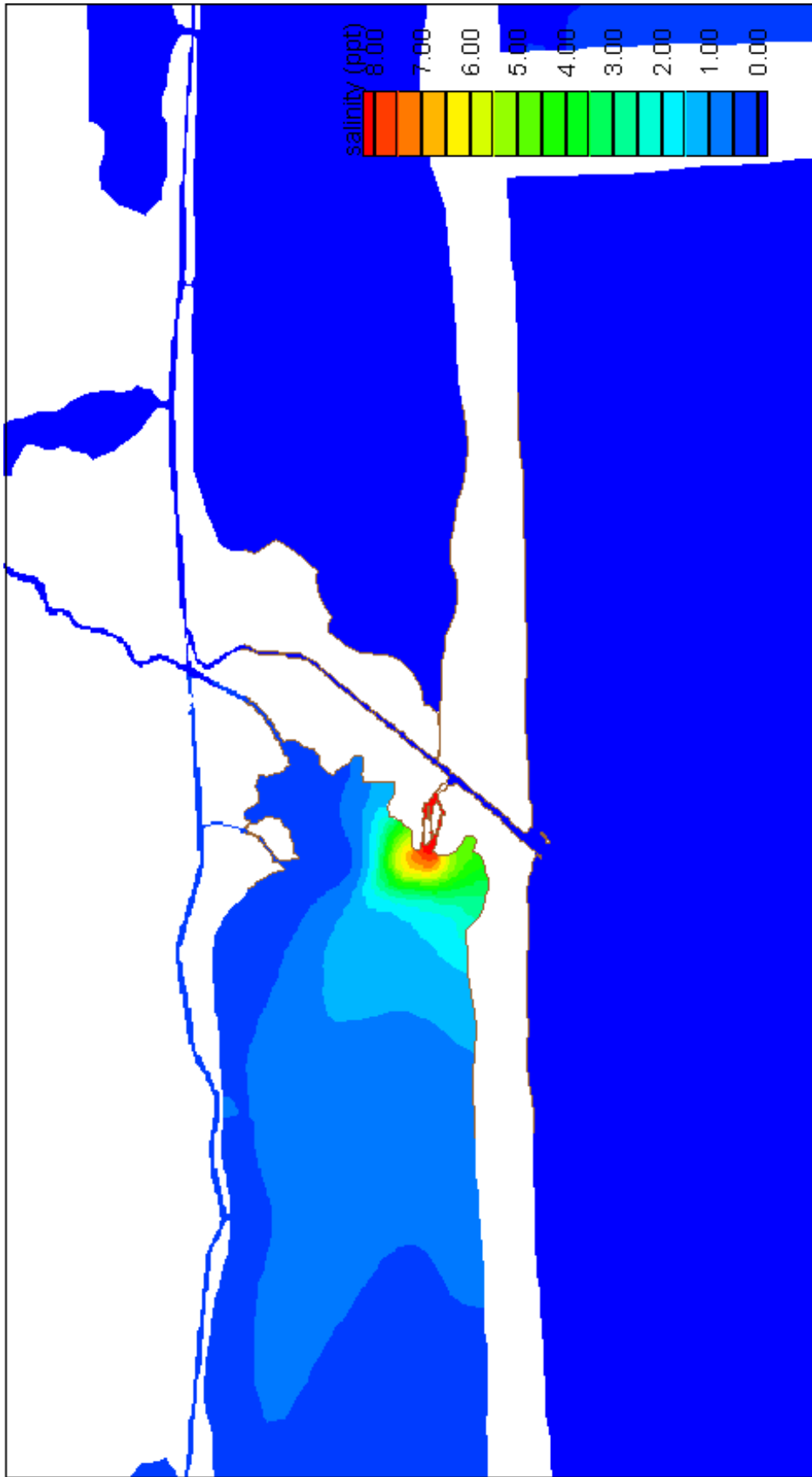
Salinity Difference, Scenario K, High River Discharge
 Scenario K: Parker's Cut (4' X 20') with bypass channel around diversion dam (4' X 20')



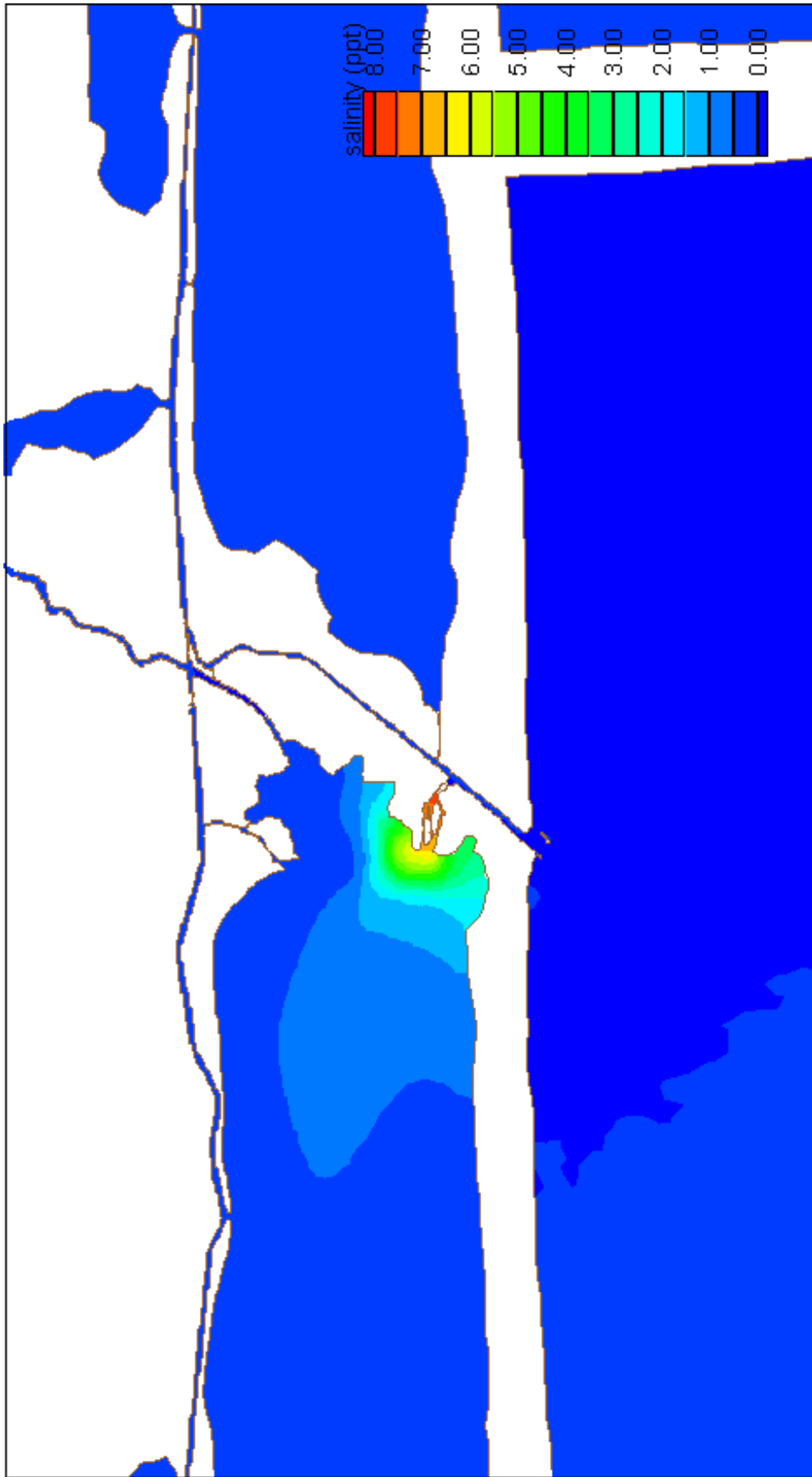
Salinity Difference, Scenario L, Low River Discharge
 Scenario L: Parker's Cut sized to be stable (estimated at 2-4' X 350') with bypass channel around diversion dam (4' X 20')



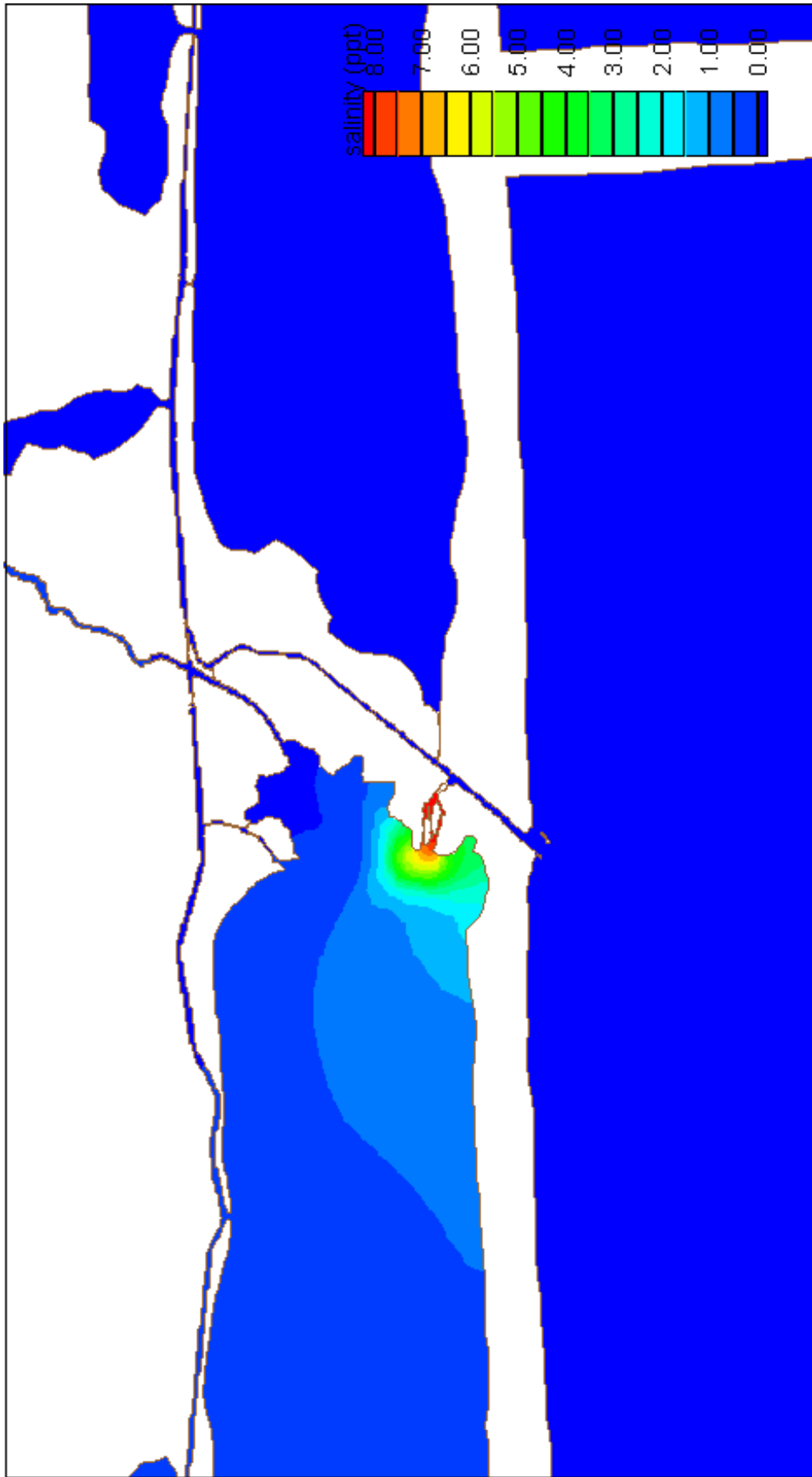
Salinity Difference, Scenario L, Medium River Discharge
 Scenario L: Parker's Cut sized to be stable (estimated at 2-4' X 350') with bypass channel around diversion dam (4' X 20')



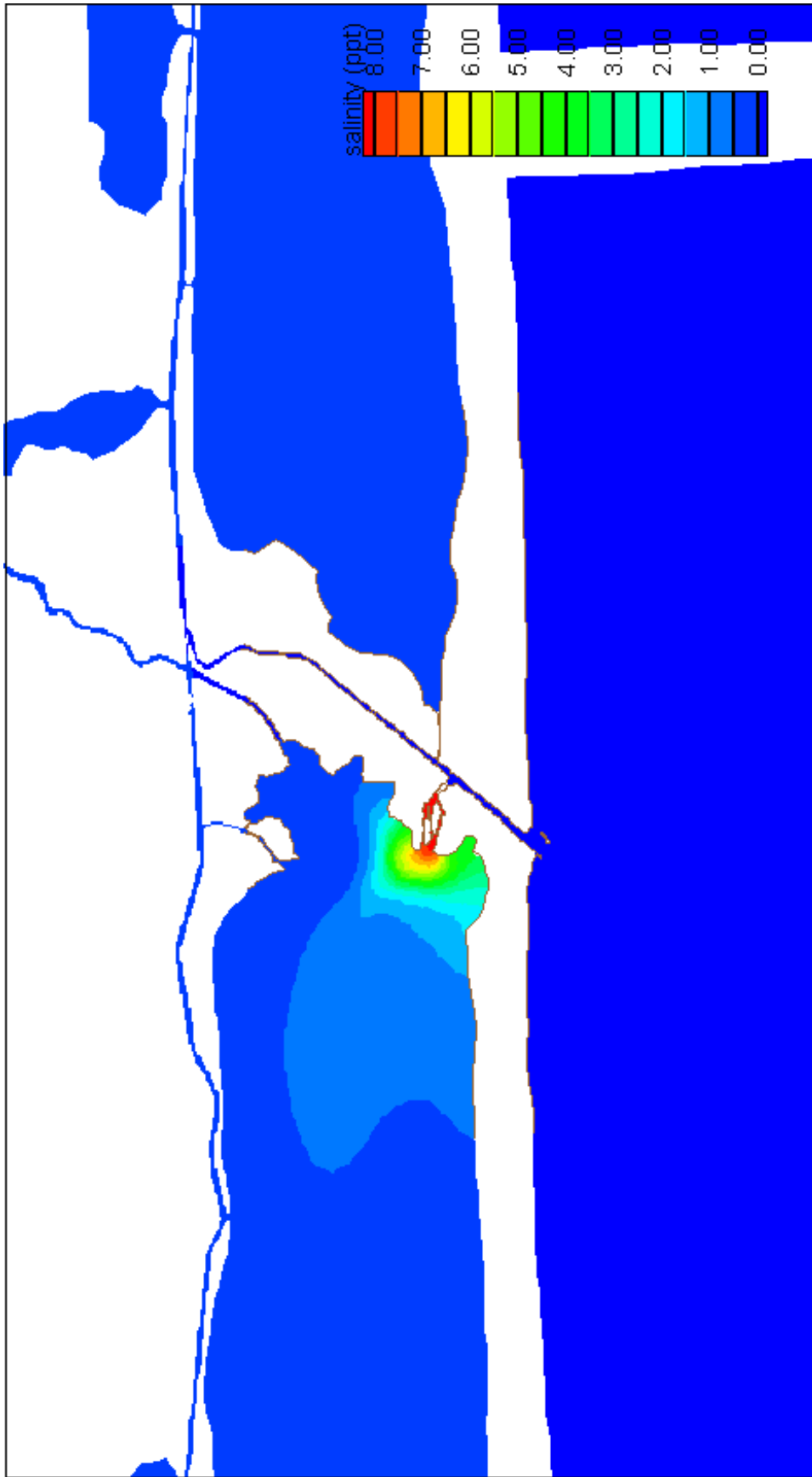
Salinity Difference, Scenario L, High River Discharge
 Scenario L: Parker's Cut sized to be stable (estimated at 2-4' X 350') with bypass channel around diversion dam (4' X 20')



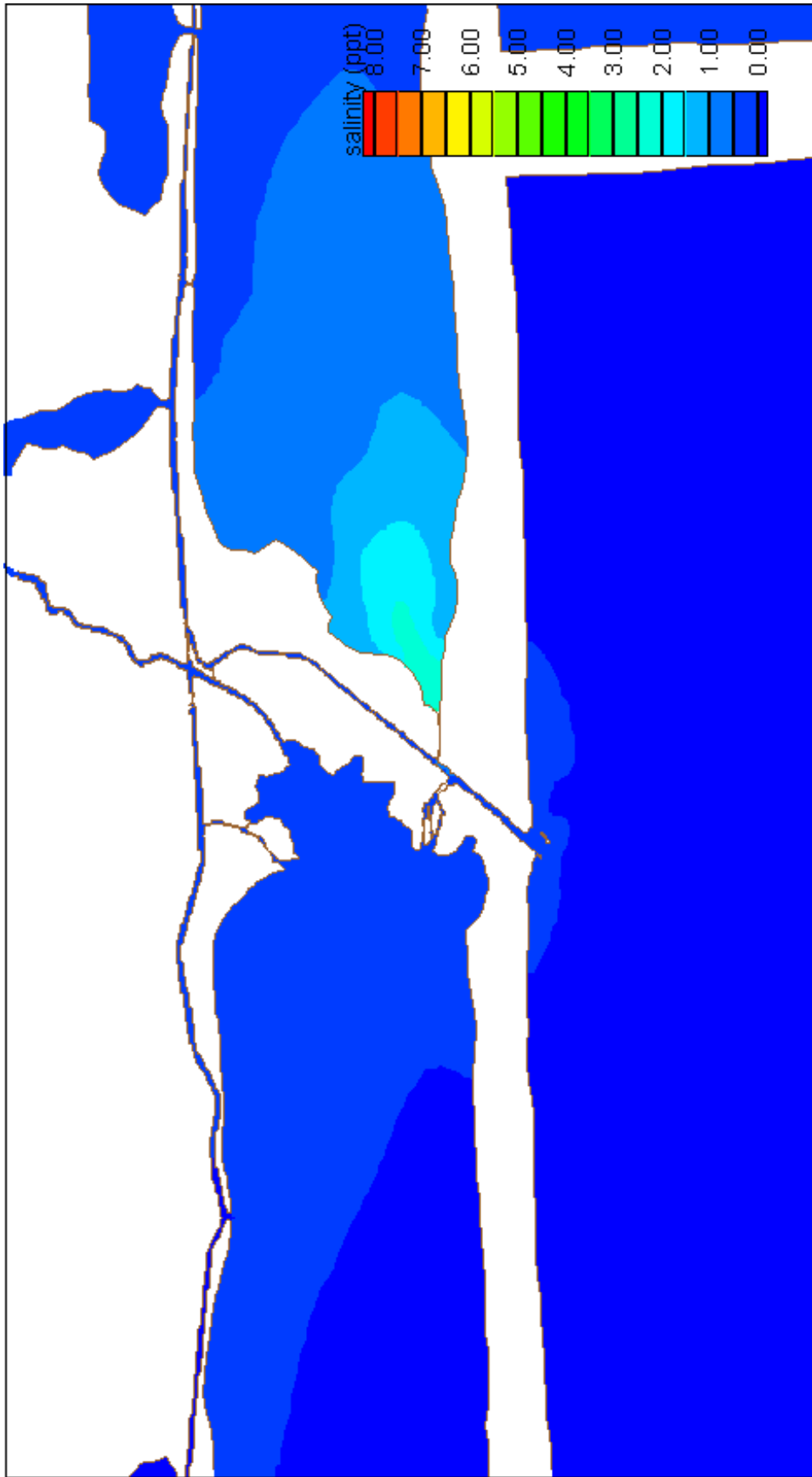
Salinity Difference, Scenario M, Low River Discharge
Scenario M: Parker's Cut (5' X 100')



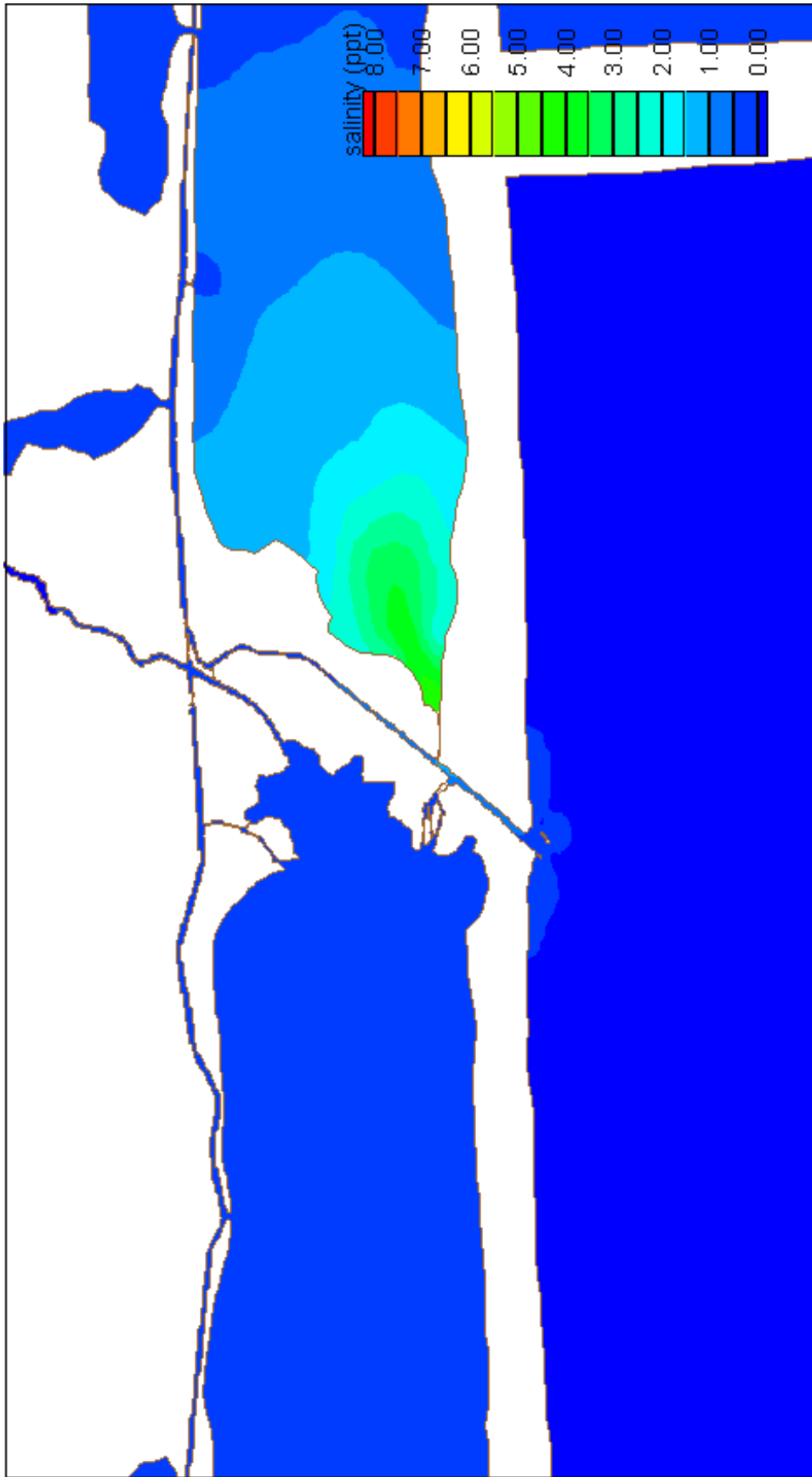
Salinity Difference, Scenario M, Medium River Discharge
Scenario M: Parker's Cut (5' X 100')



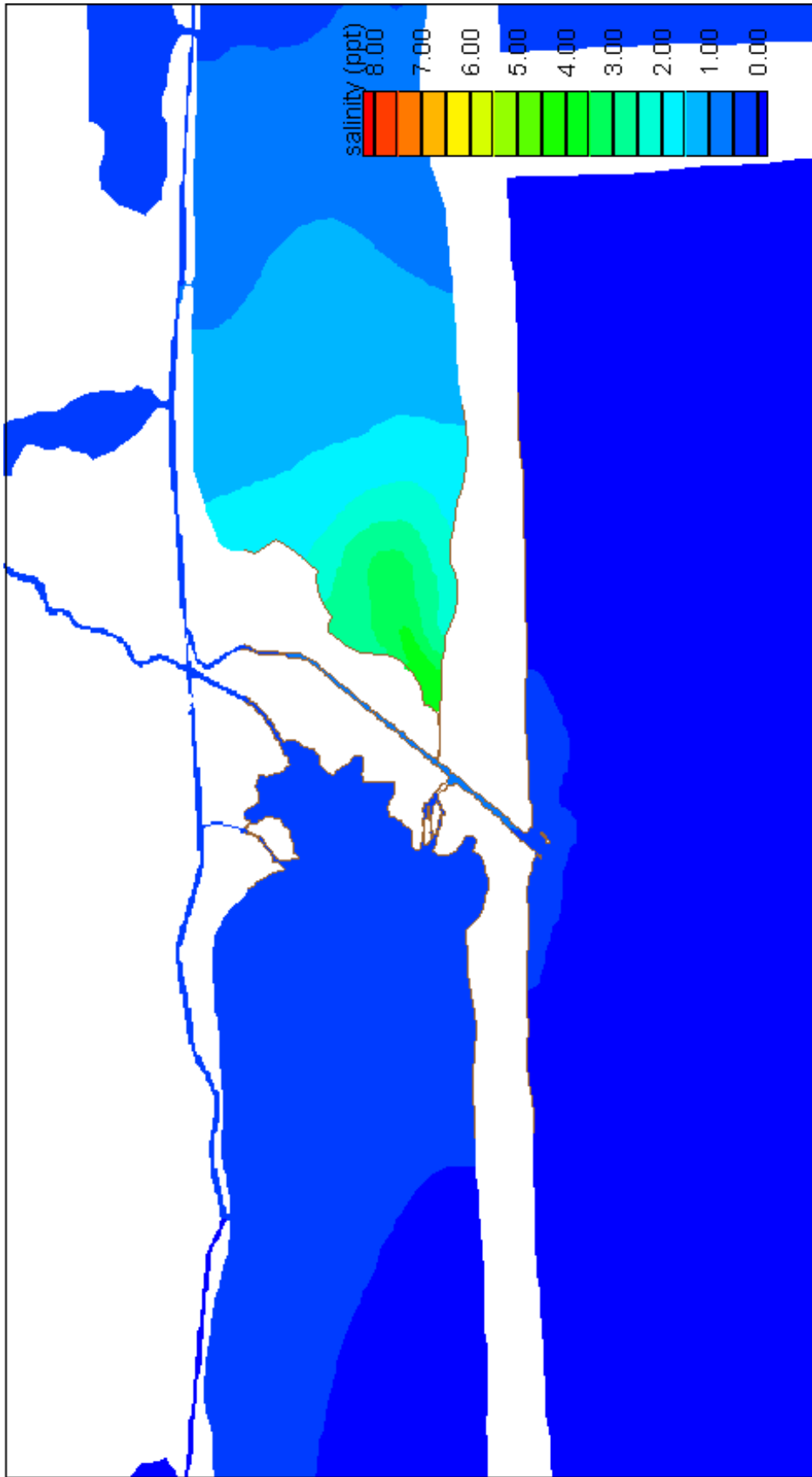
Salinity Difference, Scenario M, High River Discharge
 Scenario M: Parker's Cut (5' X 100')



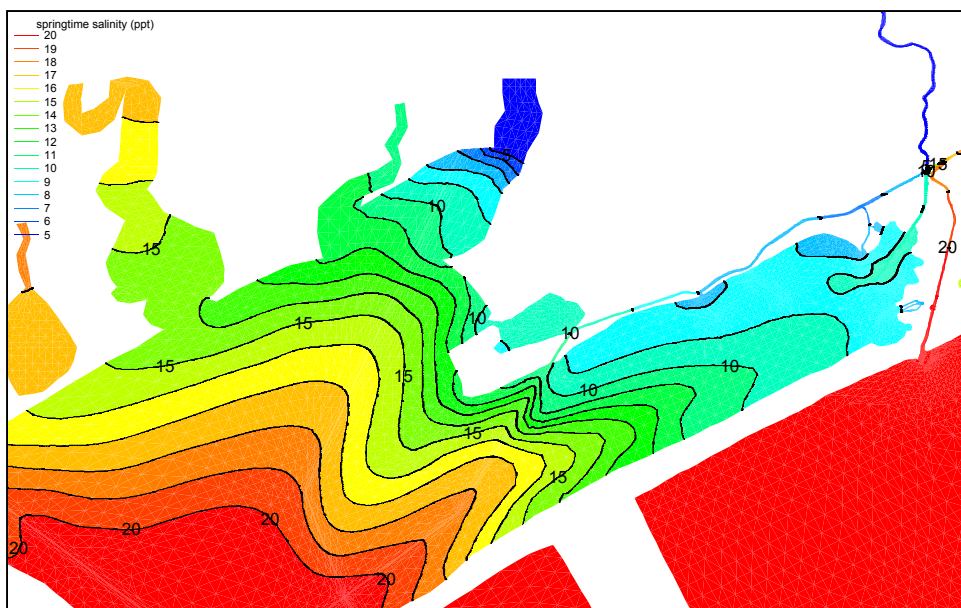
Salinity Difference, Scenario N, Low River Discharge
Scenario N: Southwest Cut (5' X 200')



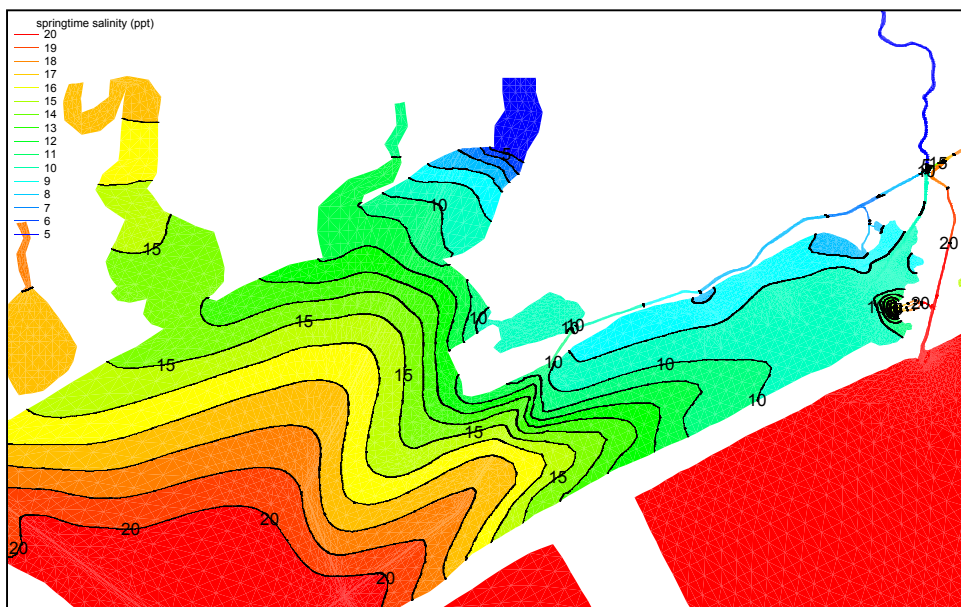
Salinity Difference, Scenario N, Medium River Discharge
Scenario N: Southwest Cut (5' X 200')



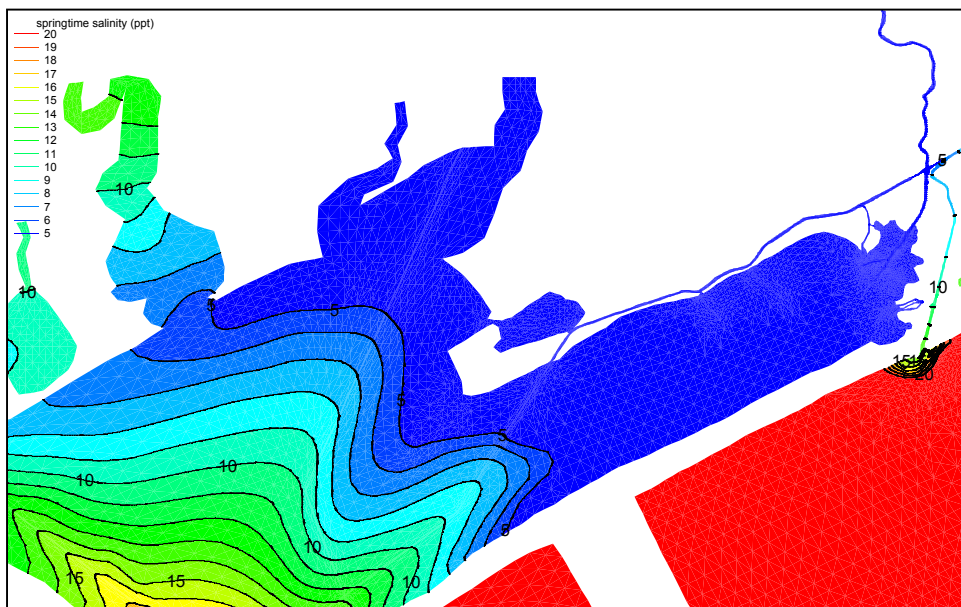
Salinity Difference, Scenario N, High River Discharge
Scenario N: Southwest Cut (5' X 200')



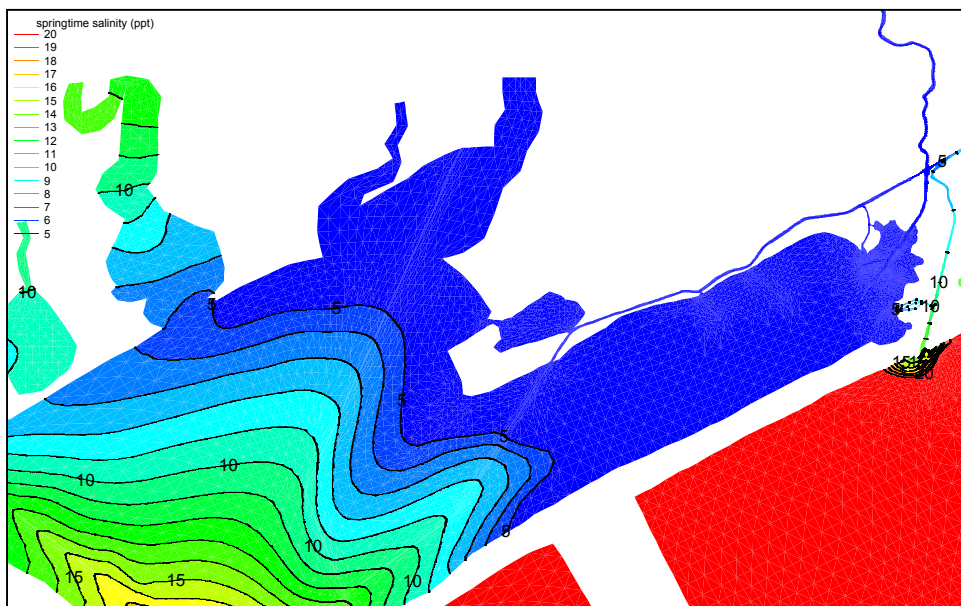
Average Springtime Salinity, Scenario A, High River Discharge
Scenario A: Existing Conditions



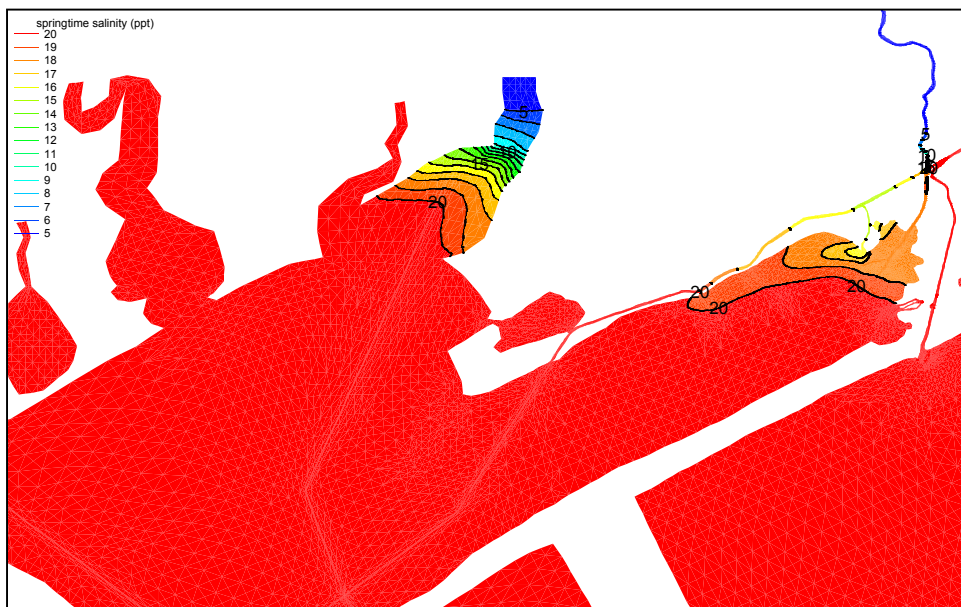
Average Springtime Salinity, Scenario B, High River Discharge
Scenario B: Parker's Cut (4' x 20')



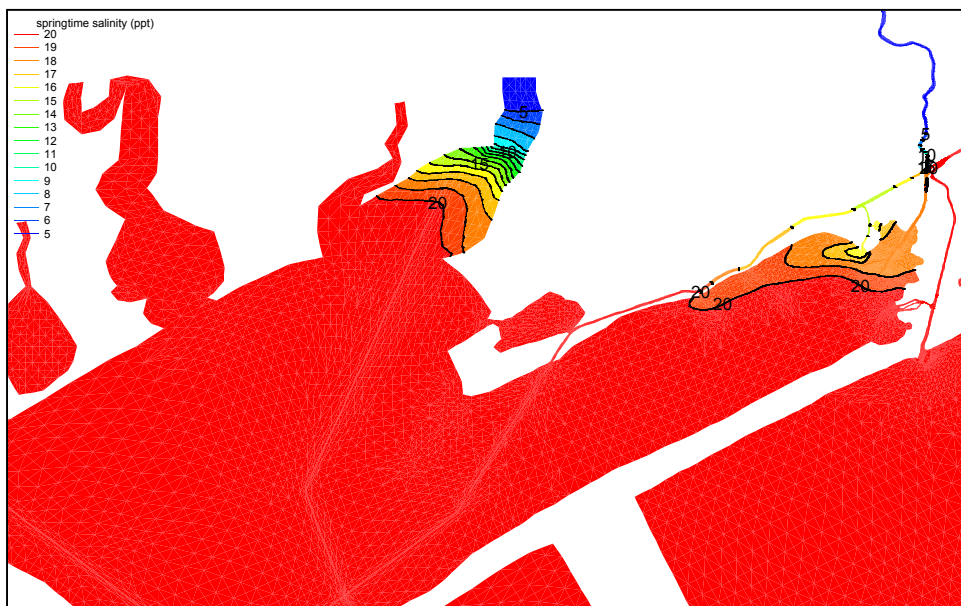
Average Springtime Salinity, Scenario A, Medium River Discharge
 Scenario A: Existing Conditions



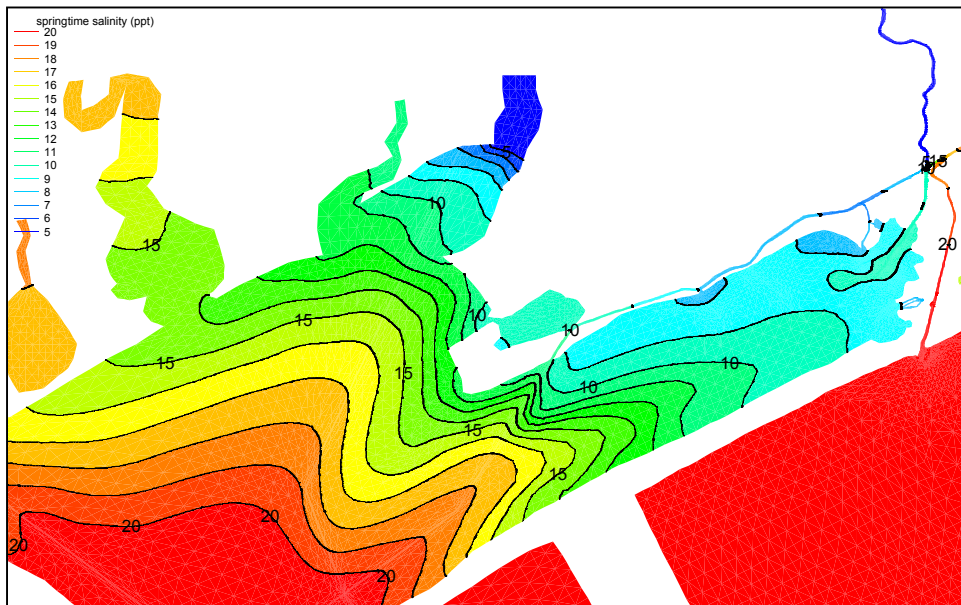
Average Springtime Salinity, Scenario B, Medium River Discharge
 Scenario B: Parker's Cut (4' x 20')



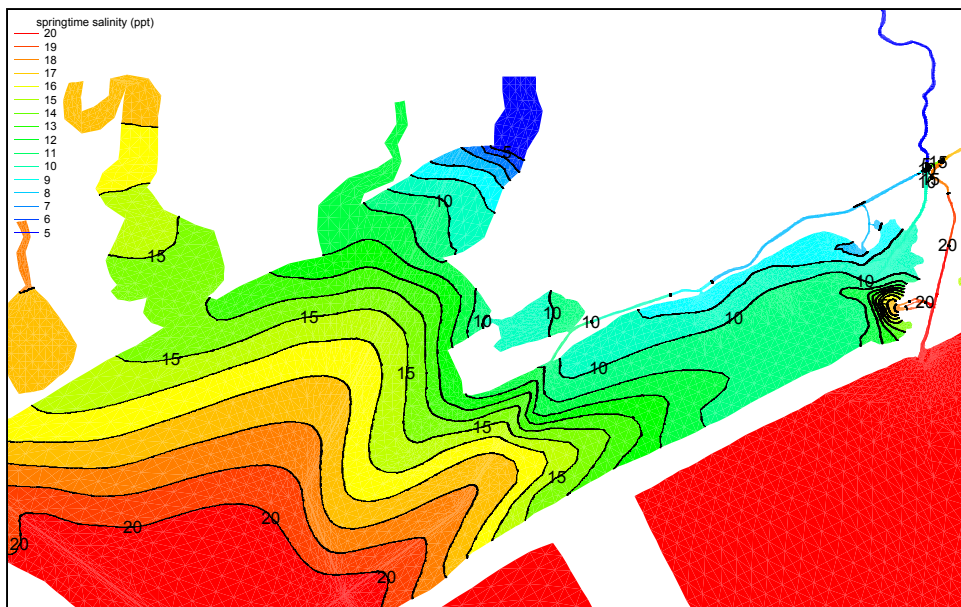
Average Springtime Salinity, Scenario A, Low River Discharge
 Scenario A: Existing Conditions



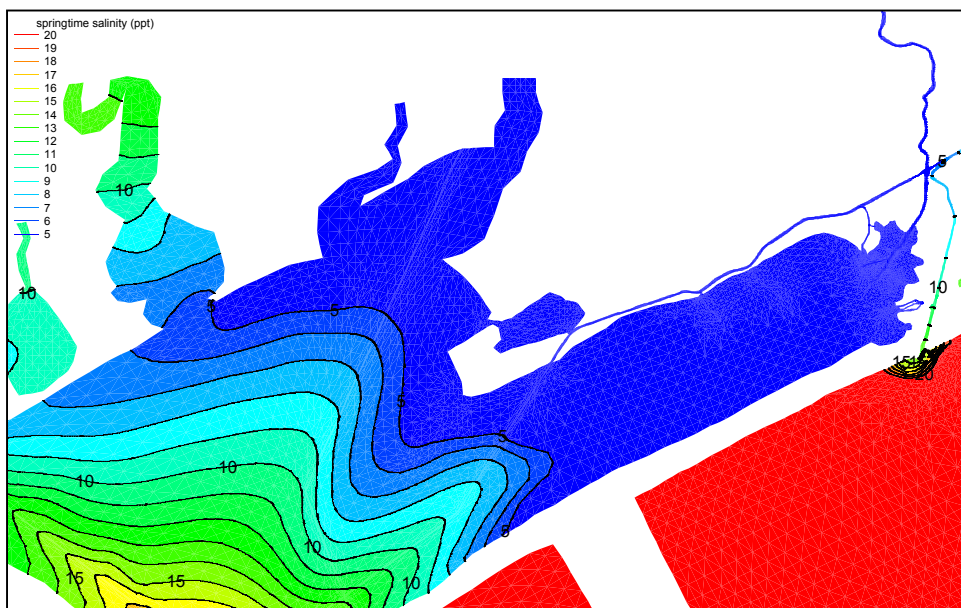
Average Springtime Salinity, Scenario B, Low River Discharge
 Scenario B: Parker's Cut (4' x 20')



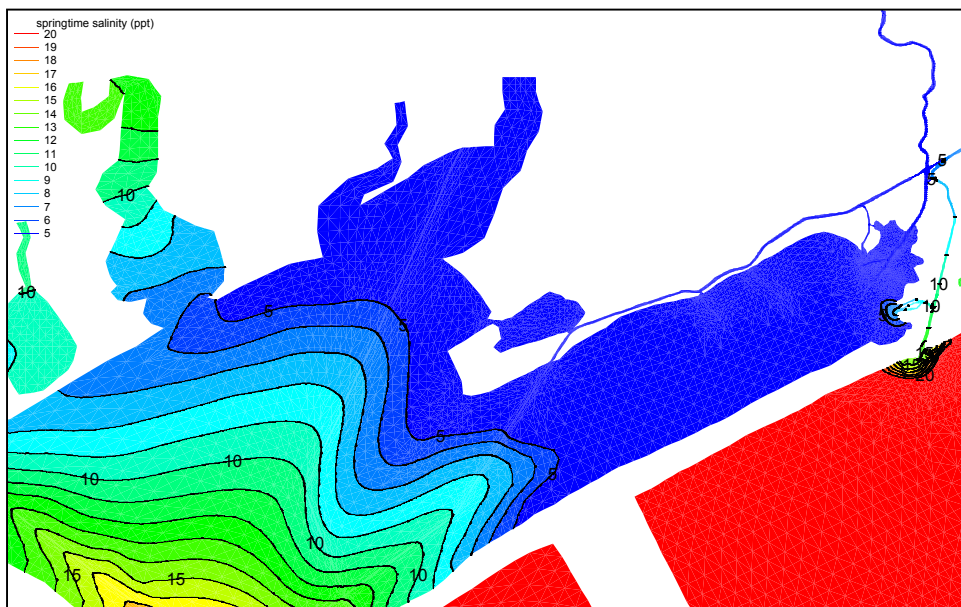
Average Springtime Salinity, Scenario A, High River Discharge
Scenario A: Existing Conditions



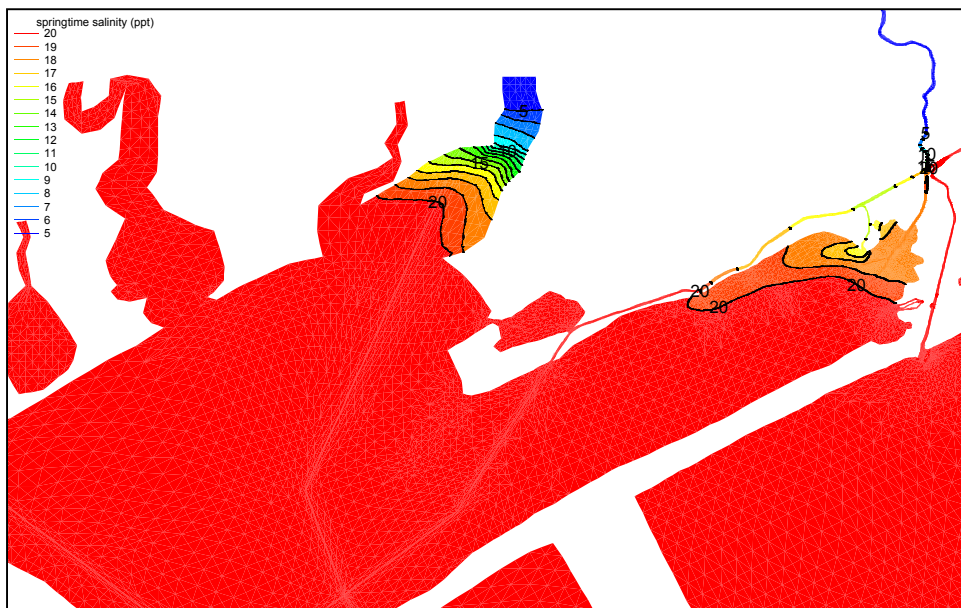
Average Springtime Salinity, Scenario L, High River Discharge
Scenario L: Parker's Cut sized to be stable (estimated at 2-4' x 350') with bypass channel around diversion dam (4' x 20')



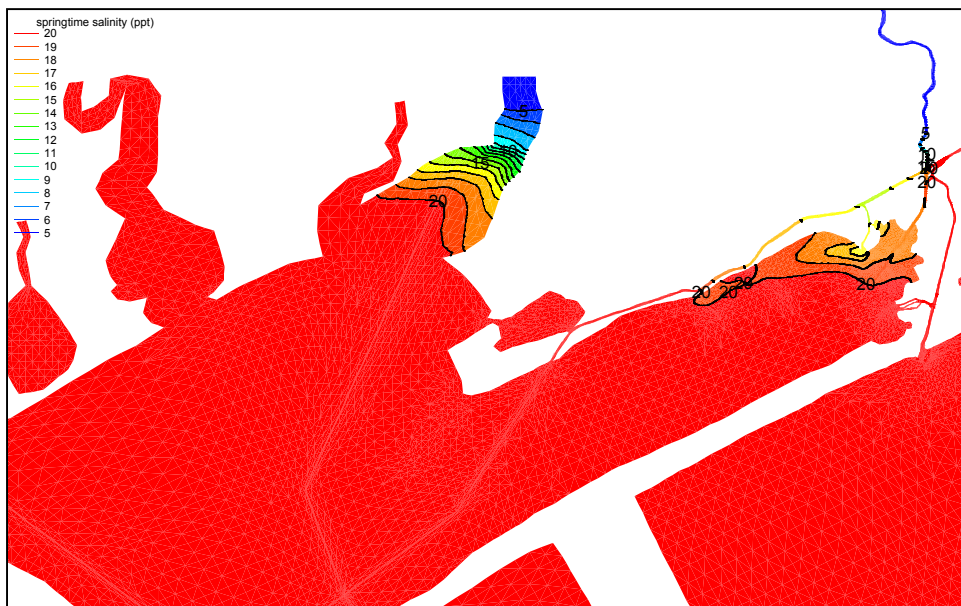
Average Springtime Salinity, Scenario A, Medium River Discharge
Scenario A: Existing Conditions



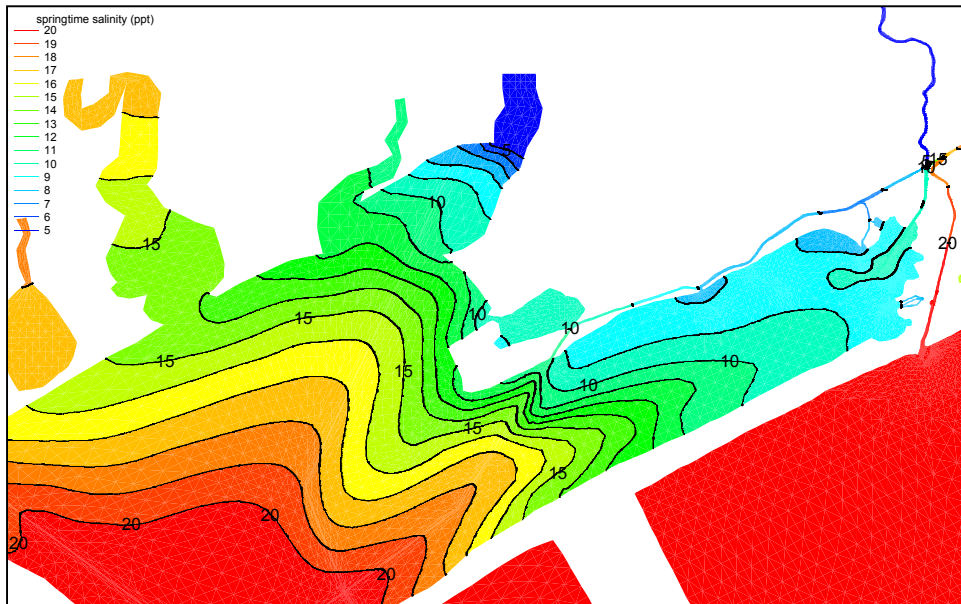
Average Springtime Salinity, Scenario L, Medium River Discharge
Scenario L: Parker's Cut sized to be stable (estimated at 2-4' x 350') with bypass channel around diversion dam (4' x 20')



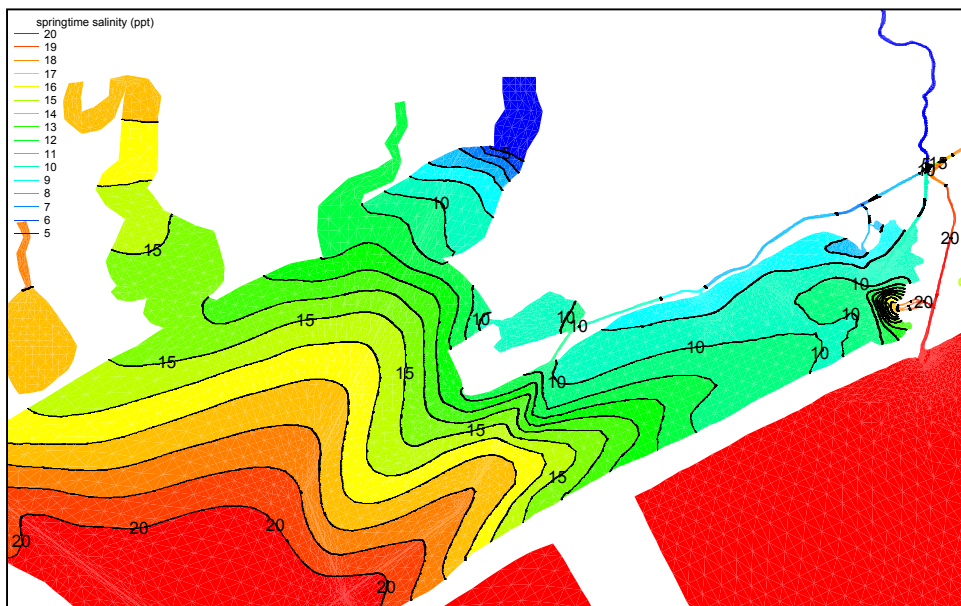
Average Springtime Salinity, Scenario A, Low River Discharge
Scenario A: Existing Conditions



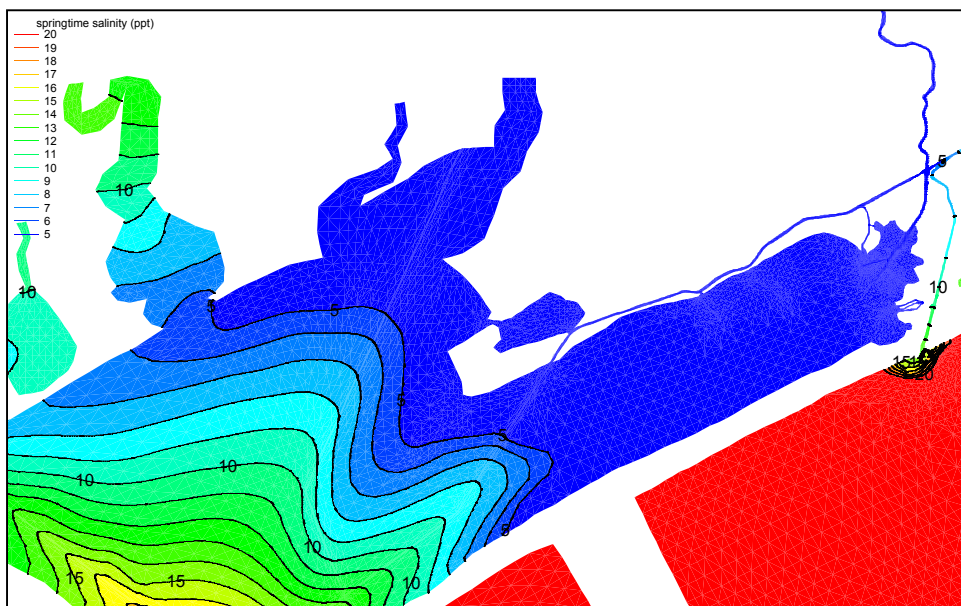
Average Springtime Salinity, Scenario L, Low River Discharge
Scenario L: Parker's Cut sized to be stable (estimated at 2-4' x 350') with bypass channel around diversion dam (4' x 20')



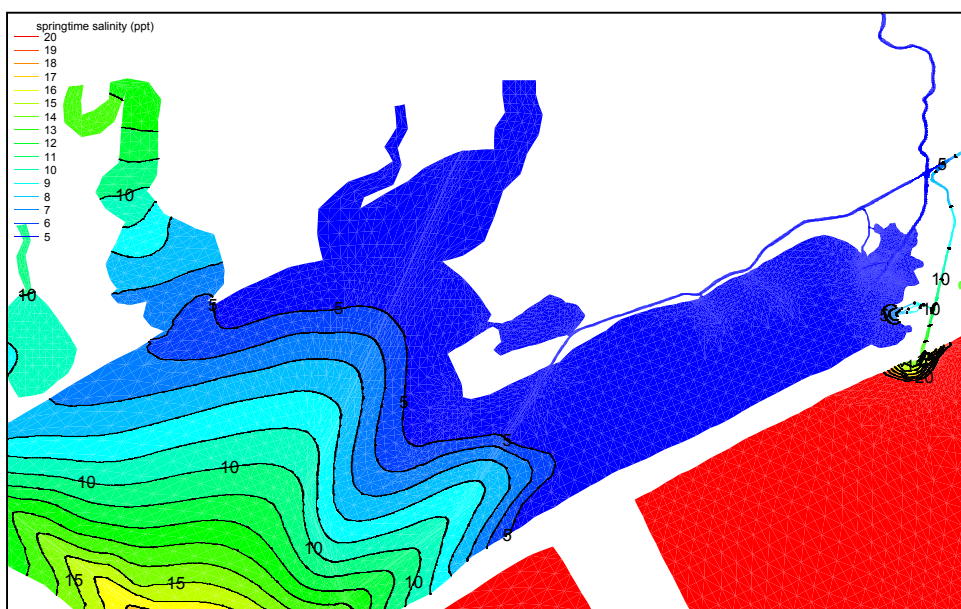
Average Springtime Salinity, Scenario A, High River Discharge
Scenario A: Existing Conditions



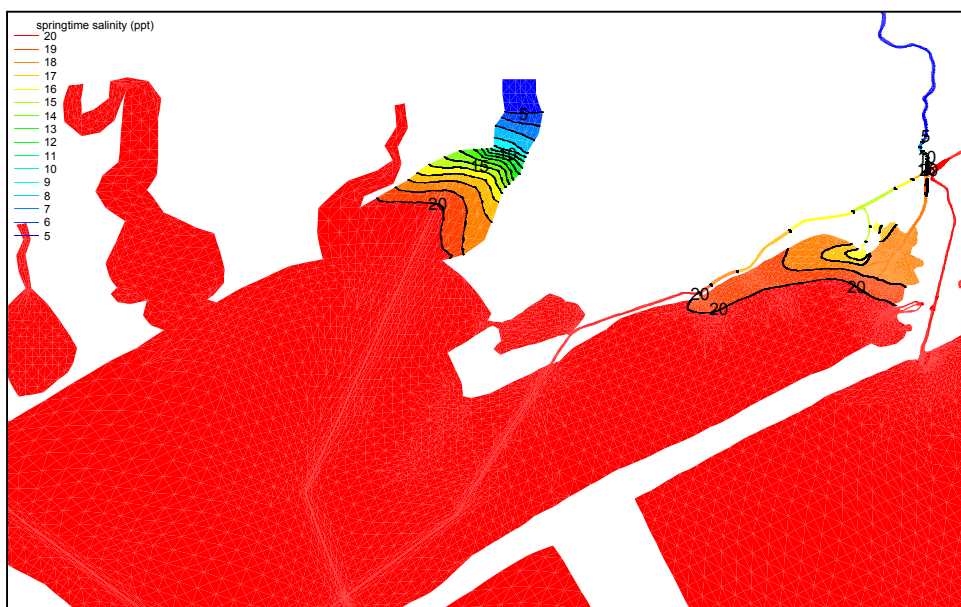
Average Springtime Salinity, Scenario M, High River Discharge
Scenario M: Parker's Cut (5' x 100')



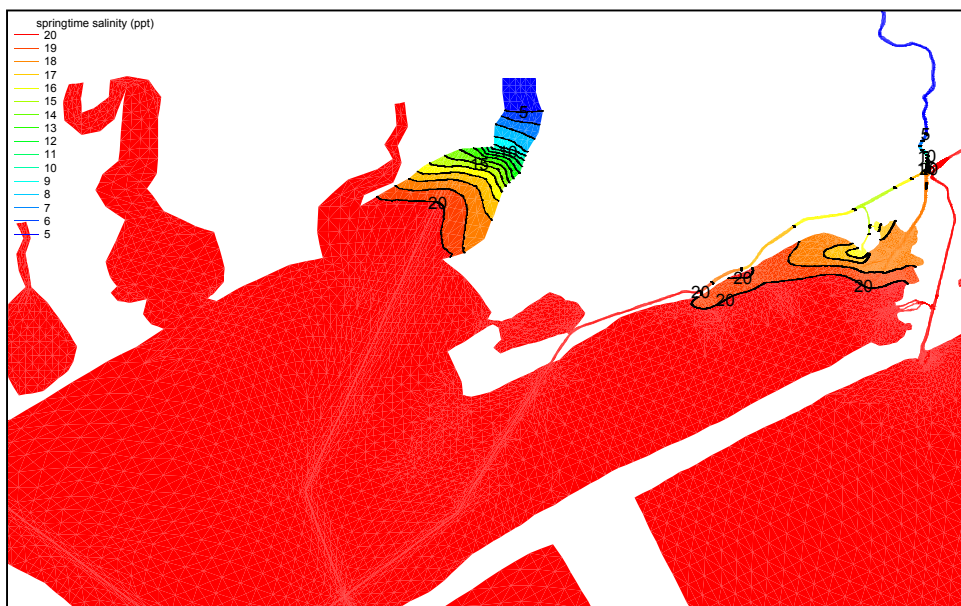
Average Springtime Salinity, Scenario A, Medium River Discharge
Scenario A: Existing Conditions



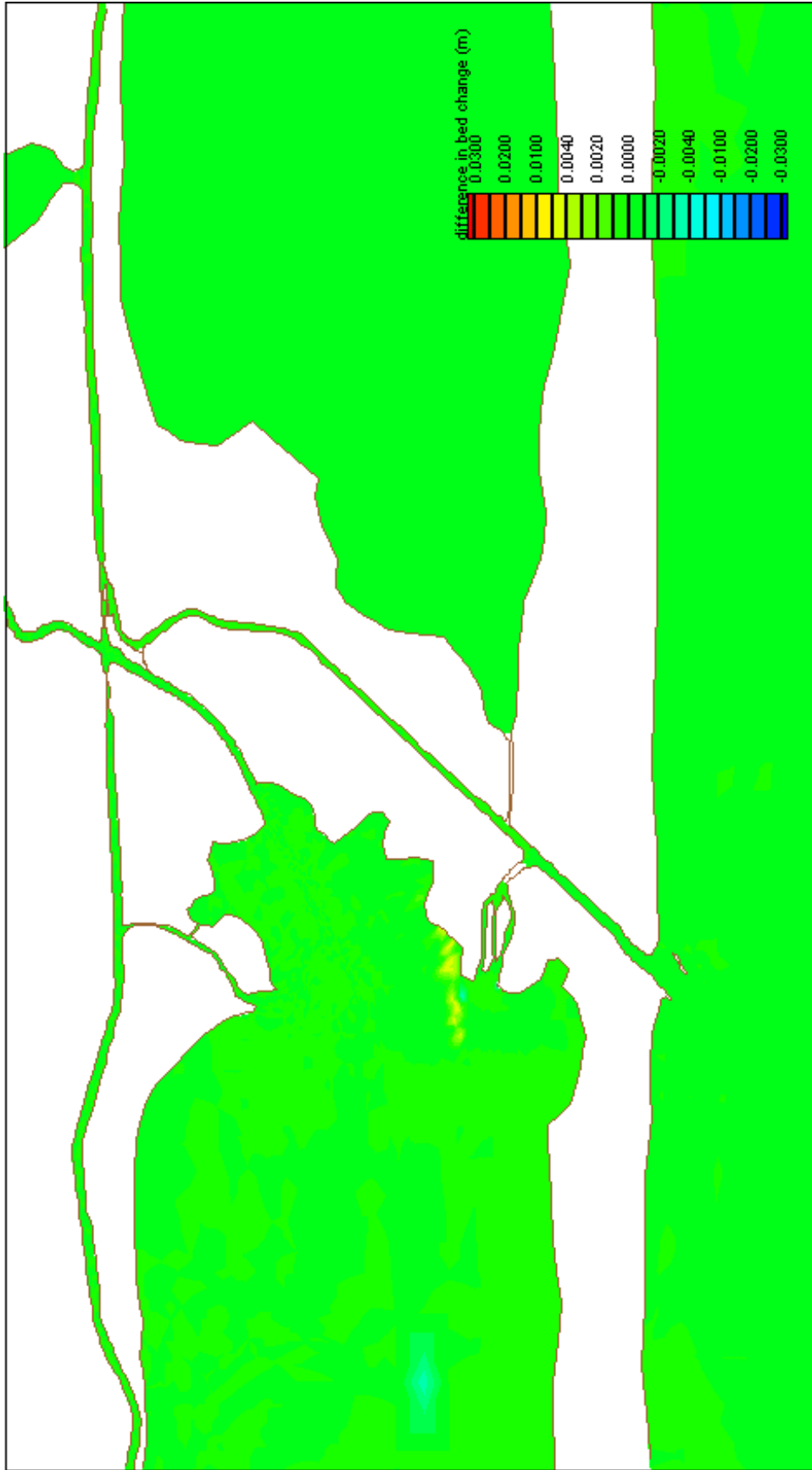
Average Springtime Salinity, Scenario M, Medium River Discharge
Scenario M: Parker's Cut (5' x 100')



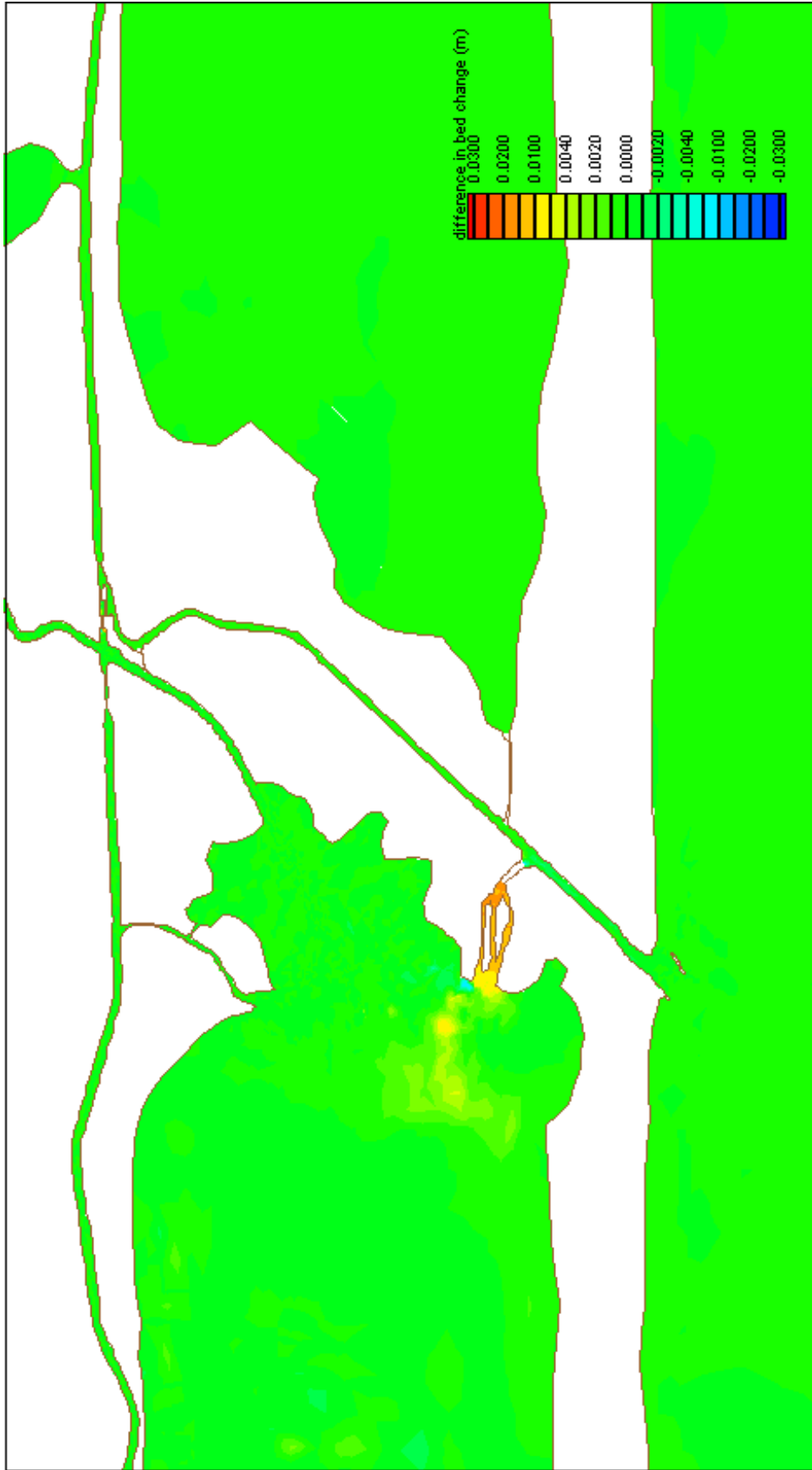
Average Springtime Salinity, Scenario A, Low River Discharge
Scenario A: Existing Conditions



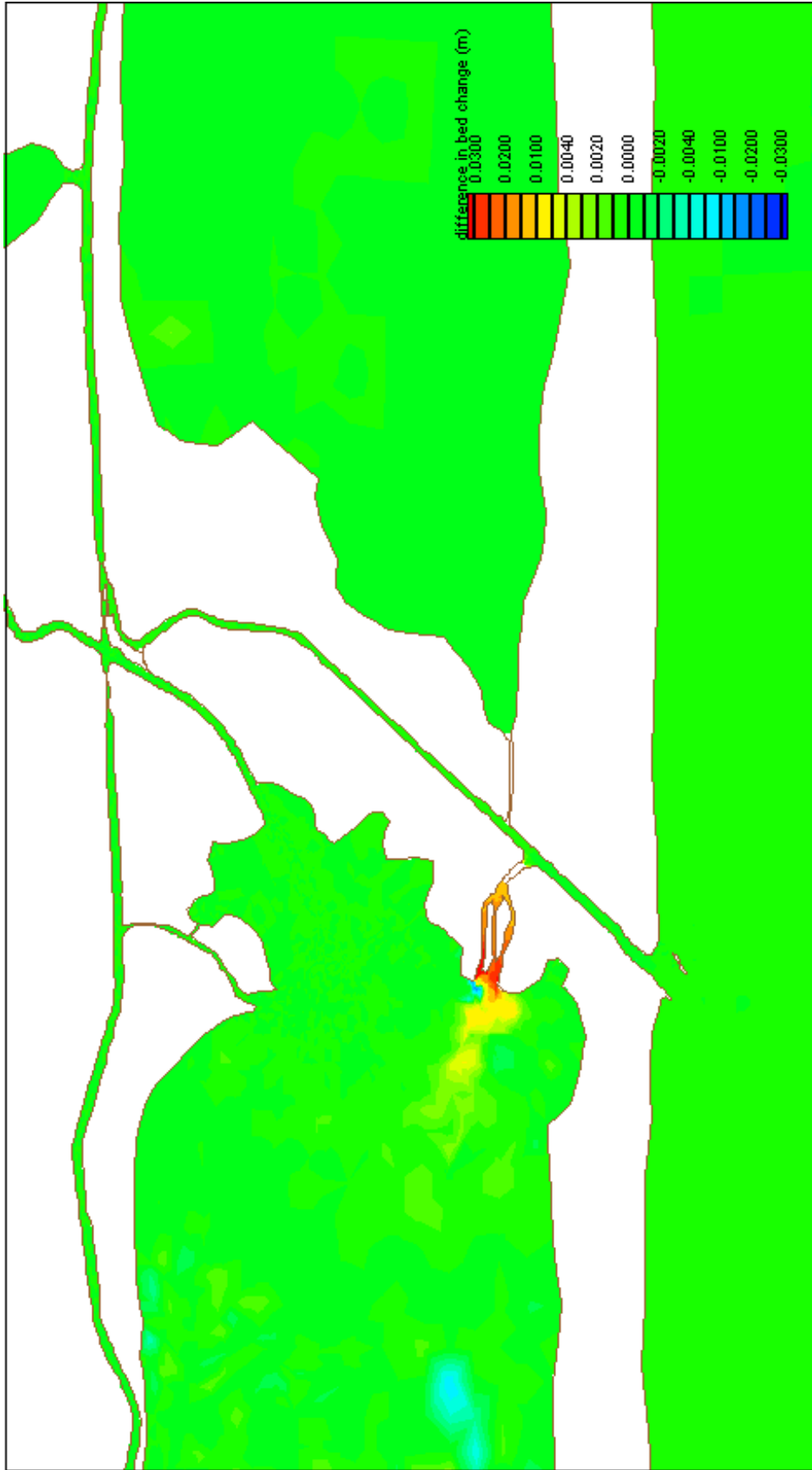
Average Springtime Salinity, Scenario M, Low River Discharge
Scenario M: Parker's Cut (5' x 100')



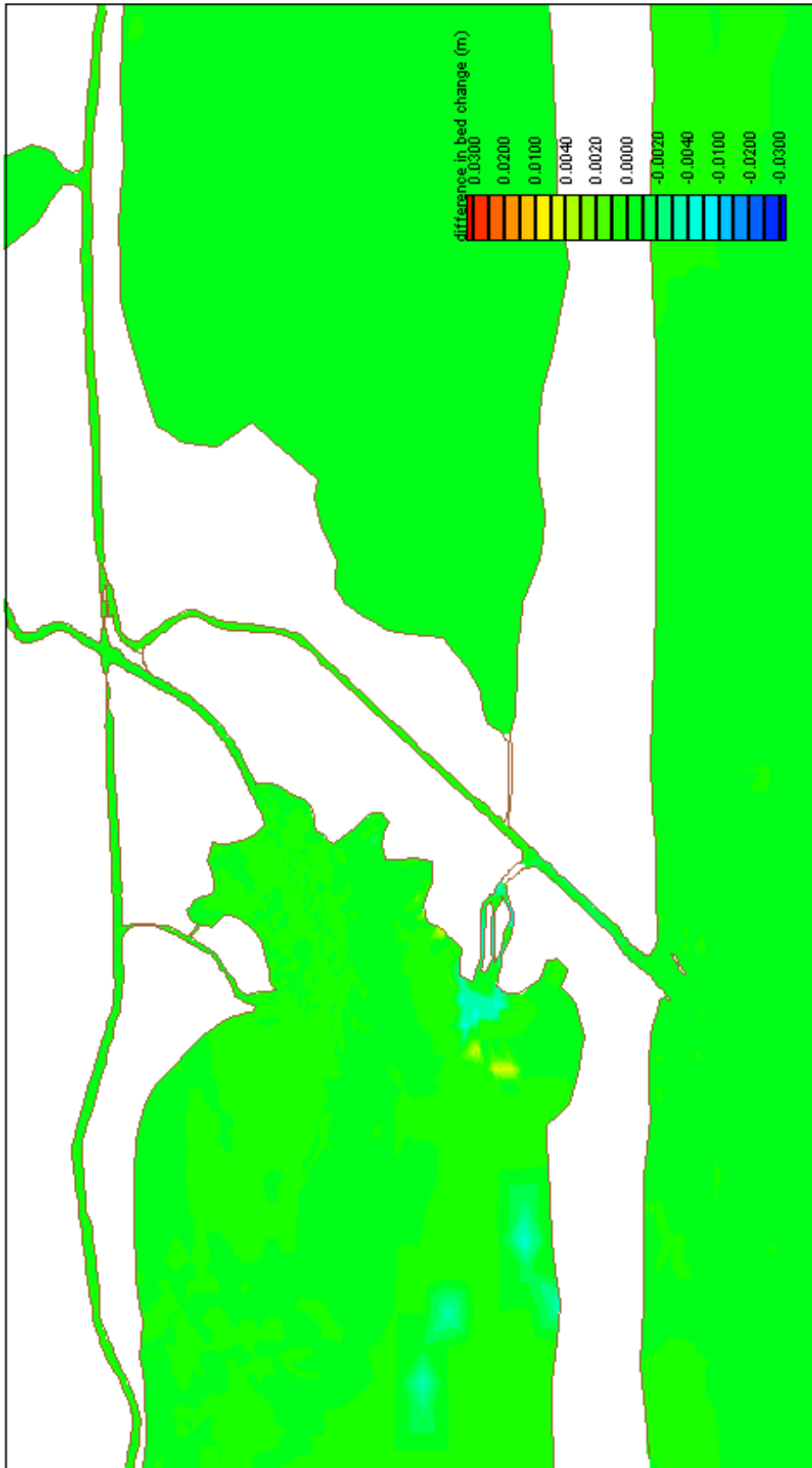
Difference in Bed Change, Scenario B, Low Discharge
Scenario B: Parker's Cut (4' X 20')



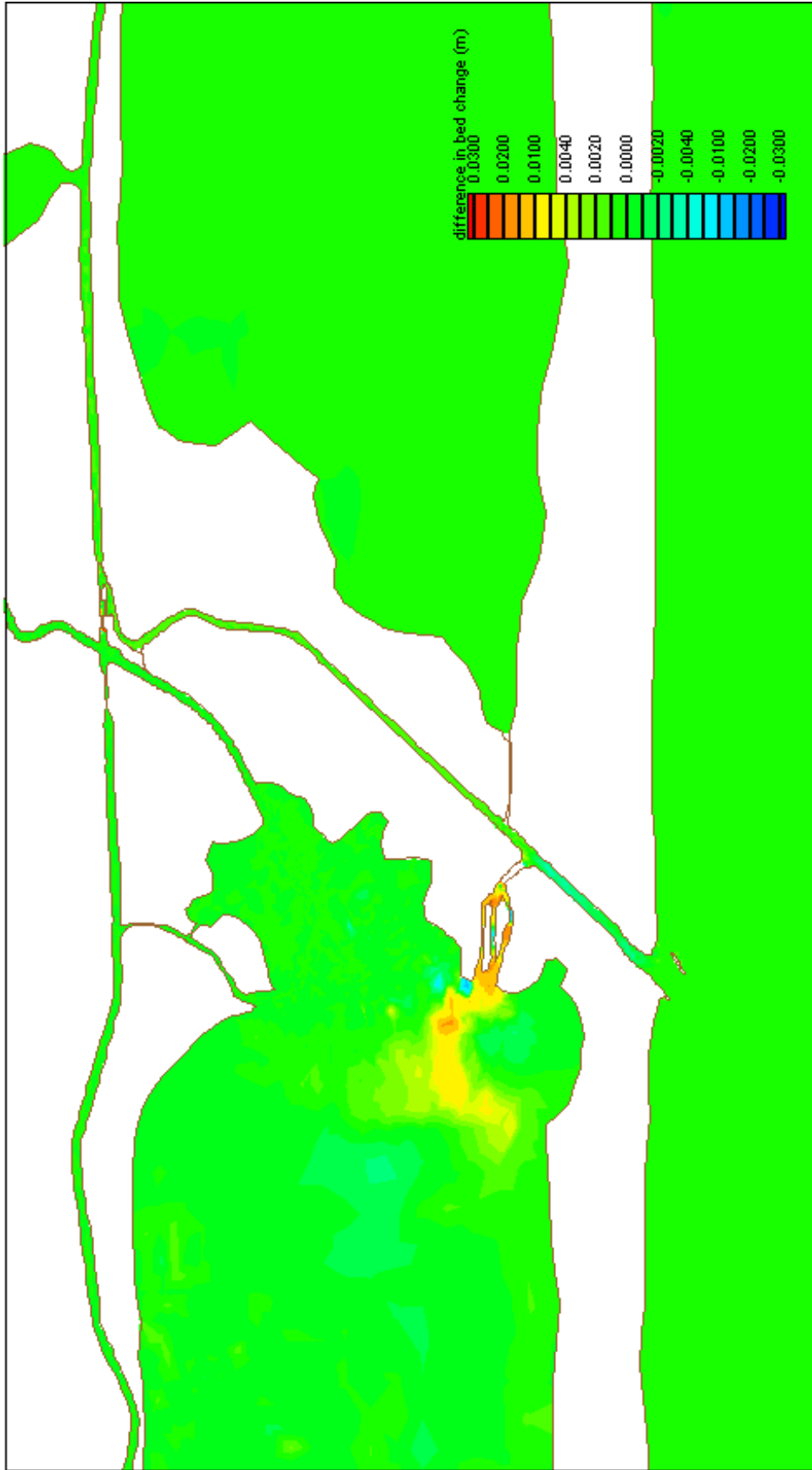
Difference in Bed Change, Scenario B, Medium Discharge
Scenario B: Parker's Cut (4' X 20')



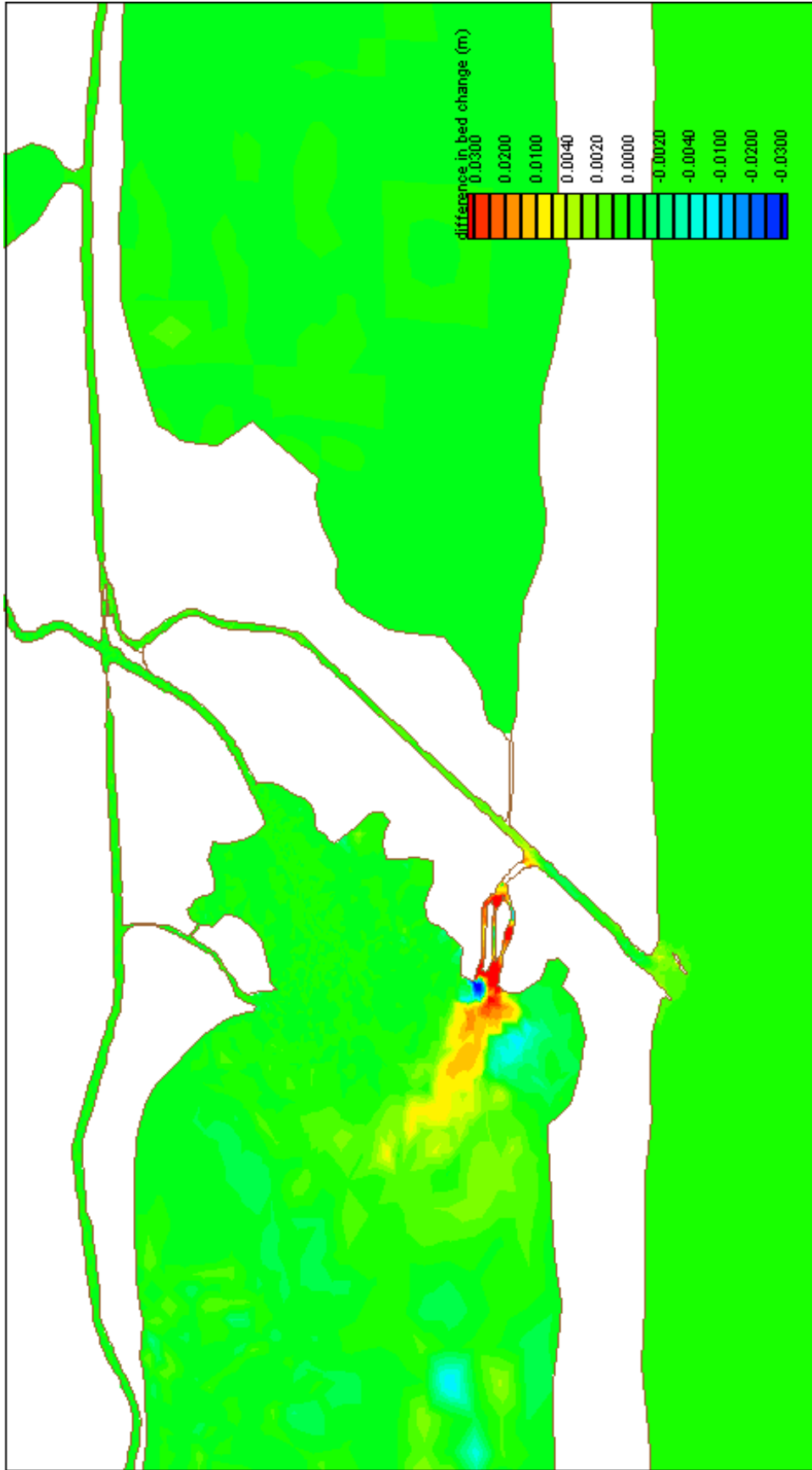
Difference in Bed Change, Scenario B, High Discharge
Scenario B: Parker's Cut (4' X 20')



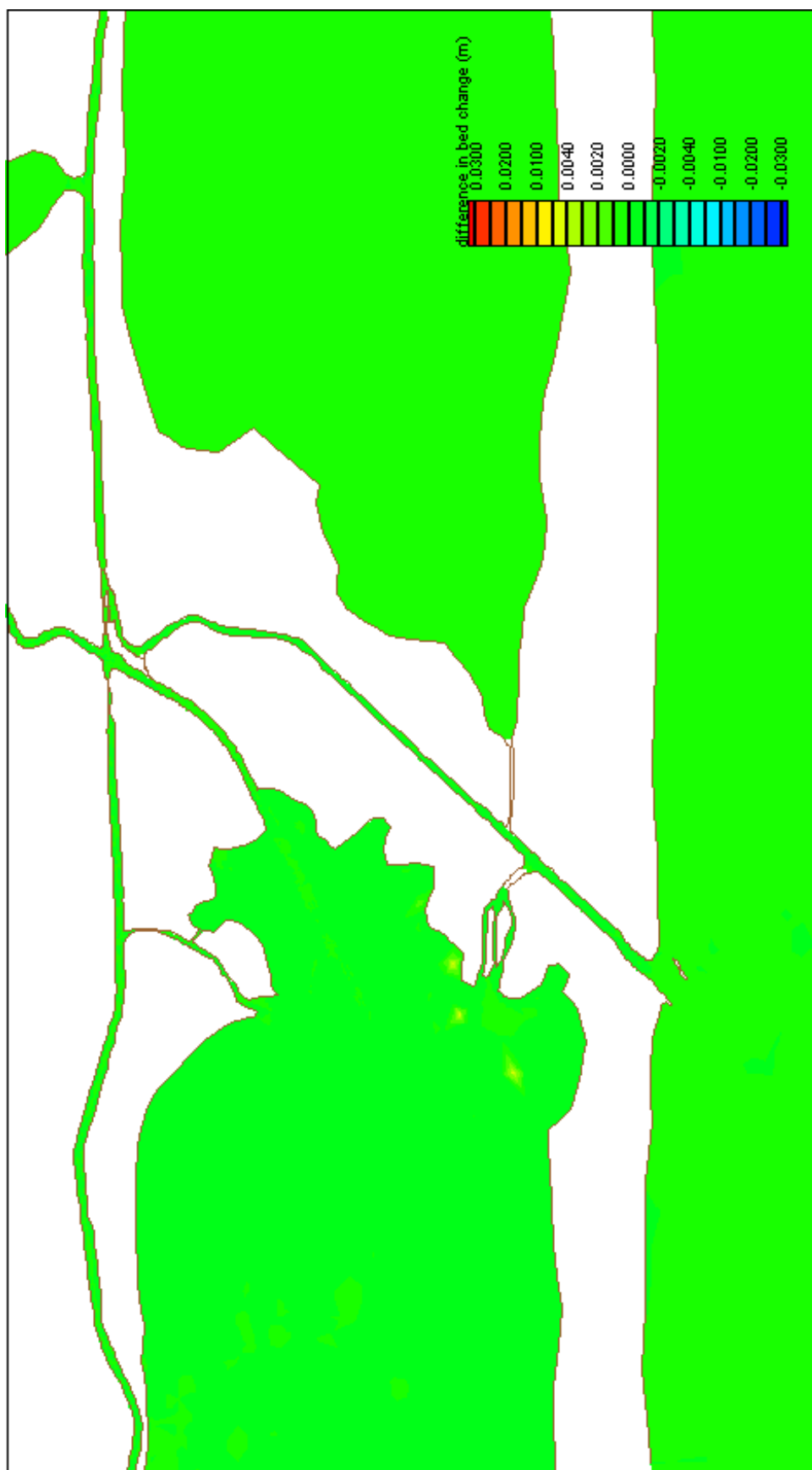
Difference in Bed Change, Scenario C, Low Discharge
 Scenario C: Parker's Cut (7' X 50')

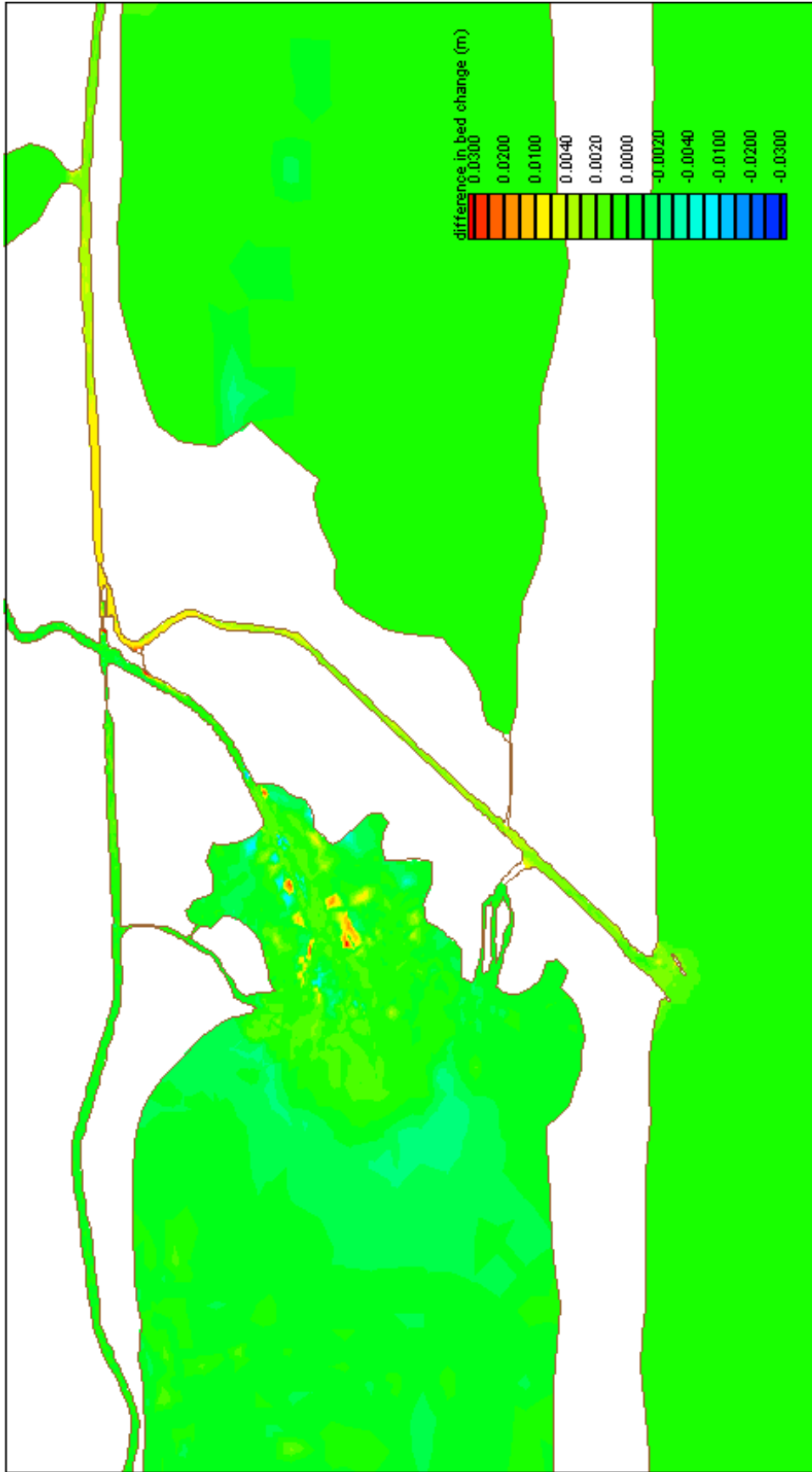


Difference in Bed Change, Scenario C, Medium Discharge
Scenario C: Parker's Cut (7' X 50')

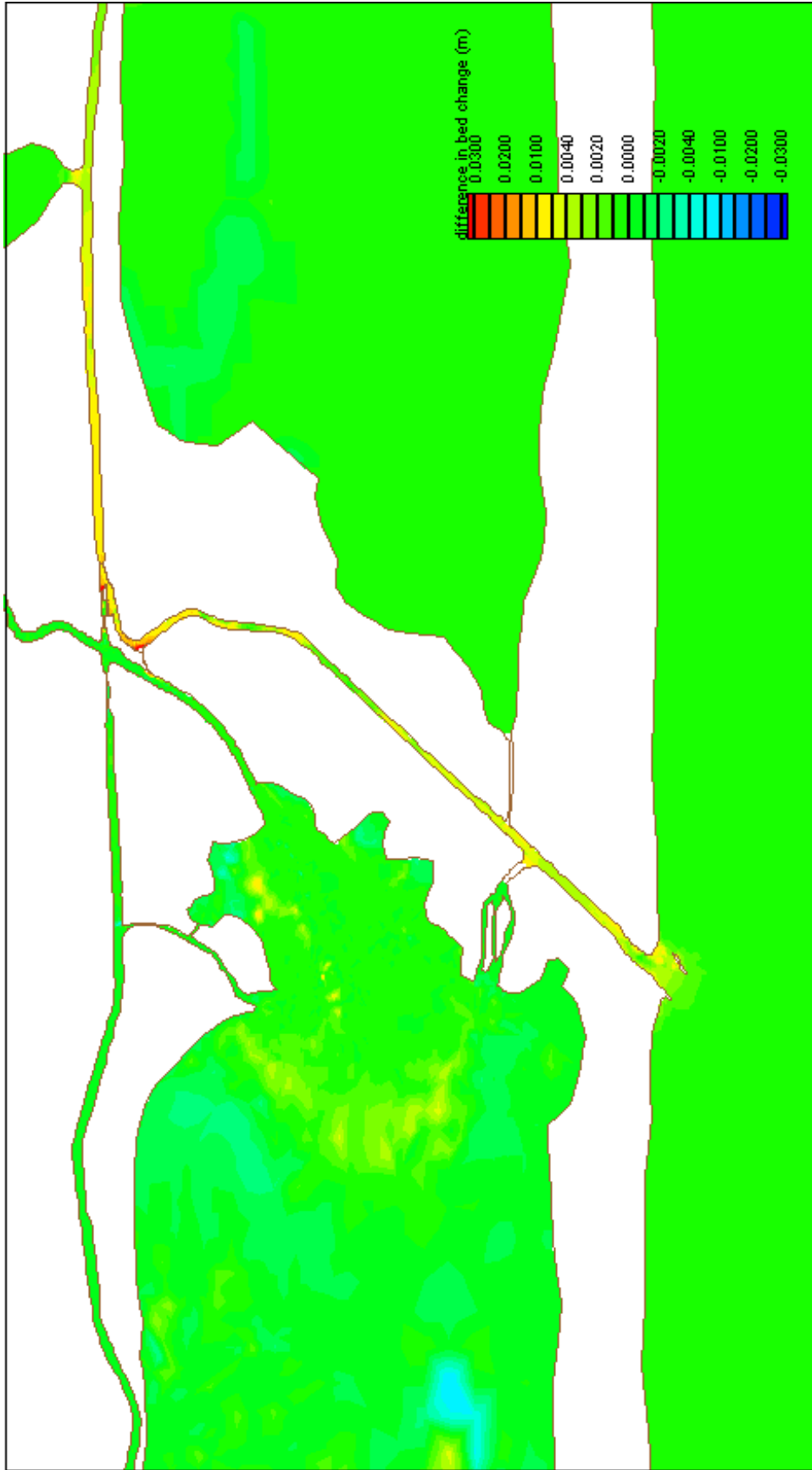


Difference in Bed Change, Scenario C, High Discharge
Scenario C: Parker's Cut (7' X 50')

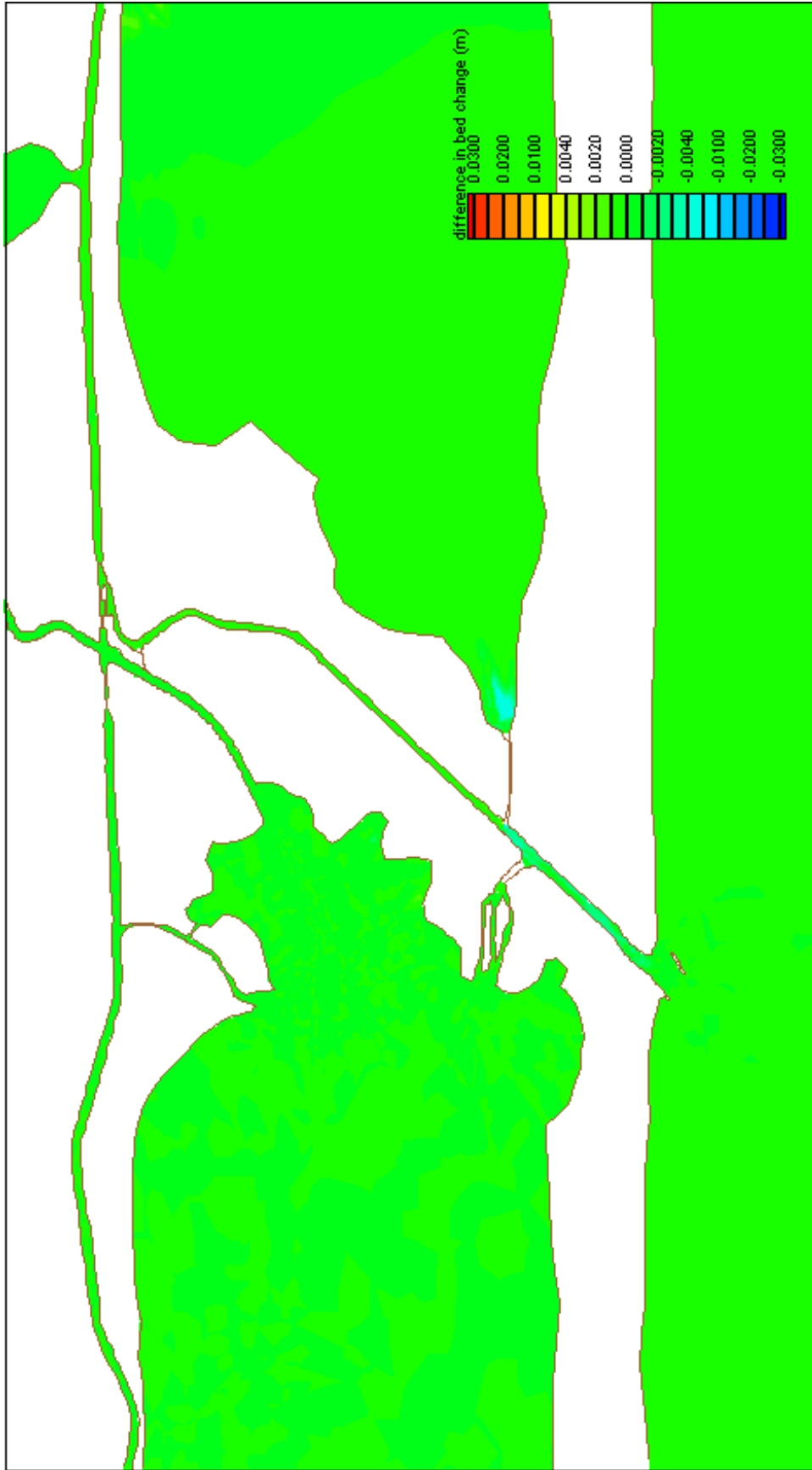




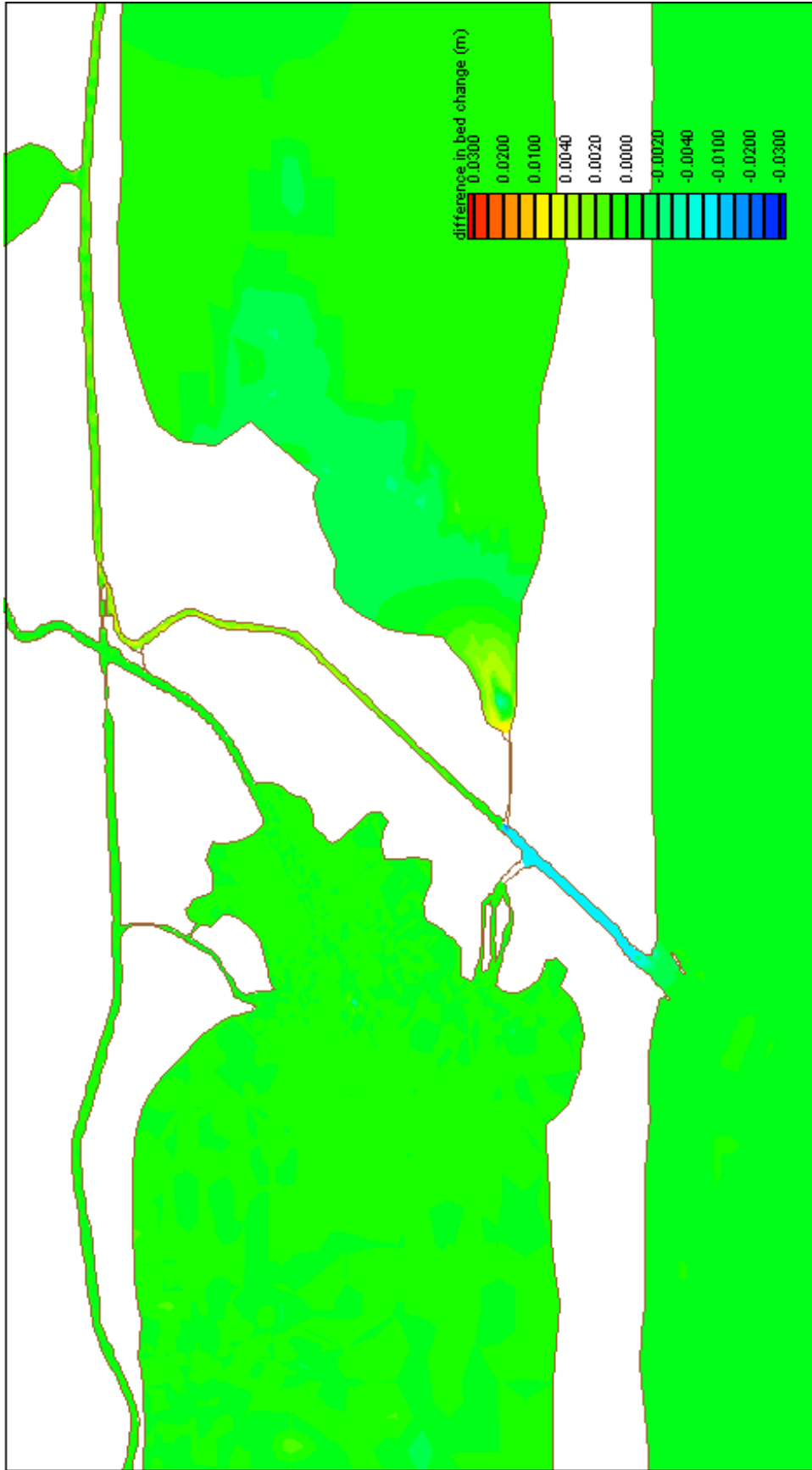
Difference in Bed Change, Scenario D, Medium Discharge
 Scenario D: Bypass channel around diversion dam (4' X 20')



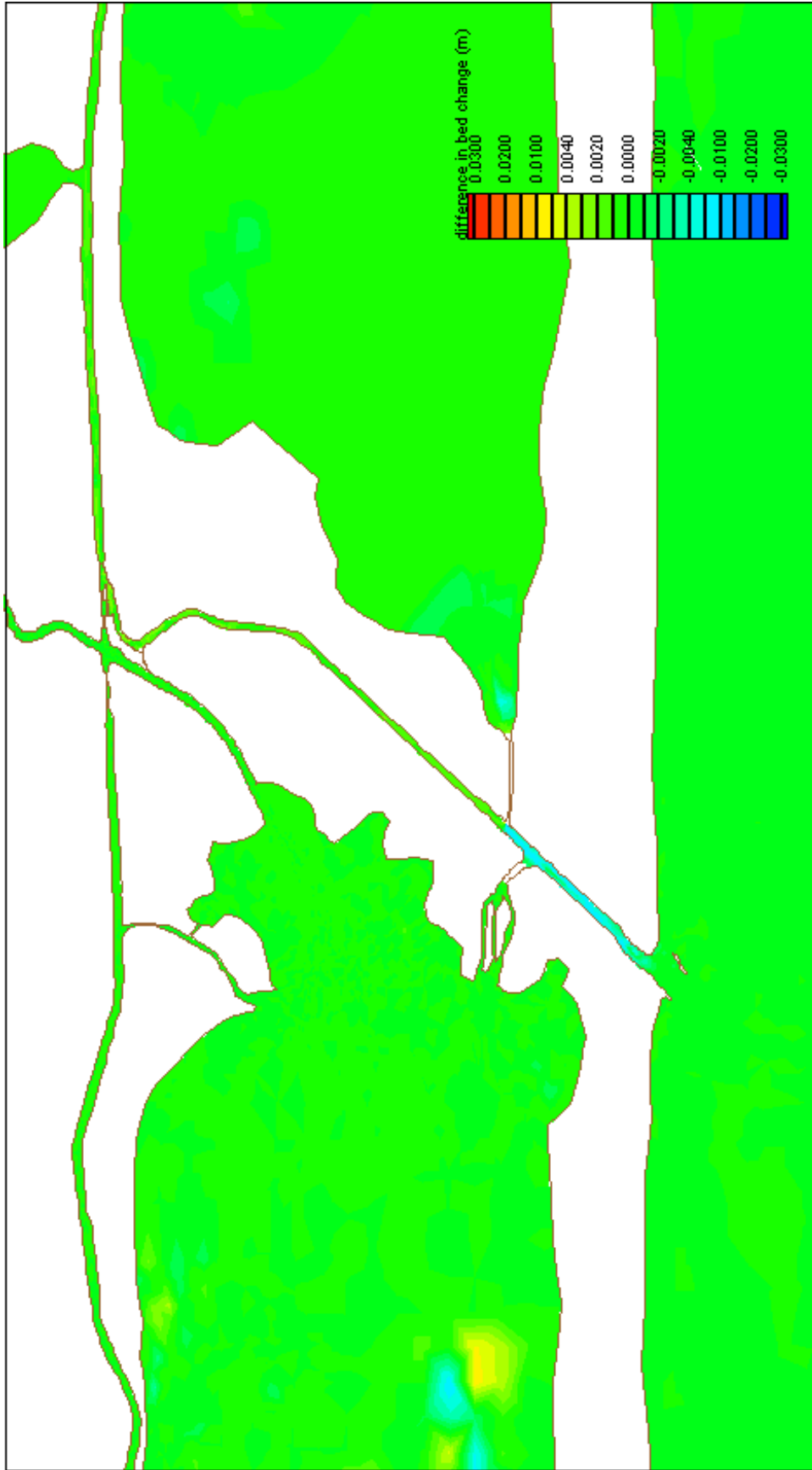
Difference in Bed Change, Scenario D, High Discharge
Scenario D: Bypass channel around diversion dam (4' X 20')



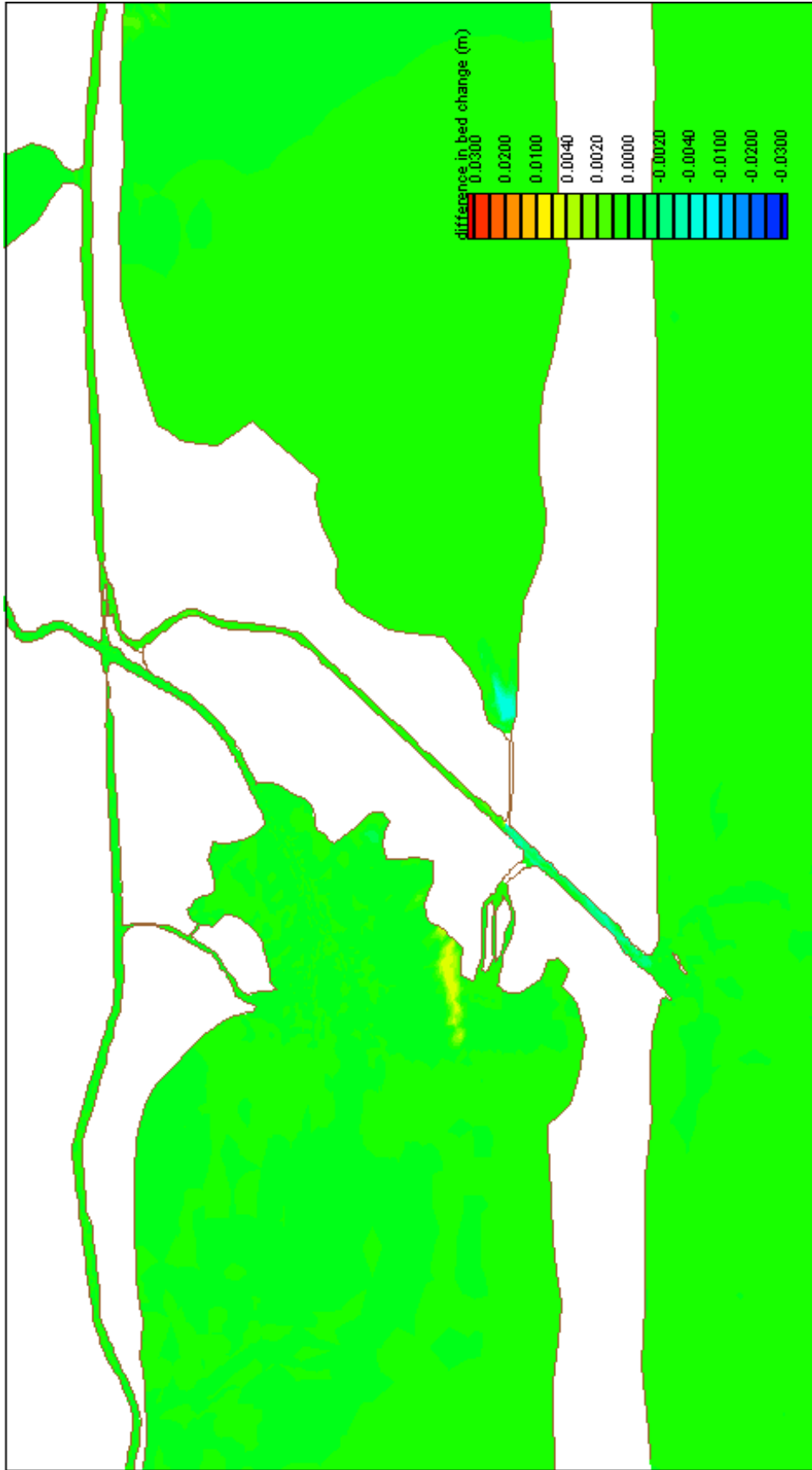
Difference in Bed Change, Scenario G, Low Discharge
Scenario G: Southwest Cut (5' X 100')



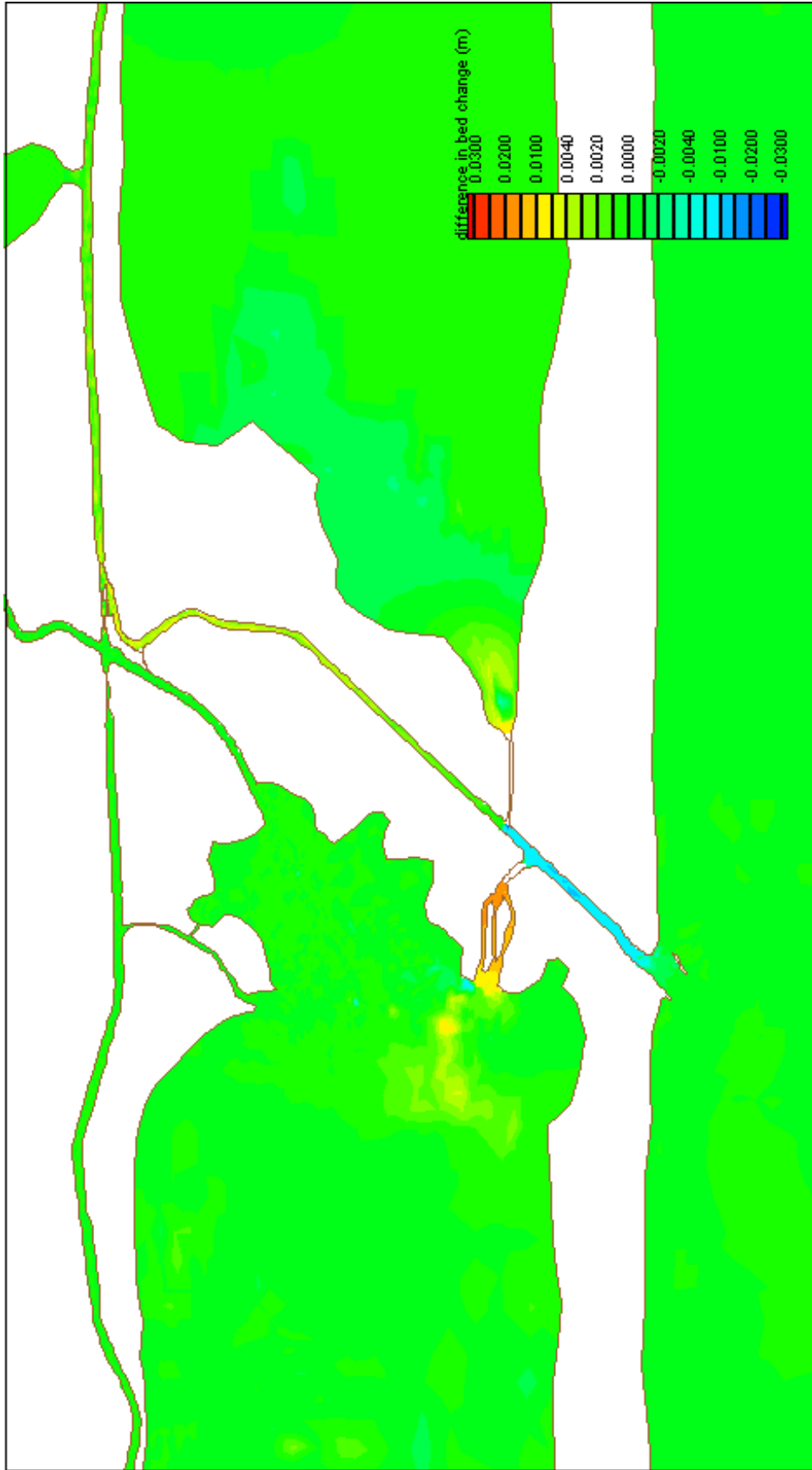
Difference in Bed Change, Scenario G, Medium Discharge
Scenario G: Southwest Cut (5' X 100')



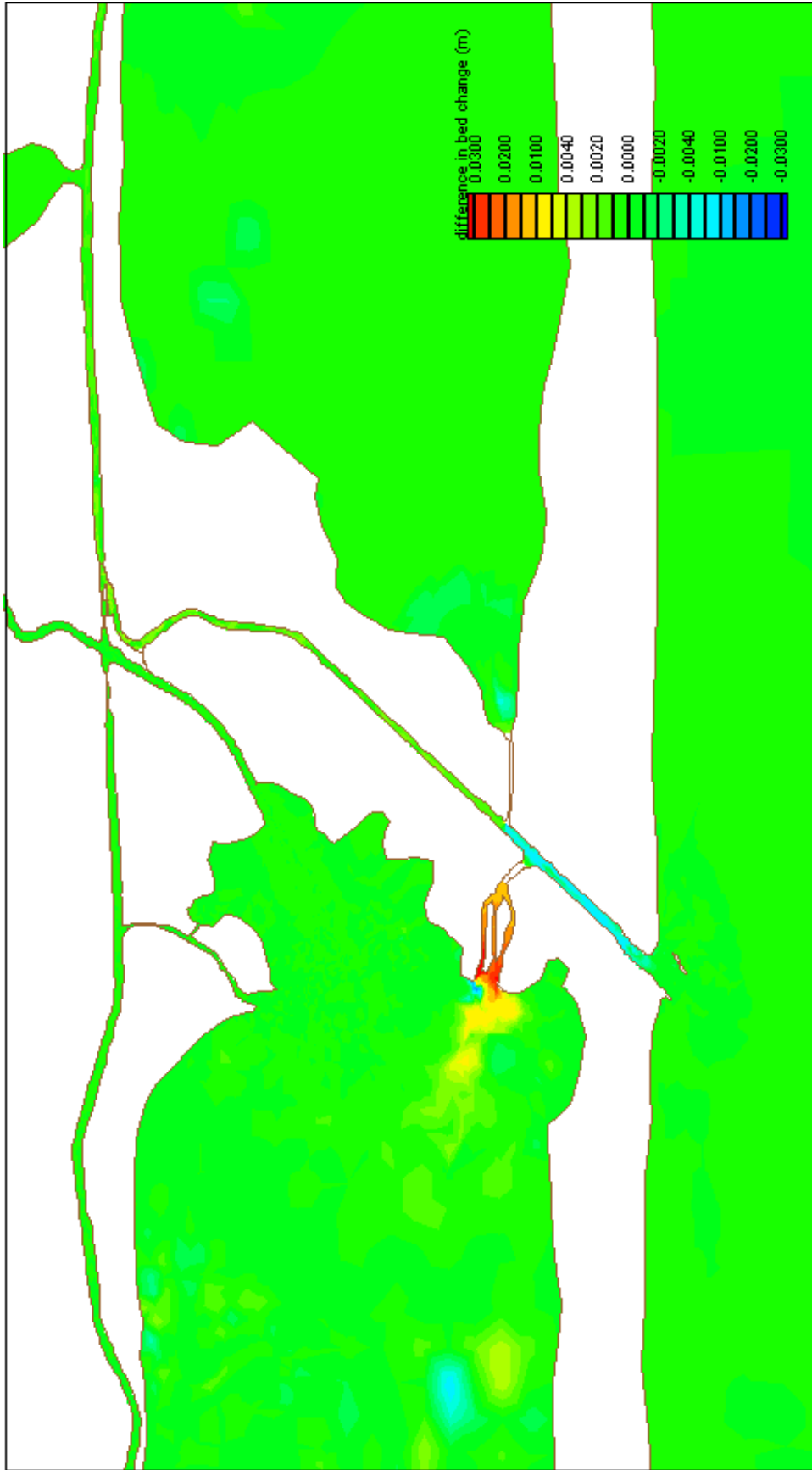
Difference in Bed Change, Scenario G, High Discharge
Scenario G: Southwest Cut (5' X 100')



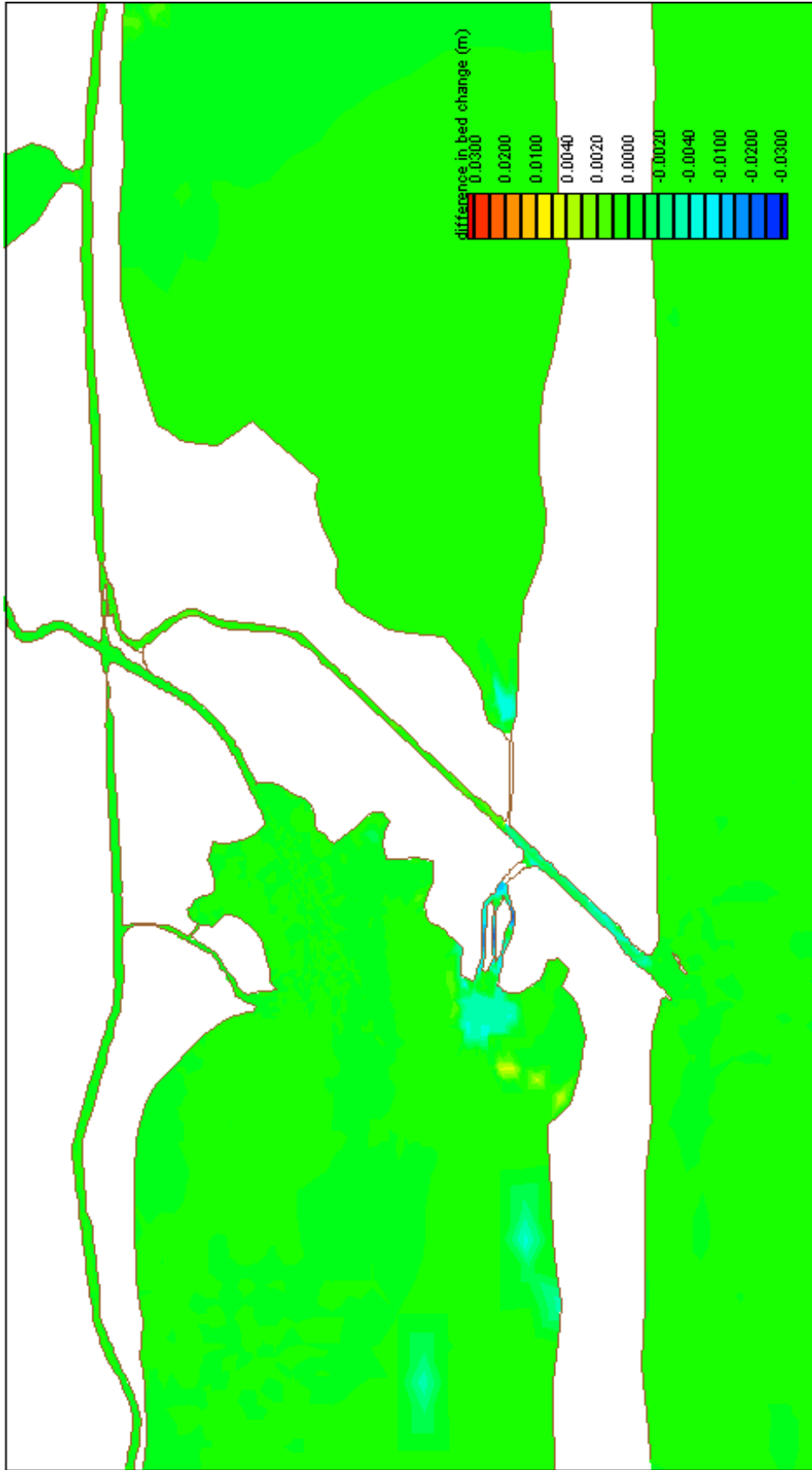
Difference in Bed Change, Scenario H, Low Discharge
Scenario H: Southwest Cut (5' X 100') with Parker's Cut (4' X 20')



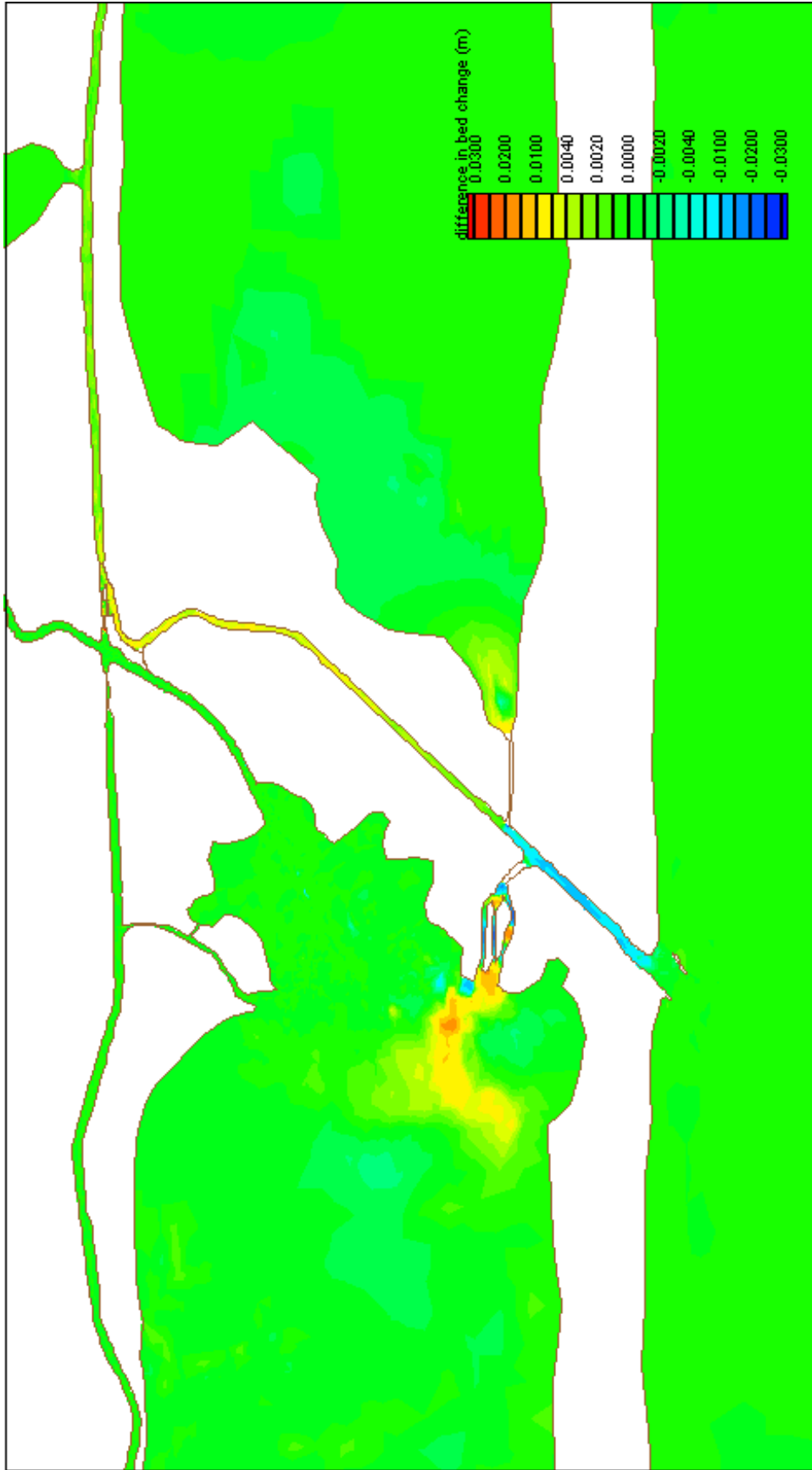
Difference in Bed Change, Scenario H, Medium Discharge
 Scenario H: Southwest Cut (5' X 100') with Parker's Cut (4' X 20')



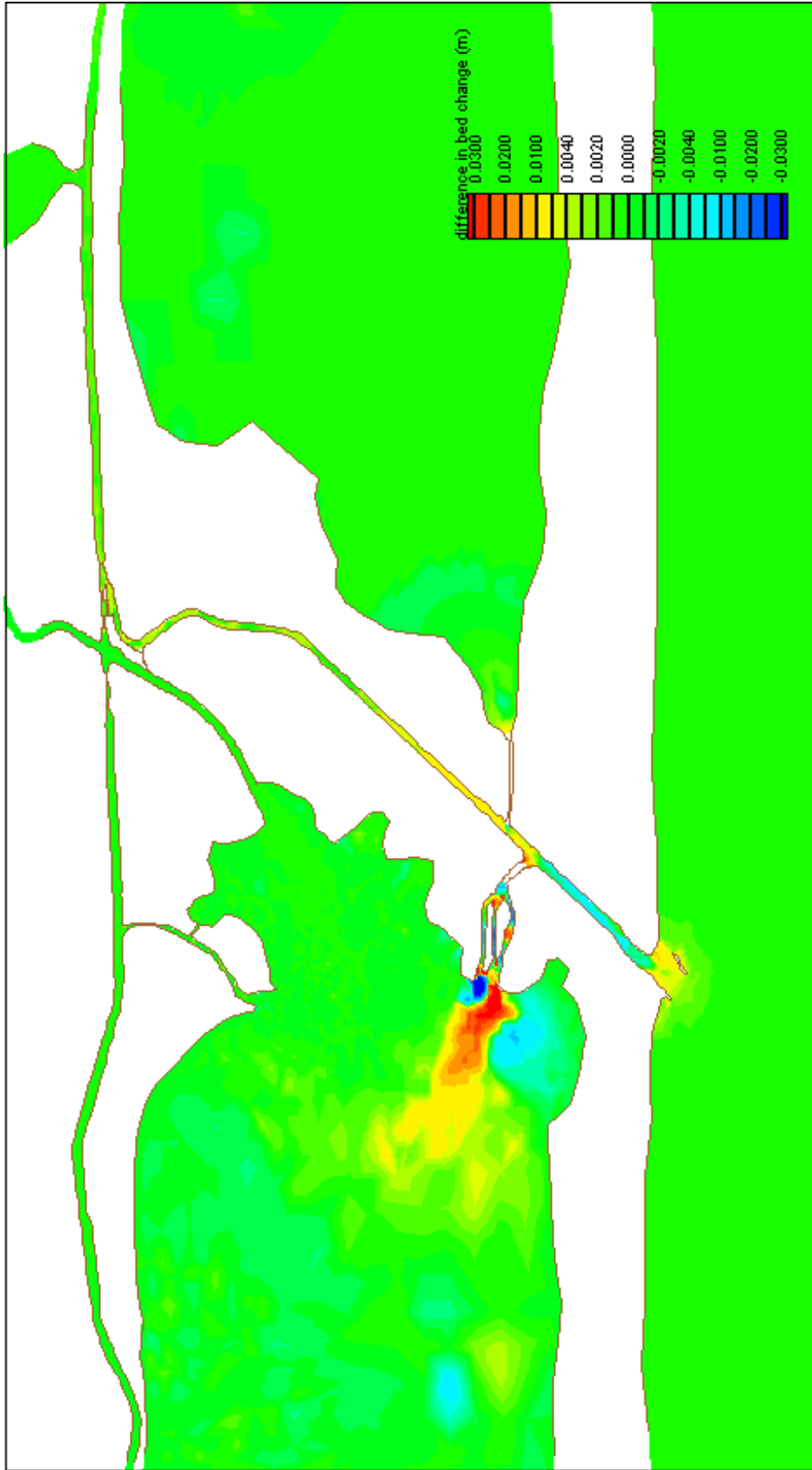
Difference in Bed Change, Scenario H, High Discharge
Scenario H: Southwest Cut (5' X 100') with Parker's Cut (4' X 20')



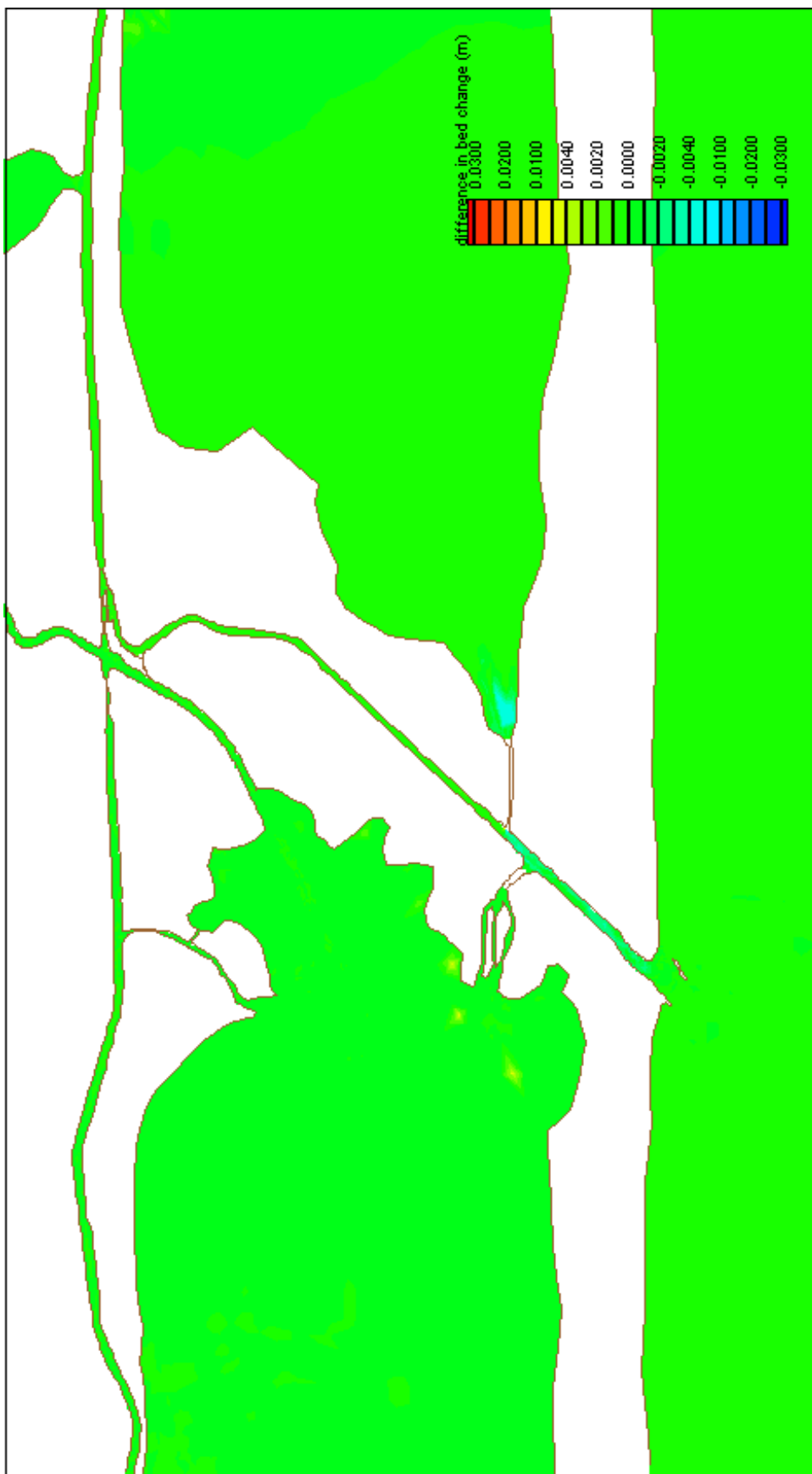
Difference in Bed Change, Scenario I, Low Discharge
 Scenario I: Southwest Cut (5' X 100') with Parker's Cut sized to be stable (estimated at 2-4' X 350')



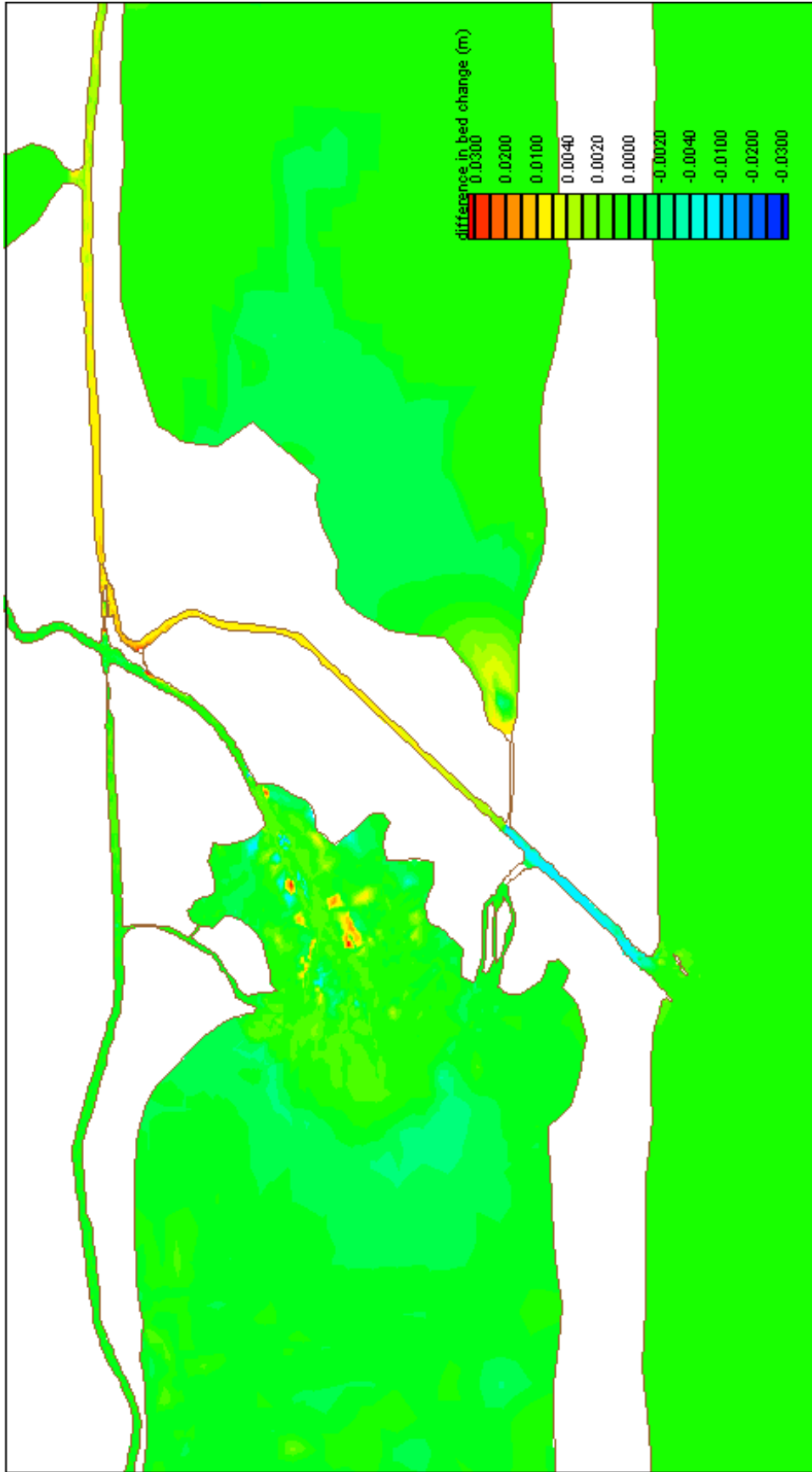
Difference in Bed Change, Scenario I, Medium Discharge
 Scenario I: Southwest Cut (5' X 100') with Parker's Cut sized to be stable (estimated at 2-4' X 350')



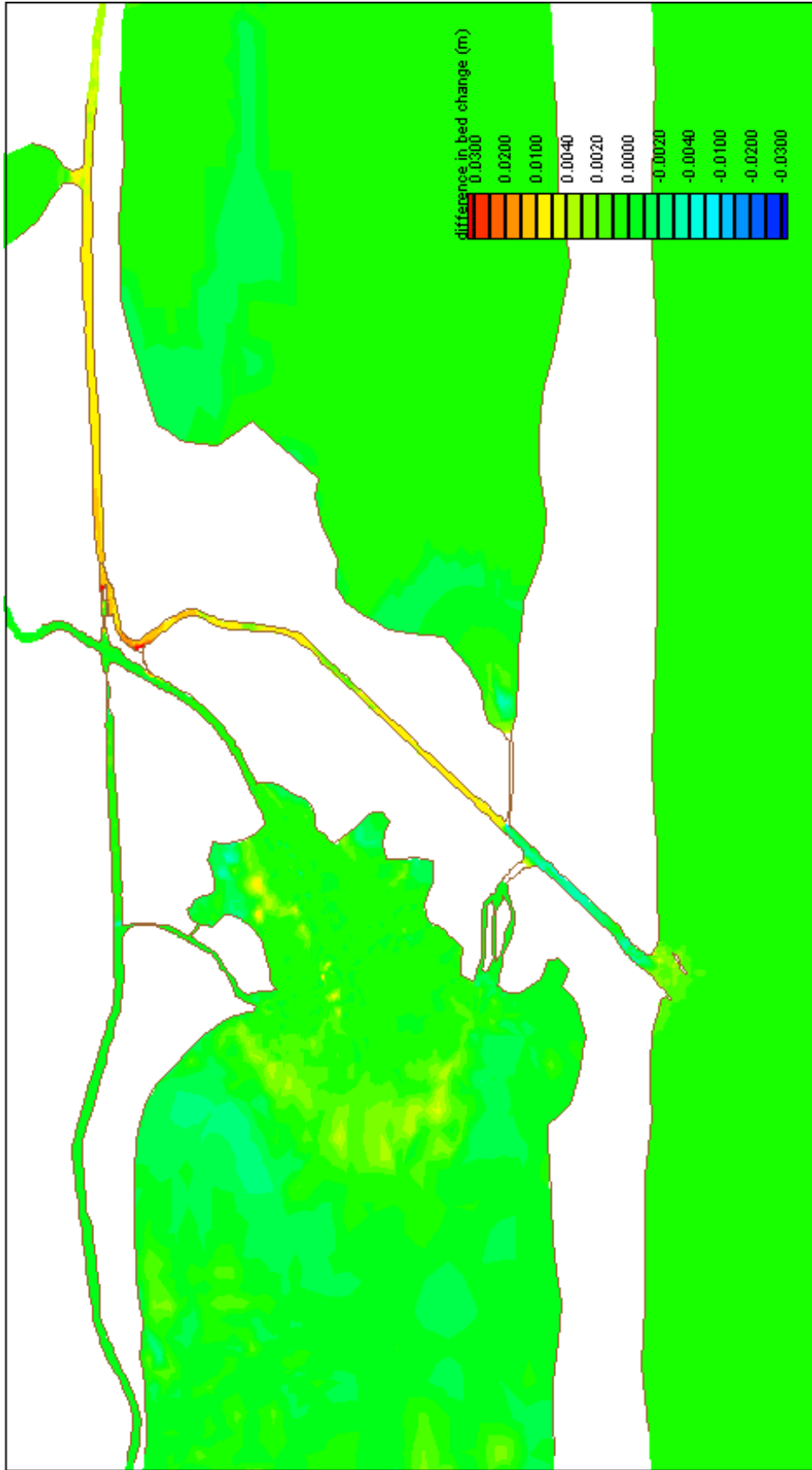
Difference in Bed Change, Scenario I, High Discharge
 Scenario I: Southwest Cut (5' X 100') with Parker's Cut sized to be stable (estimated at 2-4' X 350')



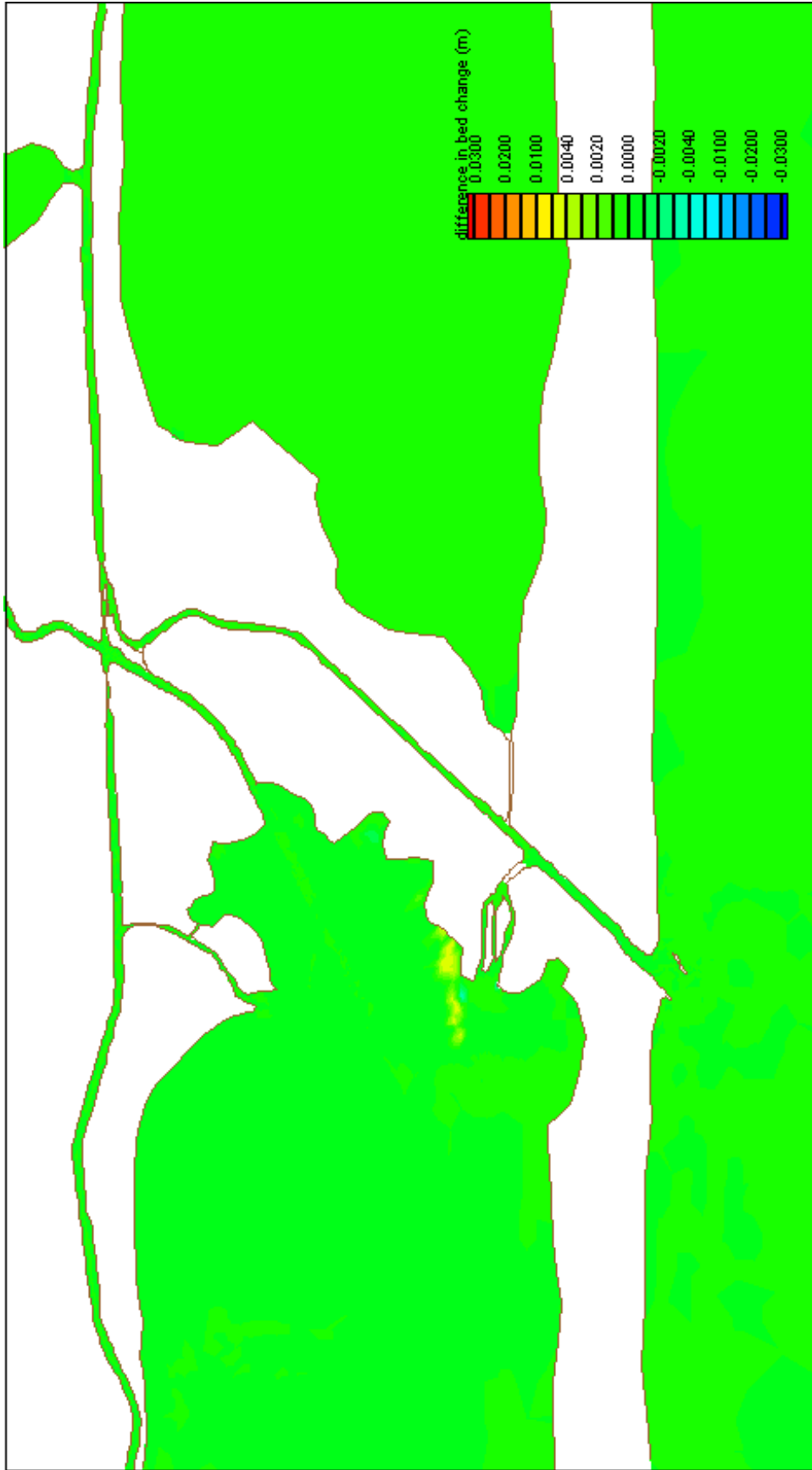
Difference in Bed Change, Scenario J, Low Discharge
 Scenario J: Southwest Cut (5' X 100') with bypass channel around diversion dam (4' X 20')



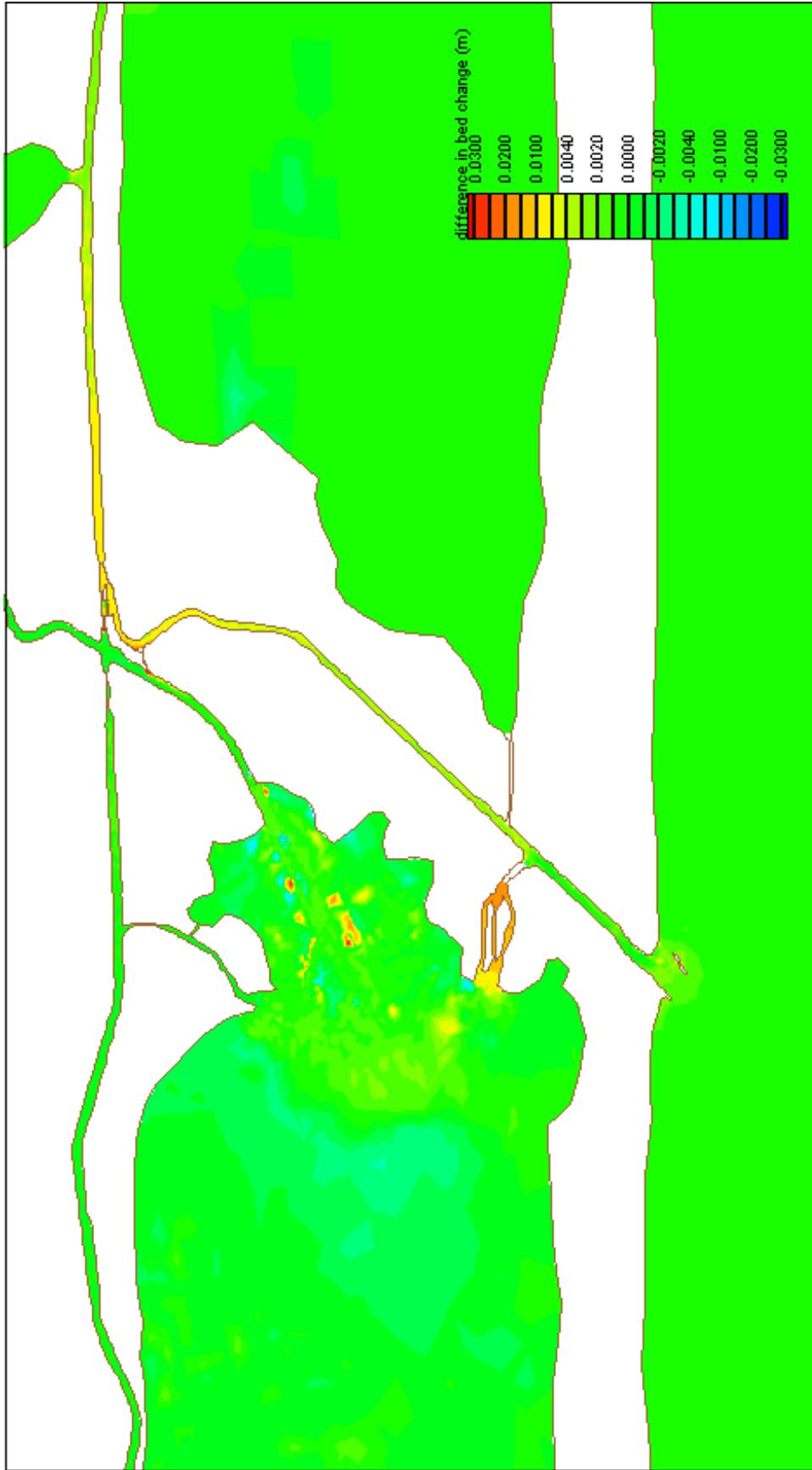
Difference in Bed Change, Scenario J, Medium Discharge
 Scenario J: Southwest Cut (5' X 100') with bypass channel around diversion dam (4' X 20')



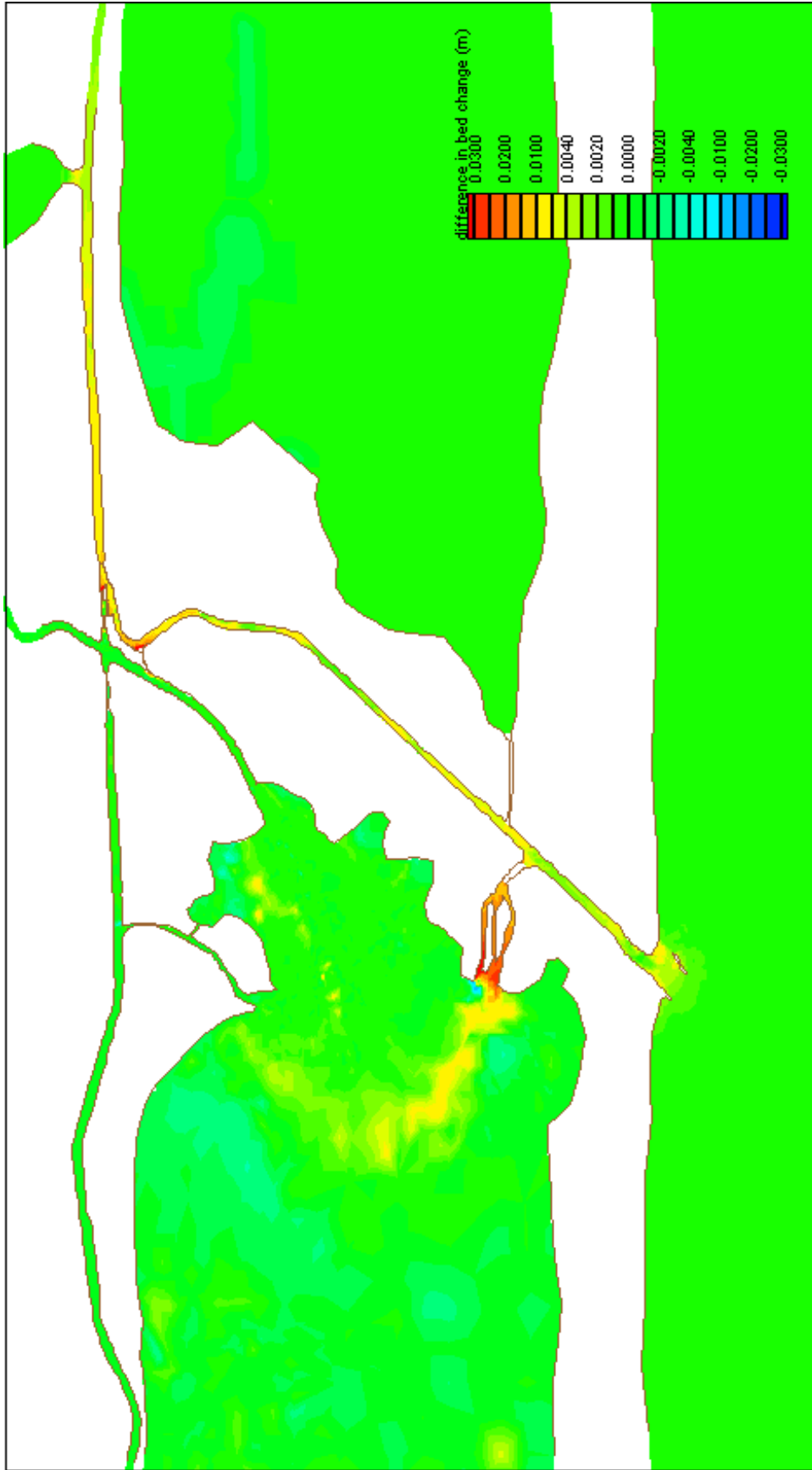
Difference in Bed Change, Scenario J, High Discharge
 Scenario J: Southwest Cut (5' X 100') with bypass channel around diversion dam (4' X 20')



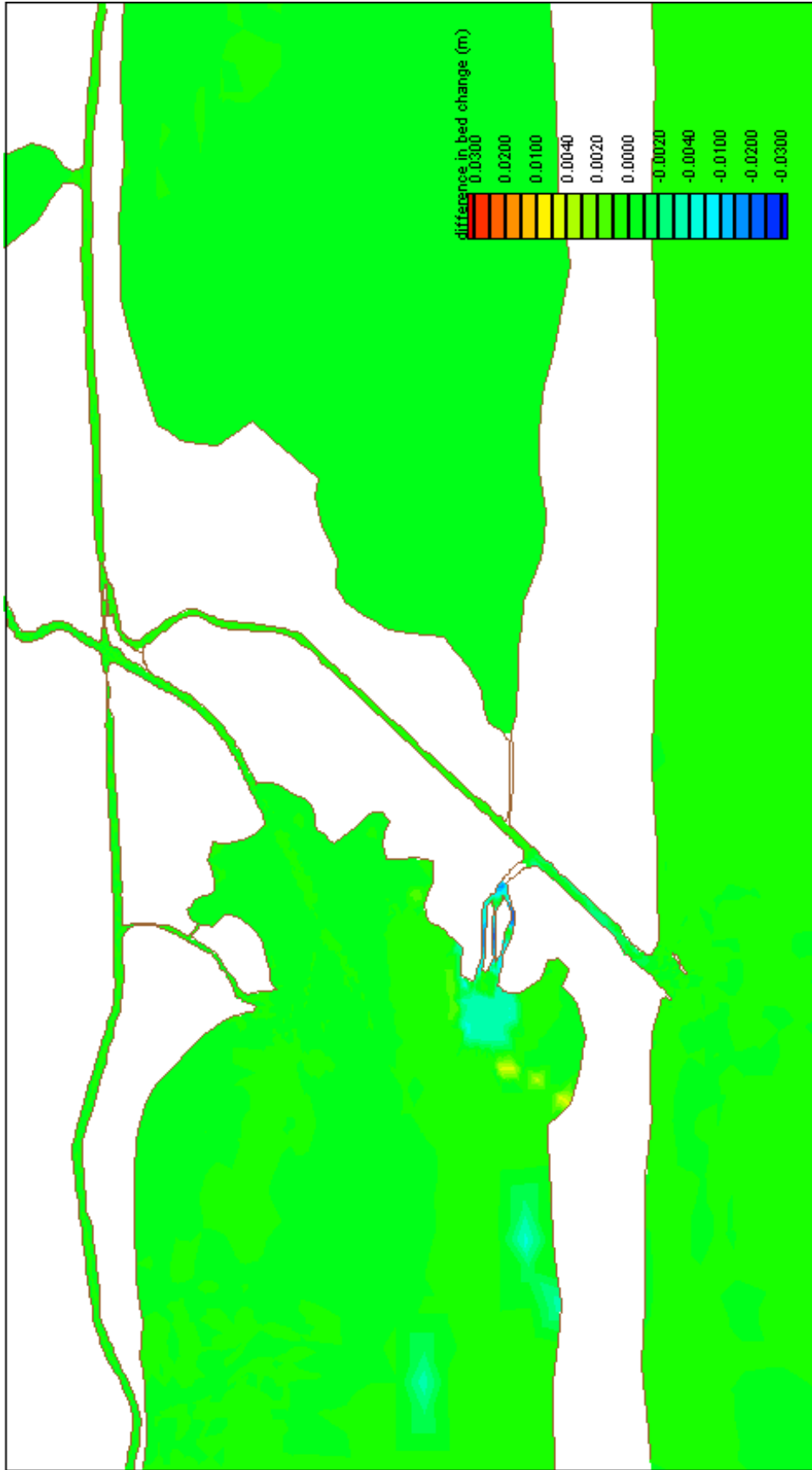
Difference in Bed Change, Scenario K, Low Discharge
Scenario K: Parker's Cut (4' X 20') with bypass channel around diversion dam (4' X 20')



Difference in Bed Change, Scenario K, Medium Discharge
 Scenario K: Parker's Cut (4' X 20') with bypass channel around diversion dam (4' X 20')

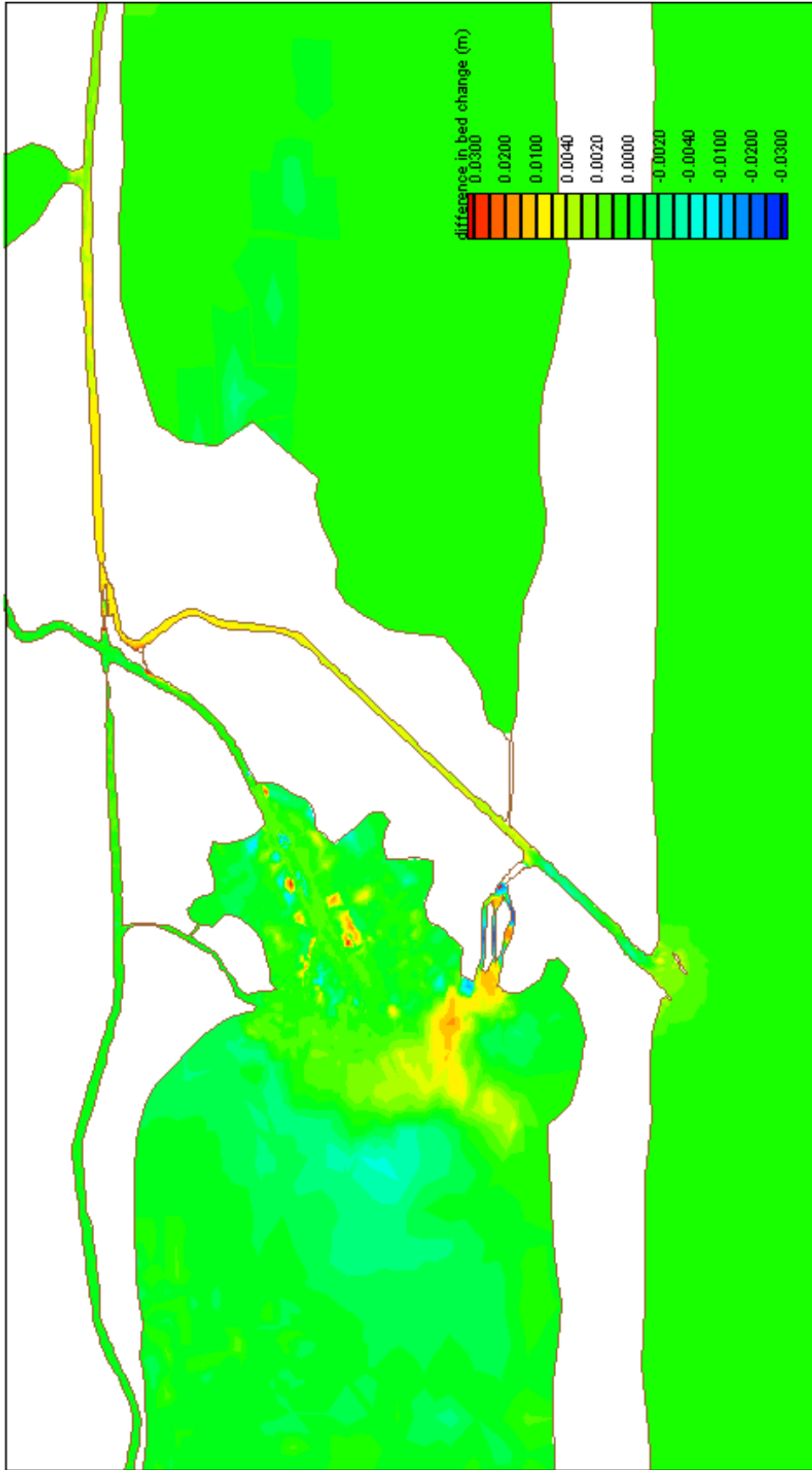


Difference in Bed Change, Scenario K, High Discharge
 Scenario K: Parker's Cut (4' X 20') with bypass channel around diversion dam (4' X 20')

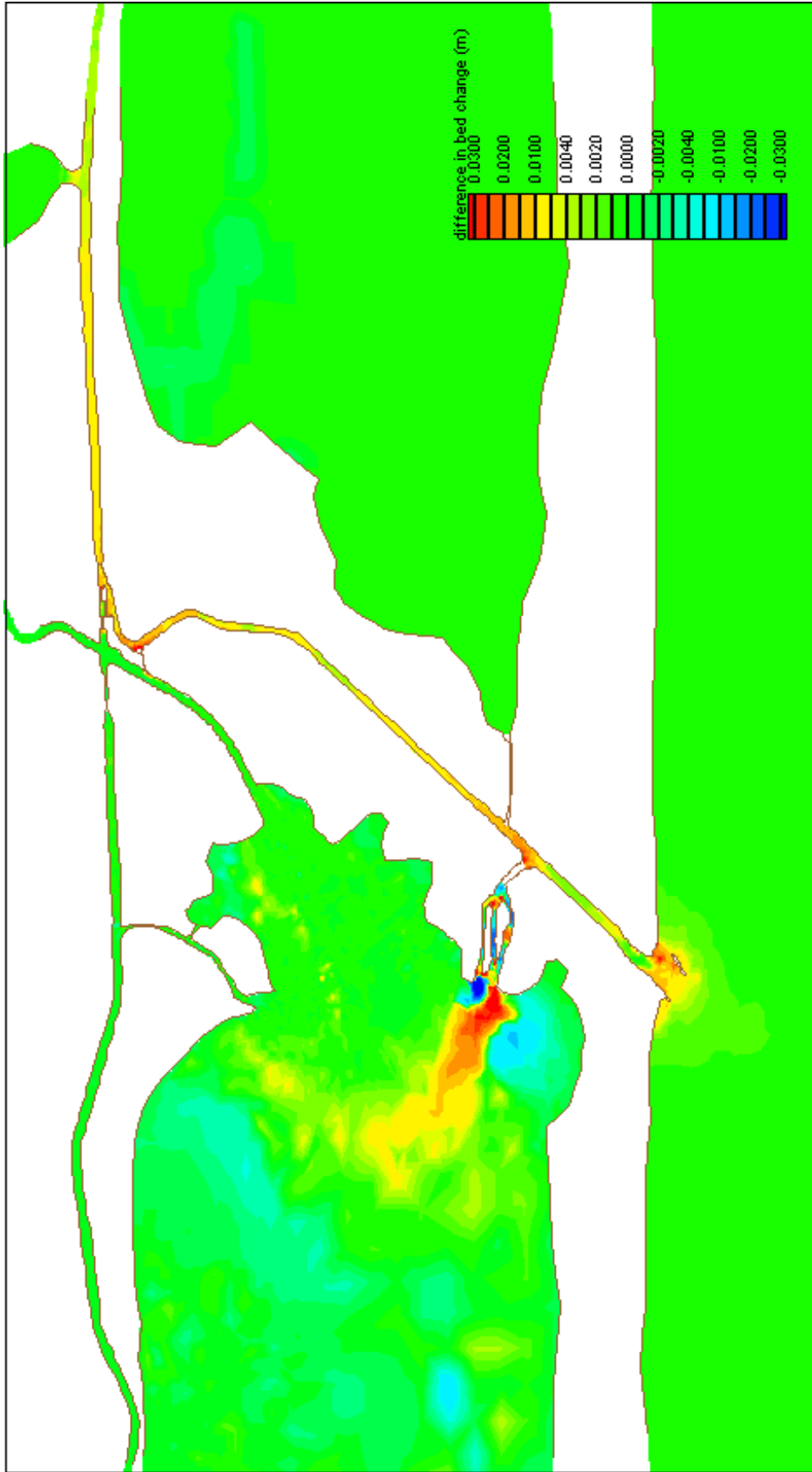


Difference in Bed Change, Scenario L, Low Discharge

Scenario L: Parker's Cut sized to be stable (estimated at 2-4' X 350') with bypass channel around diversion dam (4' X 20')

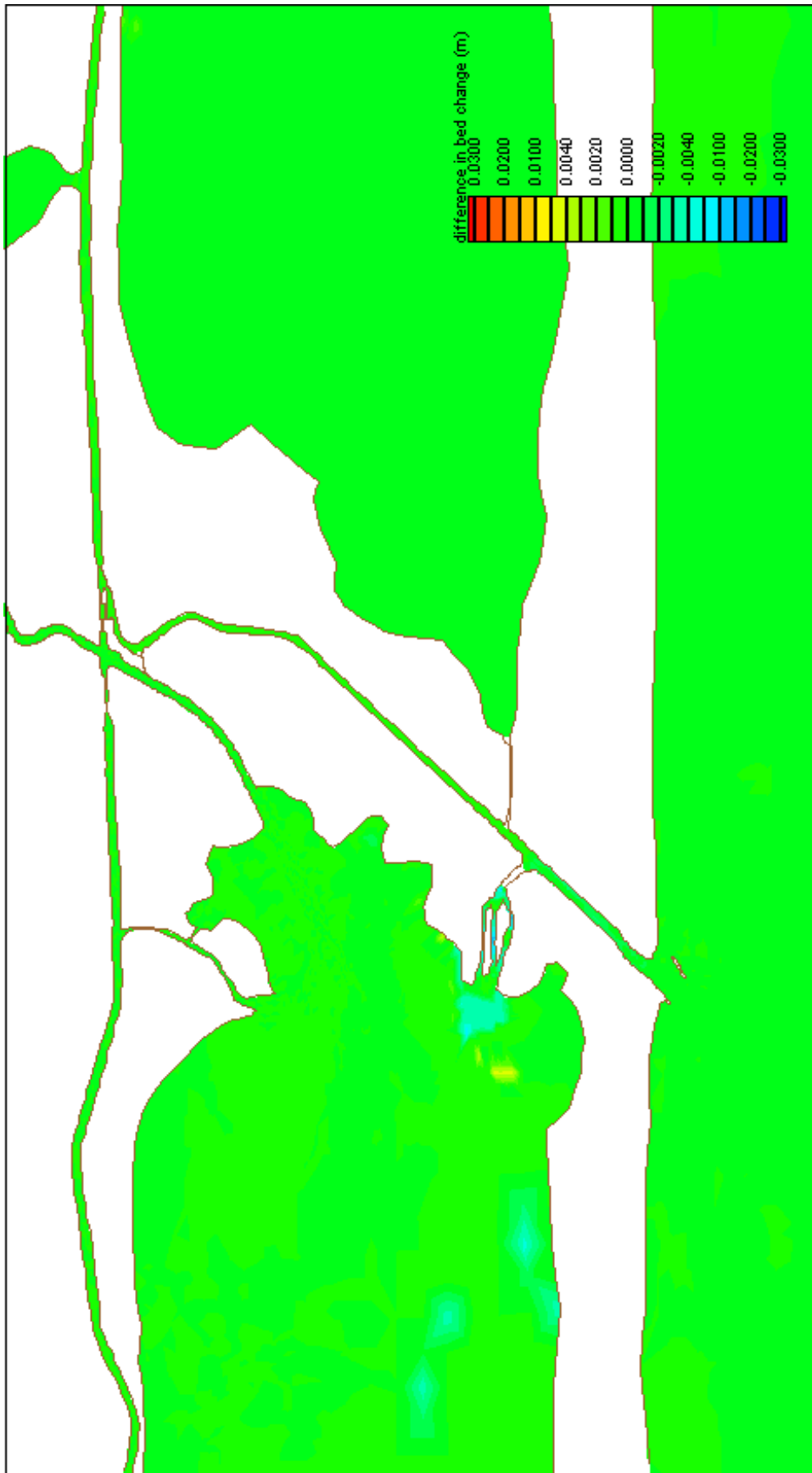


Difference in Bed Change, Scenario L, Medium Discharge
 Scenario L: Parker's Cut sized to be stable (estimated at 2-4' X 350') with bypass channel around diversion dam (4' X 20')

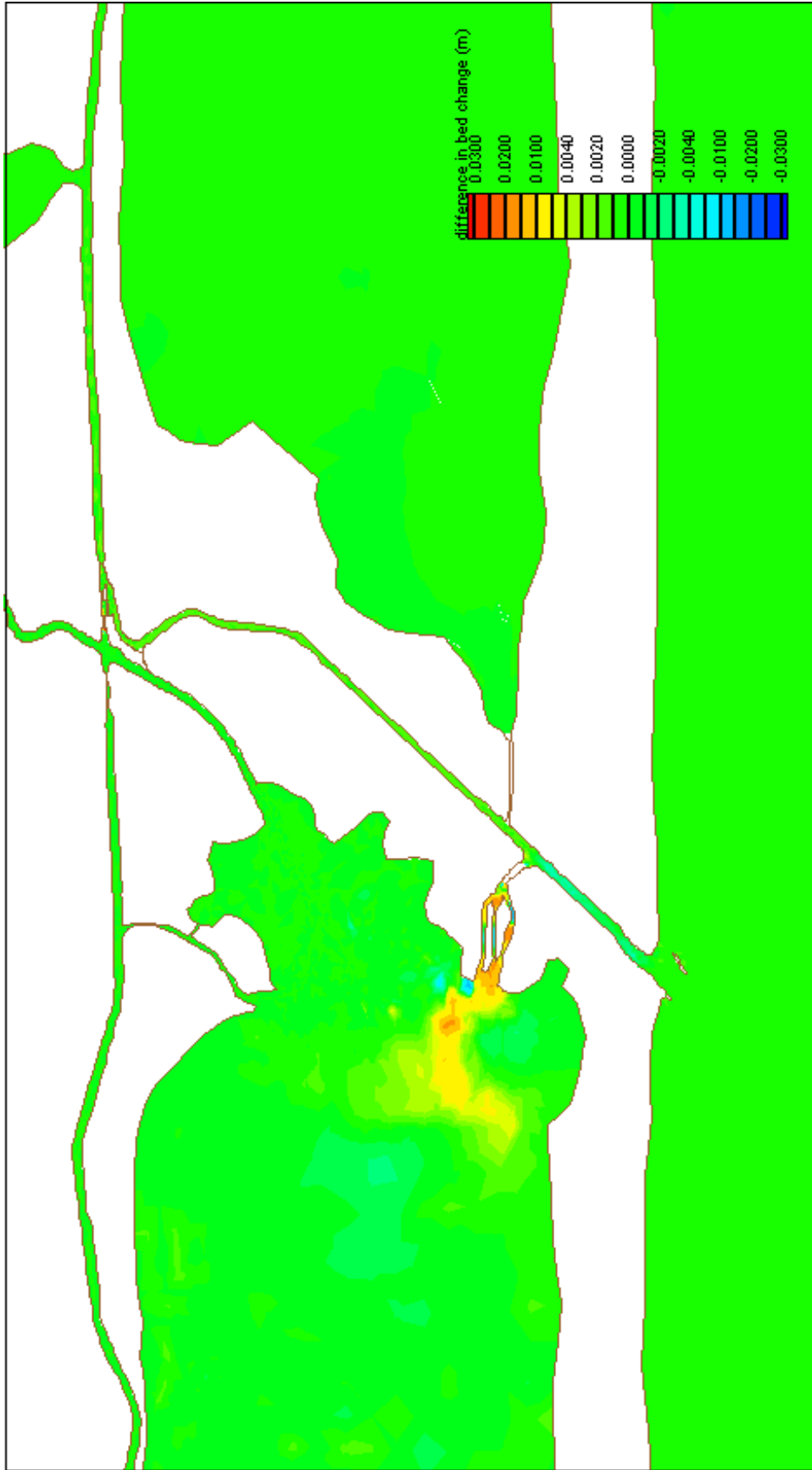


Difference in Bed Change, Scenario L, High Discharge

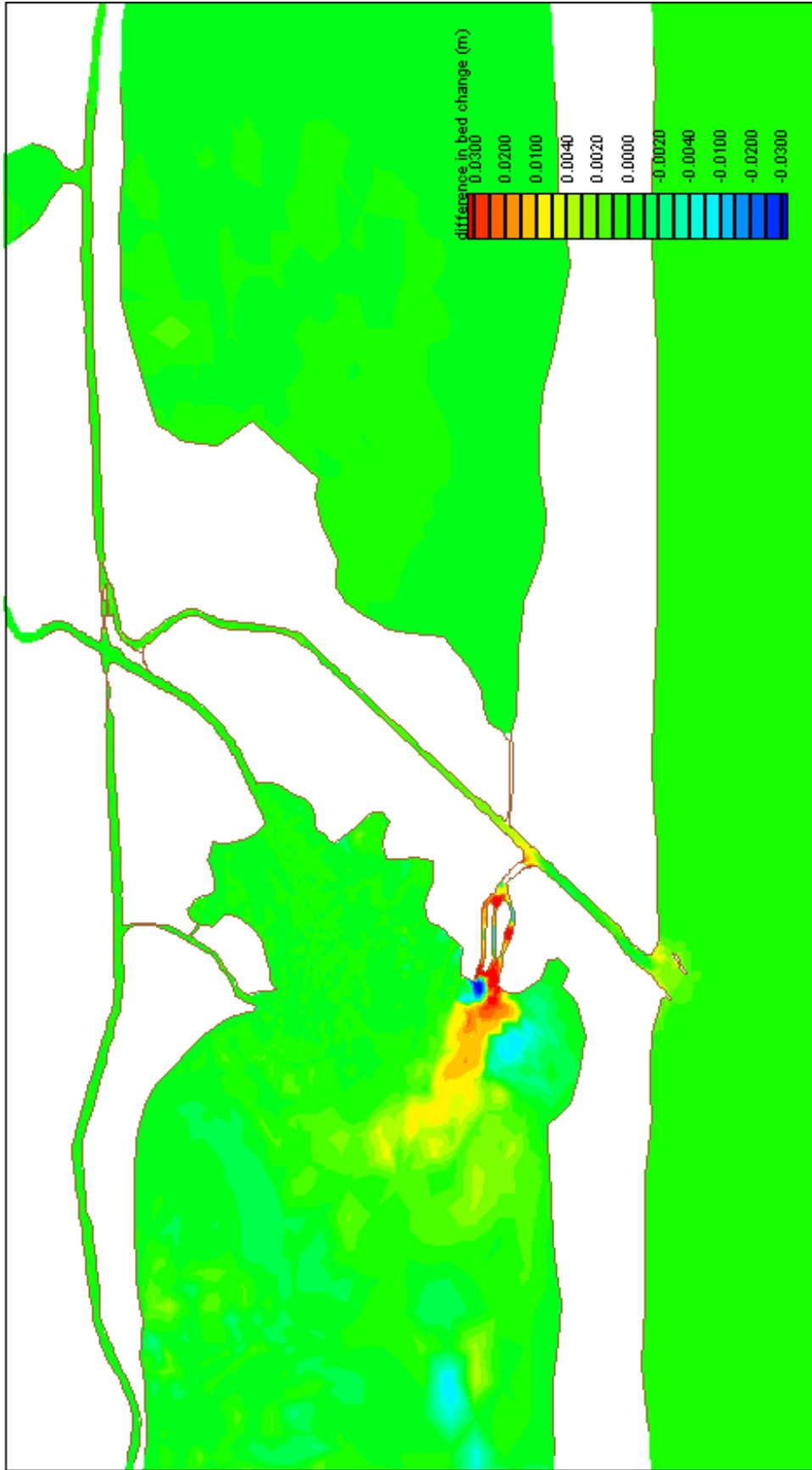
Scenario L: Parker's Cut sized to be stable (estimated at 2-4' X 350') with bypass channel around diversion dam (4' X 20')



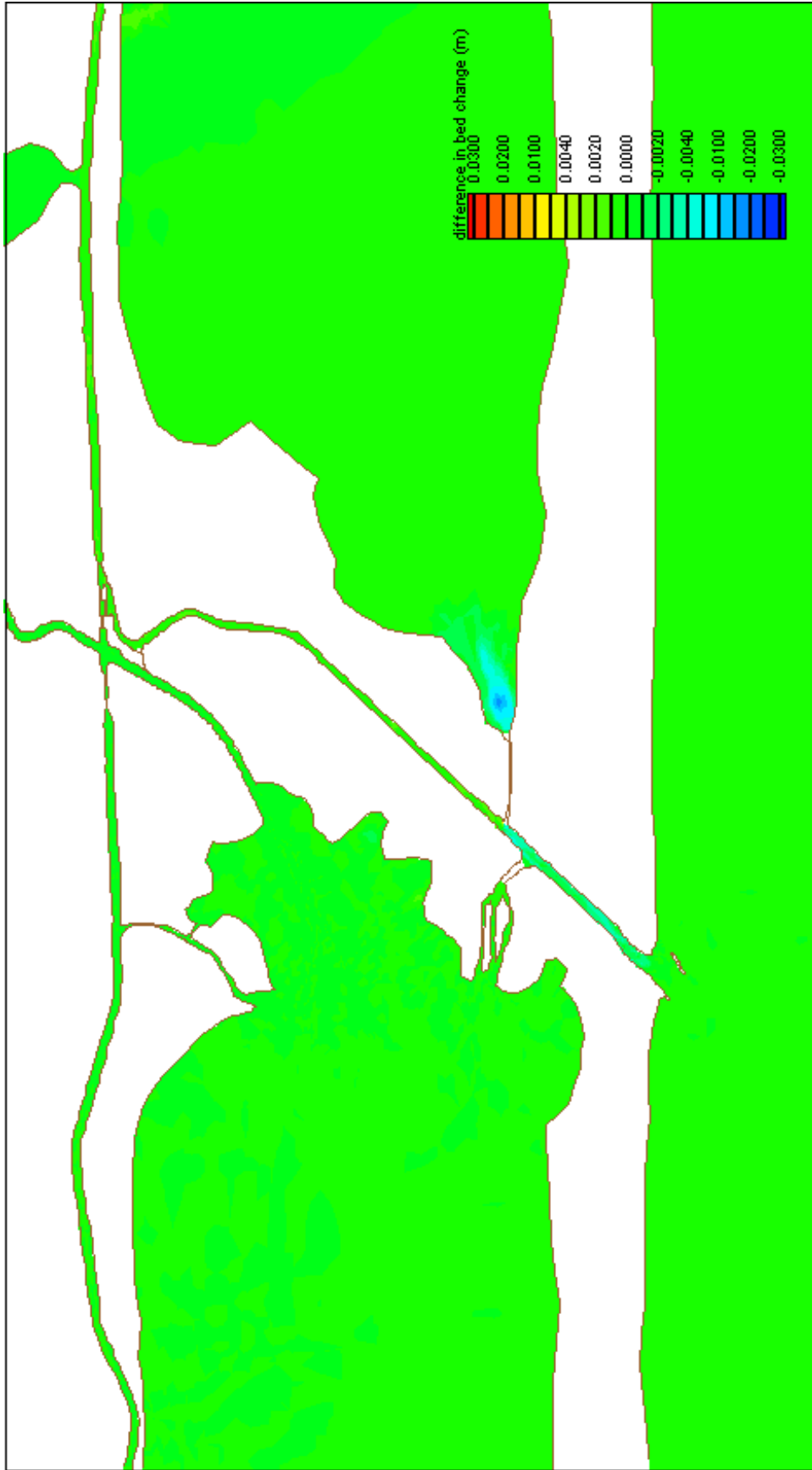
Difference in Bed Change, Scenario M, Low Discharge
 Scenario M: Parker's Cut (5' X 100')



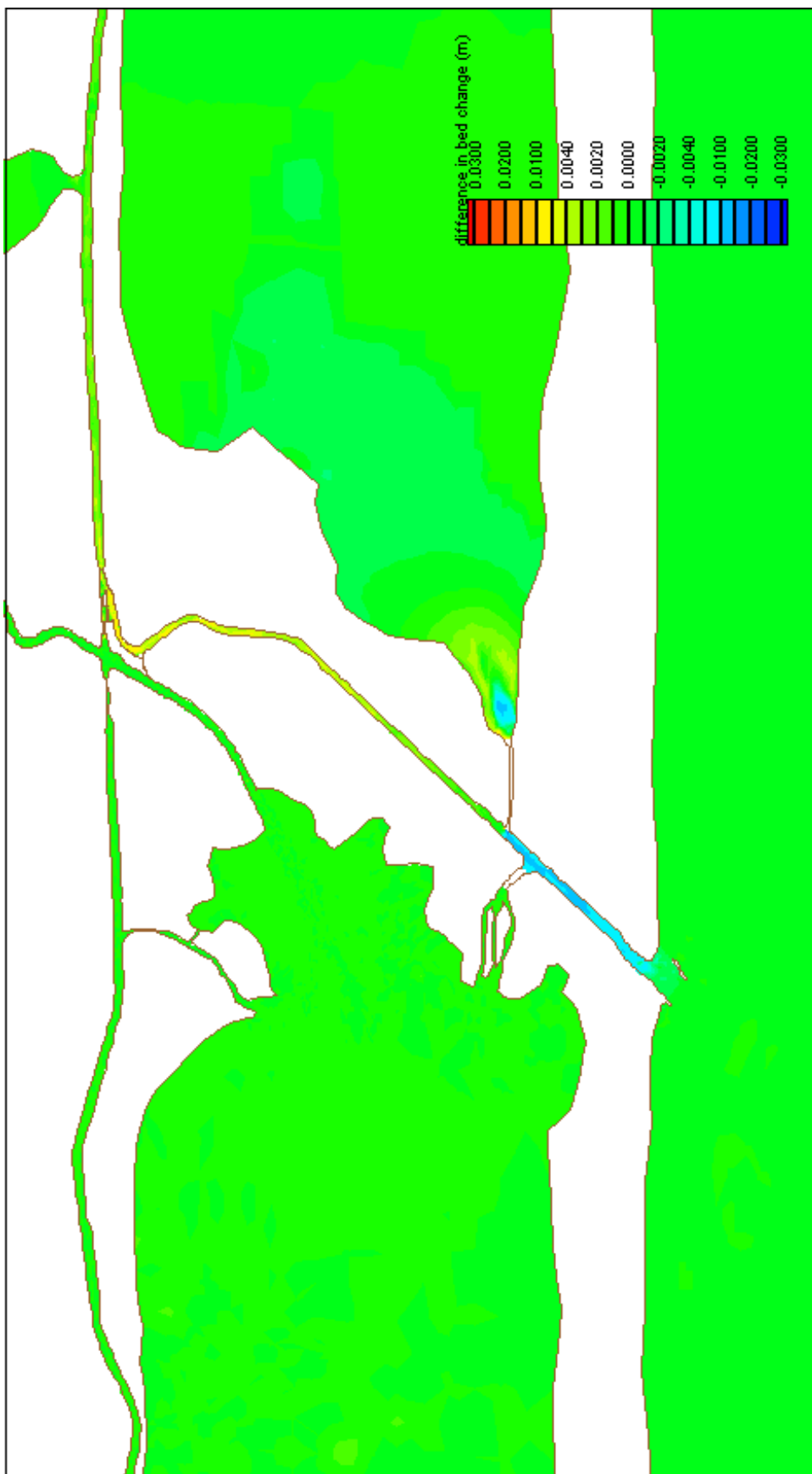
Difference in Bed Change, Scenario M, Medium Discharge
Scenario M: Parker's Cut (5' X 100')



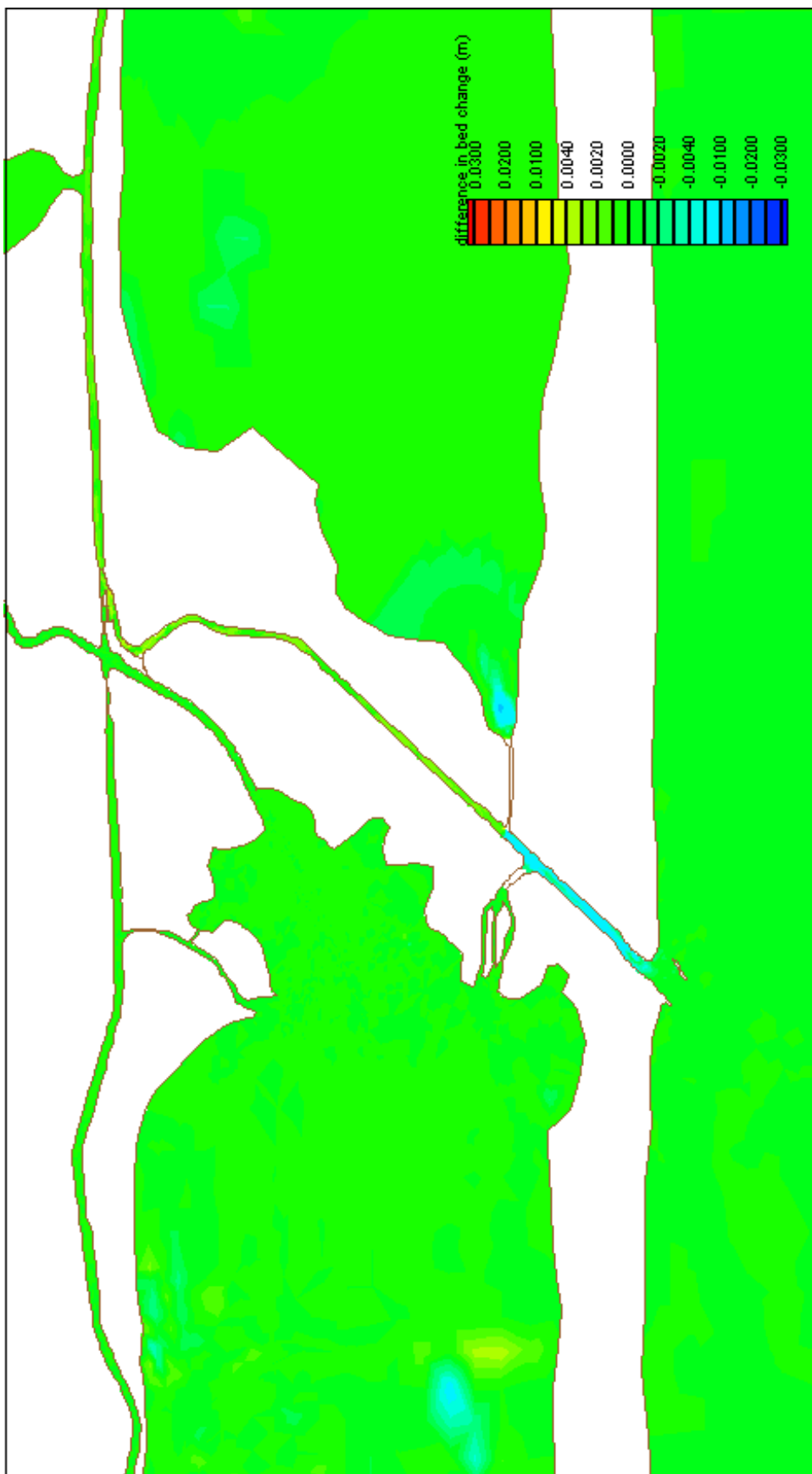
Difference in Bed Change, Scenario M, High Discharge
 Scenario M: Parker's Cut (5' X 100')



Difference in Bed Change, Scenario N, Low Discharge
Scenario N: Southwest Cut (5' X 200')



Difference in Bed Change, Scenario N, Medium Discharge
Scenario N: Southwest Cut (5' X 200')



Difference in Bed Change, Scenario N, High Discharge
Scenario N: Southwest Cut (5' X 200')